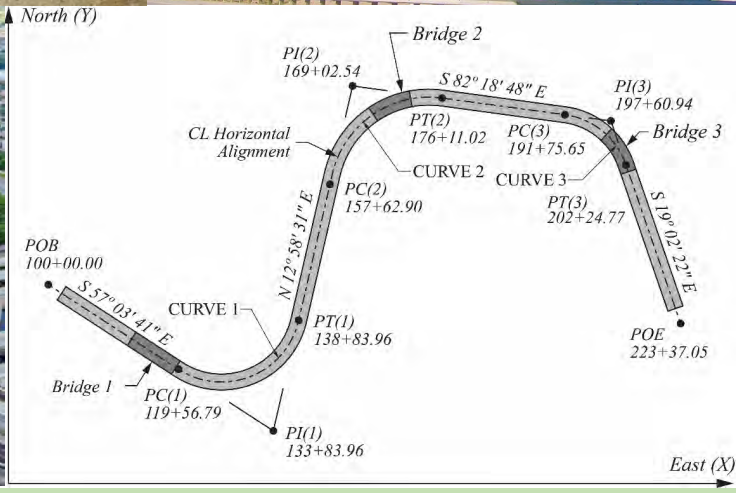

Bridge Geometry Manual

Publication No. FHWA-HIF-22-034
Infrastructure Office of Bridges and Structures

April 2022

U.S. Department of Transportation
Federal Highway Administration

FOREWORD

Documenting a bridge's geometry accurately on bridge layouts and detailed drawings during the design process is fundamental to successful bridge construction. Detailed bridge geometry provides the information necessary to establish analytical models for bridge superstructures and substructures. Geometric constraints often dictate the type of bridge to be built at a specific site. As such, determining bridge geometry is central to the work of bridge engineers and technicians.

The purpose of this manual is to provide bridge engineers and technicians with a basic framework for evaluating and computing the various components of bridge geometry. The manual includes practical examples for implementing the topics discussed. Reference is also made to numerous outside resources for further direction and discussion. The manual is organized into three Parts including General Topics, Concrete Topics, and Steel Topics. While separation among Parts maintains a focused approach, discussion topics inherently overlap with broad applicability across multiple chapters.

Joseph L. Hartmann, PhD, P.E.
Director, Office of Bridges and Structures
Office of Infrastructure
Federal Highway Administration

Cover photos source: HDR, PCI, PCI, PCI (clockwise from upper left)

Notice

This document is disseminated under the sponsorship of the U.S. Department of Transportation (USDOT) in the interest of information exchange. The U.S. Government assumes no liability for the use of the information contained in this document.

The U.S. Government does not endorse products or manufacturers. Trademarks or manufacturers' names appear in this report only because they are considered essential to the objective of the document. They are included for informational purposes only and are not intended to reflect a preference, approval, or endorsement of any one product or entity.

Nonbinding Contents

The contents of this document do not have the force and effect of law and are not meant to bind the public in any way. This document is intended only to provide clarity to the public regarding existing requirements under the law or agency policies. While this document contains nonbinding technical information, you must comply with the applicable statutes or regulations.

Quality Assurance Statement

The Federal Highway Administration (FHWA) provides high-quality information to serve Government, industry, and the public in a manner that promotes public understanding. Standards and policies are used to ensure and maximize the quality, objectivity, utility, and integrity of its information. FHWA periodically reviews quality issues and adjusts its programs and processes to ensure continuous quality improvement.

TECHNICAL REPORT DOCUMENTATION PAGE

1. Report No. FHWA-HIF-22-034	2. Government Accession No.	3. Recipient's Catalog No.
4. Bridge Geometry Manual		5. Report Date 6. Performing Organization Code:
7. Author(s) John Corven, P.E., Corven Engineering, a Hardesty Hanover Company; Thomas Eberhardt, P.E., HDR; Brian Watson, P.E., HDR; Brandon Chavel, P.E., PhD., NSBA; Jason Mash, P.E., Markosky; Duncan Paterson, P.E, PhD., HDR; Thomas Anthony, P.E., Markosky.		8. Performing Organization Report No.
9. Performing Organization Name and Address AASHTO with Precast/Prestressed Concrete Institute (PCI) 8770 W. Bryn Mawr Avenue, Suite 1150 Chicago, IL 60631-3517 HDR Engineering, Inc. 301 Grant Street, Suite 1700 Pittsburgh, PA 15219-1408		10. Work Unit No. 11. Contract or Grant No. DTFH61-13-D-00010 Task No. 5010. DTFH61-14-D-00049
12. Sponsoring Agency Name and Address Office of Bridges and Structures Federal Highway Administration 1200 New Jersey Ave SE Washington, DC 20590		13. Type of Report and Period 14. Sponsoring Agency Code
15. Supplementary Notes		
16. Abstract Determining bridge geometry is central to the work of bridge engineers and technicians. This Manual provides geometric parameters, characteristics, behaviors, and calculations for the evaluation and design of various bridge types. The Manual is organized in three parts: General, Concrete, and Steel.		
17. Key Words Geometry, concrete, steel, bridge	18. Distribution Statement No restrictions. This document is available to the public through the National Technical Information Service, Springfield, VA 22161. https://www.ntis.gov	

19. Security Classif. (of this report) Unclassified	20. Security Classif. (of this page) Unclassified	21. No. of Pages	22. Price

Form DOT F 1700.7 (8-72) Reproduction of completed page authorized.

SI* (MODERN METRIC) CONVERSION FACTORS

APPROXIMATE CONVERSIONS TO SI UNITS

Symbol	When You Know	Multiply By	To Find	Symbol
		LENGTH		
in	inches	25.4	millimeters	mm
ft	feet	0.305	meters	m
yd	yards	0.914	meters	m
mi	miles	1.61	kilometers	km
		AREA		
in^2	square inches	645.2	square millimeters	mm^2
ft^2	square feet	0.093	square meters	m^2
yd^2	square yard	0.836	square meters	m^2
ac	acres	0.405	hectares	ha
mi^2	square miles	2.59	square kilometers	km^2
		VOLUME		
fl oz	fluid ounces	29.57	milliliters	mL
gal	gallons	3.785	liters	L
ft^3	cubic feet	0.028	cubic meters	m^3
yd^3	cubic yards	0.765	cubic meters	m^3
		NOTE: volumes greater than 1000 L shall be shown in m^3		
		MASS		
oz	ounces	28.35	grams	g
lb	pounds	0.454	kilograms	kg
T	short tons (2000 lb)	0.907	megagrams (or "metric ton")	Mg (or "t")
		TEMPERATURE (exact degrees)		
^oF	Fahrenheit	5 (F-32)/9 or (F-32)/1.8	Celsius	^oC
		ILLUMINATION		
fc	foot-candles	10.76	lux	lx
fl	foot-Lamberts	3.426	$candela/m^2$	cd/m^2
		FORCE and PRESSURE or STRESS		
lbf	poundforce	4.45	newtons	N
lbf/in^2	poundforce per square inch	6.89	kilopascals	kPa

APPROXIMATE CONVERSIONS FROM SI UNITS

Symbol	When You Know	Multiply By	To Find	Symbol
		LENGTH		
mm	millimeters	0.039	inches	in
m	meters	3.28	feet	ft
m	meters	1.09	yards	yd
km	kilometers	0.621	miles	mi
		AREA		
mm^2	square millimeters	0.0016	square inches	in^2
m^2	square meters	10.764	square feet	ft^2
m^2	square meters	1.195	square yards	yd^2
ha	hectares	2.47	acres	ac
km^2	square kilometers	0.386	square miles	mi^2
		VOLUME		
mL	milliliters	0.034	fluid ounces	fl oz
L	liters	0.264	gallons	gal
m^3	cubic meters	35.314	cubic feet	ft^3
m^3	cubic meters	1.307	cubic yards	yd^3
		MASS		
g	grams	0.035	ounces	oz
kg	kilograms	2.202	pounds	lb
Mg (or "t")	megagrams (or "metric ton")	1.103	short tons (2000 lb)	T
		TEMPERATURE (exact degrees)		
^oC	Celsius	1.8C+32	Fahrenheit	^oF
		ILLUMINATION		
lx	lux	0.0929	foot-candles	fc
cd/m^2	$candela/m^2$	0.2919	foot-Lamberts	fl
		FORCE and PRESSURE or STRESS		
N	newtons	0.225	poundforce	lbf
kPa	kilopascals	0.145	poundforce per square inch	lbf/in^2

Table of Contents

List of Figures

List of Tables

PART 1 – GENERAL TOPICS

Chapter 1 – Introduction

Determining bridge geometry is central to the work of bridge engineers and technicians. Geometric constraints often dictate the type of bridge to be built at a specific site. Expressing the geometry in accurate layouts and detailed drawings is fundamental to successful bridge construction. Detailed bridge geometry provides the information needed to establish analytical models for bridge superstructures and substructures.

Bridge geometry is typically established to follow a determined roadway alignment. Roadway geometric designers take a number of variables into consideration when establishing these alignments. They work within the limits of a particular site to optimize the functionality of a roadway while considering user safety. The resulting impact on bridge geometry can be small when roadway needs are straightforward, as for simple grade separations, or quite complex, as in the case of congested urban interchanges. **Figure 1.1** shows the bridge structures for a complex, multilevel, directional urban interchange.

Source: PCI

Figure 1.1 Bridges Within a Complex Urban Interchange

1.1 Influence of Bridge Geometry on Bridge Type, Span Length, and Layout

Of the many factors influencing bridge design, geometric constraints may be the most significant. This is not to downplay the importance of factors such as durability, maintainability, construction cost, environmental appropriateness, and aesthetics. This section presents a brief overview of the various ways in which geometry affects bridge design.

1.1.1 Horizontal Curvature

Horizontal curvature can be an influential geometric constraint during the selection of a bridge's superstructure type. The degree of horizontal curvature, in conjunction with desired span lengths, can dictate the available superstructure options that can be economically utilized.

Bridges that lie along straight (tangent) alignments can be constructed with any superstructure type. The most common of these are straight steel plate girders and pretensioned concrete girders. These straight superstructure members can also be used for bridges that follow alignments with small amounts of curvature, within reasonable span lengths, as shown in **Figure 1.2**. In these instances, the straight elements form chords to the horizontal alignment between the piers.

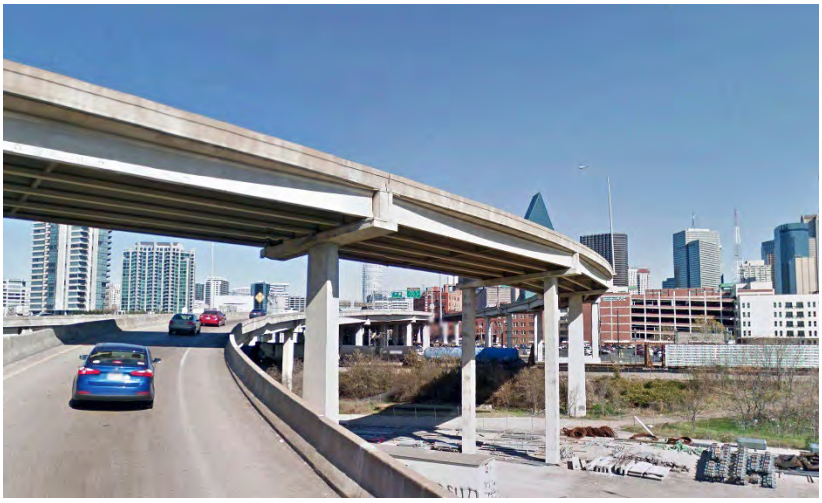

Source: PCI

Figure 1.2 Curved Bridge with Straight Precast Concrete Girders

Curved bridges with long span requirements or sharply curved bridges with moderate or long spans can limit the available superstructure options. Superstructure types for these bridges historically consisted of curved steel girders, as shown in **Figure 1.3**, or cast-in-place concrete box girders. Precast concrete segmental box girder bridges, introduced in the United States in the 1970s, have provided an economical means of building highly curved bridges with prefabricated concrete elements. The more recent introduction of curved, spliced U-girder bridges has provided another means.

Source: PCI

Figure 1.3 Curved Bridge with Curved Steel Box Girders

1.1.2 Vertical and Horizontal Clearances

A project's vertical and horizontal clearance requirements often dictate bridge superstructure type. The elevations of grade separation bridges are established to provide needed vertical clearances. Horizontal clearances to piers and abutments are located with appropriate clear setbacks. These setbacks may be reduced when protective guardrails are used. Multidirectional and multilevel interchanges, such as that shown in **Figure 1.4**, are highly constrained geometrically. Bridge elevations and structure depths are chosen to accommodate a stacking of vertical clearance needs. Pier locations, which establish span lengths and therefore superstructure type, are located not to conflict with the roadways below.

Source: PCI

Figure 1.4 Multi-level Interchange Spans Influenced by Vertical and Horizontal Clearances

Bridges over navigable waterways have strict horizontal and vertical constraints at navigation channels. **Figure 1.5** shows an elevation of a main span of a long bridge over water that crosses a navigation channel. If approach lengths are short, a lower bridge elevation with a bascule or lift span at the channel may be the appropriate choice.

Source: PCI

Figure 1.5 Bridge Elevation Providing Vertical and Horizontal Clearance over Navigable Waterway

1.1.3 Skewed Alignment Crossings

Horizontal and vertical constraints also play an important role in the selection of bridge substructure types and dimensions. This is often the case for bridges that cross underlying roadways with significant skews. In these cases, the economics of the project may benefit from moderate superstructure span lengths and special substructure bents designed to support the bridge over the underlying roadways. The most common special bents include hammerhead piers (T-piers), straddle bents, integral T-piers, and C-piers. **Figure 1.6** shows a skewed crossing by a transit bridge that utilizes straddle bents, T-piers, and integral T-piers to maintain typical superstructure spans. Three C-piers are used to support the bridge in **Figure 1.7** as it crosses a local divided highway at a significant skew.

Source: PCI

Figure 1.6 Hammerhead Piers (T-Piers), Straddle Bents, and Integral T-Piers

Source: PCI

Figure 1.7 C-Piers

1.2 Terminology

This section presents terminology related to roadway geometry and bridge structures that will be used throughout this manual. It is noted that there is some variability and interchangeability in some terms, depending on the governing highway agency and bridge and roadway disciplines. Other terms related to specific geometric characteristics are used in subsequent chapters. Common variable or interchangeable terms are presented where applicable. Definitions in this manual are provided only for ease of use and to improve the clarity of this manual. Unless indicated by citation to Federal law or regulations, the definitions, notations, and equations that follow are provided to assist in using this manual and their use is not required.

1.2.1 Roadway Cross-Section Terminology

Figure 1.8 shows a typical cross section of a two-lane divided highway. Definitions for the roadway features are given below.

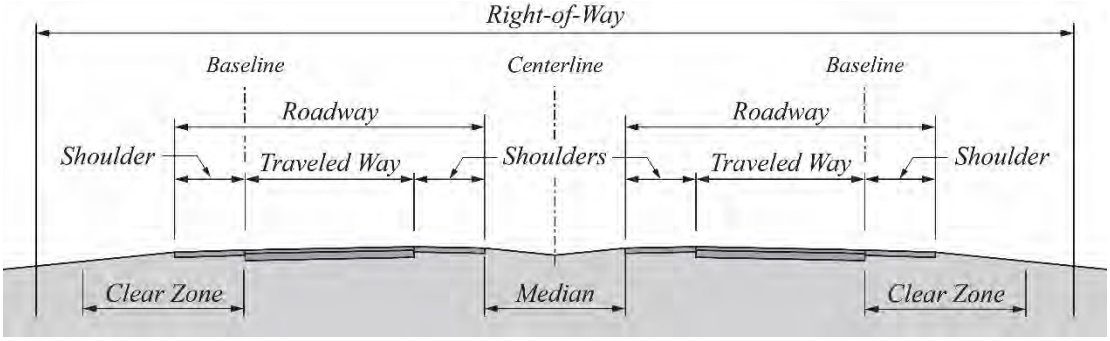

Source: PCI

Figure 1.8 Divided Highway Cross Section

- Roadway: A portion of a highway, including shoulders, for vehicular use. A roadway consists of the traveled way and shoulders. A divided highway has two or more roadways.
- Centerline (CL) of cross section: Line within the cross section that serves as the reference for roadway geometrics. The CL typically lies in the median for a divided highway as depicted in **Figure 1.8.** The CL may coincide with another given cross-section feature for other types of roadway cross sections.
- Roadway baseline (BL): Line used to locate the roadways within the cross section. The BL often coincides with the physical location of a roadway feature, such as a lane or shoulder line.
- Traveled way: The portion of the roadway for the movement of vehicles, exclusive of shoulders. This includes travel lanes, turning lanes, acceleration lanes, deceleration lanes, and auxiliary lanes.
- Lane: A portion of a traveled way marked for use by a single line of vehicles.
- Shoulders: The portion of the roadway contiguous with the traveled way that accommodates stopped vehicles, emergency use, and lateral support of subbase, base, and surface courses.
- Median: The portion of a highway separating opposing directions of the traveled way.
- Clear zone: The unobstructed, relatively flat area provided beyond the edge of the traveled way for the recovery of errant vehicles. The clear zone includes any shoulders or auxiliary lanes.
- Right-of-way: Land, property, or interest therein that is acquired, dedicated, or reserved for highway purposes.

Figure 1.9 shows one direction of the divided highway cross section of **Figure 1.8**. Several features of the cross section are shown in this figure.

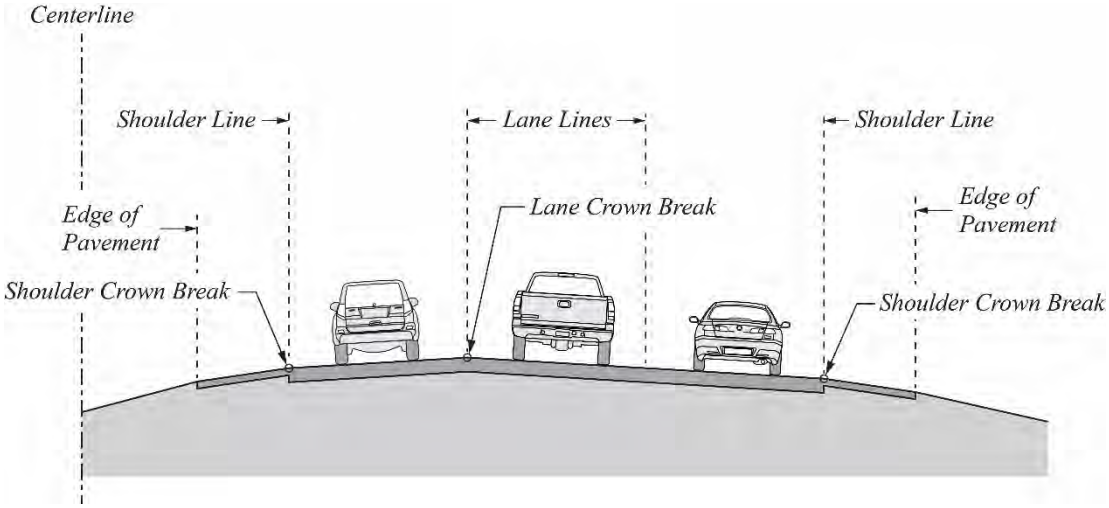

Source: PCI

Figure 1.9 Locations within a Highway Cross Section

Definitions:

- Lane lines: Lines that define the limits of the width of a lane. Lane lines lie between adjacent lanes.
- Shoulder lines: Lines that define the edge of the outermost lanes and the beginning of the shoulders.
- Edge of pavement: Lines that define the outer edge of the shoulders.
- Lane crown break: The transverse location, typically falling on a lane line, where the cross slope of the cross section changes to accommodate horizontal curvature and roadway drainage.

  Shoulder crown break: The transverse location of crown break between the outermost lanes and the shoulders.

1.2.2 Bridge Structure Terminology

Figure 1.10 shows a typical cross section of a girder bridge superstructure. This bridge carries a roadway that consists of two lanes and two shoulders. **Figure 1.11** shows detail A, which focuses on the connection of the deck slab to the longitudinal girders. Additional terms are used that complement the previously provided roadway terms.

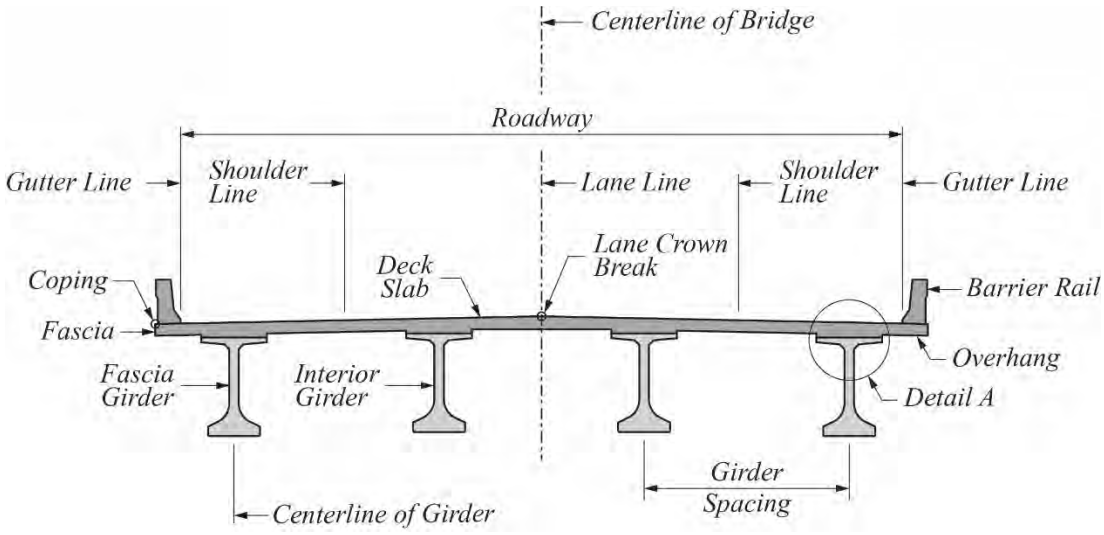

Source: PCI

Figure 1.10 Typical Bridge Superstructure Cross Section

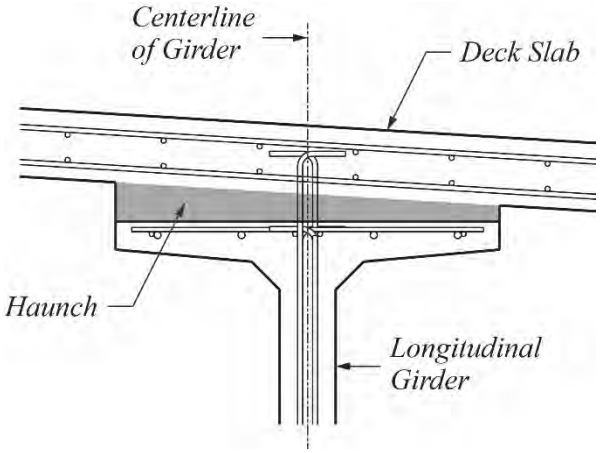

Source: PCI

Figure 1.11 Detail A: Connection of Deck Slab to the Longitudinal Girder

Superstructure terms:

- CL of bridge: The line that sets the geometric center of a bridge. The CL may or may not coincide with another feature of the highway geometry.
- Roadway: As given for roadway cross sections.
- Lane line: As given for roadway cross sections.
- Shoulder line: As given for roadway cross sections.
- Gutter line: Similar to the edge of pavement for roadways, these lines lie at the toe of the barrier railing or face of a curb or sidewalk.
- Deck slab: A solid concrete slab resisting and distributing wheel loads to the supporting components. The deck slab is typically cast in place, but may be precast concrete, with either partial or full-depth precast panels. Transverse or longitudinal post-tensioning may be used in deck slabs.

Composite behavior can be achieved by engaging horizontal shear reinforcement protruding from the longitudinal girders. Deck slabs of monolithic box-girder cross sections are typically specified by a combination of top slabs and cantilever overhangs.

- Haunch: Concrete between the top flange of the longitudinal girder and the bottom of the deck slab that accommodates differences in girder and deck slab geometry. The haunch is cast with the deck slab (see **Figure 1.11**).
- Deck fascia: The outermost vertical face of the deck slab.
- Coping (or coping lines): The lines that describe the top of the outermost portions of the deck slab.
- Barrier rail: Structural member attached to or cast on the deck slab to prevent vehicles, pedestrians, or cyclists from falling off the structure.
- Fascia girder: The outermost longitudinal girder of bridge cross section consisting of multiple longitudinal girders.
- Interior girder: A longitudinal girder located between two fascia girders.
- CL of girder: A vertical line passing through the center of a girder used to locate the transverse location of longitudinal girders within the bridge cross section.
- Girder spacing: The transverse spacing between girder CLs.

Figure 1.12 shows a typical transverse elevation of a bridge pier supporting the superstructure cross section shown in **Figure 1.10.** Though there are many possible configurations of bridge piers, the one shown in **Figure 1.12** is used to show substructure terminology. **Figure 1.13** shows an enlargement of detail B shown in **Figure 1.12**. This figure shows details related to bridge bearings.

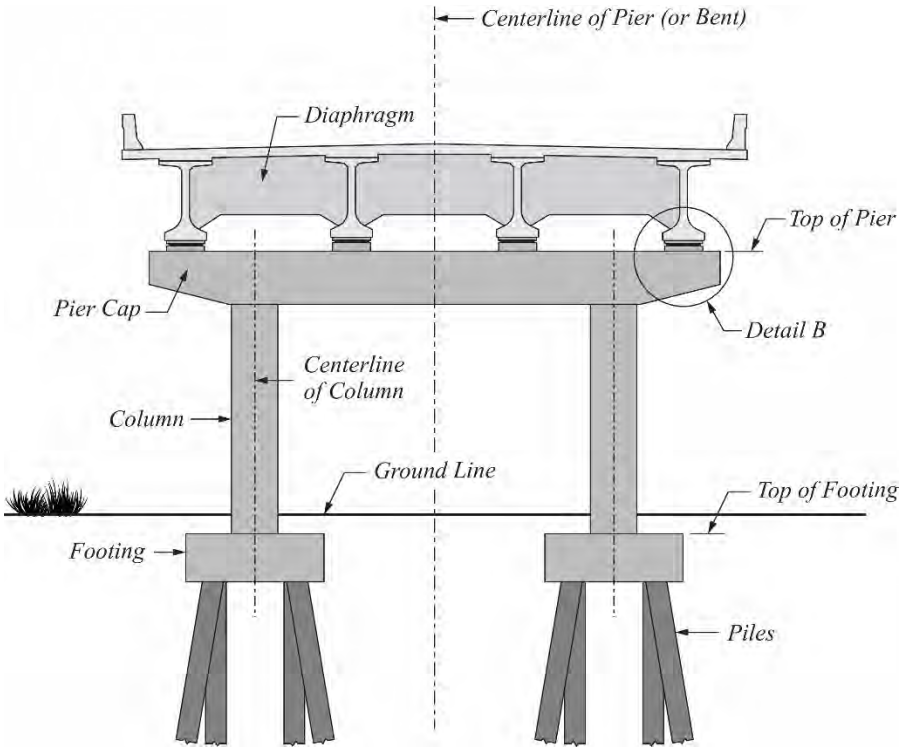

Source: PCI

Figure 1.12 Transverse Elevation of Typical Bridge Pier

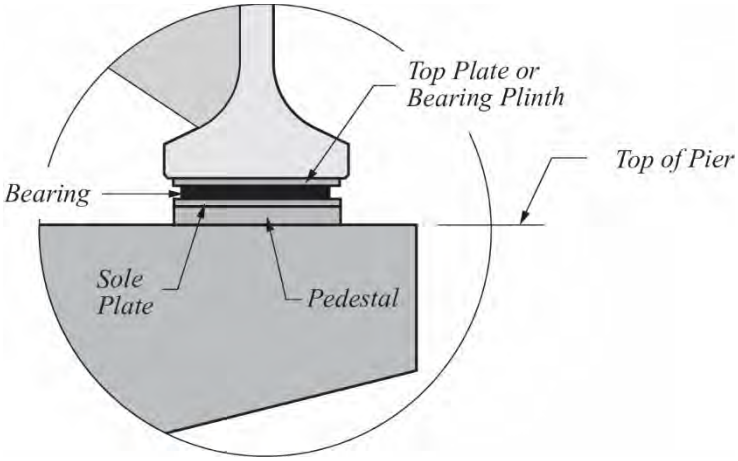

Source: PCI

Figure 1.13 Detail B: Bridge Bearing Details

Substructure terms:

- Pier (bent): A substructure unit that supports the spans of a multispan superstructure at intermediate locations between the abutments. The pier is supported by foundation elements that together are called a substructure.
- CL of pier: A line at the geometric center of the pier from which the pier geometry is referenced.
- Pier cap (bent cap): That portion of the pier on which the bearings are placed to support the bridge superstructure. Top-of-pier elevations are computed from roadway geometry and features of the superstructure cross section.
- Column: A vertical supporting element in a pier. **Figure 1.12** shows a pier consisting of multiple columns. Pier, pier shaft, and column are used interchangeably when the pier consists of a singular vertical element.
- CL of column: A line that sets the transverse location of columns within the pier elevation.
- Diaphragm: Concrete cast, or steel member erected, between girders to provide stability and load distribution. The use, size, and locations of diaphragms vary greatly among governing highway agencies.
- Footing: Reinforced concrete member that transfers loads from the columns to the earth, in the case of spread footings, or to other supporting elements, such as piles or shafts. The top of footing is typically placed at a specified distance below the ground line.
- Foundation: The supporting material or structural elements below the substructure used to transmit bridge forces to the supporting soils or rock. In **Figure 1.12**, this includes the footings and the supporting piles.
- Bearing: Load-carrying element that supports the bridge superstructure while allowing translation, rotation, or translation with rotation. Common bearing types include elastomeric bearing pads, pot bearings, disc bearings, spherical bearings, rocker bearings, and roller-pin bearings. Bearings are typically positioned flat and horizontal in both the longitudinal and transverse directions.

- Pedestal: A reinforced concrete member cast on the top of the pier, on which the bearing is placed. The pedestal is typically cast after the pier cap to achieve desired tolerances in elevation. The top of the pedestal, the bearing seat, is cast flat and horizontal.
- Top plate (or bearing plinth) and sole plate: The top plate is a steel plate attached to the bottom flange of a beam that accommodates girder geometry and distributes the load between beam and bearing. A concrete bearing plinth that is either packed or grouted in place is sometimes used instead of the top plate. In some bearing configurations, a sole plate placed beneath the bearing is used to distribute loads to the pedestal.

Chapter 2 – Roadway Horizonal Geometry

2.1 Introduction

This chapter describes the elements used for a roadway's plan view geometry. **Figure 2.1** presents a plan view of a roadway project that contains three bridges. The path that the roadway follows in plan view is called the *horizontal alignment*. As seen in section A-A of **Figure 2.1**, the horizontal alignment line coincides with the centerline (CL) of the roadway. Depending on the governing highway agency, the horizontal alignment line may lie at other transverse locations offset from the CL of a roadway, such as a lane line, shoulder line, or gutter line.

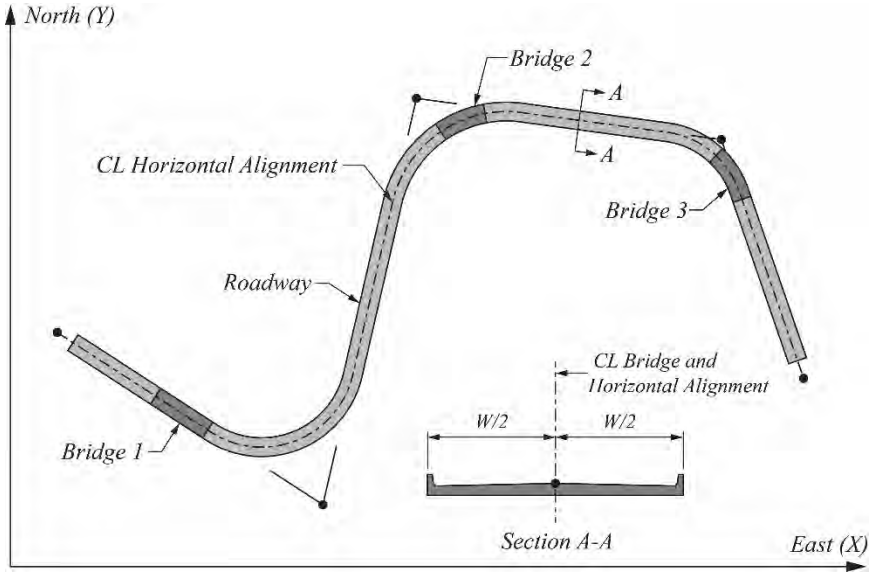

Source: PCI

Figure 2.1 Horizontal Roadway Alignment with Bridges

The horizontal alignment shown in **Figure 2.1** is composed of straight and curved elements. The lengths and curvature of these elements are selected by the highway engineer to fit project and site constraints. The design should conform to the requirements of the highway's functional classification while maintaining driving safety for the planned design speed. Horizontal alignments of roadways typically consist of the following elements:

- Tangent (straight) sections
- Circular curved sections
- Compound (multiple) circular curved sections
- Spiral sections
- Compound (multiple) spiral sections

The horizontal alignment shown in **Figure 2.1** will be developed throughout this chapter and will serve as the basis for various example calculations.

2.2 Coordinate Systems

2.2.1 Two-Dimensional Coordinate System for Horizontal Alignments

Horizontal alignment geometry is described in a two-dimensional (2D) plan view plane. A Cartesian coordinate system is utilized to establish the plan view, with the *X* axis oriented to the east and the *Y* axis oriented to the north. **Figure 2.2** shows the horizontal alignment of the example roadway shown in this type of coordinate system. The location of any point *P* on the horizontal alignment is determined by the corresponding *X* and *Y* coordinates in the coordinate system. Historical surveying convention typically reports the position of a point on the horizontal alignment by north and east coordinates.

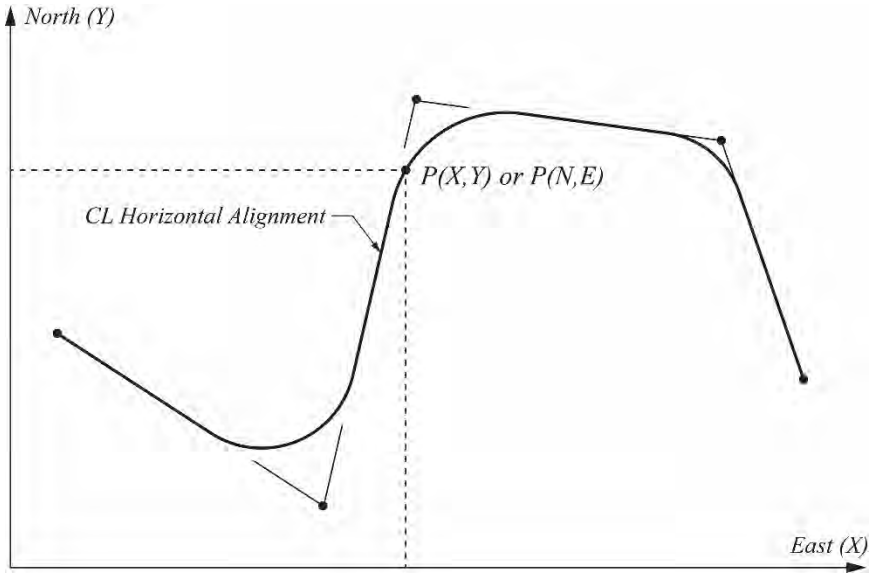

Source: PCI

Figure 2.2 Horizontal Roadway Alignment Coordinate System

The origin of the coordinate system for a particular project is established by the governing agency. These coordinate systems and the corresponding set of reference points describe geodetic datum networks that are used to locate points in North America. A datum is a formal description of the shape of the Earth along with an "anchor" point for the coordinate system. The first datum established in 1927 replaced a system of longitudes and latitudes. This datum is referred to as the North American Datum of 1927 (NAD 27). It was determined by a point (Meades Ranch Station) and azimuth on the Clarke ellipsoid of 1866.

In 1983, a more accurate datum, the North American Datum of 1983 (NAD 83), was developed. This system was based on a geocentric reference system with no datum point. The datum was based on the newer GRS80 ellipsoid. As satellite technology advanced, even more accurate datums could be achieved. This led to the development of a network of Continuously Operating Reference Stations (CORS). The National Geodetic Survey has embarked upon a series of adjustments over the years to increase the accuracy of the datum within this network. The first datum refinement, which resulted in the High Accuracy Reference Network (HARN), was completed in 1998. The HARN updated selected survey stations using Global Positioning System (GPS) observations. The second datum refinement occurred in 2007 with the National Spatial Reference System readjustment. This datum is known as NAD 83 (NSRS2007) and allowed for increased accuracies in the elevation component of the survey. The final and most recent adjustment is referred to as NAD 83 (2011). This was a further refinement of physical benchmarks (such as brass disc benchmarks).

Care should be taken to verify the datum preferred for a particular project. All these datums take an elliptical surface of the earth and project it (either Mercator or Lambert projections) onto a 2D plane surface for ease in the survey layout of a project. The resulting 2D Cartesian coordinate system is called the State Plane Coordinate System (SPCS). The SPCS consists of 124 geographic zones that together comprise the entire United States. Each State contains one or more state plane zones with the boundaries generally following county lines.

The units of the Cartesian coordinates (X,Y) or (N,E) are most typically meters, feet, or U.S. Survey Feet. The U.S. Survey Foot accounts for the discrepancy between historical North American survey systems and the international definition of the foot. The U.S. Survey Foot is 1200/3937 m. The International Foot is 0.3048 m. The difference between the U.S. Survey Foot and International Foot can have an impact on geographically large projects. The dimensioning and detailing of individual bridge members are typically not affected by the type of foot unit used on a project.

2.2.2 Three-Dimensional Coordinate System for Geometric Calculations

The three-dimensional (3D) global coordinate system for geometric calculations in this manual is the orthogonal system shown in **Figure 2.3**. The sign convention for rotations is established by the vector cross products of the unit vectors of the principal axes, following the right-hand rule.

2.3 Project Baseline

The example horizontal alignment shown in **Figure 2.2** is set by a series of control points that help define the orientation of the horizontal alignment of the roadway. These control points are

- Point of beginning - *POB*
- Point of intersection - *PI*(n), where n = number of points
- Point of ending - *POE*

The chain of chords between the control points is called the *project baseline*, or *baseline*. **Figure 2.4** shows the chords of the baseline for the example alignment of this chapter. As indicated from the naming convention of the control points, baselines are direction dependent. The baseline begins with the *POB*, passes through the successive *PI*s, and ends with the *POE*. **Figure 2.4** shows the direction of the example alignment.

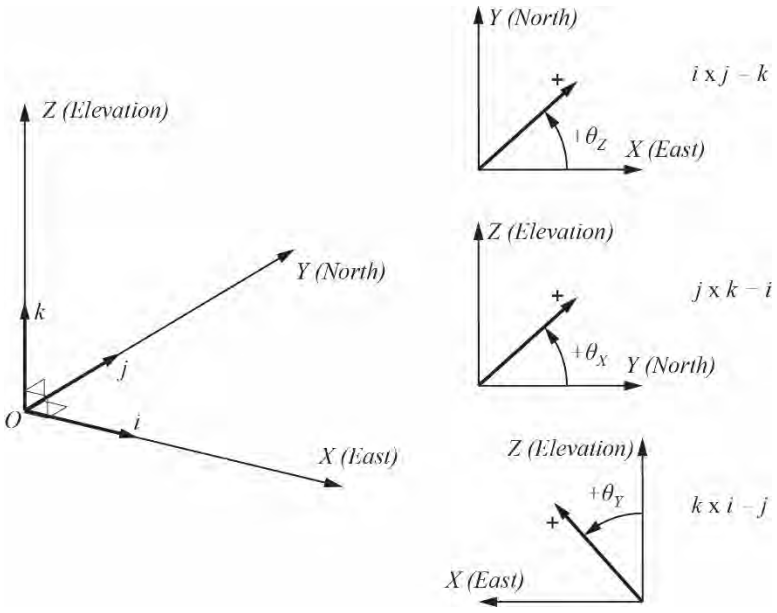

(a) (b)

Source: PCI

Figure 2.3 3D Coordinate System and Sign Conventions for General Geometric Calculations

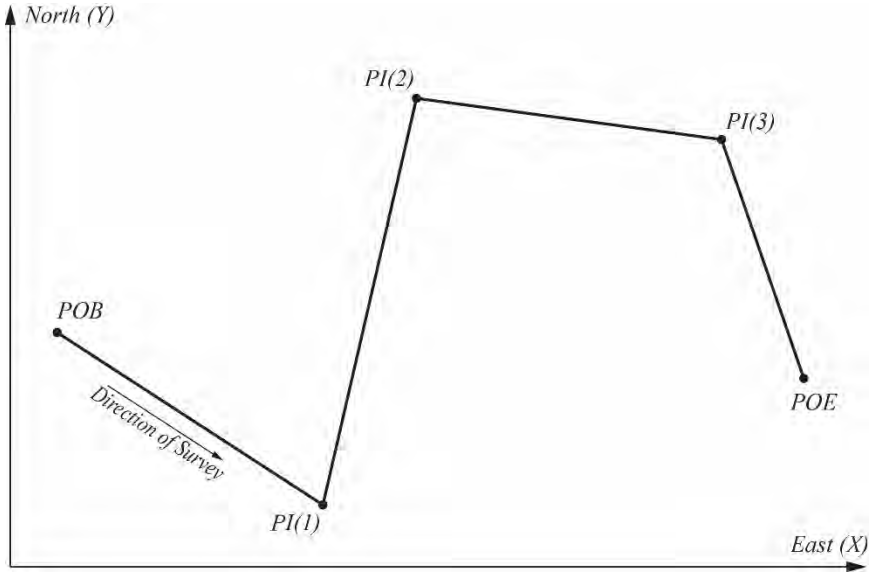

Source: PCI

Figure 2.4 Horizontal Alignment Control Points and Project Baseline

The orientation of the individual baseline chords is defined in this manual in one of two ways:

- A direction angle referenced from the X or east axis. The range of the direction angle is from zero to 360 degrees. (Note: Direction angles when referenced to the Y or north axis are called azimuth bearings).

- A compass bearing relative to north and south compass directions. Chords that are not aligned with the north or south axis are specified by an orientation to either the east or the west. The range of compass bearings in their respective directions is from zero to 90 degrees.

Figure 2.5 and **Figure 2.6** show the naming and sign conventions to describe the baseline chord orientations for the two methods used in this manual.

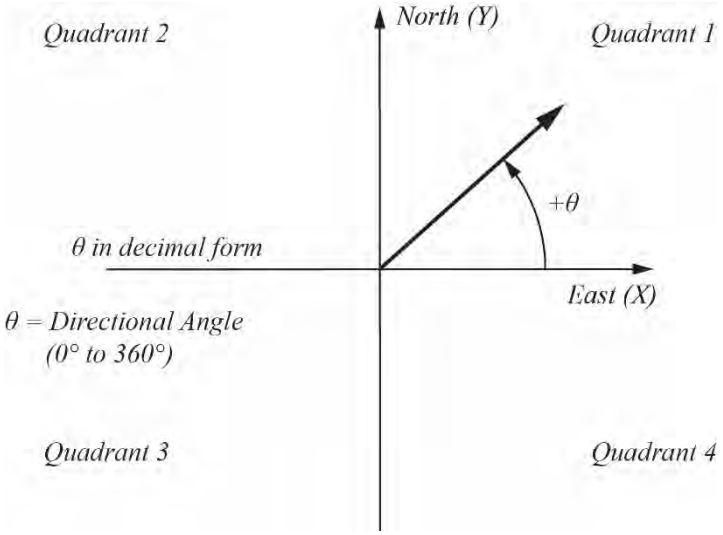

Source: PCI

Figure 2.5 Resulting Signs for Bearing Angles by Eq.(2.1)

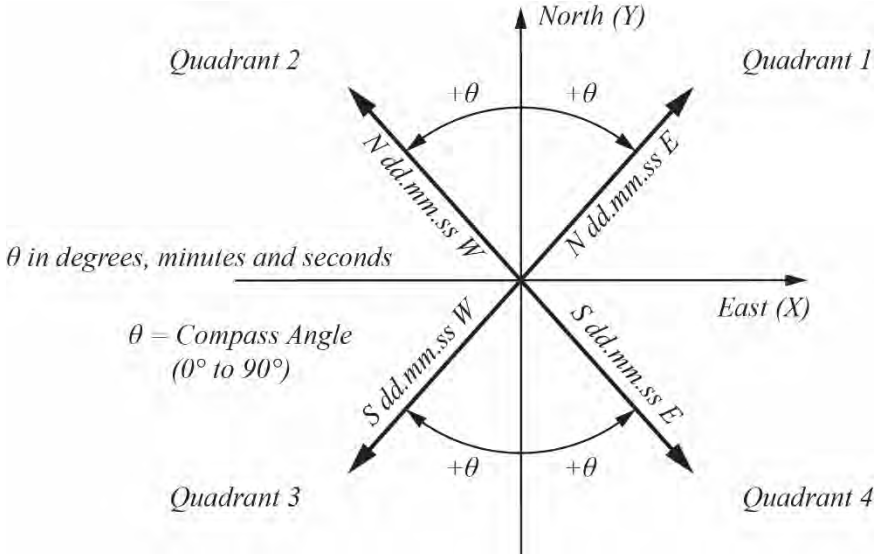

Source: PCI

Figure 2.6 Traditional Surveying Sign Convention for Bearings

Direction angles for baseline chords are calculated using the X and Y coordinate information of the survey control points. If the beginning control point of a chord has the coordinates (X_i, Y_i) and the control point at the end of the chord has the coordinates (X_{i+1}, Y_{i+1}), then the bearing of the chord is found as

$$\theta_i = \tan^{-1}\left(\frac{\Delta Y_i}{\Delta X_i}\right) \tag{2.1}$$

where ΔX_i and ΔY_i are defined as

$$\Delta X_i = X_{i+1} - X_i \tag{2.2}$$

$$\Delta Y_i = Y_{i+1} - Y_i \tag{2.3}$$

The nature of the tangent function is such that, to have direction angle results vary from zero to 360 degrees, quadrant-specific expressions are required. The direction angles by quadrant are

$$\text{Quadrant 1 } (\Delta X > 0, \Delta Y > 0) \qquad \theta_i = \tan^{-1}\left(\frac{\Delta Y_i}{\Delta X_i}\right) \tag{2.4}$$

$$\text{Quadrant 2 } (\Delta X < 0, \Delta Y > 0) \qquad \theta_i = 180 + \tan^{-1}\left(\frac{\Delta Y_i}{\Delta X_i}\right) \tag{2.5}$$

$$\text{Quadrant 3 } (\Delta X < 0, \Delta Y < 0) \qquad \theta_i = 180 + \tan^{-1}\left(\frac{\Delta Y_i}{\Delta X_i}\right) \tag{2.6}$$

$$\text{Quadrant 4 } (\Delta X > 0, \Delta Y < 0) \qquad \theta_i = 360 + \tan^{-1}\left(\frac{\Delta Y_i}{\Delta X_i}\right) \tag{2.7}$$

The unique conditions of either ΔX_i or ΔY_i equaling zero lead to the following bearings:

$$\text{If } \Delta X_i = 0 \text{ and } \Delta Y_i = +, \text{ then } \theta = 90 \text{ degrees} \tag{2.8}$$

$$\text{If } \Delta X_i = 0 \text{ and } \Delta Y_i = -, \text{ then } \theta = 270 \text{ degrees} \tag{2.9}$$

$$\text{If } \Delta Y_i = 0 \text{ and } \Delta X_i = +, \text{ then } \theta = 0 \text{ degrees} \tag{2.10}$$

$$\text{If } \Delta Y_i = 0 \text{ and } \Delta X_i = -, \text{ then } \theta = 180 \text{ degrees} \tag{2.11}$$

Converting between the two formats of expressing baseline bearings is accomplished using the following relationships:

$$\text{If } 0 \le \theta \le 90 \text{ degrees then bearing} = \text{N}(90 \text{ degrees} - \theta)\text{E} \tag{2.12}$$

$$\text{If } 90 \text{ degrees} \le \theta \le 180 \text{ degrees then bearing} = \text{N}(\theta - 90 \text{ degrees})\text{W} \tag{2.13}$$

$$\text{If } 180 \text{ degrees} \le \theta \le 270 \text{ degrees then bearing} = \text{S}(270 \text{ degrees} - \theta)\text{W} \tag{2.14}$$

$$\text{If } 270 \text{ degrees} \le \theta \le 360 \text{ degrees then bearing} = \text{S}(\theta - 270 \text{ degrees})\text{E} \tag{2.15}$$

where

E = east
N = north
S = south
W = west

Example 2.1: Compute the baseline bearings for the example horizontal alignment of this chapter using the coordinate information for the *PIs* listed in **Table 2.1**. Express the results in traditional surveying convention.

Table 2.1 Coordinate Information for Example Alignment

Point	Number	*X*, ft	*Y*, ft
POB	1	500.0	2500.0
PI(1)	2	3340.0	660.0
PI(2)	3	4340.0	5000.0
PI(3)	4	7600.0	4560.0
POE	5	8480.0	2010.0

Compute the bearings of the baseline line chords using Eq. (2.4) through (2.7):

$$\theta_1 = 360 + \tan^{-1}\left(\frac{660.0 - 2500.0}{3340.0 - 500.0}\right) = 327.0613 \text{ degrees} \tag{2.16}$$

$$\theta_2 = \tan^{-1}\left(\frac{5000.0 - 660.0}{4340.0 - 3340.0}\right) = 77.0247 \text{ degrees} \tag{2.17}$$

$$\theta_3 = 360 + \tan^{-1}\left(\frac{4560.0 - 5000.0}{7600.0 - 4340.0}\right) = 352.3133 \text{ degrees} \tag{2.18}$$

$$\theta_4 = 360 + \tan^{-1}\left(\frac{2010.0 - 4560.0}{8480.0 - 7600.0}\right) = 289.0395 \text{ degrees} \tag{2.19}$$

Using Eq. (2.12) through (2.15), the results in traditional surveying format are

$$Bearing_1 = \text{S } 57^\circ\ 03'\ 41''\ \text{E} \tag{2.20}$$

$$Bearing_2 = \text{N } 12^\circ 58'\ 31''\ \text{E} \tag{2.21}$$

$$Bearing_3 = \text{S } 82^\circ 18'\ 48''\ \text{E} \tag{2.22}$$

$$Bearing_4 = \text{S } 19^\circ 02'\ 22''\ \text{E} \tag{2.23}$$

where:

° = degrees
‘ = minutes
“ = seconds

The resulting baseline bearings of the example horizontal alignment are shown in **Figure 2.7.**

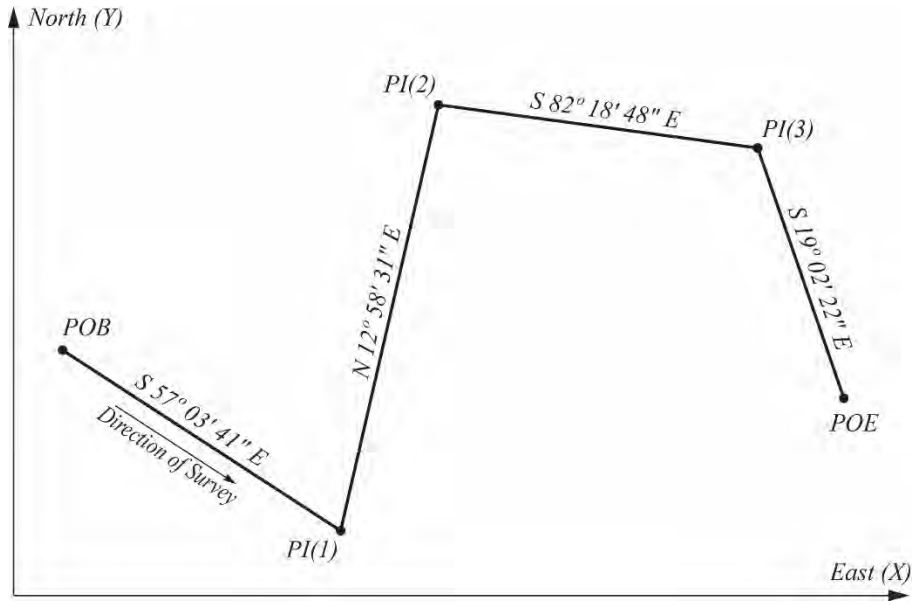

Source: PCI

Figure 2.7 Horizontal Roadway Alignment Baseline Bearings

One way to refer to the bearings of the baseline is to describe them relative to the *PI* at which they intersect. The bearing of the baseline coming into a *PI* is referred to as the *back bearing* or *bearing back*. The bearing of the baseline leaving a *PI* is referred to as the *ahead bearing* or *bearing ahead*. As an example of this terminology in **Figure 2.7**, the back and ahead bearings of *PI*(2) are

$$\text{Back bearing at PI(2)} = \text{N } 12^{\circ}58'\ 31''\ \text{E} \tag{2.24}$$

$$\text{Ahead bearing at PI(2)} = \text{S } 82^{\circ}18'\ 48''\ \text{E} \tag{2.25}$$

2.4 Stationing – Part 1

Locating a point on a baseline requires the bearings of the individual baseline chords and some measure of length along the baseline from the *POB*. The measure of length along any horizontal roadway baseline is called *stationing*. In the English system, stationing between points on an alignment is measured in increments of 100 ft and follows the format 100+00.0 (read "one hundred plus zero zero point zero"). The number to the left of the plus sign is the number of 100 ft stations from a beginning location and the number to the right of the plus sign is the length from the last even 100 ft station number.

The stationing along the baseline relative to the *POB* is found by the arithmetic sum of the lengths of the baseline chords. The length of any baseline chord L_{Bi} is found by

$$L_{Bi} = \sqrt{\left(\Delta X_i\right)^2 + \left(\Delta Y_i\right)^2} \tag{2.26}$$

The station of the *PI*s and *POE* for an alignment made up only of the baseline tangents would then be

$$Station_i = Station_{POB} + \sum_{i=1}^{n} L_{Bi} \tag{2.27}$$

Example 2.2: Using the coordinate information for the example horizontal alignment, determine the stationing of the *PI*s and *POE*. Assume the station of the *POB* to be equal to 100+00.0.

The lengths of the baseline chords are computed using the coordinate information in **Table 2.1** and Eq. (2.26).

$$L_{B1} = \sqrt{(3340.0 - 500.0)^2 + (660.0 - 2500.0)^2} = 3383.96 \text{ feet} \quad (2.28)$$

$$L_{B2} = \sqrt{(4340.0 - 3340.0)^2 + (5000.0 - 660.0)^2} = 4453.72 \text{ feet} \quad (2.29)$$

$$L_{B3} = \sqrt{(7600.0 - 4340.0)^2 + (4560.0 - 5000.0)^2} = 3289.56 \text{ feet} \quad (2.30)$$

$$L_{B4} = \sqrt{(8480.0 - 7600.0)^2 + (2010.0 - 4560.0)^2} = 2697.57 \text{ feet} \quad (2.31)$$

The stationing of the baseline control points is found by summing the chord lengths up to the point in question. These results are shown in **Table 2.2**.

Table 2.2 Baseline Chord Lengths and PI Stationing for Baseline

Point	Chord	Length, ft	Station
POB	--	--	100+00.00
--	*POB* to *PI*(1)	3383.96	--
PI(1)	--	--	133+83.96
--	*PI*(1) to *PI*(2)	4453.72	--
PI(2)	--	--	178+37.68
--	*PI*(2) to *PI*(3)	3289.56	--
PI(3)	--	--	211+27.24
--	*PI*(3) to *POE*	2697.57	--
POE	--	--	238+24.81

2.5 Circular Curves

Curved elements create a smooth driving transition between the baseline tangents. The most common of these transitions is the circular curve. **Figure 2.8** shows the layout of a circular curve connecting two baseline chords that join at a *PI*.

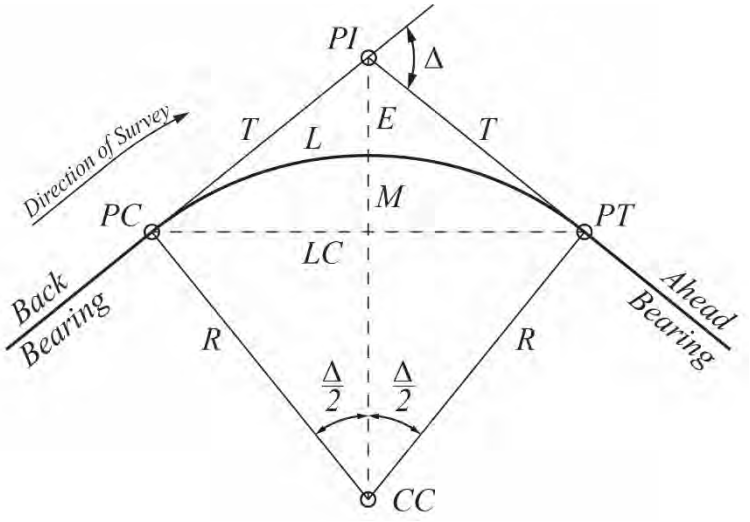

Source: PCI

Figure 2.8 Circular Curve Designations

Definitions of the quantities shown in and related to the curve in **Figure 2.8**:

PI = Point of Intersection between successive baseline chords

PC = *Point of tangent to curve - Beginning point of the circular curve, where the horizontal alignment leaves the back baseline tangent and follows the circular curve*

PT = *Point of curve to tangent - Ending point of the circular curve, where the horizontal alignment leaves the circular curve and follows the ahead baseline tangent*

CC = *Center of circular curve*

R = *Radius of circular curve*

Δ = *Deflection angle of curve—Equal to the difference in bearings of the ahead baseline tangent and back baseline tangent. The deflection angle is called a right deflection or a deflection to the right if the ahead baseline tangent is rotated clockwise from the back baseline tangent. A left deflection or deflection to the left is where the ahead baseline tangent is rotated counterclockwise from the back baseline tangent.*

D = *Degree of circular curve—Central angle subtended by an arc length of 100 ft. This is the "arc" definition of D. A 100 ft "chord" definition of D is typically used for curves on railroads.*

L = *Length of circular—Length of the portion of the circular arc between PC and PT*

LC = *Long chord length of circular curve—Length of the chord connecting PC and PT or connecting the SC and CS.*

T = *Tangent length of circular curve - Length from the PC to the PI of the circular curve which is equal to the length from the PI to the PT.*

E = *External distance from chord to circular curve - Distance from the middle of the circular curve to PI*

M = *Middle ordinate of the circular curve - Maximum perpendicular distance between the curve long chord length and the circular curve. This measurement is perpendicular to the curve long chord at its midpoint.*

Knowing the back and ahead baseline bearings and one other circular curve parameter (*L*, *R*, *T*, or the like), the other parameters of the circular curve can be computed. The deflection angle is found as the absolute value of the difference in the back and ahead baseline bearings:

$$\Delta = \left| Bearing(\ forward) - Bearing(back) \right| \tag{2.32}$$

The deflection angle in radians is found by

$$\Delta(\mathrm{rad}) = \left(\frac{\pi}{180}\right)\Delta(\mathrm{degrees}) \tag{2.33}$$

Eq. (2.34) through (2.39) define the fundamental characteristics of the circular curve:

$$L = R\Delta\ (\Delta \text{ in radians}) \quad = R\Delta\left(\frac{\pi}{180}\right)(\Delta \text{ in degrees}) \tag{2.34}$$

$$D = \frac{100}{R}\left(\frac{180}{\pi}\right)\ (\mathrm{degrees}) \tag{2.35}$$

$$LC = 2R\sin\left(\frac{\Delta}{2}\right) \tag{2.36}$$

$$T = R\tan\left(\frac{\Delta}{2}\right) \tag{2.37}$$

$$E = R\left(\left(1/\cos\left(\frac{\Delta}{2}\right)\right)-1\right) \tag{2.38}$$

$$M = R\left(1-\cos\left(\frac{\Delta}{2}\right)\right) \tag{2.39}$$

Example 2.3: Using the bearing information of Example 1, determine the circular curve parameters for a horizontal curve at *PI*(2) with a radius of 1250 ft.

The back and ahead baseline bearings in directional angle form at *PI*(2) previously computed are

$$\theta_2 = 77.0247 \text{ degrees} \tag{2.40}$$

$$\theta_3 = -7.6867 \text{ degrees} \tag{2.41}$$

The deflection angle is found by Eq. (2.32):

$$\Delta = \left|-7.6867 \text{ degrees} - 77.0247 \text{ degrees}\right| = 84.7114 \text{ degrees} \tag{2.42}$$

The clockwise rotation of the ahead baseline relative to the back baseline indicates a right deflection.

The curve parameters can be computed using Eq. (2.34) through (2.39):

$$L = (1250)(84.7114)\left(\frac{\pi}{180}\right) = 1848.12 \textit{ feet} \tag{2.43}$$

$$D = \frac{100}{12050}\left(\frac{180}{\pi}\right) = 4.58366 \text{ degrees} = 4^\circ 35' 01'' \tag{2.44}$$

$$LC = 2(1250)\sin\left(\frac{84.7114}{2}\right) = 1684.33 \text{ feet} \tag{2.45}$$

$$T = (1250)\tan\left(\frac{84.7114}{2}\right) = 1139.64 \text{ feet} \tag{2.46}$$

$$E = (1250)\left(\left(1/\cos\left(\frac{84.7114}{2}\right)\right)-1\right) = 441.53 \text{ feet} \tag{2.47}$$

$$M = (1250)\left(1-\cos\left(\frac{84.7114}{2}\right)\right) = 326.28 \text{ feet} \tag{2.48}$$

2.6 Stationing – Part 2

Introducing curved highway elements shortens the total length of the horizontal alignment compared with the sum of the baseline chords. Likewise, stationing along the horizontal alignment should consider the lengths of the circular curves and the remaining lengths of tangent runs along the baseline. The stations of the *PI*s also should be revised so that they are locatable .

Figure 2.9 shows the example alignment with circular curves added at each *PI*. The horizontal alignment now consists of tangent runs and lengths of circular curves.

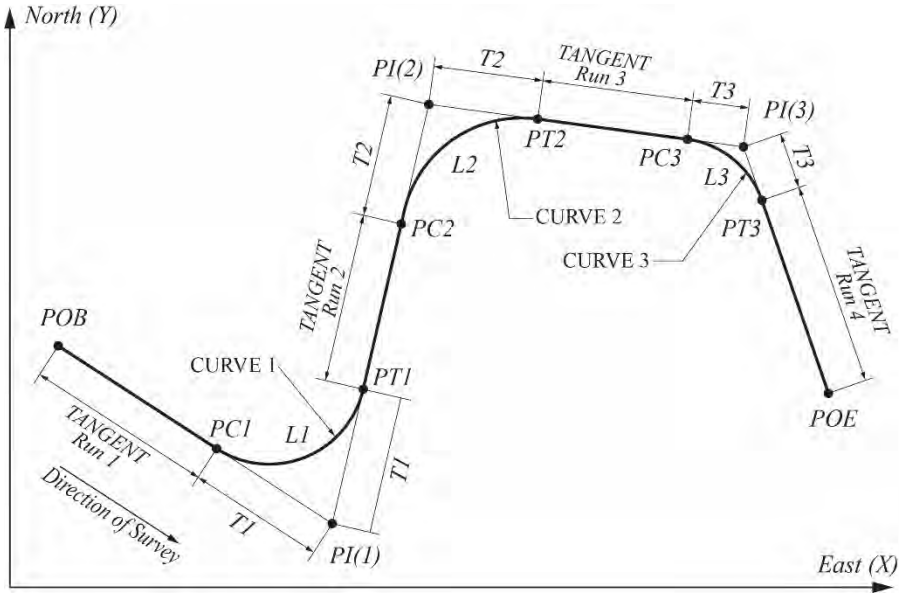

Source: PCI

Figure 2.9 Horizontal Alignment with Circular Curves Added

The first tangent run is from the *POB* to the *PC* of curve 1. The length of this tangent run is the length of the first baseline chord less the tangent length of the first curve:

$$TangentRun_1 = L_{S1} - T_1 \tag{2.49}$$

The lengths of tangent runs between intermediate *PI*s are equal to

$$TangentRun_i = L_{Si} - T_{i-1} - T_i \tag{2.50}$$

The length of the last tangent run is equal to

$$TangentRun_n = L_{Sn} - T_{n-1} \tag{2.51}$$

The station of a point on the horizontal alignment is found by the cumulative length of tangent run and curve length (or portion thereof) from the *POB* to the point. The stations of the first *PC* and *PT* are

$$Station(PC_1) = Station(POB) + TangentRun_1 \tag{2.52}$$

$$Station(PT_1) = Station(PC_1) + L_1 \tag{2.53}$$

The stations of subsequent beginnings and endings of horizontal curves are found by

$$Station(PC_i) = Station(PT_{i-1}) + TangentRun_i \tag{2.54}$$

$$Station(PT_i) = Station(PC_i) + L_i \tag{2.55}$$

Though the *PI*s are no longer on the horizontal alignment, it is still important to locate them by station. The convention adopted is that the station of a *PI* is equal to the station of the previous *PC* point plus the tangent length for that curve. In equation form, this convention is

$$Station(PI_i) = Station(PC_i) + T_i \tag{2.56}$$

The station of the *POE* is found by adding the last length of tangent run to the station of the last *PT*. If there are *n* curves, then there are *n*+1 lengths of tangent runs. The station of the *POE* is then

$$Station(POE) = Station(PT_n) + TangentRun_{n+i} \tag{2.57}$$

Example 2.4: Using the information developed in previous examples and the curve data in **Table 2.3** determine the stationing of the *PI*s and circular curve control points for the example problem of this chapter. The station of the *POB* is 100+00.0.

Table 2.3 Example Alignment Circular Curve Parameters

Curve	*R*, ft	*Δ*, rad	*L*, ft	*T*, ft
1	1000.0	1.919222 (*L*)	1919.22	1427.18
2	1250.0	1.478492 (*R*)	1848.12	1139.64
3	950.0	1.104336 (*R*)	1049.12	585.29

First compute the tangent run lengths along the alignment:

$$TangentRun_1 = 3383.96 - 1427.18 = 1956.78 \text{ feet} \quad (2.58)$$

$$TangentRun_2 = 4453.72 - 1427.18 - 1139.64 = 1886.90 \text{ feet} \quad (2.59)$$

$$TangentRun_3 = 3289.56 - 1139.64 - 585.29 = 1564.63 \text{ feet} \quad (2.60)$$

$$TangentRun_4 = 2697.57 - 585.29 = 2112.28 \text{ feet} \quad (2.61)$$

Determine the stations at the beginning and end of the circular curves:

$$Station(PC_1) = 100 + 00.00 + 1956.78 \text{ feet} = 119 + 56.78 \quad (2.62)$$

$$Station(PT_1) = 119 + 56.78 + 1919.22 \text{ feet} = 138 + 76.00 \quad (2.63)$$

$$Station(PC_2) = 138 + 76.00 + 1886.90 \text{ feet} = 157 + 62.90 \quad (2.64)$$

$$Station(PT_2) = 157 + 62.90 + 1848.12 \text{ feet} = 176 + 11.02 \quad (2.65)$$

$$Station(PC_3) = 176 + 11.02 + 1564.63 \text{ feet} = 191 + 75.65 \quad (2.66)$$

$$Station(PT_3) = 191 + 75.65 + 1049.12 \text{ feet} = 202 + 24.77 \quad (2.67)$$

Finally, determine the stations of the *PI*s and *POE*:

$$Station(POB) = 100 + 00.00 \quad (2.68)$$

$$Station(PI_1) = 100 + 00.00 + 1956.78 \text{ feet} + 1427.18 \text{ feet} = 133 + 83.96 \quad (2.69)$$

$$Station(PI_2) = 157 + 62.90 \text{ feet} + 1139.64 \text{ feet} = 169 + 2.54 \quad (2.70)$$

$$Station(PI_3) = 191 + 75.65 \text{ feet} + 585.29 \text{ feet} = 197 + 60.94 \quad (2.71)$$

$$Station(POE) = 202 + 24.77 \text{ feet} + 2112.28 \text{ feet} = 223 + 37.05 \quad (2.72)$$

The resulting stationing at the *PI*s and curve points is shown in **Figure 2.10**.

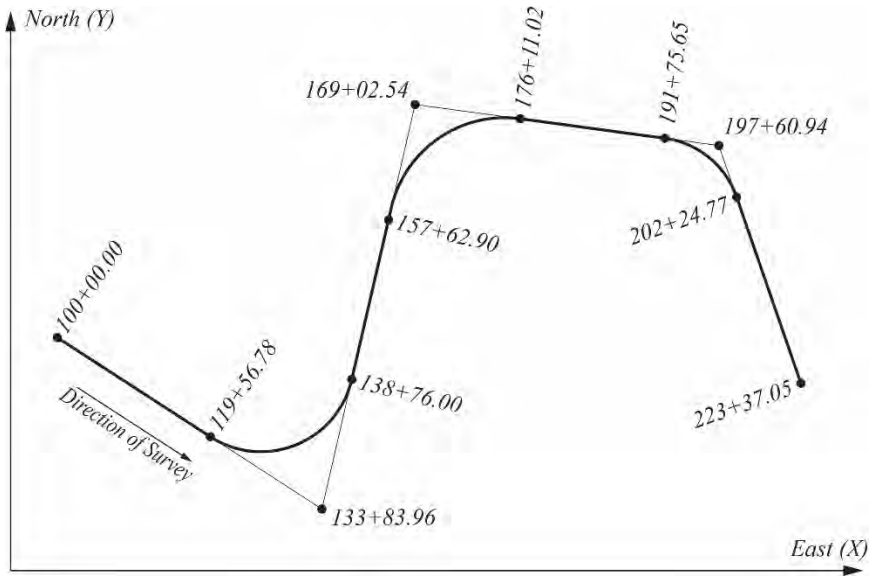

Source: PCI

Figure 2.10 Stationing along the Example Horizontal Alignment

2.7 Transition Spirals

Circular curves allow for a smooth transition between the baseline chords of a horizontal alignment. At the transition points *PC* and *PT*, however, a circular curve introduces an instantaneous change in radius (infinite radius to the curve radius and vice versa). This change in radius introduces a sudden horizontal centrifugal force tending to move a vehicle away from the center of the circular curve. When the centrifugal force is small, its influence can be mitigated by a punctual change in the cross slope of the roadway and driver steering within the travel lane. In severe instances, transitioning curve elements, or *transition spirals*, can be added between tangents and circular curves.

The transition spiral is a curve that transitions between tangent runs and circular curves, or between two circular curves, without abrupt changes in radii. The transition spiral is called a simple spiral if it connects a straight line and a circular curve, with a radius that varies from infinity to the radius of the circular curve. A compound spiral connects two circular curves, with radii varying from the radius of the first curve to the radius of the second curve. **Figure 2.11** shows a *PI* of a horizontal alignment with back and ahead tangents composed of a circular curve with equal-length entry/exit transition spirals. Transitional spiral curves are very important for rail alignments and are typically used for mainline tracks.

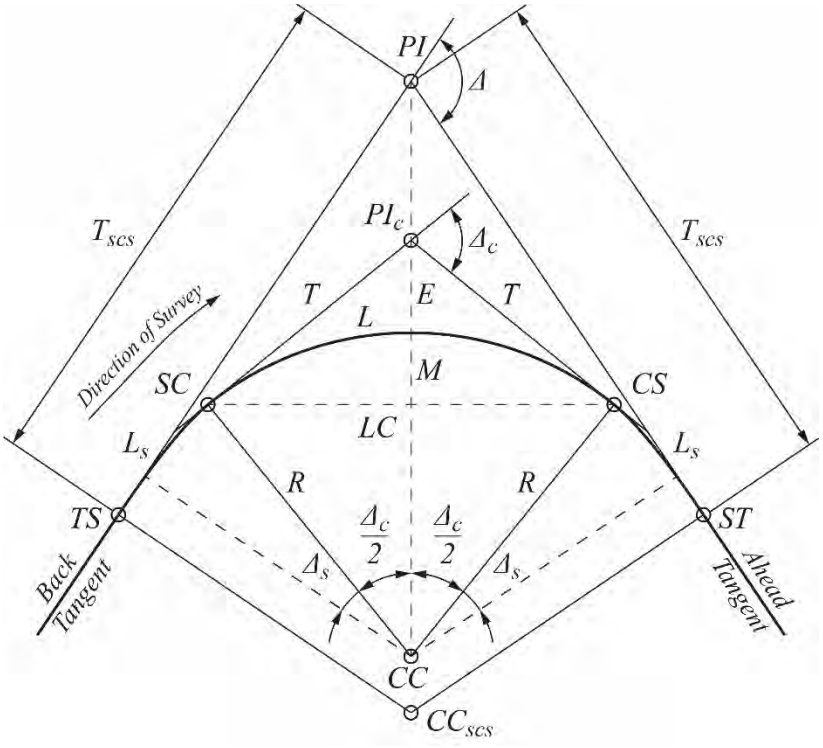

Source: PCI

Figure 2.11 Circular Curve with Equal Length Transition Spirals

Definitions of the quantities shown and related to the curve in **Figure 2.11** that are in addition to the quantities shown in **Figure 2.8** follow.

PI_c = *Point of intersection of the circular curve only*

TS = *Point of tangent to spiral—Beginning point of the spiral, where the horizontal alignment leaves the back baseline tangent*

SC = *Point of spiral to curve—The terminal point where the spiral reaches the radius of the circular curve and the circular curve begins*

CS = *Point of curve to spiral—End of the circular curve and beginning of the exiting transition spiral*

ST = *Point of spiral to tangent—Ending point of the spiral, where the radius is infinite and the horizontal alignment leaves the spiral and follow the ahead baseline tangent*

CC_{scs}= *Center of the curve containing the entry spiral, circular curve, and exit spiral*

Δ_c = *Deflection angle of the circular curve when spirals are used*

Δ_s = *Deflection angles of the spirals (equal in* **Figure 2.11***)*

D_s = *Degree of the spiral*

L_s = *Length of spiral*

T_{scs} = *Tangent length of curve containing the entry spiral, circular curve, and exit spiral*

The spiral used in highway applications is the clothoid, or Euler spiral, in which the instantaneous radius at any point along the spiral is inversely proportion to the length along the spiral to the point.

Figure 2.12 shows a picture of a simple spiral of length L_s, beginning at *TS* and ending at *SC*, where the instantaneous radius is *R*. The deflection angle of the spiral in radians is given by

$$\Delta_s = \frac{L_s}{2R} \quad \text{(rad)} \tag{2.73}$$

Point *A* is located at a length *l* along the spiral. The angle subtended by the portion of spiral with length *l* can be found by

$$\delta = \left(\frac{l}{L_s}\right)^2 \Delta_s \quad \text{(rad)} \tag{2.74}$$

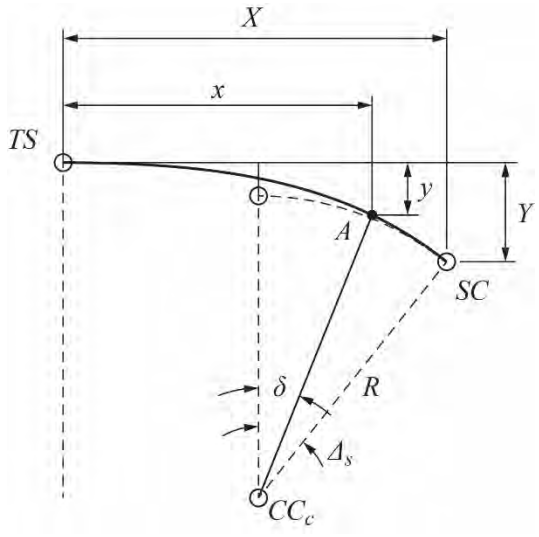

Source: PCI

Figure 2.12 Layout of a Simple Spiral

The coordinates of points along the spiral relative to the *TS* can be found by the following equations that represent in series form the integration of trigonometric sines and cosines:

$$x = l\left[1 - \frac{\delta^2}{5(2!)} + \frac{\delta^4}{9(4!)} + \frac{\delta^6}{13(6!)} + ...\right] \tag{2.75}$$

$$y = l\left[\frac{\delta}{3} - \frac{\delta^3}{7(3!)} + \frac{\delta^5}{11(5!)} - \frac{\delta^7}{15(7!)} + ...\right] \tag{2.76}$$

where δ = angle subtended by the portion of the spiral with length *l*, rad

l = the length along the spiral from *TS* to the point being located

The coordinates of the *SC* are found by substituting L_s and Δ_s into Eq. (2.75) and (2.76):

$$X = L_s\left[1 - \frac{\Delta_s^2}{10} + \frac{\Delta_s^4}{216} + \frac{\Delta_s^6}{9360} + ...\right] \tag{2.77}$$

$$Y = L_s\left[\frac{\Delta_s}{3} - \frac{\Delta_s^3}{42} + \frac{\Delta_s^5}{1320} - \frac{\Delta_s^7}{75{,}600} + ...\right] \tag{2.78}$$

Sufficient accuracy for most highway geometry calculations is found by using the first three terms of Eq. (2.75) through (2.78).

Figure 2.13 shows another view of the simple spiral of **Figure 2.12**. In this figure, a point of intersection PI_s has been located at the intersection of the back tangent and ahead tangents of the spiral. The dimension from the *TS* to the *PI* is called the long tangent T_{long}. The dimension from the PI_s to the *SC* is called the short tangent T_{short}. The long and short tangent lengths are computed using Eq. (2.79) and 2.80.

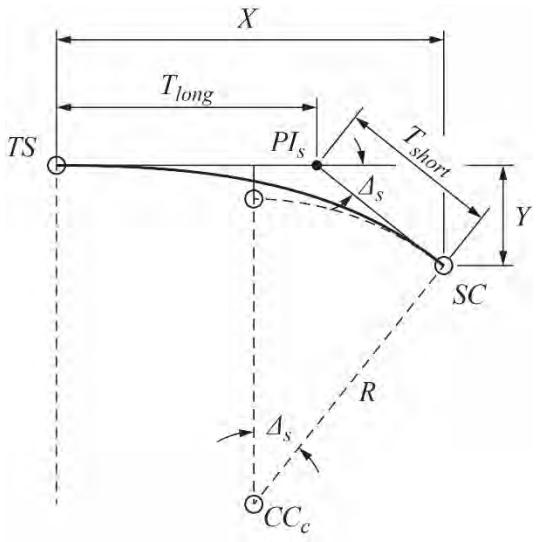

Source: PCI

Figure 2.13 Spiral PI and Tangent Lengths

$$T_{long} = X - \frac{Y}{\tan \Delta_s} \tag{2.79}$$

$$T_{short} = \frac{Y}{\sin \Delta_s} \tag{2.80}$$

The coordinates and characteristic dimensions of the simple spiral have been developed in local coordinate system with origin at the *TS*. These coordinates can be transformed to the global system of a project for incorporation into a project specific alignment.

Chapter 3 – Roadway Vertical Geometry

3.1 Introduction

Vertical profiles are used to set elevations along roadway projects. Vertical profiles are made up of a series of constant grade lines connected at vertical points of intersection (*VPI*s). The entire contiguous series of line segments depicts the *profile grade line* (*PGL*). **Figure 3.1** shows a 2D representation of a *PGL* that will serve as an example vertical alignment in this section. The *PGL* is given in a coordinate system where the x axis is stationing along an associated baseline and the y axis is elevation. As with horizontal alignments, *PGL*s are direction dependent. The *PGL* begins with the vertical point of beginning *VPOB*, passes through the successive *VPI*s, and ends with the vertical point of ending *VPOE*.

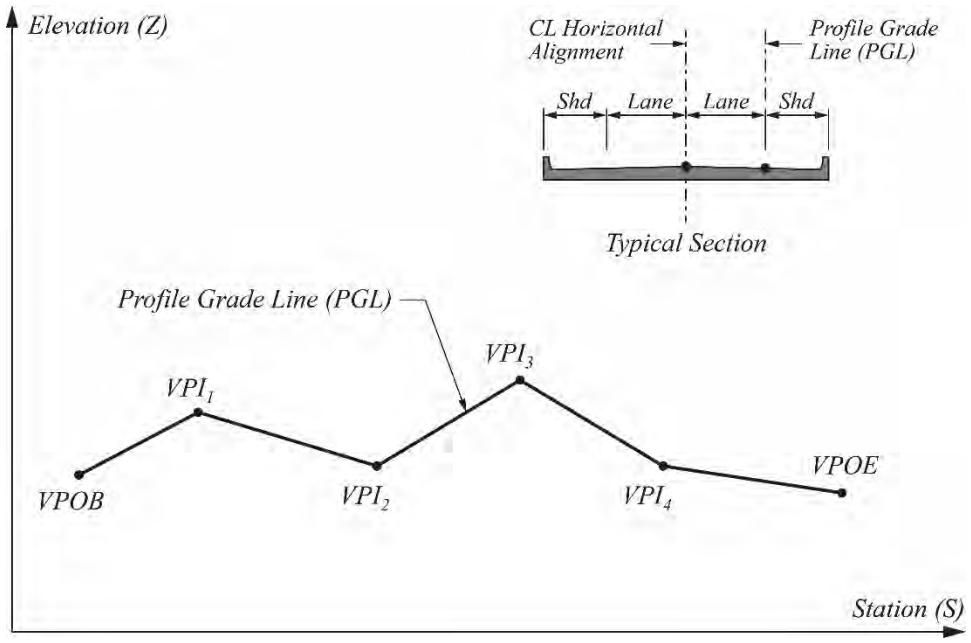

Source: PCI

Figure 3.1 Typical Vertical Profile

The PGL shown in **Figure 3.1** follows a horizontal alignment different from the centerline horizontal alignment. The transverse location of the *PGL* can vary greatly between transportation agencies or the type of roadway being designed. Typical locations for *PGL*s include edge of pavement, lane lines, shoulder lines, centerlines, and locations of cross-section crown break. In some instances, such as divided highways, one vertical profile is used to control the elevations of multiple roadways. The *PGL* may be located with a roadway in this case but may follow an independent horizontal alignment.

3.2 Vertical Grades

Figure 3.2 shows a chord of a *PGL* between two *VPI*s. The first *VPI* of the chord shown in **Figure 3.2** is VPI_i, which has the coordinates (S_i, Z_i). The second *VPI* of the line segments is VPI_{i+1}, with coordinates (S_{i+1}, Z_{i+1}).

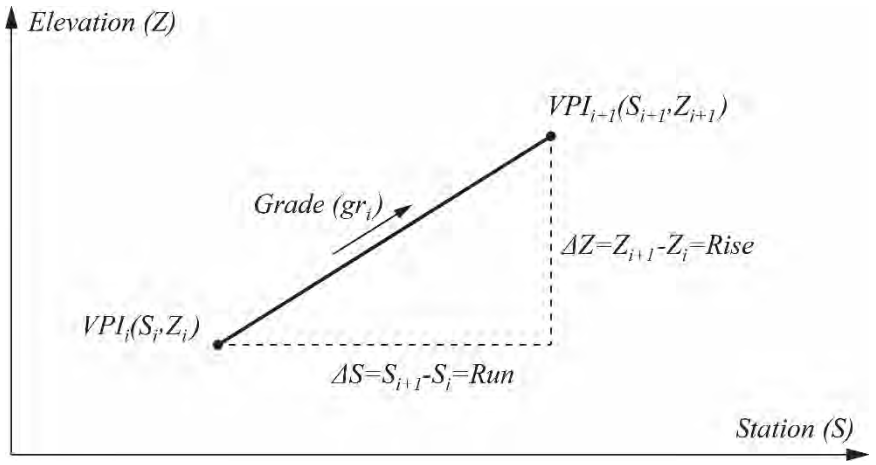

Source: PCI

Figure 3.2 Vertical Grade

The change in station between the two *VPI*s is called to the *run* of the line segment. The change in elevation between the two points is called the *rise*. The run and rise in equation form are

$$\text{Run} = \Delta S = S_{i+1} - S_i \tag{3.1}$$

$$\text{Rise} = \Delta Z = Z_{i+1} - Z_i \tag{3.2}$$

The vertical grade of this line segment of the *PGL* is the inclination of the roadway surface (the rise divided by the run). Grades are expressed in both decimal and percentage forms. When expressed as a percentage, the grade is

$$gr_i = \left(\frac{\text{Rise}}{\text{Run}}\right)100 \tag{3.3}$$

Positive grades increase in elevation with station and negative grades decrease with station.

Example 3.1: Using the coordinate information for the example vertical alignment shown below in **Figure 3.3**, determine the grades of the *PGL*.

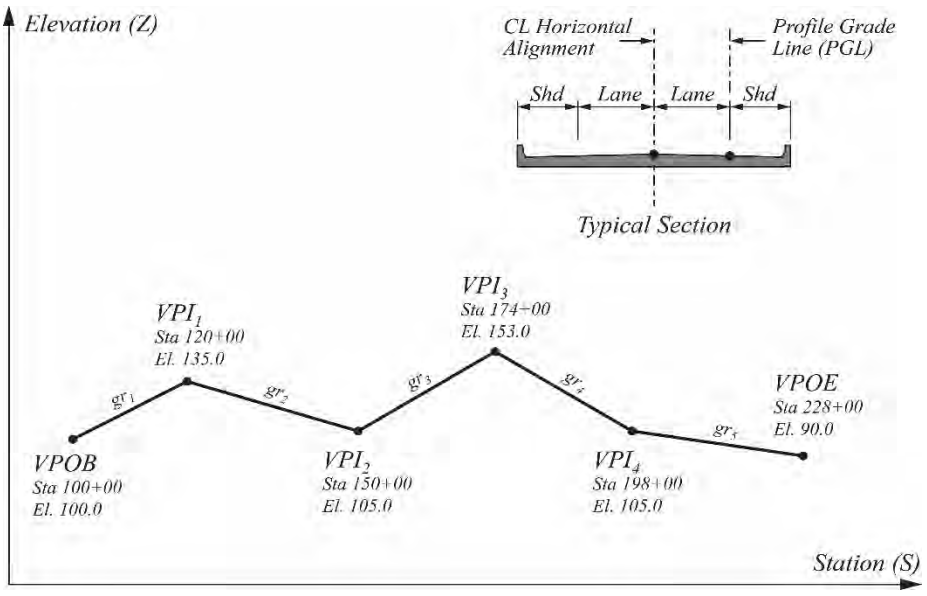

Source: PCI

Figure 3.3 Example Vertical Profile

The grades of the *PGL* line segments are computed using the coordinate information shown previously and Eq. (3.3).

$$gr_1 = \left(\frac{(135.0-100.0)}{12{,}000.0-10{,}000.0}\right)100 = +1.75\% \tag{3.4}$$

$$gr_2 = \left(\frac{(105.0-135.0)}{15{,}000.0-12{,}000.0}\right)100 = -1.0\% \tag{3.5}$$

$$gr_3 = \left(\frac{(153.0-105.0)}{17{,}400.0-15{,}000.0}\right)100 = +2.0\% \tag{3.6}$$

$$gr_4 = \left(\frac{(105.0-153.0)}{19{,}800.0-17{,}400.0}\right)100 = -2.0\% \tag{3.7}$$

$$gr_5 = \left(\frac{(90.0-105.0)}{22{,}800.0-19{,}800.0}\right)100 = -0.5\% \tag{3.8}$$

3.3 Vertical Curves

Vertical curves are used to provide a smooth transition between line segments of a vertical profile. These transitions are typically accomplished with parabolic curves. Parabolas are used because rate of change of grade is constant with distance. **Figure 3.4** shows the vertical profile studied in **Figure 3.1** with the addition of parabolic vertical curves.

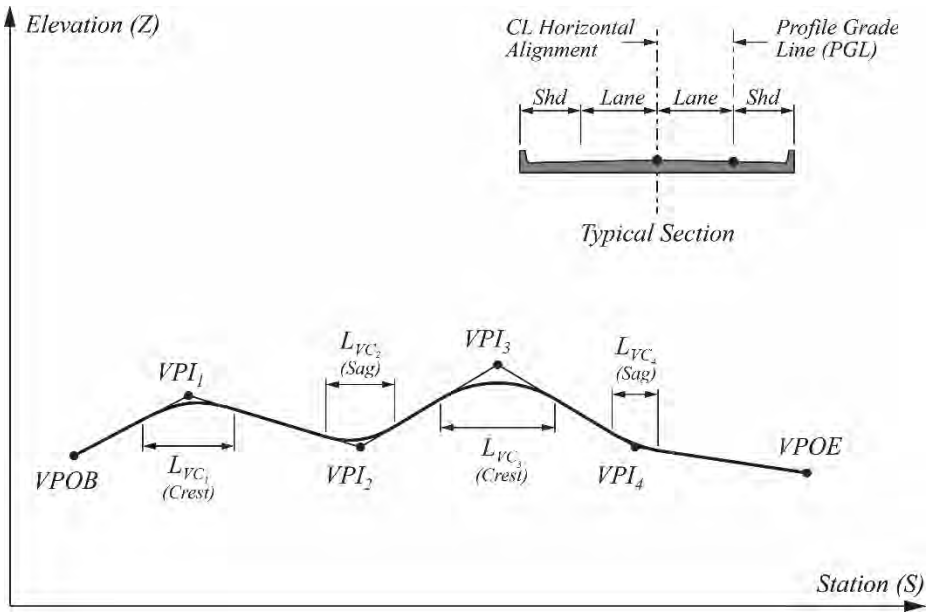

Source: PCI

Figure 3.4 Vertical Profile with Vertical Curves

Figure 3.5 shows details of a typical parabolic curve used in vertical profiles. The curve begins at the *VPC*, the point of transition from the vertical tangent alignment to the vertical curve. The vertical curve ends at the *VPT*, the point of transition from the vertical curve to the vertical tangent alignment of constant grade. As shown in **Figure 3.5**, the stationing difference from the *VPC* to the *VPI* is equal to half of the length of the vertical curve. This makes the stationing difference from the *VPI* to the *VPT* also equal to half of the curve length. This type of vertical parabolic curve is called a symmetric vertical curve and is the most common form of parabolic curve used.

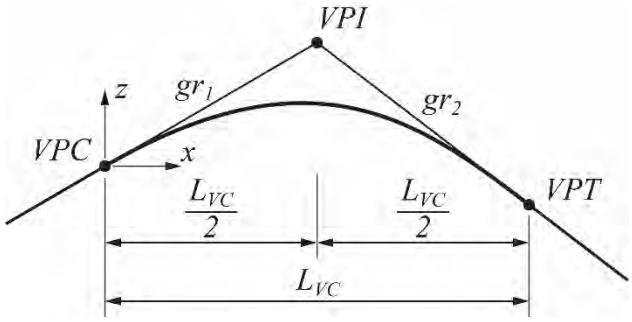

Source: PCI

Figure 3.5 Symmetric Parabolic Vertical Curves

The terms shown in **Figure 3.4** and **Figure 3.5** and the equations that follow are

gr_1 = Grade of the vertical profile at the beginning of the vertical curve

gr_2 = Grade of the vertical profile at the end of the vertical curve

L_{VC} = Length of vertical curve

S = Local stationing distance from the *VPC*

VPC = Vertical point of curvature

VPI = Vertical point of intersection

VPT = Vertical point of tangency

Z(*S*) = Elevation from the *VPC*

Z_{VPC} = Elevation at a *VPC*

Z_{VPI} = Elevation at a *VPI*

Z_{VPT} = Elevation at a *VPT*

Exit and entry grades of the vertical curve are computed in accordance with Section 3.2. Respecting the sign convention established and using decimal expressions for the grade, the elevations of the *VPC* and *VPT* are found by

$$Z_{VPC} = Z_{VPI} - gr_1\left(\frac{L_{VC}}{2}\right) \tag{3.9}$$

$$Z_{VPT} = Z_{VPI} + gr_2\left(\frac{L_{VC}}{2}\right) \tag{3.10}$$

Derivation of the equation for the symmetric parabolic vertical curve begins with the general quadratic expression:

$$Z = a_1S^2 + a_2S + a_3 \tag{3.11}$$

The *Z* term in Eq. (3.11) is elevation and the *S* term is stationing measured from the *VPC*. The slope at any location along the vertical curve is found as the first derivative of Eq. (3.11):

$$\frac{dZ}{dS} = 2AS + B \tag{3.12}$$

The slope at the beginning of the vertical curve is equal to g_1. The slope at the end of the vertical curve is equal to g_2. Combining Eq. (3.11) and (3.12) with the boundary conditions produces the general equation for elevation at a station *S* along a parabolic vertical curve:

$$Z(S) = \left(\frac{gr_2 - gr_1}{2L_{VC}}\right)S^2 + gr_1S + E_{VPC} \tag{3.13}$$

The grade along the vertical curve is

$$gr(S) = \left(\frac{gr_2 - gr_1}{L_{VC}}\right)S + gr_1 \tag{3.14}$$

Example 3.2: Using the information from **Figure 3.3** and **Figure 3.6**, and previously computed grades, find the stations and elevations of the *VPC* and *VPT* for the four vertical curves in the *PGL*.

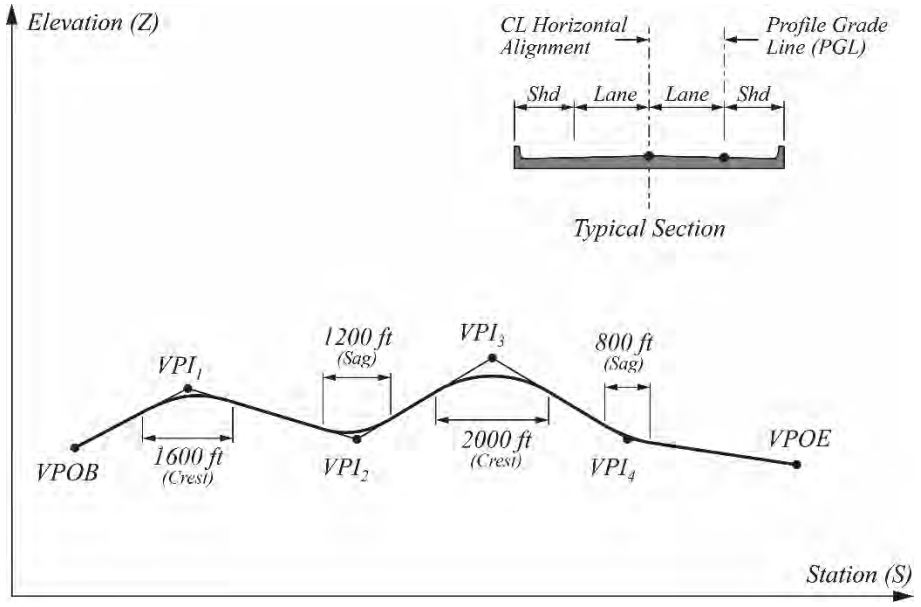

Source: PCI

Figure 3.6 Example Vertical Profile

Stations of the *VPC*s are found by subtracting half of the length of the symmetric vertical curve from the station of the corresponding *VPI*. The stations of the *VPT*s are found by adding half of the curve length to the *VPI* stations. Elevations of the *VPC*s and *VPT*s are found by either adding or subtracting from the *VPI* elevation, the local grade multiplied by half of the length of the corresponding vertical curve. The results are as follows:

Table 3.1 VPC and VPT Stations and Elevations

Curve	*VPC* station	*VPT* station	*VPC* elevation, ft	*VPT* elevation, ft
1	112+00	128+00	121.0	127.0
2	144+00	156+00	111.0	117.0
3	164+00	184+00	133.0	133.0
4	194+00	202+00	98.0	88.0

Example 3.3: Using the information from the previous examples, find the elevations and grades at tenth points along the length of the first vertical curve in the *PGL* shown in **Figure 3.6**.

Eq. (3.13) and (3.14) are used for this solution. Grades were previously computed in Example 3.1. The length of the curve is 1600 ft. The elevation and station of the *VPC* of this curve were computed in Example 3.2. Substituting known values into Eq. (3.13) and (3.14) yields

$$Z(S) = \left(\frac{-0.01 - 0.0175}{2(1600)}\right)S^2 + 0.0175S + 121.0 \tag{3.15}$$

$$gr(S) = \left(\frac{-0.01 - 0.0175}{1600}\right)S + 0.0175 \tag{3.16}$$

Applying Eq. (3.15) and (3.16) at the first 1/10 point of the 1600 ft vertical curve results in the following:

$$Z(160) = \left(\frac{-0.01 - 0.0175}{2(1600)}\right)(160)^2 + 0.0175(160) + 121.0 = 123.58 \text{ ft} \tag{3.17}$$

$$gr(160) = \left(\frac{-0.01 - 0.0175}{1600}\right)(160) + 0.0175 = 0.01475 \tag{3.18}$$

Computed in similar fashion, the results for all tenth points are as follows:

Table 3.2 Vertical Curve 1 Elevations and Grades

Point	*S*	Elevation, ft	Grade
$0.0L_{vc}$	0.0	121.00	0.01750
$0.1L_{vc}$	160	123.58	0.01475
$0.2L_{vc}$	320	125.72	0.01200
$0.3L_{vc}$	480	127.42	0.00925
$0.4L_{vc}$	640	128.68	0.00650
$0.5L_{vc}$	800	129.50	0.00375
$0.6L_{vc}$	960	129.88	0.00100
$0.7L_{vc}$	1120	129.82	-0.00175
$0.8L_{vc}$	1280	129.32	-0.00450
$0.9L_{vc}$	1440	128.38	-0.00725
$1.0L_{vc}$	1600	127.00	-0.01000

3.4 Vertical Curve High Points and Low Points

Two types of vertical curves are identified in **Figure 3.4** and **Figure 3.6**. Crest curves occur where grades reduce with increasing station. Sag curves occur where grades increase with increasing station. It may be necessary to compute the elevation of the high point on a crest vertical curve or a low point on a sag vertical curve. **Figure 3.7** depicts these points for the two types of curves.

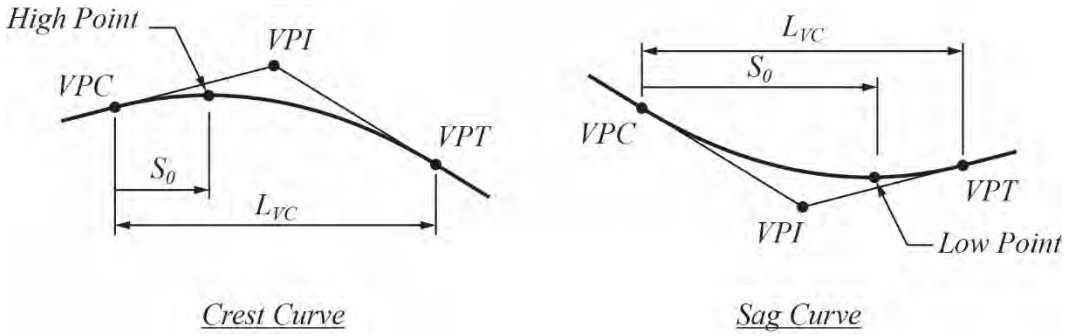

Source: PCI

Figure 3.7 High Point and Low Point for Crest and Sag Vertical Curves, respectively

The high point or low point of the curves shown in **Figure 3.7** occurs where the grade of the vertical curve equals zero (distance S_0). Setting Eq. (3.14) equal to zero and rearranging to solve for *s*:

$$S_0 = -\left(\frac{gr_1}{gr_2 - gr_1}\right)L_{VC} \tag{3.19}$$

$$Z(S_0) = Z_{VPC} - \left(\frac{gr_1^2}{gr_2 - gr_1}\right)\left(\frac{L_{VC}}{2}\right) \tag{3.20}$$

Eq. (3.20) is only valid when the high or low point lies with the limits of the vertical curve. This will be the case only when there is a change of sign in the grades connected by the vertical curve. When the sign remains the same for the two grades, the high and low points for these curves occur at either the *VPC* or *VPT*.

Example 3.4: Find the high point station and elevation of the vertical curve in Example 3.3.

Using Eq. (3.19) and (3.20):

$$S_0 = -\left(\frac{0.0175}{-0.01-0.0175}\right)(1600) = 1018.1818 \text{ ft} \tag{3.21}$$

$$Z(1600) = \left(\frac{0.0175}{-0.01-0.0175}\right)(1018.1818)^2 + 0.0175(1018.1818) + 121.0 = 129.9091 \text{ ft} \tag{3.22}$$

The station at which the high point elevation is found is equal to the station of the V_{PC} plus the distance S_0.

$$S = S_{VPC} + S_0 = (112+00) + 1018.1818 = 122 + 18.1818 \tag{3.23}$$

Chapter 4 – Roadway Superelevation

4.1 Introduction

A vehicle traveling along a curved alignment experiences centrifugal forces acting away from the center of curvature. The centrifugal force is a function of the radius of curvature, vehicle weight, and vehicle velocity. Centrifugal forces on a flat roadway are resisted by friction forces acting between the tires of the vehicle and the roadway. The frictional forces are equal to the tire normal forces multiplied by a friction coefficient between the tires and roadway. **Figure 4.1** shows the forces acting on a vehicle following a curved alignment on a flat roadway. The eccentricity of the centrifugal force to the roadway creates different normal forces on the wheels and, as a result, different frictional forces. Excessive speed can lead to radial forces greater than the frictional resistance offered between the roadway and the tires, leading to the lateral sliding of the vehicle across the roadway surface.

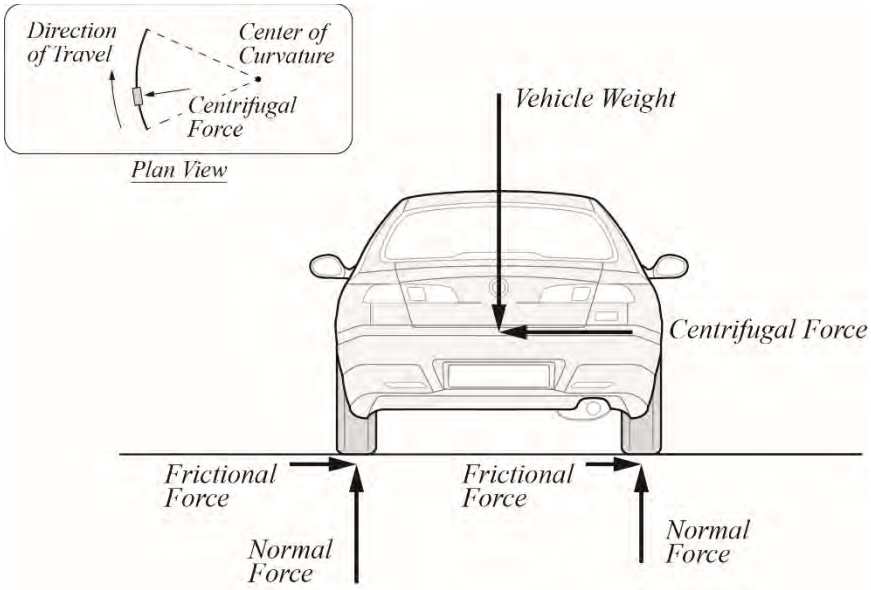

Source: PCI

Figure 4.1 Forces Acting on a Vehicle Following a Curved Alignment on a Flat Roadway

The effects of the centrifugal force on rider comfort and safety can be overcome by introducing a sloping roadway as shown in **Figure 4.2**. The horizontal centrifugal force is now resisted by the horizontal components of the frictional force and the vehicle normal forces. The sloping of the roadway as shown in **Figure 4.2** is referred to as *superelevating* the roadway. An elevation change of a point on the cross section due to sloping the roadway is the *superelevation* of the point (an elevation that is *superimposed* onto the *profile grade line* [*PGL*] elevation). The amount of the roadway slope is called the roadway *cross slope*. The value of a roadway cross slope is most commonly expressed as a percentage of the transverse rise over a unit horizontal run.

Sign conventions for roadway superelevation and cross slope vary among transportation agencies. For this manual, a positive superelevation moves the right edge of pavement down from horizontal when looking in the direction of increasing station. **Figure 4.3** shows the terms and sign convention for superelevation in this manual.

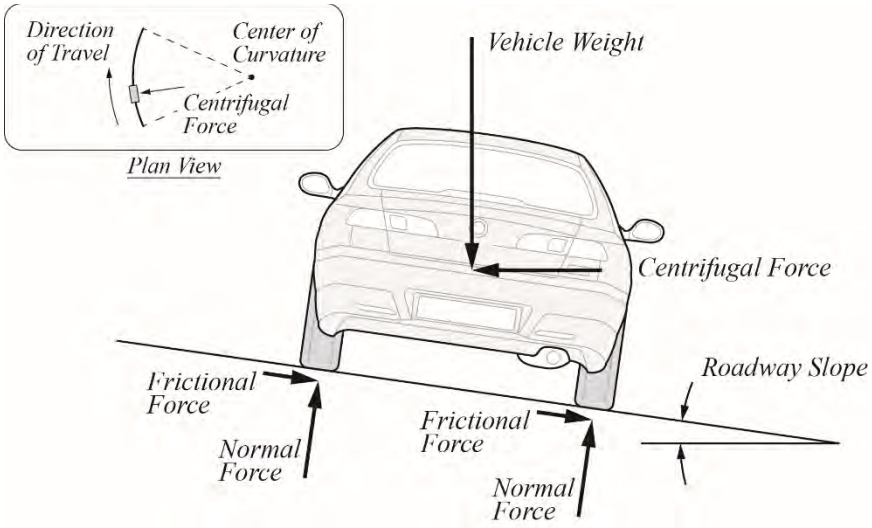

Source: PCI

Figure 4.2 Forces Acting on A Vehicle Following a Curved Alignment on a Superelevated Roadway Cross Slope

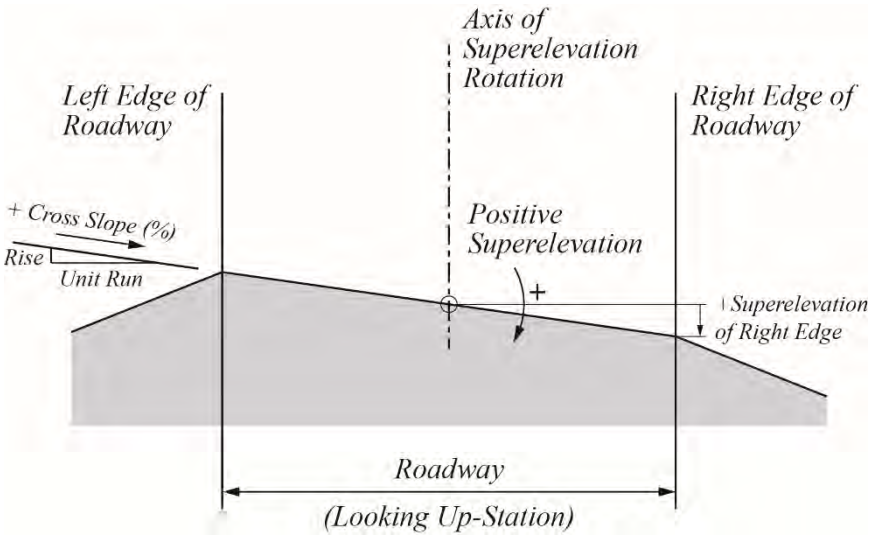

Source: PCI

Figure 4.3 Superelevation and Sign Convention

The degree of roadway curvature and the vehicle design speed are primary factors affecting the rate of a roadway's superelevation. Other factors, however, can also affect the need for superelevation:

- Climate conditions—frequency of water, ice, and snow
- Terrain conditions—flat, rolling, or mountainous
- Roadway location—rural or urban
- Nature of traffic—percentage of trucks, frequency of slow-moving vehicles, etc.

Consult the governing transportation agency for applicable superelevation information.

4.2 Normal Crown

The previous section discussed the use of a superelevated roadway to maintain rider comfort and safety for roadways on curved alignments. Roadways on tangent alignments also require some

minimum value of cross slope to allow water to drain from the travel lanes. Typical values for minimum lane cross slope are 2 percent or ¼ inch per foot. Shoulders of roadways on tangent alignments may have a greater cross slope to further facilitate drainage. The combined shape of the sloping lane and shoulder lines on tangent roadway alignments is called the *normal crown* of the roadway. **Figure 4.4** shows the cross section of a two-way roadway on a tangent alignment. **Figure 4.5** shows a corresponding typical layout of the normal crown for the two-lane roadway.

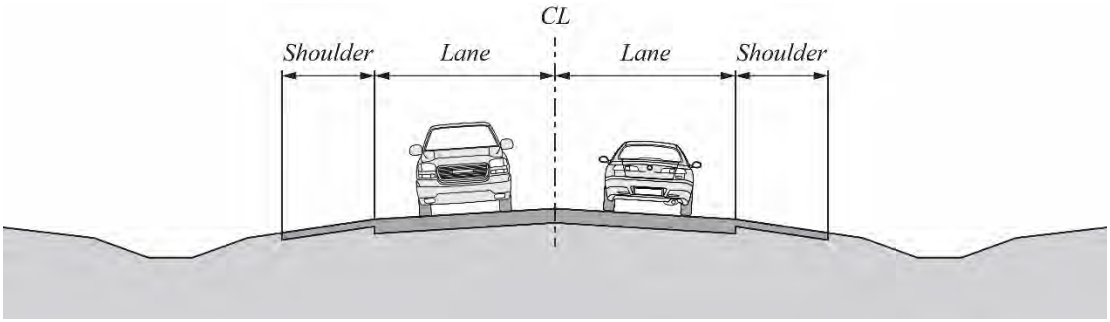

Source: PCI

Figure 4.4 Two-Lane Roadway Cross Section

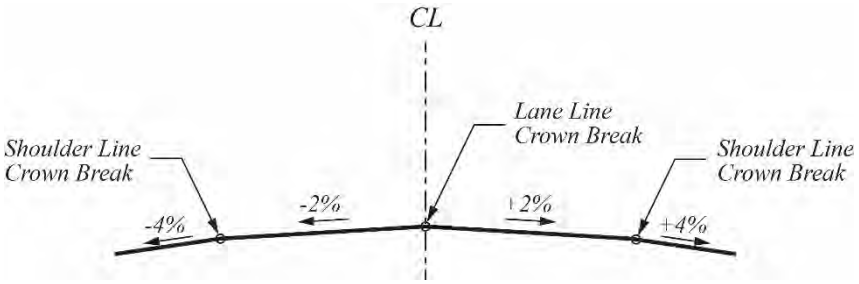

Source: PCI

Figure 4.5 Cross Section for a Two-Lane Roadway on a Tangent Alignment

Elevations of points in a cross section on a tangent alignment, relative to the *PGL*, are found by summing increments of the horizontal transverse offset to the point multiplied by the cross slopes of the normal crown. Absolute elevations are found by adding these relative elevations to the *PGL* elevation at the station of the cross section.

Cross slopes of the various elements of the normal crown differ with the type of roadway and the number of travel lanes. Two common cross sections and normal crown diagrams are shown in **Figure 4.6** and **Figure 4.7**. **Figure 4.6** shows the normal crown for a two-lane, one-direction ramp common in urban interchanges. In this case, the normal crown has a constant cross slope of 2 percent across the entire width of the roadway. **Figure 4.7** shows a three-lane, one-direction roadway of a divided highway, typical of an interstate highway.

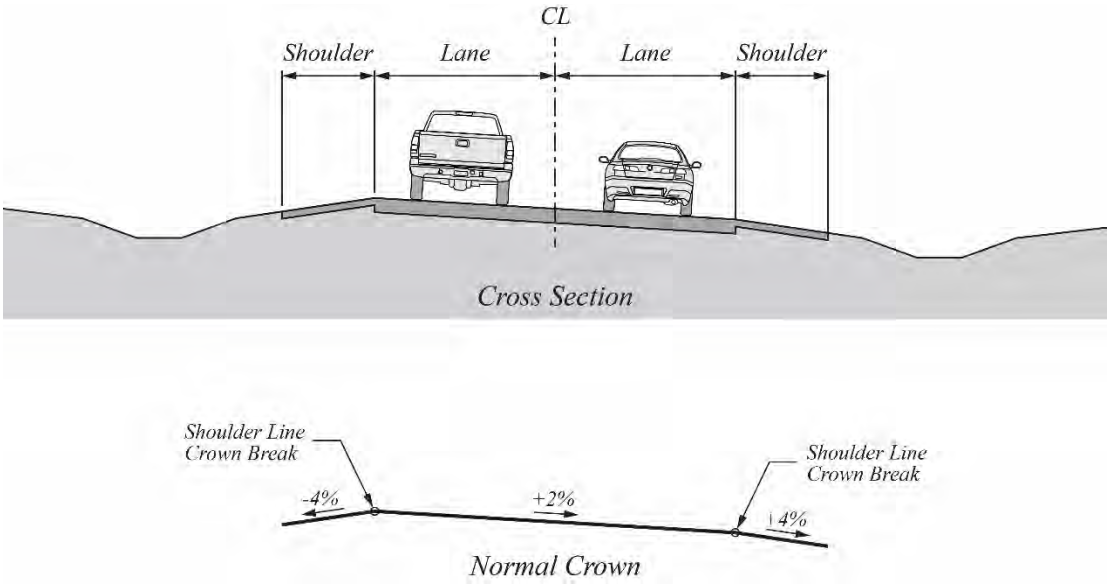

Source: PCI

Figure 4.6 Two-Lane One-Direction Ramp Cross Section

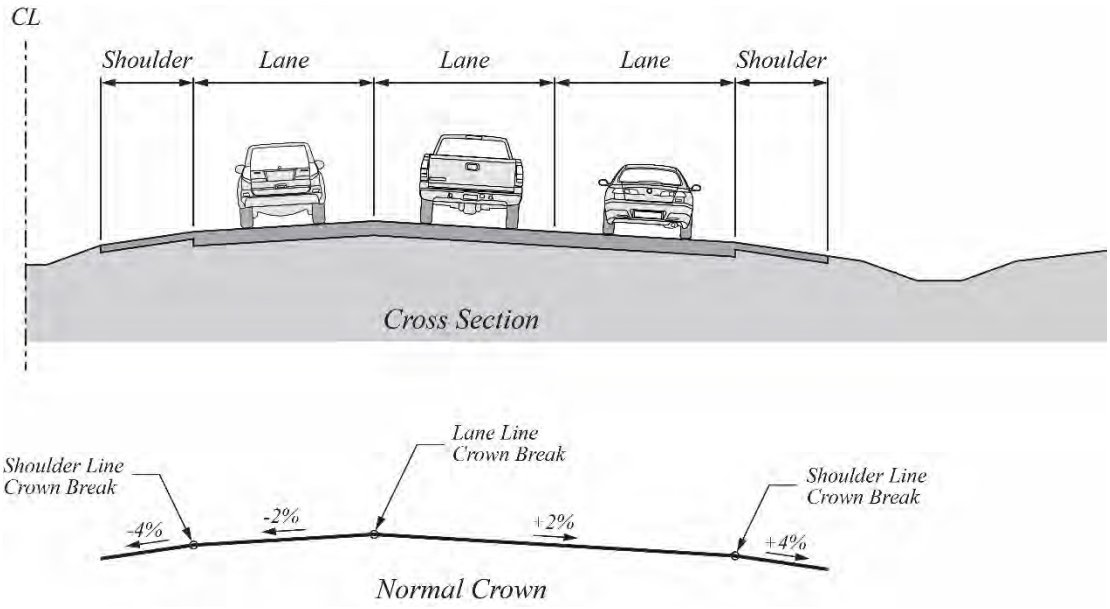

Source: PCI

Figure 4.7 Three-Lane, One-Direction Interstate Cross Section

4.3 Pivot Point

The application of superelevation to the normal crown of a cross section involves the selection of a point about which to rotate the roadway surface, or the *pivot point*. Common locations of pivot points are lane lines, shoulder lines, or gutter lines. **Figure 4.8** shows an example cross section looking up-station of a two-lane, one-directional bridge at normal crown. The normal crown of this example comprises a constant 2 percent cross slope across the entire width of the bridge. The horizontal alignment, found along the centerline of the bridge, contains a sharp curve to the right. Vertical elevations are specified along the profile grade line, which is located at the right side of the right travel lane. **Figure 4.9, Figure 4.10,** and **Figure 4.11** compare the bridge cross section at a maximum

superelevation rate of 8 percent with the cross section at normal crown (**Figure 4.8**), for three different transverse locations of the pivot point locations.

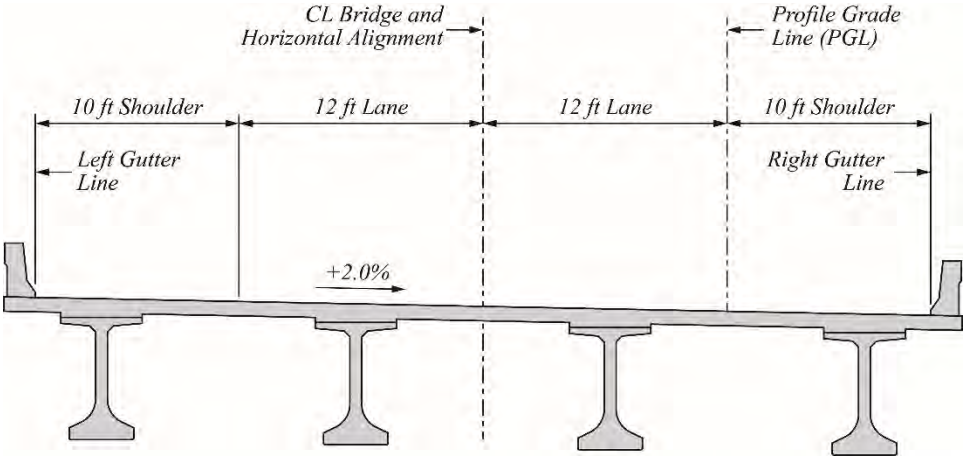

Source: PCI

Figure 4.8 Two-Lane, One-Direction Ramp Bridge Structure at Normal Crown

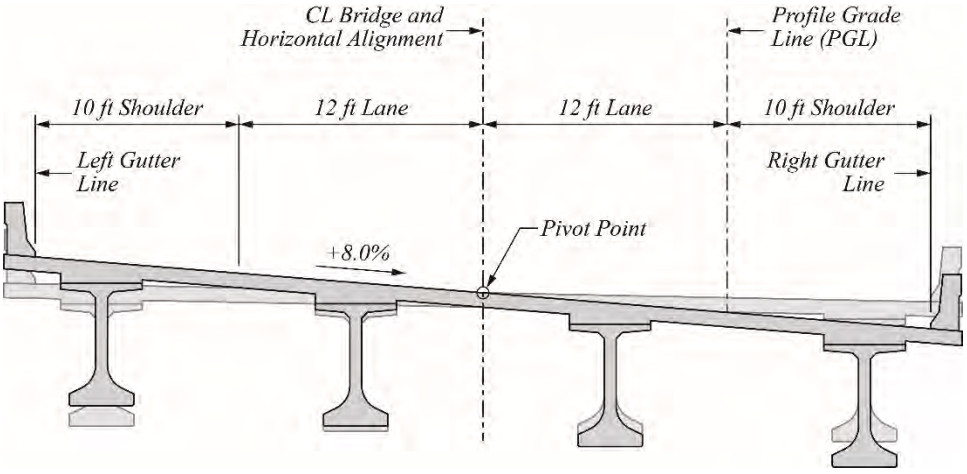

Source: PCI

Figure 4.9 Maximum Superelevation with Pivot Point at Centerline Bridge

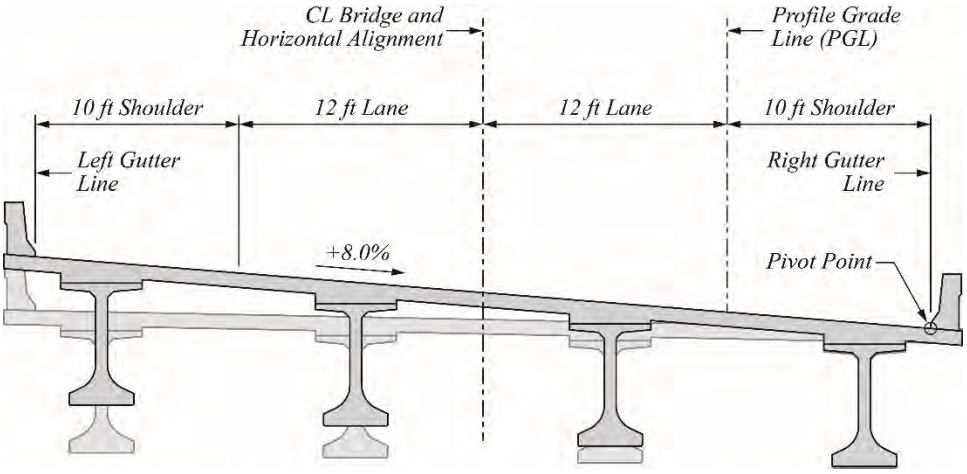

Source: PCI

Figure 4.10 Maximum Superelevation with Pivot Point at the Right Gutter Line

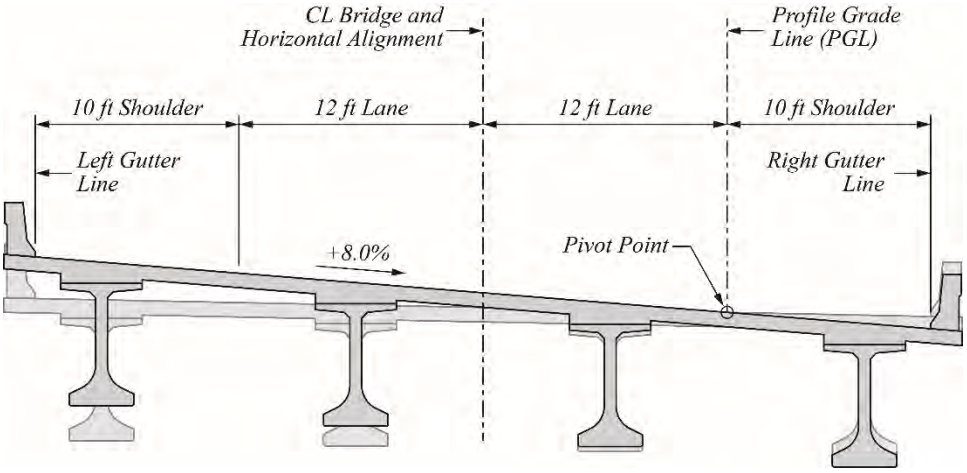

Source: PCI

Figure 4.11 Maximum Superelevation with Pivot Point at the Profile Grade Line

The transverse location of the pivot point is chosen based on several considerations:

- Additional localized vertical grade: The rise and fall of the bridge deck with superelevation, at points offset from the pivot point, either adds or subtracts from the grade of the bridge as given along the *PGL*. This additional grade can lead to an awkward, or even unsafe, driving experience. For a given transition length, the center pivot location shown in **Figure 4.9** produces the least influence on grade within the travel lanes. The increase in grade for a pivot point located at the gutter line as shown in **Figure 4.10** is nearly three times as much as a center pivot location. This increase, however, can be mitigated by specifying longer superelevation transitions.
- Bridge deck drainage: When severe superelevation coincides with a relatively flat vertical profile or one containing sag curves, a pivot point location at a gutter line as shown in **Figure 4.10** can help prevent low points along a bridge deck. The elevation drop of the right gutter line from a centerline pivot point, as shown in **Figure 4.9,** can exacerbate this issue. The placement of additional bridge deck drains or scuppers in these locations can be used to address this concern.

- Merging/exiting alignments: A pivot point location on the *PGL*, as shown in **Figure 4.11**, can facilitate the establishment of vertical profiles of ramp alignments that might be merging onto or exiting from a mainline alignment. Grades and elevations of the two roadways can be established without corrections for cross slope.

4.4 Superelevation Transitions and Superelevation Diagrams

Moving from normal crown to the maximum superelevation needed for a horizontal curve should be done gradually over a distance that maintains safe driving speed. This is accomplished by introducing *superelevation transitions* located at the interfaces between tangent and curved horizontal alignment elements.

Figure 4.12 shows a perspective view of a horizontal alignment at a horizontal curve with entry and exit transition spirals. The roadway cross section of **Figure 4.12** comprises two lanes and shoulders, with the travel lanes carrying two-directional traffic. The cross section is similar to that shown in **Figure 4.4** and **Figure 4.5**, with the exception that the travel lanes and shoulders have the same cross slopes. The pivot point for superelevation transitions is located at the center of the roadway. The superelevation transitions through this curve are as follows:

- The cross section in the tangent run is in normal crown as the curve is approached.
- While still following the entry tangent, the adverse crown to the left of the pivot point rotates to a flat cross slope. The length along the tangent over which this rotation occurs is called the *tangent runout*. The tangent runout ends at the *TS*.
- Maximum superelevation is achieved over the length of the entry transition spiral, from the *TS* to the *SC*. This length is called the *superelevation runoff* length. It is the length needed to transition from the flat cross slope to the left of the pivot point to maximum superelevation.
- At a distance along the superelevation runoff equal to the tangent runout, a constant cross slope is achieved across the cross section. The cross section is fully superelevated at this location. The entire cross section rotates about the pivot point from this location to the end of the superelevation runout at the *SC*.
- Maximum superelevation is achieved at the *SC* and is maintained throughout the length of the circular curve.
- Beginning at the *CS*, superelevation transition begins to rotate the cross section from maximum superelevation to normal crown. The full cross section first rotates about the pivot point until the cross slope to the right of the pivot point reaches that of the normal crown. The cross slope of the portion of the cross section to the left of the pivot point then rotates to zero cross slope, completing the exiting superelevation runoff at the *ST*.
- The left half of the cross section continues to rotate over the exiting tangent runout until normal crown is achieved.

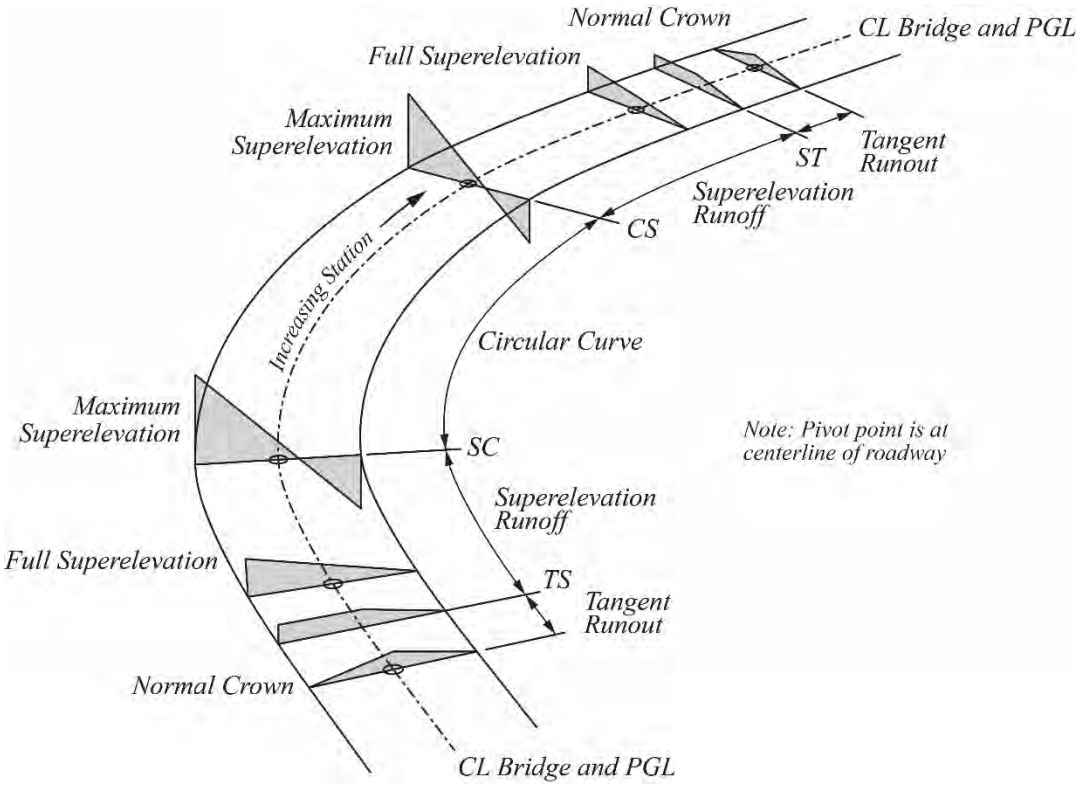

Source: PCI

Figure 4.12 Superelevation Transitions

Superelevation variations can be described in the form of a *superelevation diagram*, which plots the values of superelevation relative to the *PGL* and with respect to stationing along the horizontal alignment. **Figure 4.13** shows a superelevation diagram for the alignment shown in **Figure 4.12**.

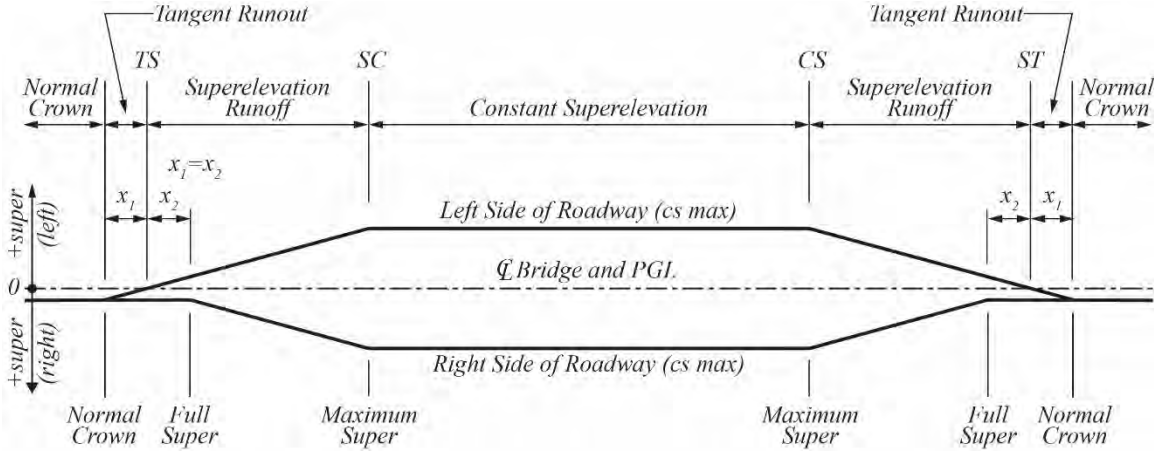

Source: PCI

Figure 4.13 Superelevation Diagram for Geometry of Fig. 4.12

The horizontal axis of the superelevation diagram in **Figure 4.13** is the *PGL*. Length along the *PGL* is measured in stations. The vertical axis is the amount of superelevation at a selected location offset from the pivot point. The vertical axis can be expressed as the value of the cross slope at locations along the transition.

The sign convention for the diagram is consistent with the sign convention for this manual. Positive superelevation lowers the edge of roadway to the right of the pivot point and is plotted below the *PGL* axis. Positive superelevation raises the edge of roadway to the left of the pivot point and is plotted above the *PGL* axis. Negative values for superelevation are plotted on the opposite side of the *PGL* from corresponding positive values.

Another example of a superelevation diagram is presented in **Figure 4.14**. This diagram is for a typical horizontal curve with transition spirals for the example bridge shown in **Figure 4.9**, with rotation about the centerline of the cross section. There is no tangent runout, as the normal crown has a constant 2 percent positive cross slope.

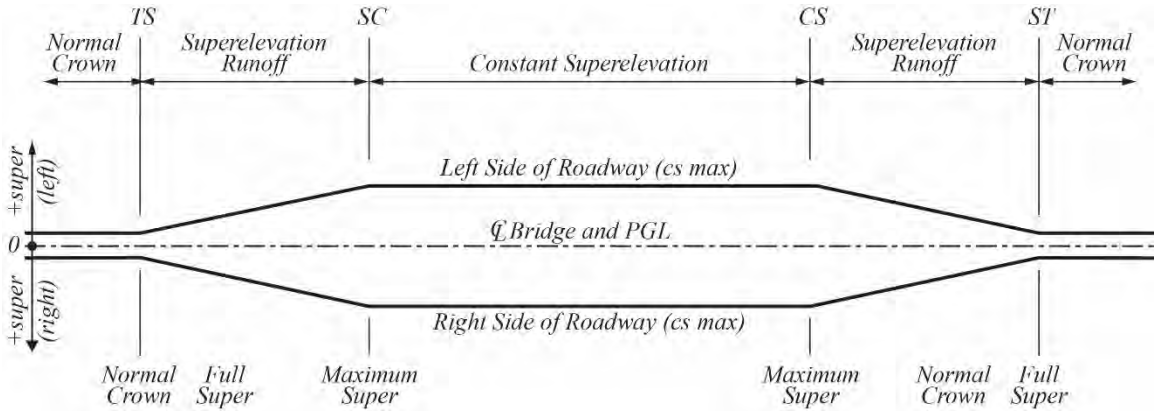

Source: PCI

Figure 4.14 Superelevation Diagram for Geometry of Fig. 4.9

Many horizontal alignments do not contain transition spirals. Tangent runouts typically occur on the entry and exiting alignment tangents when this is the case. The superelevation runoff typically begins on the entry or exiting alignment tangents and ends at some location along the circular curve. The length of the superelevation runoff, L_R, on the entry and exit tangents is typically expressed as a percentage, k_1, of the overall length of the superelevation runoff. This percentage varies among transportation agencies, but typical values range from 0.5 to 0.8 of the superelevation runoff length. **Figure 4.14** shows a superelevation diagram in the region of a *PC*. The variable k_1 is specified to locate the beginning and end of the superelevation runout.

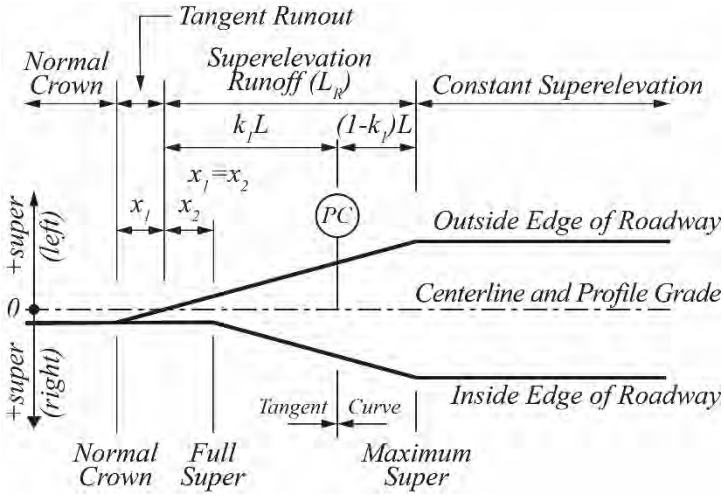

Source: PCI

Figure 4.15 Superelevation Diagram for a Horizontal Alignment without Transition Spirals

4.5 Superelevation Diagrams for Example Horizontal Alignment

Superelevations have been established for the three curves of the example horizontal alignment. The cross section of the roadway is similar to that shown in **Figure 4.4** and **Figure 4.5**, comprising two 12 ft lanes and two 10 ft shoulders. The normal crown of the cross section is different, however, in that cross slopes of plus or minus2 percent are used for the lanes and shoulders. The maximum superelevation rates for the three curves are 6 percent for the 1000 ft radius of curve 1, 5 percent for the 1250 ft radius of curve 2, and 7.5 percent for the 950 ft radius of curve 3. A one-third/two-thirds split of the superelevation runoff at the *PC*s and *PT*s was assumed. **Figure 4.16** shows the resulting superelevation diaphragms.

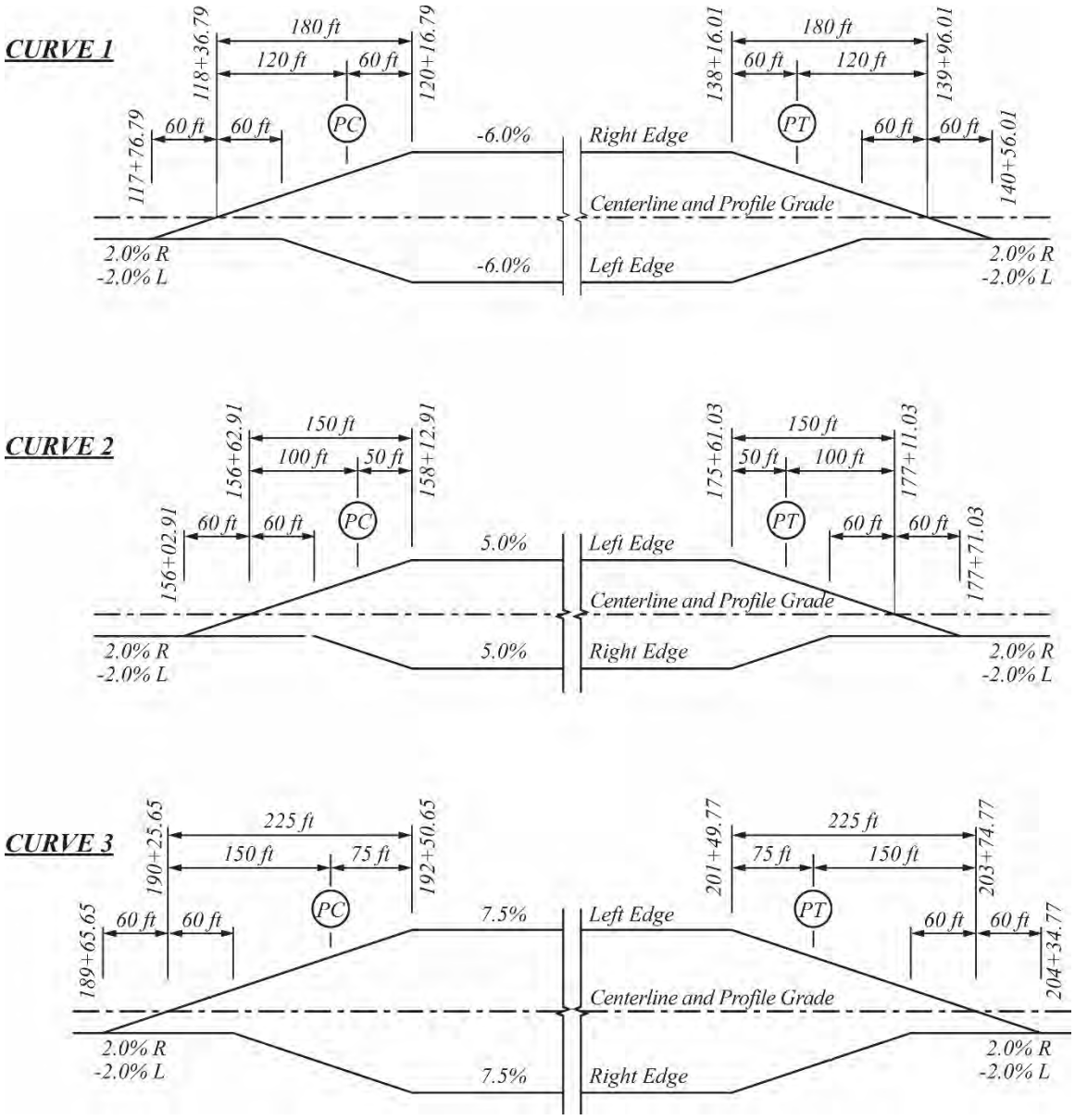

Source: PCI

Figure 4.16 Superelevation Diagram for Example Horizontal Alignment

Chapter 5 – Working with Horizontal Geometry

5.1 Introduction

This chapter contains a vector-based approach to locating and working with points on horizontal alignments. Items discussed include:

- Locating points on horizontal alignments
- Locating points offset from horizontal alignments
- Projecting points onto horizontal alignments
- Creating offset horizontal alignments

See appendix A for additional information regarding vectors and basic vector operations.

Examples in this chapter will use the horizontal alignment presented in Chapter 2. The layout of the horizontal alignment is shown in **Figure 5.1**. Key features of this horizontal alignment are shown in **Table 5.1, Table 5.2,** and **Table 5.3**. See appendix B for a complete listing of example geometry.

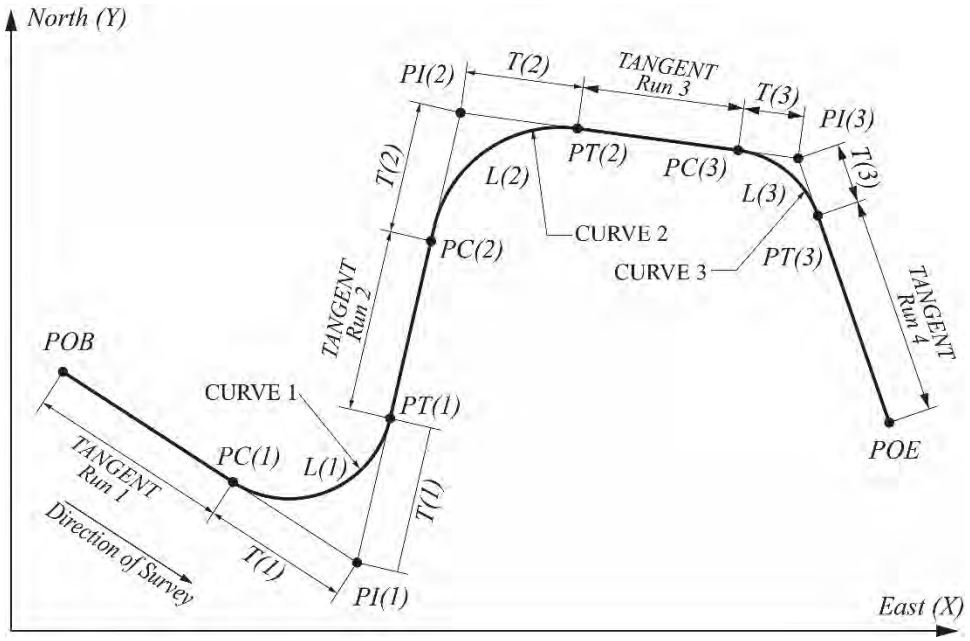

Source: PCI

Figure 5.1 Example Horizontal Alignment

Table 5.1 Horizontal Alignment PI Coordinates and Stations of Horizontal Alignment Control Points

Point	East (*X*)	North (*Y*)	Station
POB	500.0	2500.0	100+00.0000
PI(1)	3340.0	660.0	133+83.9622
PI(2)	4340.0	5000.0	169+02.5493
PI(3)	7600.0	4560.0	197+60.9533
POE	8480.0	2010.0	223+37.0702

Table 5.2 Horizontal Circular Curve Data

Curve	*R*, ft	*Δ*, rad	*L*, ft	*T*, ft
1	1000.0	1.91922267 (*L*)	1919.2227	1427.1765
2	1250.0	1.47849267 (*R*)	1848.1158	1139.6356
3	950.0	1.10433657 (*R*)	1049.1197	528.2879

Table 5.3 Horizontal Alignment Stationing

Point	Station	Length, ft	Element
POB	100+00.0000	--	--
--	--	1956.7857	Tangent run 1
PC(1)	119+56.7857	--	--
--	--	1919.2227	Curve 1
PT(1)	138+76.0083	--	--
--	--	1886.9055	Tangent run 2
PC(2)	157+62.9138	--	--
--	--	1848.1158	Curve 2
PT(2)	176+11.0296	--	--
--	--	1564.6358	Tangent run 3
PC(3)	191+75.6654	--	--
--	--	1049.1197	Curve 3
PT(3)	202+24.7851	--	--
--	--	2112.2851	Tangent run 4
POE	223+37.0702	--	--

5.2 Locating Points on Tangent Runs

Locating coordinates of points along linear elements using vector geometry requires the following information:

- Coordinates of a beginning point
- Unit vector expressing direction
- Length along the linear element from the beginning point

Convenient beginning points for horizontal alignments are points of beginning *POB*, points of intersection *PI*, or points of curve to tangent *PT*. Unit vectors are aligned with a segment of the baseline of the alignment. Lengths from beginning points are determined by station differences between the point being found and the beginning point.

Consider the first segment of the baseline of the example alignment shown in **Figure 5.1**. The vector of this baseline segment from the *POB* to *PI*(1) is

$$\overrightarrow{V_{01}} = \left(X_{PI(1)} - X_{POB}\right)i + \left(Y_{PI(1)} - Y_{POB}\right)j \tag{5.1}$$

The length of this baseline vector is equal to the baseline length from the *POB* to *PI*(1):

$$\left|\overrightarrow{V_{01}}\right| = \sqrt{\left(X_{PI(1)} - X_{POB}\right)^2 + \left(Y_{PI(1)} - Y_{POB}\right)^2} \tag{5.2}$$

The resulting unit vector for the first segment of the baseline is found by dividing the vector components by the vector length:

$$\overrightarrow{U_{01}} = \left(\frac{\left(X_{PI(1)} - X_{POB} \right)}{\left| \overrightarrow{V_{01}} \right|} \right) i + \left(\frac{\left(Y_{PI(1)} - Y_{POB} \right)}{\left| \overrightarrow{V_{01}} \right|} \right) j \tag{5.3}$$

The coordinates of a point along the first tangent run are found by first scaling the tangent run unit vector by an amount equal to the station difference between the point to be found and the station of the *POB*. This scaled vector is then added to the coordinates of the *POB*. The change in station between these two points is

$$\Delta Station = Station_P - Station_{POB} \tag{5.4}$$

The vector to be added to the coordinates of the beginning point, the *POB*, is

$$\vec{V} = \Delta Station \times \overrightarrow{U_{01}} \tag{5.5}$$

The coordinates of the point at station 110+00 are then

$$P(X,Y) = POB(X,Y) + \vec{V} \tag{5.6}$$

Example 5.1: Compute the coordinates of the point located at station 110+00 on the example horizontal alignment.

The vector of the segment of the baseline between the *POB* and *PI*(1) is

$$\begin{aligned} \overrightarrow{V_{01}} &= \left(X_{PI(1)} - X_{POB} \right) i + \left(Y_{PI(1)} - Y_{POB} \right) j = \left(3340 - 500 \right) i + \left(660 - 2500 \right) j \\ &= 2840 i - 1840 j \end{aligned} \tag{5.7}$$

The length of vector V_{01} is equal to the baseline length from the *POB* to *PI*(1):

$$\left| \overrightarrow{V_{01}} \right| = \sqrt{(2840)^2 + (-1840)^2} = 3383.9622 \text{ ft} \tag{5.8}$$

The resulting unit vector for the first segment of the baseline is

$$\begin{aligned} \overrightarrow{U_{01}} &= \left(\frac{\left(X_{PI(1)} - X_{POB} \right)}{\left| \overrightarrow{V_{01}} \right|} \right) i + \left(\frac{\left(Y_{PI(1)} - Y_{POB} \right)}{\left| \overrightarrow{V_{01}} \right|} \right) j = \left(\frac{2840}{3383.9622} \right) i + \left(-\frac{1840}{3383.9622} \right) j \\ &= 0.83925288 i - 0.54374130 j \end{aligned} \tag{5.9}$$

The significant digits in this chapter may seem extreme but should be retained because lengths between points can be long.

The change in station between these two points is

$$\Delta Station = (110 + 00) - (100 + 00) = 1000 \text{ ft} \tag{5.10}$$

The vector to be added to the coordinates of the beginning point, the *POB*, is

$$\vec{V} = 1000 \times \left(0.83925288 i - 0.54374130 j \right) = 839.25288 i - 543.74130 j \tag{5.11}$$

The coordinates of the point at station 110+00 are then

$$P(X,Y) = POB(500,2500) + \left(839.25288i - 543.74130j\right)$$
$$= \left(1339.2529, 1956.2587\right) \tag{5.12}$$

The location of this point is shown graphically in **Figure 5.2**:

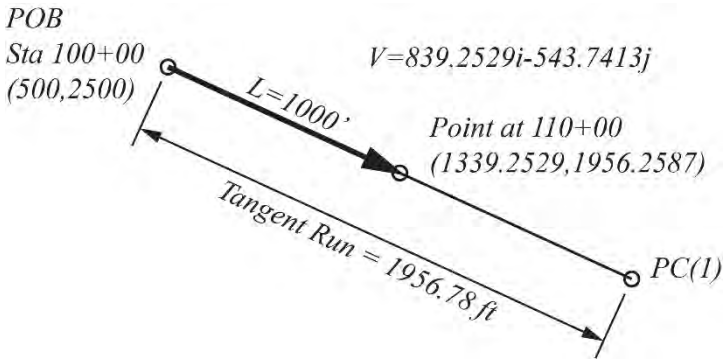

Source: PCI

Figure 5.2 Locating Point at 110+00

The previous solution is valid for stations between the station of the *POB* and the first tangent to curve point, *PC*(1). Unit vectors and beginning coordinates for other segments of the baseline should be developed for finding points along the other tangent runs of the alignment.

Example 5.2: Compute the coordinates of the point located at station 145+00 on the example horizontal alignment.

By inspection of Table 5.3, the point lies in the tangent run between *PI*(1) and *PI*(2). The beginning point of this tangent run is *PT*(1), which has a station of 138+76.0083. The vector of the segment of the baseline between *PI*(1) and *PI*(2) is

$$\overrightarrow{V_{12}} = \left(X_{PI(2)} - X_{PI(1)}\right)i + \left(Y_{PI(2)} - Y_{PI(1)}\right)j = \left(4340 - 3340\right)i + \left(5000 - 660\right)j$$
$$= 1000i + 4340j \tag{5.13}$$

The length of this vector is

$$\left|\overrightarrow{V_{12}}\right| = \sqrt{(1000)^2 + (4340)^2} = 4453.7175 \text{ ft} \tag{5.14}$$

The unit vector for this segment of the baseline is

$$\overrightarrow{U_{12}} = \left(\frac{1000}{4453.7175}\right)i + \left(\frac{4340}{4453.7175}\right)j = 0.22453153i + 0.97446684j \tag{5.15}$$

The station difference between the point being found and the beginning point of the tangent run is

$$\Delta Station = (145 + 00) - (138 + 76.0083) = 623.9917 \text{ ft} \tag{5.16}$$

The total length along this segment of the baseline from *PI*(1) to station 145+00 on the alignment is equal to the sum of the tangent length of the first circular curve plus the station difference from the point to be found and *PT*(1).

$$\text{Length} = T(1) + \Delta Station = 1427.1765 + 623.9917 = 2051.1682 \text{ ft} \tag{5.17}$$

The vector to be added to the coordinates of *PI*(1) is then

$$\vec{V} = 2051.1682 \times \left(0.22453153i + 0.97446684j\right) = 460.5519i + 1998.7954j \tag{5.18}$$

The coordinates of the point at station 145+00 are then

$$\begin{aligned} P(145+00) &= PI1(3340,660) + \left(460.5519i + 1998.7954j\right) \\ &= \left(3800.5519, 2658.7954\right) \end{aligned} \tag{5.19}$$

5.3 Locating Points Offset from Tangent Runs

Finding the coordinates for points offset perpendicularly from a point on a tangent run is facilitated by knowing the unit vectors aligned with the horizontal alignment baselines. **Figure 5.3** shows a tangent run beginning at a *PT* point. The unit vector for this tangent run has been multiplied by a change in station to locate the coordinates of point *P* on the tangent run. Points offset from the tangent run at point *P* are designated P_L (point to the left) and P_R (point to the right). These points are located by multiplying the perpendicular unit vectors by the value of the offset and adding the resulting vector to the coordinates of point *P*.

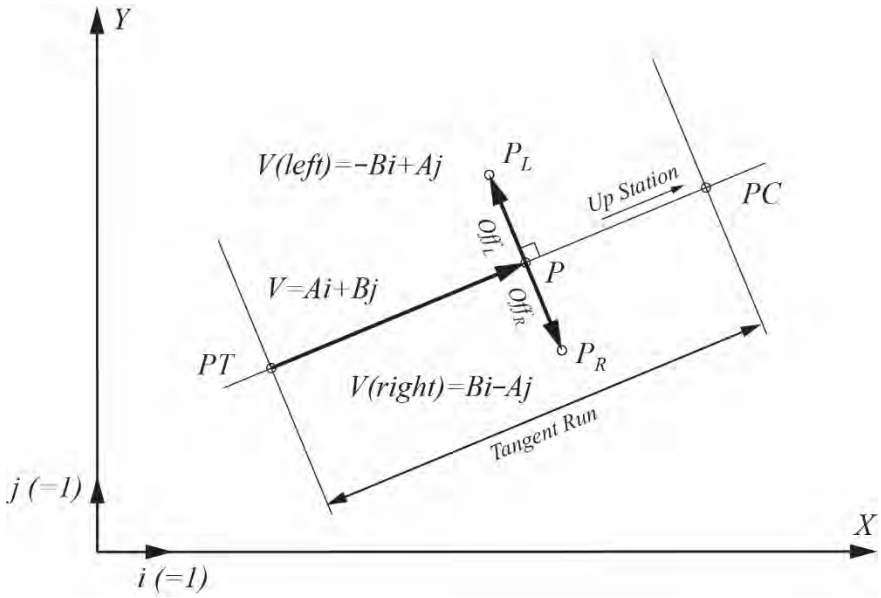

Source: PCI

Figure 5.3 Locating Points Offset from Tangent Runs

The unit vector for the tangent run in **Figure 5.3** can be found by the coordinates of the baseline on which it lies using Eq. (5.1)–(5.3) and expressed in generalized form as

$$\vec{U} = ai + bj \tag{5.20}$$

The vector from the *PC* to point *P* is found by multiplying the unit vector times the difference in stationing:

$$\vec{V} = \Delta Station\left(\vec{U}\right) = \left(STA_P - STA_{PC}\right)\left(ai + bj\right) = Ai + Bj \tag{5.21}$$

The coordinates of point *P* are found as described in the previous section by adding the vector *V* to the coordinates of the *PT*. The unit vectors perpendicular to the tangent run are

$$\overrightarrow{U}(left) = -bi + aj \tag{5.22}$$

$$\overrightarrow{U}(right) = bi - aj \tag{5.23}$$

The component terms *a* and *b* in the previous equations are those of the unit vector of the tangent run. The vectors to the offset points are found by multiplying the perpendicular unit vectors by the desired left or right offset distance Off_L or Off_R. The coordinates of the offset points are then found by adding the vectors to the coordinates of the point *P*.

Example 5.3: Compute the coordinates of points 20 ft to the left and right of the point found in Example 5.2 at station 145+00 on the example horizontal alignment.

The unit vector of the baseline from *PI*(1) to *PI*(2) and the coordinates of the point at station 145+00 were found in Example 5.2 to be

$$\overrightarrow{U_{12}} = 0.22453153i + 0.97446684j \tag{5.24}$$

$$P(145+00) = (3800.5519, 2658.7954) \tag{5.25}$$

The unit vectors perpendicular to the baseline are

$$\overrightarrow{U}(left) = -0.97446684i + 0.22453153j \tag{5.26}$$

$$\overrightarrow{U}(right) = 0.97446684i - 0.22453153j \tag{5.27}$$

The vectors to the points offset 20 ft on either side of the point at station 145+00 are

$$\overrightarrow{V}(left) = 20(-0.97446684i + 0.22453153j) = -19.4893i + 4.4906j \tag{5.28}$$

$$\overrightarrow{V}(right) = 20(0.97446684i - 0.22453153j) = 19.4893i - 4.4906j \tag{5.29}$$

The resulting coordinates of the offset points are

$$P(left) = P(145+00) + (-19.4893i + 4.4906j) = (3781.0626, 2663.2860) \tag{5.30}$$

$$P(right) = P(145+00) + (19.4893i - 4.4906j) = (3820.0412, 2654.3048) \tag{5.31}$$

Figure 5.3 shows both a left and right vector to points offset either side of the horizontal alignment. It can be seen in the previous example that a single vector—positive with an offset to the left—typically is sufficient to find points offset in either direction. A negative offset would result in an offset to the right as computed in Example 5.3.

Points located at the center of the circular curves are convenient for future geometric calculations. These points can be found as offset points to either *PC* or *PT* points, where the amount of offset is equal to the radius of the horizontal curve.

Example 5.4: Compute the coordinates of the center of the circle of horizontal curve 2.

The unit vector of the baseline from *PI*(1) to *PI*(2) and the coordinates of *PI*(1) are

$$\overrightarrow{U_{12}} = 0.22453153i + 0.97446684j \tag{5.32}$$

$$PI(1) = (3340, 660) \tag{5.33}$$

The length along the baseline from *PI*(1) to the *PC* of curve 2 is equal to the length of that segment of the baseline less the tangent length of curve 2:

$$\text{Length} = 4453.7175 - 1139.6356 = 3314.0819 \text{ ft} \tag{5.34}$$

The vector from *PI*(1) to the *PC* of curve 2 is

$$\vec{V} = 3314.0819 \times \left(0.22453153i + 0.97446684j\right) = 744.1159i + 3229.4629j \tag{5.35}$$

The coordinates of the point at the *PC* of curve 2 are then

$$P(PC2) = PI(1)(3340, 660) + \left(744.1159i + 3229.4629j\right) = \left(4084.1159, 3889.4629\right) \tag{5.36}$$

The offset to the center of the circular curve is to the right. The unit vector perpendicular and to the right of the baseline is

$$\vec{U}(right) = 0.97446684i - 0.22453153j \tag{5.37}$$

The radius of the circular curve is 1250 ft. The vector to the center of the circle is

$$\vec{V}(center) = 1250\left(0.97446684i - 0.22453153j\right) = 1218.0836i - 280.6644j \tag{5.38}$$

The resulting coordinate at the center of the circle is equal to the coordinates of *PC*(2) plus the vector to the center:

$$P(center) = P(PC2) + \left(1218.0836i - 280.6644j\right) = \left(5302.1995, 3608.7985\right) \tag{5.39}$$

5.4 Locating Points Offset from Tangent Runs at a Skew

The previous section dealt with locating points offset perpendicularly from a tangent run of a horizontal alignment. A more general case of locating points offset from an alignment is when the offset point lies along a line skew to the perpendicular direction. A common occurrence of this for bridge structures is where skew roadways are being crossed and the supporting substructure is skewed to optimize the bridge's layout.

Figure 5.4 shows a tangent run beginning at a *PT* point and ending at the *PC* point at the beginning of the next horizontal curve. The unit vector for this tangent run is that of the segment of the baseline on which it lies. Point *P* is located at a location along the tangent run at a known station. Points P_L and P_R are located along vectors with origin at point *P* and direction determined by a skew angle. The skew angle is measured relative to a direction perpendicular to the local tangent at point *P*. In the case of **Figure 5.4**, this local tangent is the tangent run. The sign convention adopted for this manual is that a plan view, counterclockwise rotation from perpendicular to the skew orientation is positive.

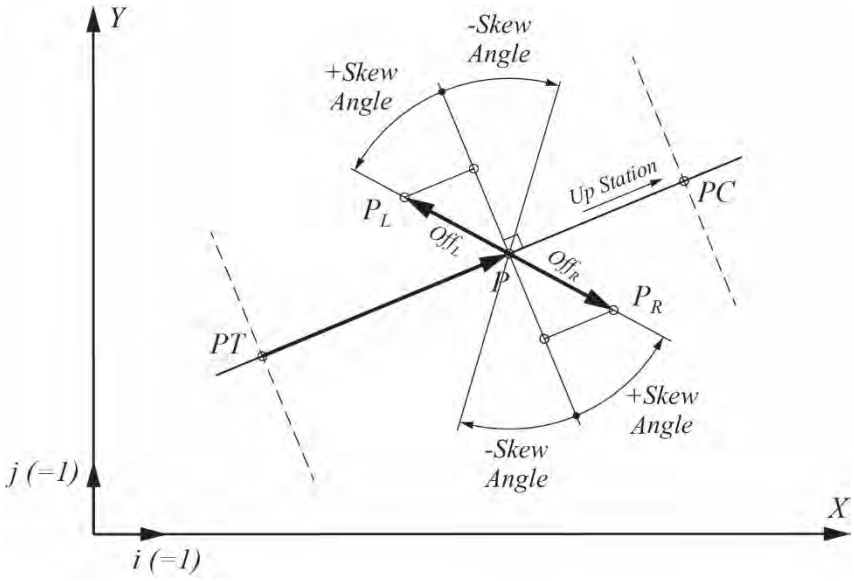

Source: PCI

Figure 5.4 Locating Points with a Skew Offset

Locating offset points P_L and P_R in **Figure 5.4** is accomplished by adding vectors from P to P_L and P to P_R to the coordinates of point P. Perpendicular vectors at point P are located first as in Section 5.3. The direction angles of the unit perpendicular vectors can be determined from the components of those vectors, respecting the guidelines developed in Section 2.3 of this manual. The direction angle of the skew vector is the sum of the direction angle of the perpendicular bearings plus the skew angle. The direction angles are used to construct the unit vectors of the skew lines. The length of the vector is the unit length multiplied by the known offset.

Example 5.5: Compute the coordinates of points 20 ft to the left and right, and with a skew of 30 degrees, of the point found in Example 5.2 at station 145+00 on the example horizontal alignment.

The unit vector of the baseline from *PI*(1) to *PI*(2) and the coordinates of the point at station 145+00 were found in Example 5.2 to be

$$\overrightarrow{U_{12}} = 0.22453153i + 0.97446684j \tag{5.40}$$

$$P(145+00) = (3800.5519, 2658.7954) \tag{5.41}$$

The unit vectors perpendicular to the baseline are

$$\overrightarrow{U}(left) = -0.97446684i + 0.22453153j \tag{5.42}$$

$$\overrightarrow{U}(right) = 0.97446684i - 0.22453153j \tag{5.43}$$

The direction angles of these vectors are

$$Brg(left) = 180 + \tan^{-1}\left(\frac{0.22453153}{-0.97446684}\right) = 167.0247 \text{ degrees} \tag{5.44}$$

$$Brg(right) = 360 + \tan^{-1}\left(\frac{-0.22453153}{0.97446684}\right) = 347.0247 \text{ degrees} \tag{5.45}$$

The direction angles of the skew vectors are

$$Brg(skew\ left) = \vec{U}(left) + \text{skew angle} = 167.0247 + 30 = 197.0247 \text{ degrees} \quad (5.46)$$

$$Brg(skew\ right) = \vec{U}(right) + \text{skew angle} = 347.0247 + 30 = 17.0247 \text{ degrees} \quad (5.47)$$

The unit vectors along the skew direction are

$$\vec{U}(skew\ left) = \cos\left(Brg\right)i + \sin\left(Brg\right)j = -0.95617879i - 0.29278341j \quad (5.48)$$

$$\vec{U}(skew\ right) = \cos\left(Brg\right)i + \sin\left(Brg\right)j = 0.95617879i + 0.29278341j \quad (5.49)$$

The skew vectors are

$$\vec{V}(skew\ left) = 20 \times \left(-0.95617879i - 0.29278341j\right) = -19.1236i - 5.8557j \quad (5.50)$$

$$\vec{V}(skew\ right) = 20 \times \left(0.95617879i + 0.29278341j\right) = 19.1236i + 5.8557j \quad (5.51)$$

The coordinates of the offset points are

$$P(skew\ left) = \left(3800.5519, 2658.7954\right) + \left(-19.1236i - 5.8557j\right) = \left(3781.4283, 2652.9397\right) \quad (5.52)$$

$$P(skew\ right) = \left(3800.5519, 2658.7954\right) + \left(19.1236i + 5.8557j\right) = \left(3819.6755, 2664.6511\right) \quad (5.53)$$

5.5 Projecting Points onto Tangent Runs

Roadway geometric information related to points of known coordinates not lying on a horizontal alignment needs a perpendicular projection of the points onto a controlling horizontal alignment. The results of the projections are stations on the controlling horizontal alignment, which in turn can be used to determine elevations and superelevation information.

Figure 5.5 shows a tangent run beginning at a *PT* point and ending at the *PC* point at the beginning of the next horizontal curve. The unit vector for this tangent run is that of the segment of the baseline on which it lies. Points P_L and P_R are points known by *X* and *Y* coordinates. Vectors *V*(*left*) and *V*(*right*) can be constructed from coordinate information of points *PT*, P_L, and P_R. The direction angle of the vectors can be determined from the vector components. Using the sign convention of this manual, points to the left of the tangent run looking up-station will have a direction angle greater than the bearing of the tangent run. Likewise, points to the right looking up-station will have a smaller direction angle bearing than that of the tangent run. Note that points before the *PT* or beyond the *PC* do not project onto this particular tangent run.

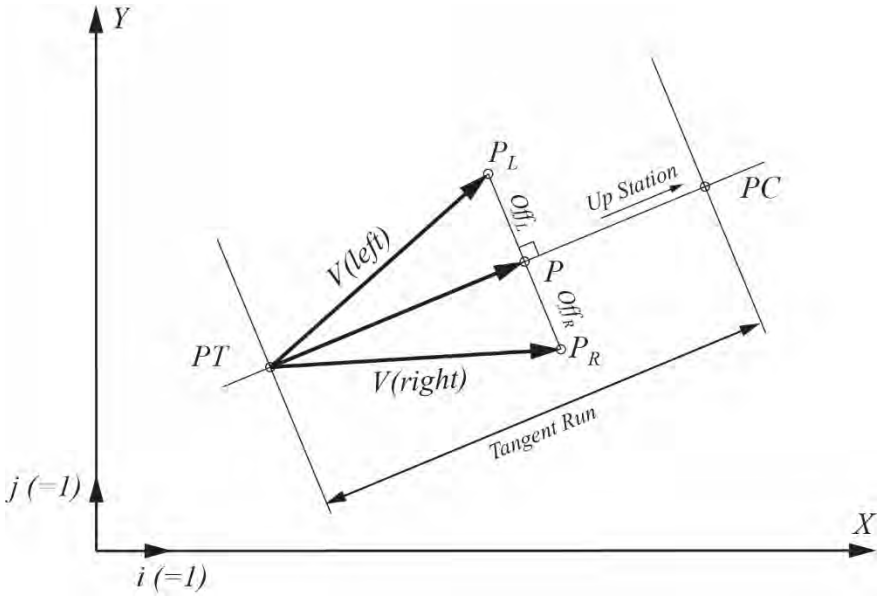

Source: PCI

Figure 5.5 Projecting Points on Tangent Runs

The vector between the *PT* and the point to be projected is

$$\vec{V} = \left(X - X_{PT}\right)i + \left(Y - Y_{PT}\right)j \tag{5.54}$$

The direction angle is found in accordance with Section 2.3 of this manual:

$$\theta = \tan^{-1}\left(\frac{Y - Y_{PT}}{X - X_{PT}}\right) \tag{5.55}$$

A triangle can be formed by a vector along the tangent run applied at the *PT*; a vector perpendicular to the tangent run applied at the desired point of projection; and a hypotenuse, which is the vector between the *PT* and the known point to project. The angle between the vector along the tangent run and the vector to the known point is found by the difference in bearing angle:

$$\Delta\theta = \theta(vector) - \theta(tangent\ run) \tag{5.56}$$

The length of the vector along the tangent run is the change in station from the *PT* to the projecting station. It is found as

$$\Delta Station = \left|\vec{V}\right|\cos\Delta\theta \tag{5.57}$$

The offset of the known point to the projected station is found in similar fashion:

$$Offset = \left|\vec{V}\right|\sin\Delta\theta \tag{5.58}$$

The direction of the offset, whether left or right looking up-station, is determined by considering the possible values for the differences in direction angle $\Delta\theta$. Using the vector approach with direction angle, the possible values for $\Delta\theta$ and direction of offset are

$$0 \le \Delta\theta \le 90 \text{ degrees} \quad \text{(offset to the left looking up-station)} \tag{5.59}$$

$$270 \text{ degrees} \le \Delta\theta \le 360 \text{ degrees} \quad \text{(offset to the right looking up-station)} \tag{5.60}$$

Note: This manual presents regions where points do and do not project onto the elements of a horizontal alignment (this section for tangent runs and Section 5.9 for circular curves). This will be the case for the great majority of horizontal alignments. There can be instances where alignments contain such significant change in direction that they double back on themselves. In these instances, points may project on one or more elements of the horizontal alignment. The station reported for the projection of the point is typically that associated with the smallest offset value.

Example 5.6: Compute the station along the example horizontal alignment at which a point with coordinates (3700, 3500) projects, provided that the unit vector of the baseline from *PI*(1) to *PI*(2) and the coordinates of *PT*1 are

$$\overrightarrow{U_{12}} = 0.22453153i + 0.97446684j \tag{5.61}$$

$$PT(1) = (3660.4461,\ 2050.7362) \tag{5.62}$$

The direction angle bearing of the unit vector following the baseline from *PI*(1) to *PI*(2) is

$$\theta = \tan^{-1}\left(\frac{Y - Y_{PT}}{X - X_{PT}}\right) = \tan^{-1}\left(\frac{0.97446684}{0.22453153}\right) = 77.02467 \text{ degrees} \tag{5.63}$$

The vector between *PT*1 and *P*(3700, 3500) is

$$\vec{V} = \left(3700 - 3660.4461\right)i + (3500 - 2050.7362)\,j = 39.5539i + 1449.2638\,j \tag{5.64}$$

The length of this vector is

$$\left|\vec{V}\right| = \sqrt{\left(39.5539\right)^2 + \left(1449.2638\right)^2} = 1449.8035 \text{ ft} \tag{5.65}$$

The direction angle bearing of this vector is

$$\theta = \tan^{-1}\left(\frac{1449.2638}{39.5539}\right) = 88.43665 \text{ degrees} \tag{5.66}$$

The difference in direction angle is

$$\Delta\theta = 88.43665 - 77.02467 = 11.41198 \text{ degrees} \tag{5.67}$$

The station onto which *P*(3700, 3500) projects is

$$\begin{aligned} Station &= Station_{PT1} + \left|\vec{V}\right|\cos\Delta\theta = (138 + 76.0083) + \left(1449.8035\cos\left(11.41198\right)\right) \\ &= 152 + 97.1489 \end{aligned} \tag{5.68}$$

The offset of the known point to the projected station is found in similar fashion:

$$Offset = \left|\vec{V}\right|\sin\Delta\theta = 1449.8035\sin\left(11.41198\right) = 286.8615 \text{ ft} \tag{5.69}$$

The magnitude of the change in angle $\Delta\theta$ indicates that the offset is to the left looking up-station.

5.6 Additional Information for Example Alignment

Additional coordinate information for key points on the example alignment presented in this manual was prepared using the vector approach described in the preceding sections. **Table 5.4** presents the information in **Table 5.3** with the addition of coordinate information. **Table 5.5** presents the information in **Table 5.2** with the addition of the coordinates at the center of the circular curves of the example alignment.

Table 5.4 Horizontal Alignment Stationing with Coordinates

Point	Station	*X*(E), ft	*Y*(N), ft	Length, ft	Element
POB	100+00.0000	500.0000	2500.0000	--	--
--	--	--	--	1956.7857	Tangent run 1
PC(1)	119+56.7857	2142.2380	1436.0148	--	--
--	--	--	--	1919.2227	Curve 1
PT(1)	138+76.0083	3660.4461	2050.7362	--	--
--	--	--	--	1886.9055	Tangent run 2
PC(2)	157+62.9138	4084.1159	3889.4629	--	--
--	--	--	--	1848.1158	Curve 2
PT(2)	176+11.0296	5469.3951	4847.5663	--	--
--	--	--	--	1564.6358	Tangent run 3
PC(3)	191+75.6654	7019.9714	4638.2861	--	--
--	--	--	--	1049.1197	Curve 3
PT(3)	202+24.7851	7790.9321	4006.7308	--	--
--	--	--	--	2112.2851	Tangent run 4
POE	223+37.0702	8480.0000	2010.0000	--	--

Table 5.5 Horizontal Circular Curve Data with Circle Center Coordinates. Note

Curve	*R*, ft	*Δ*, rad	*L*, ft	*T*, ft	*CC X*(E), ft	*CC Y*(N), ft
1	1000.0	1.91922267 (*L*)	1919.2227	1427.1765	2685.9793	2275.2677
2	1250.0	1.47849267 (*R*)	1848.1158	1139.6356	5302.1994	3608.7985
3	950.0	1.10433657 (*R*)	1049.1197	585.2879	6892.9027	3696.8226

5.7 Locating Points on Circular Curves

Points along circular curves are located by station relative to the point of tangent to curve *PC*. The vector approach to locating a point along circular curves is facilitated by knowing the coordinates of the centers of the circular curves. The coordinate of a point along the curve is found by adding a vector, with a length equal to the radius of the curve, to the coordinates of the circle center (*CC*) in the direction of the point. The direction of the vector is found by proportion of station from the *PC* to the point relative to the length of the circular curve.

Figure 5.6 presents the first circular curve of the example alignment. The deflection angle of this curve is to the left looking up-station, which is positive in the sign convention of this manual. Point *P* is located along the circular curve at a known station. The angle α is the angle subtended by the arc length along the circular curve from the *PC* to point *P*.

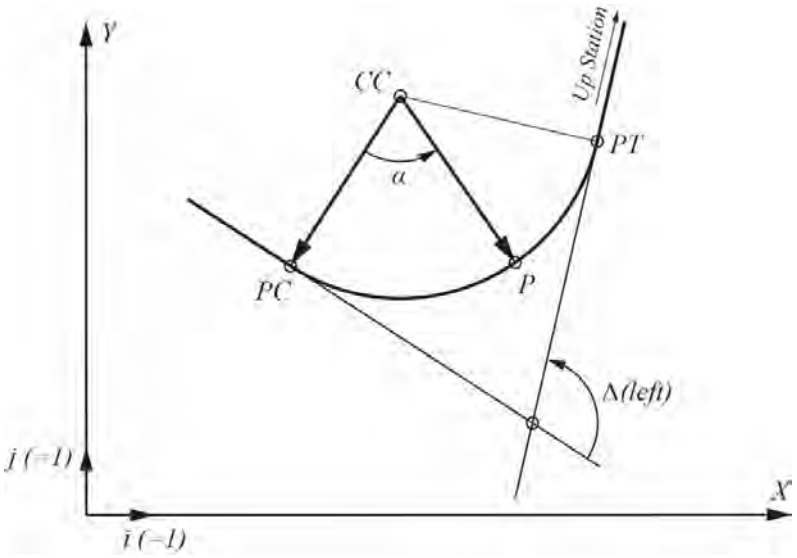

Source: PCI

Figure 5.6 Locating Points on Horizontal Curves

The vector from the circle center to the point of beginning of the curve is

$$\overrightarrow{V_{PC}} = \left(X_{PC} - X_{CC}\right)i + \left(Y_{PC} - Y_{CC}\right)j \tag{5.70}$$

The direction angle of this vector is found in accordance with section 2.3 of this manual:

$$\theta_{PC} = \tan^{-1}\left(\frac{Y_{PC} - Y_{CC}}{X_{PC} - X_{CC}}\right) \tag{5.71}$$

The angle from the *PC* to the point in question is

$$\alpha = \left(\frac{Sta_P - Sta_{PC}}{L}\right)\Delta \tag{5.72}$$

The direction angle bearing of the vector from the *CC* to point *P* is then

$$\theta_P = \theta_{PC} + \alpha \tag{5.73}$$

The unit vector in the direction from the *CC* to point *P* is

$$\overrightarrow{U_P} = \cos\left(\theta_P\right)i + \sin\left(\theta_P\right)j \tag{5.74}$$

The vector from the *CC* to point *P* is

$$\overrightarrow{V_P} = R\left(\overrightarrow{U_P}\right) = R\cos\left(\theta_P\right)i + R\sin\left(\theta_P\right)j \tag{5.75}$$

The coordinates of point *P* are found by adding the vector from the *CC* to point *P* to the coordinates of the *CC*:

$$P(X,Y) = CC\left(X,Y\right) + \left(R\cos\left(\theta_P\right)i + R\sin\left(\theta_P\right)j\right) \tag{5.76}$$

Figure 5.7 shows the second circular curve of the example alignment presented in this manual. The deflection angle of this curve is to the right looking up-station. As a result, the orientation of the vector

from the *CC* to point *P* is found by subtracting the angle α from the direction angle of the vector from the *CC* to *PC*. The equations presented in this section remain valid if the sign convention for deflection angles is maintained, with deflection angles to the right being negative.

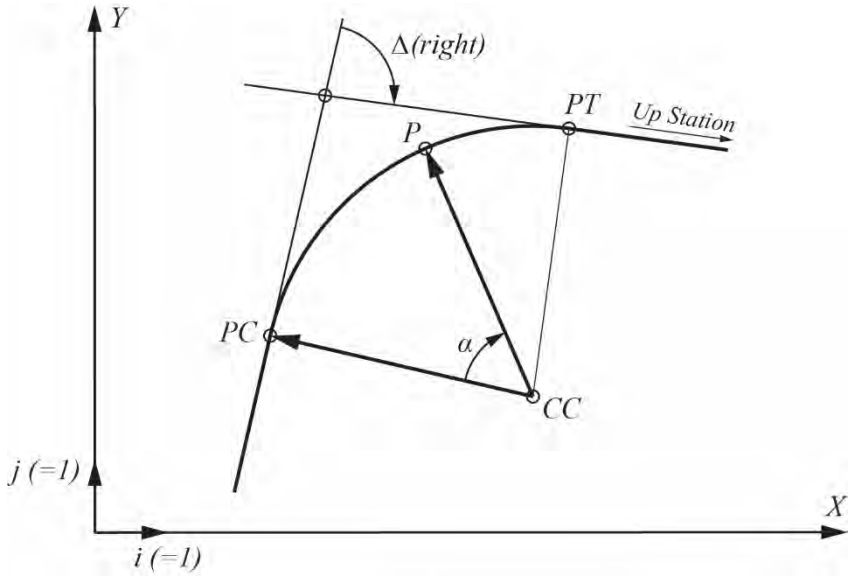

Source: PCI

Figure 5.7 Locating Points on Horizontal Curves with Negative Deflection Angles

Example 5.7: Compute the coordinates of the point located at station 130+00 on the example horizontal alignment.

By inspection of **Table 5.4**, station 130+00 lies on the first circular curve between *PC*(1) and *PT*(1). The vector from the circle center to the *PC* is

$$\begin{aligned}\overrightarrow{V_{PC}} &= \left(2142.2380 - 2685.9793\right)i + (1436.0148 - 2275.2677)\,j \\ &= -543.7413i - 839.2529\,j\end{aligned} \tag{5.77}$$

The direction angle of this vector is found in accordance with Section 2.3 of this manual:

$$\theta_{PC} = 180 + \tan^{-1}\left(\frac{-839.2529}{-543.7413}\right) = 237.06131 \text{ degrees} \tag{5.78}$$

The angle from the *PC* to the point in question is

$$\alpha = \left(\frac{\left(130+00\right) - \left(119+56.7857\right)}{1919.2227}\right)109.963359° = 59.771776 \text{ degrees} \tag{5.79}$$

The direction angle to the vector from the *CC* to point *P* is then

$$\theta_P = \theta_{PC} + \alpha = 237.06131 + 59.77178 = 296.88309 \text{ degrees} \tag{5.80}$$

The unit vector in the direction from the *CC* to point *P* is

$$\overrightarrow{U_P} = 0.45139296i - 0.89232527\,j \tag{5.81}$$

The vector from the *CC* to the point located at station 130+00 is

$$\overrightarrow{V_P} = 1000\left(0.45139296i - 0.89232527j\right) = 451.39296i - 892.325275j \tag{5.82}$$

The coordinates of the point at station 130+00 are found by adding the vector from *CC* to point *P* to the coordinates of *CC*:

$$\begin{aligned} P(X,Y) &= \left(2685.9793, 2275.2677\right) + \left(451.3930i - 892.3253j\right) \\ &= \left(3137.3723, 1382.9424\right) \end{aligned} \tag{5.83}$$

5.8 Locating Points Offset from Circular Curves

Coordinates of points offset from points at known stations along circular curves are computed in a similar manner to points offset from tangent runs (Section 5.4). Rather than computing vectors perpendicular to the tangent alignment, the radial vector from the *CC* to the known point *P* is used.

Figure 5.8 shows the first circular curve of the example alignment of this manual. Point *P* has been located based on its station along the circular curve in accordance with the previous section. The length of the vector used to locate point *P* was equal to the radius of the circular curve. Lengths of the vectors to points offset from the alignment are equal to the radius of the circular curve plus or minus the value of the offset. For curves with a positive deflection angle (left deflections looking up-station), a positive offset to the left will reduce the magnitude of the radial vector. Negative offsets to the right will increase the magnitude of the radial vector. The lengths of the locating vectors become

$$\left|\vec{V}\right|(left) = R - Off_L \tag{5.84}$$

$$\left|\vec{V}\right|(right) = R + Off_R \tag{5.85}$$

Vectors to the offset points are found by ratio of the length to the offset to the radius of the circular curve:

$$\overrightarrow{V_{OFF}} = \left(\frac{\left|\vec{V}\right|}{R}\right)\overrightarrow{V_P} \tag{5.86}$$

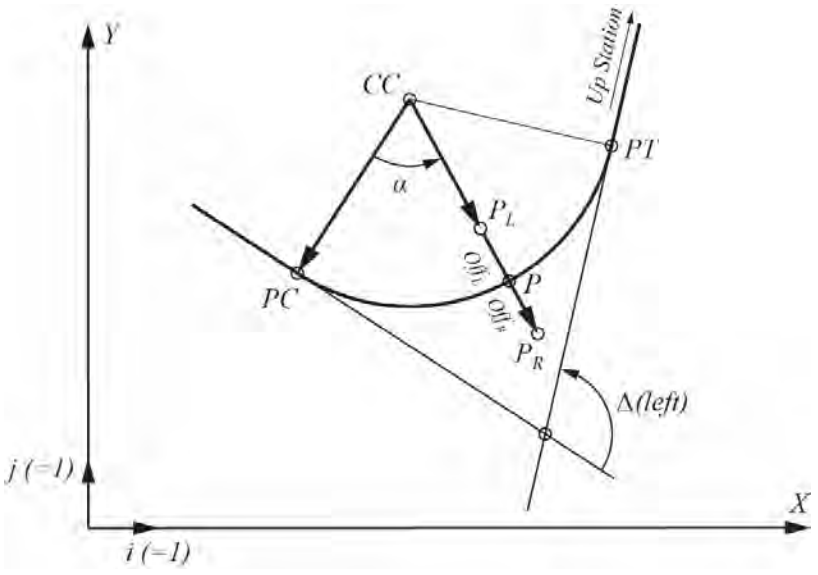

Source: PCI

Figure 5.8 Locating Points Offset from Horizontal Curves

For curves with negative deflections in the sign convention of this manual (right deflections looking up-station), the offsets add and subtract differently for positive and negative offsets. For curves with negative deflection angles, the lengths of the locating vectors are

$$\left|\vec{V}\right|(left) = R + Off_L \tag{5.87}$$

$$\left|\vec{V}\right|(right) = R - Off_R \tag{5.88}$$

Example 5.8: Compute the coordinates of the point offset 10 ft to the right of the point located at station 130+00 on the example horizontal alignment.

The vector from the *CC* to the point located at station 130+00 and the coordinates of that point as determined in Example 5.7 are

$$\overrightarrow{V_P} = 1000\left(.45139296i - .89232527j\right) = 451.39296i - 892.325275j \tag{5.89}$$

$$P(X,Y) = \left(3137.3723, 1382.9424\right) \tag{5.90}$$

For an offset of 10 ft to the right for this curve with a positive deflection angle, the locating vector is

$$\begin{aligned}\overrightarrow{V_{OFF}} &= \left(\frac{\left|\vec{V}\right|}{R}\right)\overrightarrow{V_P} = \left(\frac{R + Offset}{R}\right)\overrightarrow{V_P} = \left(\frac{1000+10}{1000}\right)\overrightarrow{V_P} = 1.01\overrightarrow{V_P} \\ &= 1.01\left(451.39296i - 892.325275j\right) = 455.906890i - 901.248528j\end{aligned} \tag{5.91}$$

The coordinates of point *P* are found by adding the vector from the *CC* to point *P* to the coordinates of the *CC*:

$$\begin{aligned}P_{OFF}(X,Y) &= \left(2685.9793, 2275.2677\right) + \left(455.906890i - 901.248528j\right) \\ &= \left(3141.8862, 1374.0192\right)\end{aligned} \tag{5.92}$$

5.9 Projecting Points onto Circular Curves

Projecting points onto circular curves involves determining the length along the circular curves at which the points are radially offset. With regard to a horizontal alignment, the resulting projection is expressed by the projecting station and corresponding radial offset.

Radial lines of a circular curve pass through the circle center. Only points that lie between radial lines that pass through the *PC* and *PT* will project onto a circular curve of a horizontal alignment. **Figure 5.9** shows the first circular curve of the example alignment. Also shown are two regions that contain points that can be projected onto the circular curve. Points that lie outside of these regions do not project to the curve.

Vectors for points within the projecting regions from the circle center to the points will be radial to the circular curve. Figure 5.9 shows two points that will project to the circular curve. Point P_1 lies to the left of the circular curve when looking up-station in the projecting region on the curve side of the *CC*. The left offset of this point is positive in the sign convention of this manual. Points in this region to the right of the circular curve will have negative offsets. Point P_2 lies on the far side of the *CC* in the second projecting region. These points are seldom of interest in roadway geometry and are not addressed in

this manual. Note that points in this second region would also project to tangent runs on either side of this curve.

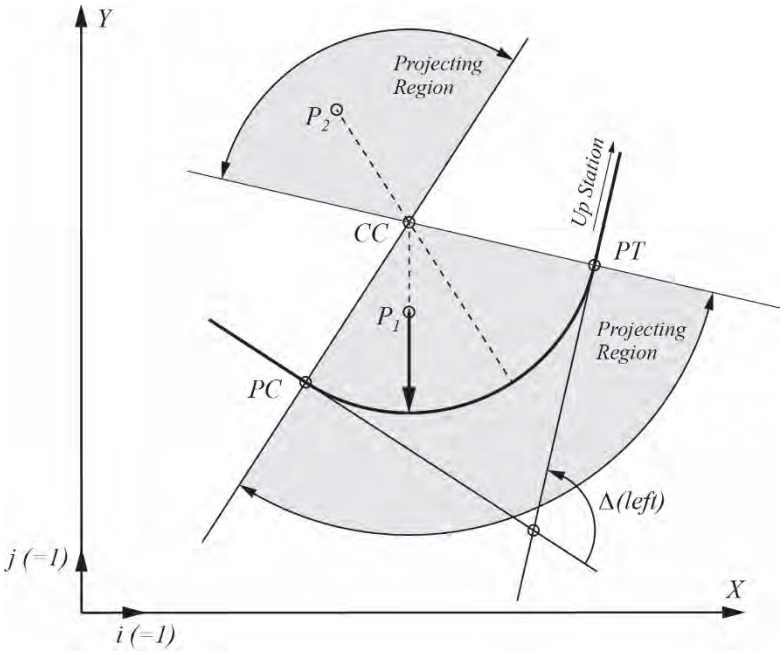

Source: PCI

Figure 5.9 Projection Regions of Points on Circular Curves

Figure 5.10 shows a known point *P* offset from a circular curve. A vector from the *CC* to point *P* can be established from coordinate information. This vector can be used to determine the station and offset of the projection of point *P*.

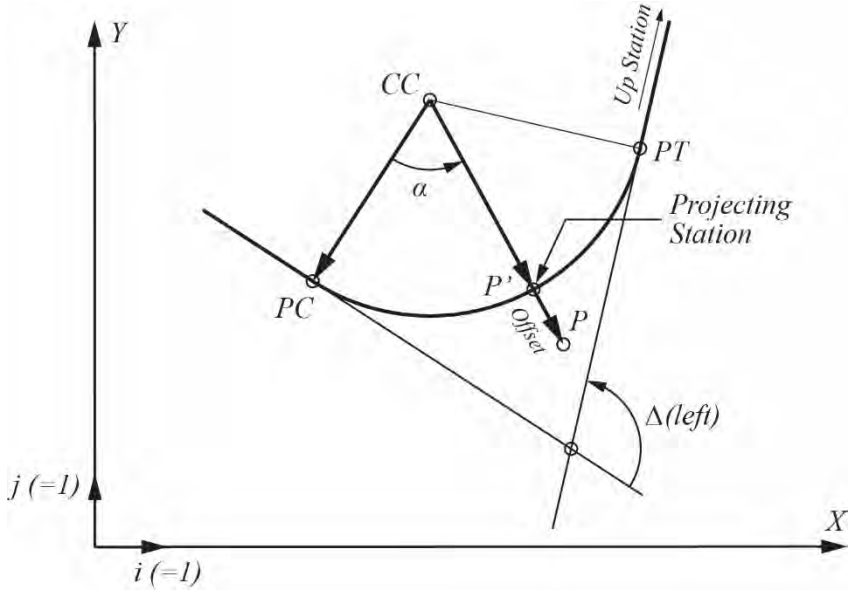

Source: PCI

Figure 5.10 Determining Station and Offset along a Circular Curve

The vector from the circle center to point *P* is

$$\overrightarrow{V_P} = \left(X_P - X_{CC}\right)i + \left(Y_P - Y_{CC}\right)j \tag{5.93}$$

The direction angles of these two vectors are found in accordance with Section 2.3 of this manual:

$$\theta_P = \tan^{-1}\left(\frac{Y_P - Y_{CC}}{X_P - X_{CC}}\right) \tag{5.94}$$

The angle from the *PC* to the point in question is

$$\alpha = \theta_P - \theta_{PC} \tag{5.95}$$

The length along the circular curve through which the vector from the *CC* to point *P* intersects it is

$$l = \left(\frac{\alpha}{\Delta}\right)L \tag{5.96}$$

The station to the intersecting point, which is the projecting station, is

$$Station_P = Station_{PC} + l \tag{5.97}$$

The radial offset at the projecting station is equal to the radius of the circular curve less the length of the vector from the *CC* to point *P*:

$$Offset = R - \left|\overrightarrow{V_P}\right| \tag{5.98}$$

To maintain the sign convention of this manual, a correction in sign needs to be made as a function of the sign of the deflection angle. The revised expression for offset becomes

$$Offset = \frac{\Delta}{\left|\Delta\right|}\left(R - \left|\overrightarrow{V_P}\right|\right) \tag{5.99}$$

Example 5.9: Project a point with the coordinates of (3394.8102, 1541.8110) onto curve 1 of the example horizontal alignment. Determine the projecting station and offset.

Using the information in Section 5.6, the vector of the *CC* to the *PC* and *CC* to point *P* are

$$\begin{aligned}\vec{V}_{CC-PC} &= \left(2142.2380 - 2685.9793\right)i + \left(1436.0148 - 2275.2677\right)j \\ &= -543.7413i - 839.2529j\end{aligned} \tag{5.100}$$

$$\begin{aligned}\vec{V}_{CC-P} &= \left(3394.8102 - 2685.9793\right)i + \left(1541.8110 - 2275.2677\right)j \\ &= 708.8309i - 733.4567j\end{aligned} \tag{5.101}$$

The length of this vector is

$$\left|\vec{V}_{CC-P}\right| = \sqrt{\left(708.8309'\right)^2 + \left(-733.4567'\right)^2} = 1020 \text{ ft} \tag{5.102}$$

The direction angles for these two vectors relative to the x axis are

$$\theta_{PC} = 180 + \tan^{-1}\left(\frac{-839.2529}{-543.7413}\right) = 237.061310 \text{ degrees} \tag{5.103}$$

$$\theta_P = 360 + \tan^{-1}\left(\frac{-733.2529}{708.8309}\right) = 314.021820 \text{ degrees} \tag{5.104}$$

The angle between the vector to point *P* and the vector to the *PC* is

$$\alpha = 314.021820 - 237.061310 = 76.960510 \text{ degrees} \tag{5.105}$$

The length along the circular curve through which the vector from the *CC* to point *P* intersects it is

$$l = \left(\frac{76.960510^\circ}{109.963359^\circ} \right) 1919.2227' = 1343.2143 \text{ ft} \tag{5.106}$$

The station to the intersecting point, which is the projecting station, is

$$Station_P = (119 + 56.7857) + 1343.2143 = 133 + 00 \tag{5.107}$$

The radial offset at the projecting station is equal to the radius of the circular curve less the length of the vector from the *CC* to point *P*:

$$Offset = \frac{109.963359 \text{ degrees}}{|109.963359 \text{ degrees}|}(1000 \text{ ft} - 1020 \text{ ft}) = -20 \text{ ft} \quad \text{(offset to the right)} \tag{5.108}$$

5.10 Offset Alignments

Additional horizontal alignments offset from the control horizontal alignment of a roadway may be needed to develop bridge geometry. These offset alignments might be profile grade lines or pivot point lines that are different from the control alignment. Curved girder bridges often use offset alignments to determine the centerline of the curved girders.

Figure 5.11 shows the first horizontal curve of the example alignment. A new horizontal alignment at a fixed offset is desired. The deflection angles of the original curve and the offset curve are the same. This results in the *PC*s and *PT*s of the two curves lying on the same radial lines passing through the common center of the two curves. This also results in lengths of tangent runs of the offset alignment being equal to those of the original alignment.

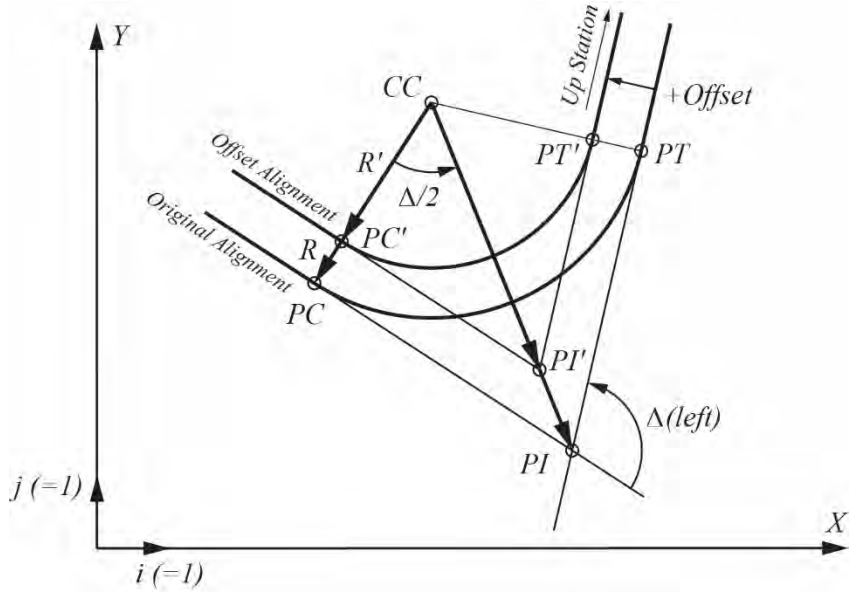

Source: PCI

Figure 5.11 Finding Offset Alignments

The vector from the circle center to the *PI* of the known alignment is found by known coordinate information:

$$\vec{V}_{PI} = (X_{PI} - X_{CC})i + (Y_{PI} - Y_{CC})j \tag{5.109}$$

Considering that the two circular curves are concentric, it can be shown that the vector from the circle center to the *PI* of the offset alignment is equal to

$$\vec{V}_{PI'} = \left(\frac{R'}{R}\right)\vec{V}_{PI} \tag{5.110}$$

The vector from the *PI* of the known alignment minus the vector to the *PI* of the offset alignment is the vector difference of the two vectors from the circle center:

$$\Delta\vec{V} = \vec{V}_{PI'} - \vec{V}_{PI} = \left(\frac{R'}{R} - 1\right)\vec{V}_{PI} \tag{5.111}$$

The coordinates of the offset *PI* are found by adding this vector difference to the *PI* coordinates of the known *PI*:

$$PI'(X,Y) = PI(X,Y) + \Delta\vec{V} = PI(X,Y) + \left(\frac{R'}{R} - 1\right)\vec{V}_{PI} \tag{5.112}$$

The *POB* and *POE* of the offset alignment are located as offset points to the first and last tangent run using the approach described in Section 5.3. Note that significant accuracy is important in computing the offset *PI* locations to ensure that the resulting baselines are parallel.

Example 5.10: Find the alignment control points for an alignment offset 12 ft to the right of the centerline alignment of the example alignment.

The offset *POB* and *POE* are found by adding vectors perpendicular to the first and last tangent runs, scaled to a length of -12 ft to the coordinates of the centerline *POB* and *POE*.

$$\begin{aligned} POB' &= (500, 2500) + (-6.5248956i - 10.0710346j) \\ &= (493.4751044, 2489.9289654) \end{aligned} \tag{5.113}$$

$$\begin{aligned} POE' &= (8480, 2010) + (-11.3435300i - 3.9146300j) \\ &= (8468.6564700, 2006.0853700) \end{aligned} \tag{5.114}$$

The vectors from the circle centers to the *PI*s of the centerline alignment are

$$\begin{aligned} \vec{V}_{CC1-PI1} &= (3340 - 2685.979298)i + (660 - 2275.267700)j \\ &= 654.020702i - 1615.267700j \end{aligned} \tag{5.115}$$

$$\begin{aligned} \vec{V}_{CC2-PI2} &= (4340 - 5302.199416)i + (5000 - 3608.798529)j \\ &= -962.199416i + 1391.201471j \end{aligned} \tag{5.116}$$

$$\begin{aligned} \vec{V}_{CC3-PI3} &= (7600 - 6892.902672)i + (4560 - 3696.822560)j \\ &= 707.097328i + 863.177440j \end{aligned} \tag{5.117}$$

The coordinates of the *PI*s of the offset alignment are

$$PI(1)'(X,Y) = (3430,660) + \left(\frac{1012}{1000} - 1\right)\vec{V}_{CC1-PI1} = (3347.848248, 640.616788) \quad (5.118)$$

$$PI(2)'(X,Y) = (4340,5000) + \left(\frac{1238}{1250} - 1\right)\vec{V}_{CC2-PI2} = (4349.237114, 4986.644466) \quad (5.119)$$

$$PI(3)'(X,Y) = (7600,4560) + \left(\frac{938}{950} - 1\right)\vec{V}_{CC3-PI3} = (7591.068244, 4549.096706) \quad (5.120)$$

PART 2 – CONCRETE TOPICS

Chapter 6 – Geometry of Straight Bridges with Straight Precast Concrete Girders

6.1 Introduction

This chapter presents geometric calculations typical of straight bridges that lie on tangent runs. With regard to the superstructures of straight bridges, consideration will be given to the determination of

- Deck coordinates, elevations, grades, and cross slopes
- Girder elevations and haunch thicknesses

For substructure elements, consideration will be given to the determination of

- Bearing and bearing seat dimensions and orientations
- Pier cap layout and elevations

The scope of this chapter is limited to the discussion of girder-supported bridges with composite decks using the following longitudinal flexural elements:

- Precast concrete bulb-tee girders
- Precast concrete U-girders
- Steel plate girders
- Steel trapezoidal box girders

The approach to this chapter is to work through the geometry of an example straight bridge that follows the horizontal alignment, vertical profile, and superelevation descriptions in previous chapters. This example bridge will consist of precast concrete bulb-tee girders. Subsequent sections will then discuss differences in the geometry of straight bridges built with the three other girder types.

6.2 Example Bridge

Figure 6.1 shows a plan view of the horizontal alignment previously developed in this manual. The coordinates of the control points of the alignment baseline are provided in **Table 6.1**. A summary of the geometry of the example horizontal alignment, along with vertical profile and superelevation data, is provided in appendix B.

Table 6.1 Coordinates of Baseline Control Points for the Example Alignment

Point	Number	*X*, ft	*Y*, ft
POB	1	500.0	2500.0
PI(1)	2	3340.0	660.0
PI(2)	3	4340.0	5000.0
PI(3)	4	7600.0	4560.0
POE	5	8480.0	2010.0

Also shown in **Figure 6.1** is bridge 1, which is the example bridge for this chapter. The bridge lies on the initial tangent run of the example alignment, beginning at station 110+70 and ending at station 118+50. The bridge ends before the beginning of the first horizontal curve of the alignment. **Figure 6.2** shows a plan view layout of bridge 1. The bridge consists of six spans of 130 ft, for a total length of 780

ft. Abutments 1 and 7 at the ends of the bridge, and piers 2, 3, and 6, are oriented perpendicular to the alignment. Piers 4 and 5 are oriented with a skew of 30 degrees to accommodate an underlying roadway.

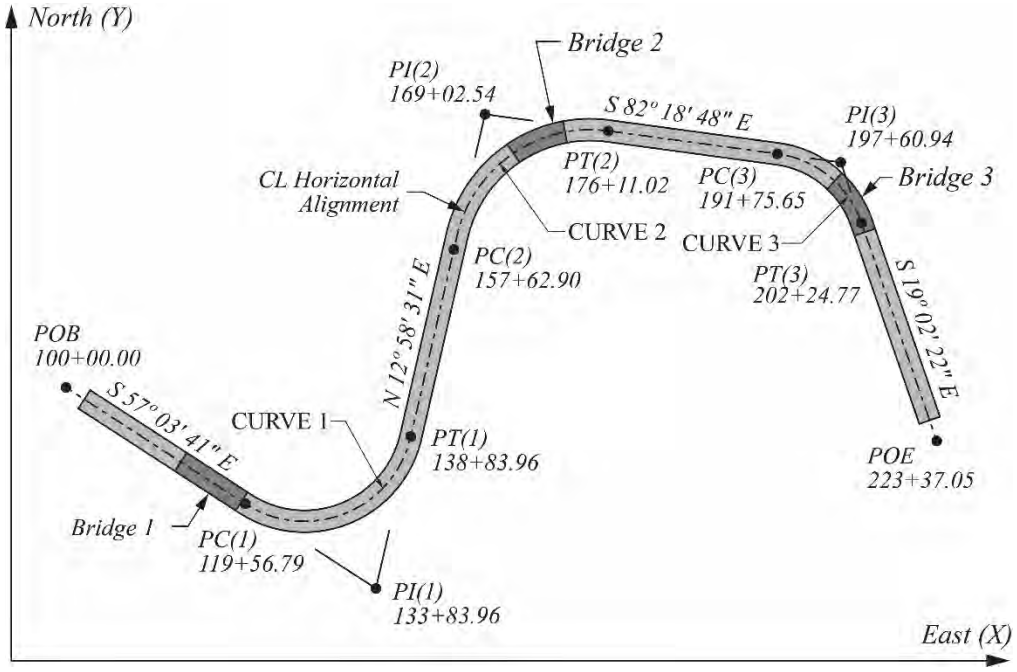

Source: PCI

Figure 6.1 Example Horizontal Alignment

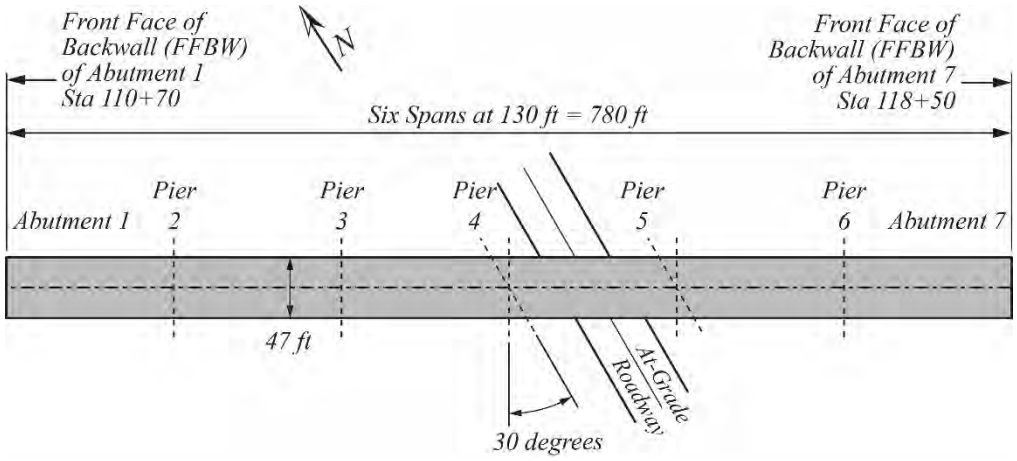

Source: PCI

Figure 6.2 Plan View of Example Bridge (Bridge 1)

The cross section of bridge 1 is shown in **Figure 6.3**. The centerline of the bridge coincides with the project horizontal alignment and *PGL*. The bridge roadway consists of two 12 ft travel lanes and two 10 ft shoulders. The out-to-out width of the bridge is 47 ft 0 in. Normal crown for the cross section consists of plus or minus 2 percent cross slopes about a crown break that coincides with the centerline of the bridge. The layout of the cross section is composed of four 72 in. bulb-tee girders with a centerline spacing of 12 ft 6 in. The girders support an 8 in. thick concrete deck slab.

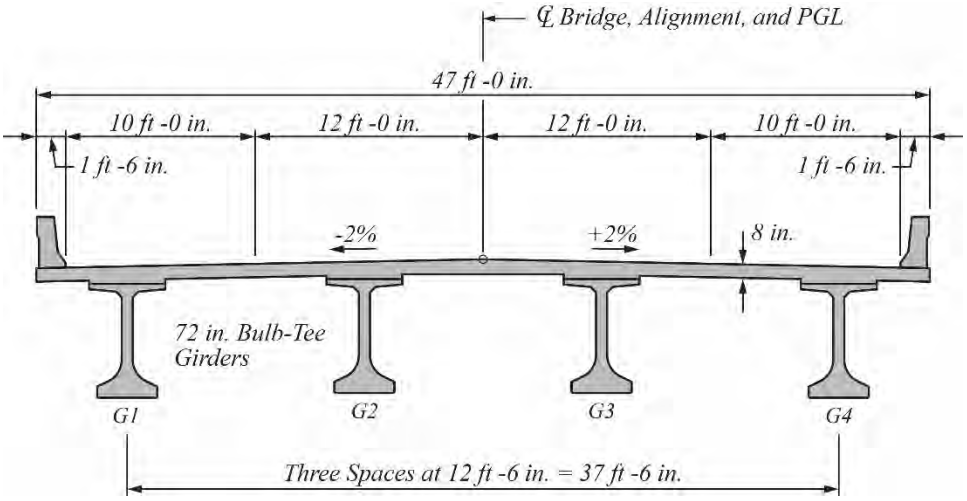

Source: PCI

Figure 6.3 Bridge 1 Cross Section

6.3 Example Geometry Calculations

6.3.1 Locate Coordinates of the Centerline of Bridge at Abutments and Pier Stations

Example 5.1 in Chapter 5 located the coordinates of a point at station 110+00 on the first tangent run of the example alignment using vector methods. That same approach is used to find the centerline coordinates at the stations of the piers.

The unit vector for the first tangent run was found in Example 5.1 as

$$\overrightarrow{U_{01}} = 0.83925288i - 0.54374130j \tag{6.1}$$

The unit vector is multiplied by the stationing difference between the pier stations and the *POB* station (100+00) and added to the coordinates of the *POB* (500, 2500) to find the coordinates at the pier stations. **Table 6.2** shows the change in station, components of the change in station multiplied by the corresponding components of the unit vectors, and the resulting coordinates at abutments and piers.

Table 6.2 Centerline Bridge Coordinates at Abutments and Piers

Pier	Station	*ΔSta*, ft	*ΔSta*(u_i), ft	*ΔSta*(u_j), ft	*CL X*(E), ft	*CL Y*(N), ft
Abt. 1	110+70	1070.0	898.00	581.80	1398.00	1918.20
2	112+00	1200.0	1007.10	652.49	1507.10	1847.51
3	113+30	1330.0	1116.21	723.18	1616.21	1776.82
4	114+60	1460.0	1225.31	793.86	1725.31	1706.14
5	115+90	1590.0	1334.41	864.55	1834.41	1635.45
6	117+20	1720.0	1443.51	935.24	1943.51	1564.76
Abt. 7	118+50	1850.0	1552.62	1005.92	2052.62	1494.08

6.3.2 Locate Coordinates of the Coping Lines at Abutment and Pier Stations

The coping lines are offset half of the bridge width from the centerline of the bridge. The left coping line is offset -23.5 ft from centerline and the right coping line is offset +23.5 ft. Points are located using the vector techniques presented in Section 5.3. The perpendicular unit vector to the right of the first tangent run is

$$\overline{U_R} = -0.54374130i - 0.83925288j \tag{6.2}$$

The perpendicular offset vectors to the coping lines are

$$\overline{V}(23.5) = -12.78i - 19.72j \tag{6.3}$$

$$\overline{V}(-23.5) = 12.78i + 19.72j \tag{6.4}$$

The offset vectors are added to the coordinates at the abutment and pier stations along the centerline to find the coordinates of the coping lines at those stations. **Table 6.3** shows the resulting coordinates for the coping line at the centerline of pier stations.

Table 6.3 Coping Line Coordinates at Abutment and Pier Stations

Pier	*CL X*(E), ft	*CL Y*(N), ft	*Left X*(E), ft	*Left Y*(N), ft	*Right X*(E), ft	*Right Y*(N), ft
Abt. 1	1398.00	1918.20	1410.78	1937.92	1385.22	1898.47
2	1507.10	1847.51	1519.88	1867.23	1494.33	1827.79
3	1616.21	1776.82	1628.98	1796.55	1603.43	1757.10
4	1725.31	1706.14	1738.09	1725.86	1712.53	1686.42
5	1834.41	1635.45	1847.19	1655.17	1821.63	1615.73
6	1943.51	1564.76	1956.29	1584.49	1930.74	1545.04
Abt. 7	2052.62	1494.08	2065.40	1513.80	2039.84	1474.36

6.3.3 Locate Coordinates of Coping Lines along the Skew of Piers 4 and 5

Piers 4 and 5 are oriented with a +30-degree skew in the sign convention of this manual. The coordinates of the coping lines along the skew lines of the centerline of these piers can be found using the vector methods shown in Section 5.4. The perpendicular unit vector to the right of the first tangent run is

$$\overline{U_R} = -0.54374130i - 0.83925288j \tag{6.5}$$

The direction angle of this unit vector is found from Eq. (2.6):

$$\theta = 180 + \tan^{-1}\left(\frac{\Delta Y_i}{\Delta X_i}\right) = 180 + \tan^{-1}\left(\frac{-0.83925288}{-0.54374130}\right) = 237.0613 \text{ degrees} \tag{6.6}$$

The direction angle of the skew pier orientation is

$$\theta = 237.0613 + 30 = 267.0613 \text{ degrees} \tag{6.7}$$

The unit vector of the skew pier orientation is

$$\overline{U}(\text{skew right}) = \cos\left(267.0613\right)i + \sin\left(267.0613\right)j \tag{6.8}$$

which becomes

$$\overline{U}(\text{skew right}) = -0.05126734i - 0.99868497j \tag{6.9}$$

The offset dimension to the right coping line along the skew pier orientation is

$$Offset = \frac{23.5}{\cos\left(30\right)} = 27.1355 \text{ ft} \tag{6.10}$$

The offset vectors to the left and right coping line along the skew pier orientation are

$$\bar{V}(\text{skew left}) = 1.3912i + 27.0998j \quad (6.11)$$

$$\bar{V}(\text{skew right}) = -1.3912i - 27.0998j \quad (6.12)$$

The offset vectors are added to the coordinates at the pier stations along the centerline to find the coordinates of the coping lines along the skew pier orientation. **Table 6.4** shows the resulting coordinates for the coping line of piers 4 and 5.

Table 6.4 Coping Line Coordinates along Skew at Piers 4 and 5

Pier	*CL X*(E), ft	*CL Y*(N), ft	*Left X*(E), ft	*Left Y*(N), ft	*Right X*(E), ft	*Right Y*(N), ft
4	1725.31	1706.14	1726.70	1733.24	1723.92	1679.04
5	1834.41	1635.45	1835.80	1662.55	1833.02	1608.35

6.3.4 Compute Elevations of Centerline Bridge at Abutment and Pier Stations

Figure 6.4 shows the vertical profile for the example alignment was developed in chapter 3. **Figure 6.5** shows a closer view of the beginning of the vertical profile, from the *VPOB* through the first vertical curve. **Figure 6.5** also shows the location of bridge 1 along the vertical profile. The first span of the bridge lies on the 1.75 percent constant grade that begins with the *VPOB*. The remaining five spans lie along the first vertical curve.

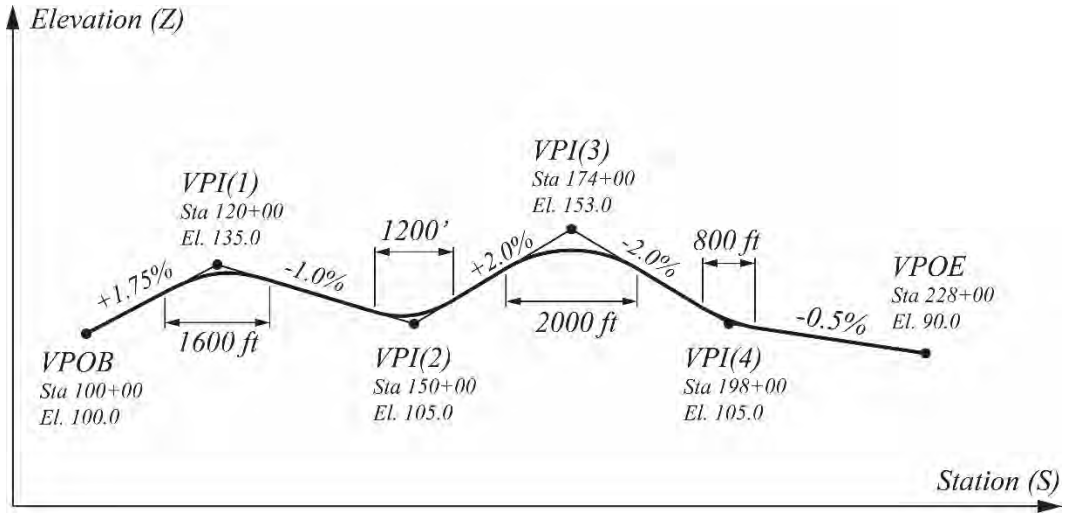

Source: PCI

Figure 6.4 Vertical Profile for Example Alignment

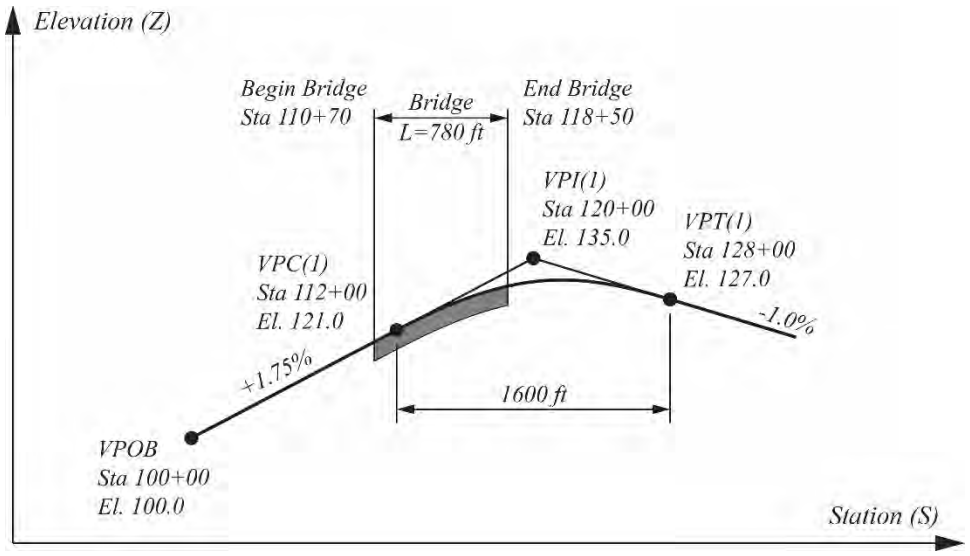

Source: PCI

Figure 6.5 Vertical Profile at Bridge 1

Points along the constant grade portion of the profile beginning with the *VPOB* are found by

$$Z(\Delta Sta) = Z_{VPOB} + gr_1 \Delta Sta = 100.0 + 0.0175\Delta Sta \tag{6.13}$$

Elevations along the first vertical curve are found by

$$Z(\Delta Sta) = \left(\frac{gr_2 - gr_1}{2L_{VC}}\right)\Delta Sta^2 + gr_1 \Delta Sta + Z_{VPC} \tag{6.14}$$

which becomes

$$Z(\Delta Sta) = \left(\frac{-.01 - .0175}{2(1600)}\right)\Delta Sta^2 + 0.0175\Delta Sta + 121.0 \tag{6.15}$$

Instantaneous grades along the first vertical curve are found by

$$gr(\Delta Sta) = \left(\frac{gr_2 - gr_1}{L_{VC}}\right)\Delta Sta + gr_1 = \left(\frac{-0.01 - .00175}{1600}\right)\Delta Sta + 0.0175 \tag{6.16}$$

Table 6.5 shows the resulting elevations and grades along the centerline of the alignment at the stations of the piers computed using Eq. (6.13), (6.14), and (6.16).

Table 6.5 Centerline Alignment Elevations and Grades at Pier Stations

Pier	Station	Elevation, ft	Grade
Abt. 1	110+70	118.73	0.0175
2	112+00	121.00	0.0175
3	113+30	123.13	0.0153
4	114+60	124.97	0.0130
5	115+90	126.52	0.0108
6	117+20	127.78	0.0086
Abt. 7	118+50	128.74	0.0063

6.3.5 Compute Elevations of Coping Lines at Abutment and Pier Stations

Elevations of points across the cross section of a straight bridge are computed by subtracting relative elevations within the normal crown from the *PGL* elevations. The relative elevations are found by considering the cross slopes, crown points, and transverse dimensions of the normal crown of the roadway.

Bridge 1 coping elevations are found by subtracting from the *PGL* the 2 percent cross slope multiplied by half the bridge width (23.5 ft). The differential elevations of the left and right coping lines of bridge 1 are

$$\Delta Z_{left} = \left(-0.02\left(-23.5 \text{ ft}\right)\right) = 0.47 \text{ ft} \tag{6.17}$$

$$\Delta Z_{right} = \left(0.02\left(23.5 \text{ ft}\right)\right) = 0.47 \text{ ft} \tag{6.18}$$

The final elevations are found by subtracting these differential elevations from the *PGL* elevations. The results for the left and right coping elevations are shown in **Table 6.6**.

Table 6.6 Coping Line Elevations at Pier Locations

Pier	Station	*CL* elevation, ft	Left coping elevation, ft	Right coping elevation, ft
Abt. 1	110+70	118.73	118.26	118.26
2	112+00	121.00	120.53	120.53
3	113+30	123.13	122.66	122.66
4	114+60	124.97	124.50	124.50
5	115+90	126.52	126.05	126.05
6	117+20	127.78	127.31	127.31

Table 6.6 shows the elevations for the left and right coping at abutment 1 and the five pier locations. The elevations for the coping lines at abutment 7 are not shown in this table. The reason for this is that Eq. (6.17) and (6.18) are valid only for locations where the cross section is in normal crown. A portion of the last span of bridge 1 includes the beginning of the tangent runout leading to curve 1. As curve 1 is to the left, the left coping remains at the normal crown position through the tangent runout and into the superelevation runoff. The right coping rises throughout the tangent runout.

Figure 6.1 shows a portion of the superelevation diagram for curve 1 of bridge 1. The location of the front face of back wall station is also shown in **Figure 6.6**. The cross slope on the right side of the *PGL* has changed from +2.0 percent to -0.44 percent.

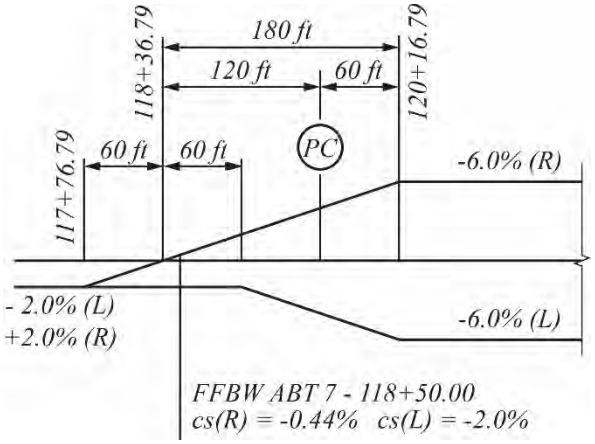

Source: PCI

Figure 6.6 Curve 1 Entry Superelevation Diagram

The differential elevation of the right coping line relative to the bridge centerline is

$$\Delta Z_R = \left(-0.0044\left(23.5 \text{ ft}\right)\right) = 0.10 \text{ ft} \tag{6.19}$$

Subtracting the negative differential elevation from the *PGL* produces an elevation of the right coping at the front face of backwall (*FFBW*) of abutment 7 that is higher than the *PGL* elevation. The elevation of the left coping line at this location is still 0.47 ft lower than the *PGL* elevation. **Table 6.7** shows the results for the left and right coping elevations. The cross section of the bridge at the *FFBW* of abutment 7 is shown in **Figure 6.7.**

Table 6.7 Coping Line Elevations at Front Face of Backwall of Abutment 7

Pier	Station	*CL* elevation, ft	Left coping elevation, ft	Right coping elevation, ft
Abt. 7	118+50	128.74	128.27	128.84

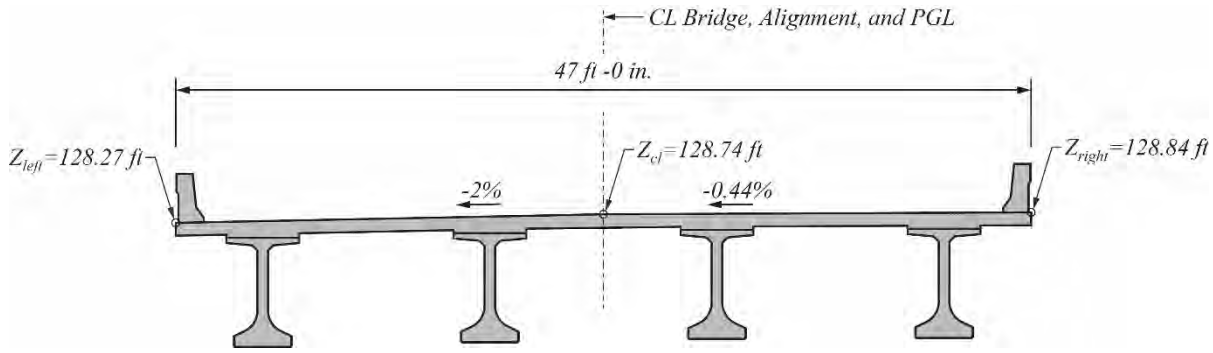

Source: PCI

Figure 6.7 Superelevations at Station of Front Face of Backwall at Abutment 7

6.4 Haunch Thickness

The bridge deck slab is cast to produce a desired roadway surface. Precast, prestressed concrete girders of straight bridges have fabrication constraints that keep girders from exactly following the intended profile of the deck slab. Haunches, similar to that shown in **Figure 6.8**, are cast to make up the difference in geometry between the deck slab and the girders. Horizontal shear reinforcement in the deck slab and prestressed girders develops composite behavior of the deck–girder cross section. The

working point *WP* for haunch thickness calculations is located at the top center of the precast concrete girder as shown in **Figure 6.8**.

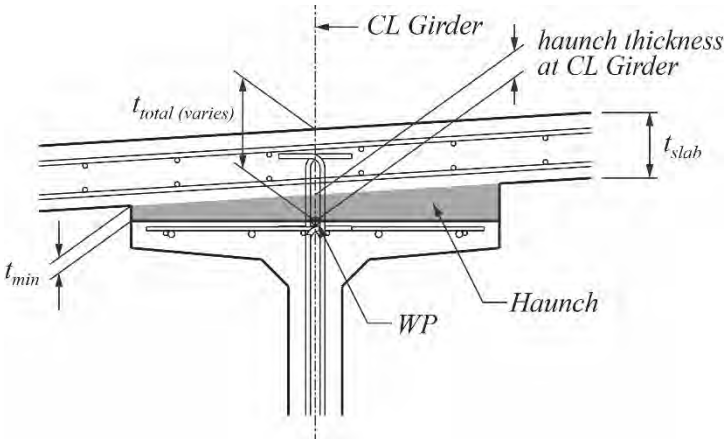

Source: PCI

Figure 6.8 Typical Haunch for a Girder–Deck Slab Bridge

The remainder of this section will develop haunch thicknesses for the precast concrete bulb-tee girders for example bridge 1. Differences in haunch characteristics for the other girder types will be discussed in later sections.

6.4.1 Haunch Thickness for Precast Concrete Bulb-Tee Girders

The thicknesses of haunches along the length of a girder vary to accommodate geometric and deflection characteristics of each girder in a bridge. Girder haunch thicknesses calculated at the centerlines of the bearings can affect the elevations at which the girders are erected.

Haunch thicknesses along the centerline of the precast concrete girders are found by considering the following factors:

- Minimum haunch thickness
- Deck slab cross slope across the top flange
- Deck slab vertical profile along the length of the girder
- Noncomposite girder deflections and camber
- Composite girder permanent deflections

6.4.1.1 Adjustment for Minimum Haunch Thickness

The details of **Figure 6.8** show a minimum thickness of haunch. This minimum dimension accounts for the forming of the deck slab between the girders and the haunch itself. The minimum haunch thickness can vary with the type of forming system used for the slab. Stay-in-place forms may produce a different minimum thickness compared with formwork stick-built out of lumber. The owner agency may have minimum thickness requirements or specifications.

Minimum haunch thicknesses between 1 and 2 in. are common. For the purposes of bridge 1, the example bridge of this chapter, a minimum haunch thickness of 1 in. is used:

$$t_{min} = 1 \text{ in.} \tag{6.20}$$

The implication of this minimum thickness is that the bearing seat elevations at both ends of the girder should be lowered 1 in. to achieve proper deck geometry.

6.4.1.2 Adjustment for Cross Slope

The minimum haunch thickness is set at the low side of the deck slab at the edge of the top flange of the bulb-tee girder. **Figure 6.9** shows a cross section of a haunch with the cross slope falling to the left.

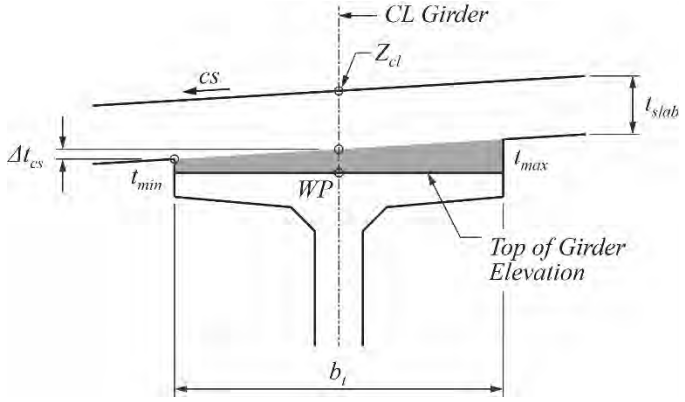

Source: PCI

Figure 6.9 Typical Haunch for Girder-Deck Slab Bridges

The magnitude of the cross slope multiplied by half the width of the top flange produces a second adjustment in haunch thickness. Expressed in equation form, the adjustment for cross slope is

$$\Delta t_{cs} = |cs| \frac{b_t}{2} \tag{6.21}$$

where

Δt_{cs} = change in haunch thickness as a result of cross slope

$|cs|$ = absolute value of the cross slope at the cross section under consideration

b_t = width of the top flange of the girder

The first five spans of bridge 1 are in normal crown, with -2 percent cross slope to the left of the centerline of the bridge and +2 percent to the right. Assuming a top flange width of 4 ft, the adjustment for cross slope for the girders in these spans is

$$\Delta t_{cs} = 0.02\left(\frac{48 \text{ in.}}{2}\right) = 0.48 \text{ in.} \tag{6.22}$$

As discussed in Section 6.3.5, a portion of the last span of bridge 1 lies on the tangent runout of the first horizontal curve of the alignment. The cross slope of the left half of the bridge remains in -2 percent cross slope over the entire span length. The vertical adjustment for cross slope of the girders to the left of centerline is 0.48 in. as computed above. The cross slope on the right side of centerline begins at +2 percent, and at station 117+76.79 begins rotating counterclockwise to a cross slope of -0.44 percent at the end of the bridge. The adjustment for cross slope for the girders to the right of the centerline of the bridge at the abutment 7 is

$$\Delta t_{cs} = 0.0044\left(\frac{48 \text{ in.}}{2}\right) = 0.1056 \text{ in.} \tag{6.23}$$

As with the minimum thickness of the haunch, the bearing seat elevations at both ends of the girder should be lowered by the cross-slope adjustment to achieve proper deck geometry.

6.4.1.3 Adjustment for Bridge Profile

A third adjustment to haunch thickness is needed to accommodate the profile grade within the span. **Figure 6.10** shows an elevation view of a span constructed with a straight, uncambered girder. The profile of this span is a constant grade, similar to span 1 of bridge 1. The minimum thickness of the haunch can be achieved throughout the span, as the deck slab and girder follow the same slope.

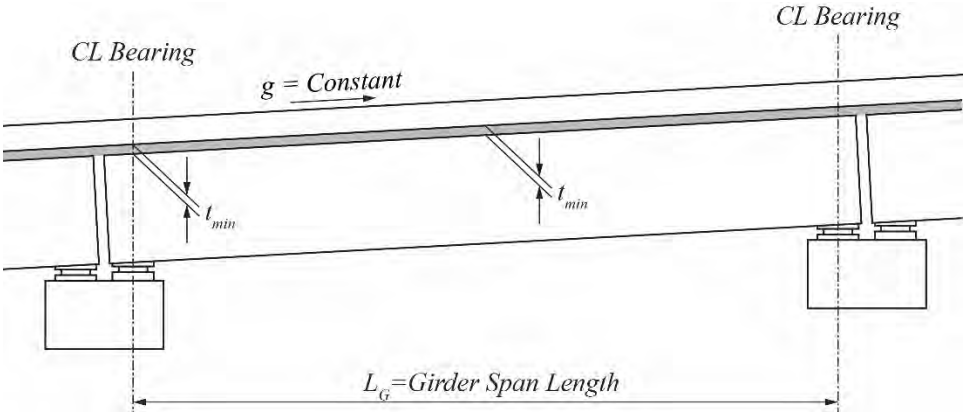

Source: PCI

Figure 6.10 Span on Constant Grade with Girder with No Camber

Figure 6.11 shows a span for which the profile is a crest vertical curve, similar to spans 2 through 6 of bridge 1. In this case, the minimum haunch thickness is located at the ends of the girder. Between the ends of the girder, the deck slab rises and falls relative to the top surface of the uncambered girder. The haunch thickness is adjusted to fill the gap between the deck slab and the top of the girder. The adjustment in the haunch thickness along the length of the girder due to the crest vertical curve can be found by subtracting the elevations at the top of deck from a reference line, which is a chord between the deck-level centerline of bearing elevations. This difference in elevation, which is equal to the haunch adjustment, is expressed as

$$\Delta t_{pr} = Z(x) - \left(Z_1 + \left(\frac{Z_2 - Z_1}{L_G} \right) x \right) \tag{6.24}$$

where

Δt_{pr} = Change in haunch thickness as a result of vertical profile
$Z(x)$ = Centerline of girder bridge deck elevation at x along the span
Z_1 = Centerline of girder bridge deck elevation at beginning of the span
Z_2 = Centerline of girder bridge deck elevation at end of the span
L_G = Girder Span length
X = Horizontal Distance from CL Bearing at beginning of the span

Note that the crest curve, in maintaining the minimum haunch thickness at the centerlines of bearing, does not cause the girder to be lowered further than the adjustments of the previous sections.

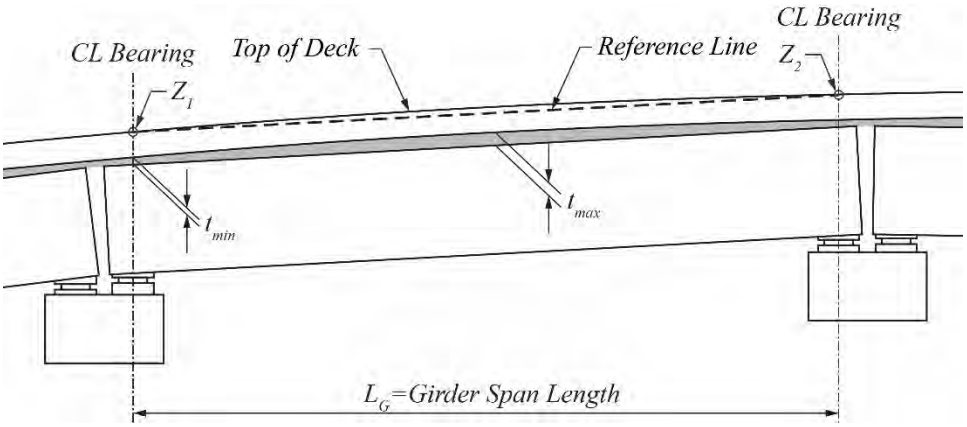

Source: PCI

Figure 6.11 Profile Grade Adjustment for Crest Curves

Figure 6.12 shows a span of a bridge with a profile that follows a sag vertical curve. In this case, the minimum thickness of haunch is located within the span, and maximum haunch thickness is at the bearings. The previous equation is used to again determine the adjustment in beam elevation and haunch thickness. Girder elevations are lowered in the case of the sag curve to accommodate the increased haunch at the bearings.

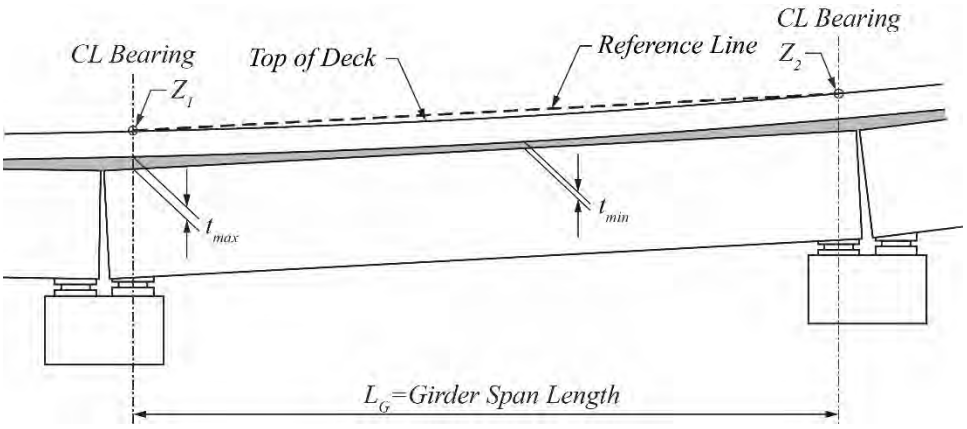

Source: PCI

Figure 6.12 Varying Haunch for Sag Curves with Girder with No Camber

It should be noted in **Figure 6.10, Figure 6.11**, and **Figure 6.12** that the ends of the girders are drawn perpendicular to the tops and bottoms of the uncambered girders. This is done to draw attention to the shape of the gaps between adjacent girder ends. Some bridge owners prefer to cast the ends of the girders, so that they are vertical in the erected position after all permanent loads are applied.

Consider the interior girder to the right of the centerline of bridge (girder 3) in span 2 of bridge 1 as an example. **Figure 6.8** presents the calculation of Eq. (6.24) for this girder at tenth-point stations along the length of the girder. The third column of **Table 6.8** lists the top of deck elevations along the centerline of girder 3 in span 2 following the vertical profile. The fourth column of **Table 6.8** lists the elevations along a straight line between the top of deck elevations at pier 2 and pier 3. The last column lists the differences in the top of deck and straight-line elevations.

Table 6.8 Bridge 1, Girder 3 in Span 2 Adjustments for Profile

Tenth point	Station	Deck elevation along *centerline* of girder, ft	Straight-line elevation, ft	Δt_{pr}, ft
1(P2)*	112+00	120.875	120.875	0
2	112+13	121.101	121.088	0.013071
3	112+26	121.3242	121.301	0.023238
4	112+39	121.5444	121.5139	0.030499
5	112+52	121.7618	121.7269	0.034856
6	112+65	121.9762	121.9399	0.036308
7	112+78	122.1877	122.1529	0.034856
8	112+91	122.3963	122.3658	0.030499
9	113+04	122.6021	122.5788	0.023237
10	113+17	122.8049	122.7918	0.013071
11(P3)*	113+30	123.0048	123.0048	0

* Tenth points 1 and 11 are at the centerline of the pier.

The maximum adjustment occurs at midspan of span 2 of bridge 1, point 6 in **Table 6.8**. The adjustment for the example of girder 3 in span 2 is then

$$\Delta t_{pr} = 0.0363 \text{ ft} = 0.44 \text{ in.} \tag{6.25}$$

6.4.1.4 Adjustment for Non-Composite Bridge Deflections

The adjustments computed in the previous sections considered the girders as rigid bodies, straight and uncambered along their length. In actuality, the prestressed concrete girders deflect at various stages of construction under the application of the prestressing force, self-weight, and superimposed dead loads. The deflected shape of the girder under the action of loads applied to the noncomposite acting girder should be considered in determining haunch dimensions and girder elevations.

Equations for noncomposite deflections in this chapter are presented in simplistic form for the purpose of presenting their impact on geometric calculations. Refer to the binding American Association of State and Highway Transportation's (AASHTO) *LRFD Bridge Design Specifications* (AASHTO BDS) (AASHTO, 2017a) (incorporated by reference per 23 CFR 625.4(d)(1)(v)) for procedures for determining these deflections, and the non-binding Precast/Prestressed Concrete Institute's *PCI Bridge Design Manual* (PCI, 2011) for supplemental material.

6.4.1.4.1 Adjustment for Camber

Girder camber is first observed in the casting yard when the force in the pretensioning strands is transferred from the stressing bulkheads to the hardened concrete. As the girder begins to deflect upward, the self-weight of the girder begins to act in the downward direction. The difference in the deflections of these two loads is the camber of the girder at transfer. This condition of camber is shown in **Figure 6.13**.

The camber at transfer can be expressed as

$$\Delta_{ce} = \Delta_{ps}(\uparrow) + \Delta_{sw}(\downarrow) \tag{6.26}$$

where

Δ_{ce} = Midspan girder camber at transfer, ft
Δ_{ps} = Upward deflection as a result of the application of the prestressing force, ft
Δ_{sw} = Downward deflection as a result of engaging the girder self-weight, ft

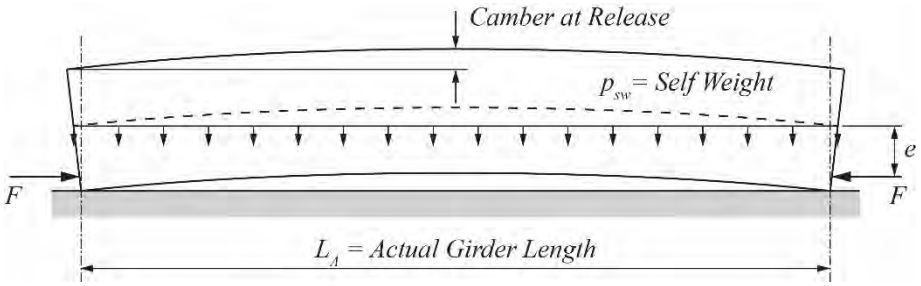

Source: PCI

Figure 6.13 Prestressed Girder Camber

For the case of a constant force of prestressing at a constant eccentricity along the entire length of the girder, the deflection resulting from the application of the prestressing force is

$$\Delta_{ps} = \frac{FeL_A^2}{8E(t)I} \tag{6.27}$$

where

F = Prestressing force after transfer, kip
e = Eccentricity of the prestressing force, ft
L_A = Actual length of the girder, ft
$E(t)$ = Modulus of elasticity of the concrete at time of transfer, kip/ft^2
t = Age of concrete at loading, days
I = Moment of inertia of the cross section of the girder, ft^4

The case of deflection based on a constant force over the full length of the girder is shown here for simplicity. More exacting calculations should be made to consider force variations over transfer lengths, debonding of strands, and draped tendons. Refer to the *PCI Design Handbook* and *PCI Bridge Design Manual* for more information regarding camber.

The deflection resulting from the self-weight of the girder is

$$\Delta_{sw} = \frac{5p_{sw}L_A^4}{384E(t)I} \tag{6.28}$$

where

p_{sw} = Uniform load of the self-weight of the girder, kip/ft

Eq. (6.26) can then be expressed as

$$\Delta_{ce} = \frac{FeL_A^2}{8E(t)I} - \frac{5p_{sw}L_A^4}{384E(t)I} \tag{6.29}$$

6.4.1.4.2 Adjustment for Noncomposite Superimposed Loads

Superimposed dead loads acting on the noncomposite girder applied after girder erection will deflect the girder in the downward direction. This deflection changes girder elevations and the needed thickness of the haunch. The noncomposite superimposed dead loads include the weight of the deck slab (including the haunch), the weight of stay-in-place forms (if used), and the weight of any permanent diaphragms placed before composite action. **Figure 6.14** shows the deflected shape of the girder under the action of a uniformly distributed superimposed dead load.

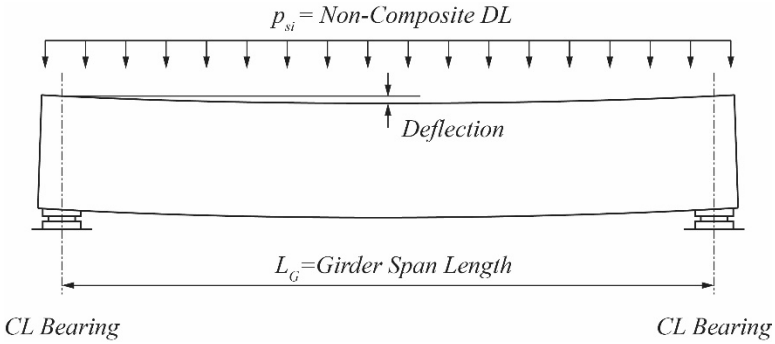

Source: PCI

Figure 6.14 Noncomposite Dead Load Deflection after Erection

The noncomposite deflections applied as a uniformly repeating load are computed as

$$\Delta_{si} = \frac{5 p_{si} L_G^4}{384 E(t) I} \tag{6.30}$$

where

p_{si} = noncomposite superimposed dead loads applied to girder

6.4.1.4.3 Total Adjustments for Noncomposite Bridge Deflections

The net camber at midspan of the girder is found as the camber at transfer (Eq. [6.29]) minus the deflection resulting from the application of superimposed dead loads (Eq. [6.30]):

$$\Delta_{nc} = \left(\frac{F e L_A^2}{8 E(t) I} - \frac{5 p_{sw} L_A^4}{384 E(t) I} \right) - \left(\frac{5 p_{si} L_G^4}{384 E(t) I} \right) \tag{6.31}$$

where

Δ_{nc} = Net camber at midspan, ft

The noncomposite net camber predicted by Eq. (6.31) is the instantaneous elastic deflection, based on prestress forces and moduli of elasticity consistent with the age of the particular loading (at transfer or at placement of noncomposite superimposed dead loads). The time-dependent nature of the concrete creep will cause the instantaneous net camber to grow with time. This camber growth should be accounted for by considering the age of the girder from transfer to casting the deck slab. The binding AASHTO BDS (AASHTO, 2017a) (incorporated by reference per 23 CFR 625.4(d)(1)(v)) and the non-binding Precast/Prestressed Concrete Institute's *PCI Bridge Design Manual* (PCI, 2011) provide detailed methodologies for including time-dependent material effects in predicting camber. For the purposes of this manual, a simplified expression is presented:

$$\Delta_{cr}(t) = \phi(t) \Delta_e \tag{6.32}$$

where

Δ_{cr} = Creep deflection at time t
Δ_e = Elastic deflection
ϕ = Creep factor from age at loading to time t
t = Time from noncomposite loading to composite behavior

The noncomposite net camber including time-dependent concrete behavior is then

$$\Delta_{nc} = \left(\frac{FeL_A^2}{8EI} - \frac{5p_{sw}L_A^4}{384EI} \right)(1+\phi_1) - \frac{5p_{si}L_G^4}{384EI}(1+\phi_2) \tag{6.33}$$

where

ϕ_1 = Creep factor for camber
ϕ_2 = Creep factor for noncomposite superimposed dead loads

Figure 6.15 shows the net deflected shape of the prestressed concrete girder considering all noncomposite deflections. The net camber Δ_{nc} is upward in **Figure 6.15**. This is typically the case for pretensioned concrete girders, as the camber values are typically greater than the other noncomposite deflections.

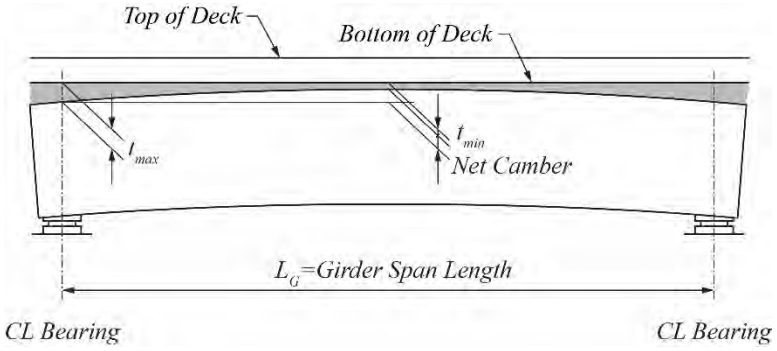

Source: PCI

Figure 6.15 Haunch Variation to Accommodate Net Camber

Girder 3 in span 2 of Bridge 1 is considered again as an example. The bulb-tee girder assumed in this example is the 72 in. Florida I-beam (FIB). The cross-sectional and other characteristics used to evaluate girder deflections are shown in **Table 6.9**. For simplicity of this example the actual girder length and girder span length are set equal to the 130 ft span length.

Table 6.9 Noncomposite Dead Load Deflection after Erection

Characteristic	Symbol	Unit	Value
Girder cross-sectional area	A	ft^2	7.35
Girder moment of inertia	I	ft^4	35.71
Actual girder length ≈ Girder Span Length	$L_A = L_G$	ft	130.0
Concrete modulus of elasticity	E	lb/ft^2	630,000.0
Prestressing force	P	kip	2400.0
Girder self-weight	p_{sw}	kip/ft	1.10
Noncomposite superimposed dead load	p_{si}	kip/ft	1.40
Eccentricity of the prestressing strands	E	ft	2.17

A constant modulus of elasticity is used in this example for simplicity. The components of the midspan deflections on the noncomposite section are

$$\Delta_{ps} = \frac{FeL_A^2}{8EI} = \frac{2400(2.17)(130)^2}{8(630{,}000)(35.71)} = 0.4890 \text{ ft} = 5.87 \text{ in.} \tag{6.34}$$

$$\Delta_{sw} = \frac{5p_{sw}L_A^4}{384EI} = \frac{5(1.1)(130)^4}{384(630{,}000)(35.71)} = 0.1818 \text{ ft} = 2.18 \text{ in.} \tag{6.35}$$

$$\Delta_{si} = \frac{5p_{si}L_G^4}{384EI} = \frac{5(1.4)(130)^4}{384(630{,}000)(35.71)} = 0.2314 \text{ ft} = 2.77 \text{ in.} \tag{6.36}$$

The net camber at midspan is found by adding time-dependent effects according to Eq. (6.34). For the purposes of this example, assume the creep factor on camber is 0.8 and the creep factor on superimposed loads is 0.2. The net camber is then

$$\Delta_{nc} = (5.87 - 2.18)(1.8) - 2.77(1.2) = 3.32 \text{ in.} \tag{6.37}$$

6.4.1.5 Deflections Resulting from Superimposed Loads on the Composite Section

Another adjustment can be added to the total haunch dimensions that accounts for the loads from the weights of traffic barriers, future wearing surface, lighting poles, signing, and utilities that are applied to the deck slab/girder composite section (Δ_{comp}). Often, these are small in magnitude and are not included in the adjustment calculations. The requirements of the agency building the bridge should be consulted as to whether the desired profile is to be achieved at the end of deck slab placement, at the end of construction, or some other time.

6.4.1.6 Summary of Haunch Thicknesses

The haunch dimensions and adjustments to girder elevations can be determined by summing the applicable adjustments described in the previous sections. The general expression for the thickness of the haunch is

$$t_{total} = t_{\min} + \Delta t_{cs} + \Delta t_{pr} + \Delta t_{nc} + \Delta t_{comp} \tag{6.38}$$

At midspan of girder 3 in span 2 of bridge 1, all adjustments in the thickness of the haunch are applicable, except for the adjustment for camber deflection. The upward camber is greater than the downward superimposed load deflection so that the adjustment is made at the ends of the girder. Assuming permanent composite deflections are small, the resulting haunch thickness at midspan is

$$t_{total} = t_{\min} + \Delta t_{cs} + \Delta t_{pr} = 1 + 0.48 + 0.44 = 1.92 \text{ in.} \tag{6.39}$$

At the ends of girder 3 in span 2, the adjustment for vertical profile does not apply, as the profile follows a crest curve (see **Figure 6.11**). The resulting haunch thickness at the ends of the girder is

$$t_{total} = t_{\min} + \Delta t_{cs} + \Delta t_{nc} = 1 + 0.48 + 3.32 = 4.80 \text{ in.} \tag{6.40}$$

6.4.2 Haunch Thickness for Precast Concrete U-girders

Adjustments to girder elevations and haunch dimensions for concrete U-girders are similar to those made for concrete bulb-tee girders. The major difference is that U-girders can be erected to a specified superelevation. **Figure 6.16** shows a U-girder positioned below the deck slab of a bridge with a constant cross slope. The U-girder in this figure has been placed to follow the slope of the bridge deck.

Haunch adjustments for cross slope in this instance are not needed in setting beam elevations. Bearing details are modified to accommodate the tilt of the U-girder.

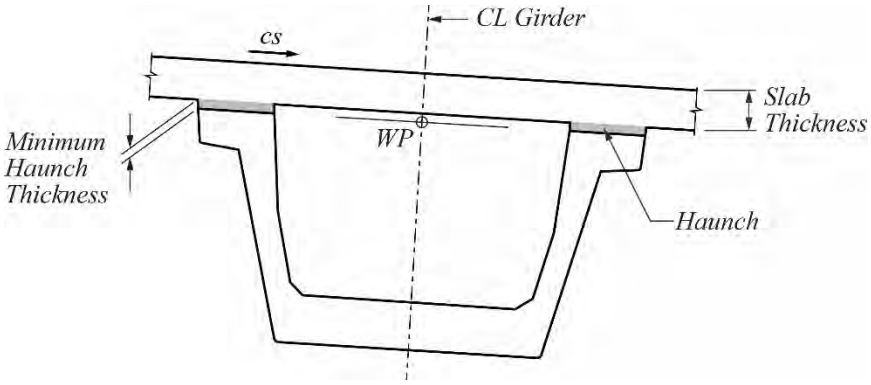

Source: PCI

Figure 6.16 Precast U-girder Placed along Cross Slope

In spans with varying superelevation, the haunches should be adjusted to accommodate the difference between deck slab and U-girder cross slope. **Figure 6.17** shows this condition. An extreme instance of this is when the U-girders are erected without cross slope and the deck slab has superelevation. More information regarding the adjustments for haunch thicknesses is provided in Chapter 9.

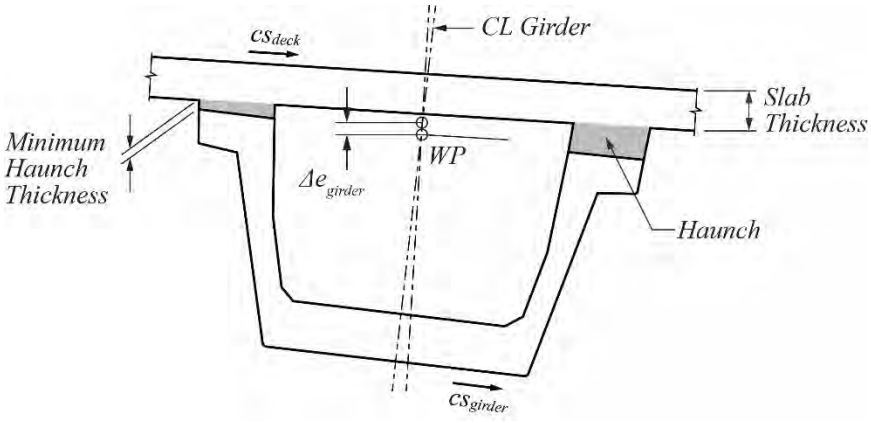

Source: PCI

Figure 6.17 Precast Concrete U-girder Placed along Cross Slope

6.4.3 Haunch Thickness for Steel Plate Girders

For a detailed discussion of steel plate girder camber and haunch, refer to Chapter 10.

Steel plate girders can be fabricated with a specified camber so that adjustments to girder elevations and haunch dimensions can be minimized. Deflections resulting from girder self-weight, superimposed dead loads on the noncomposite section, and superimposed dead loads on the composite section (if included), inverted to produce the cambered shape, are provided to the fabricator. Adjustments for bridge profile can be calculated and included with the camber information. Depending on the variability of the profile along the length of, or across the width of, the bridge, the fabricator may fabricate one girder shape for a range of profile adjustments. An additional minimum haunch thickness may be used to account for the fabricated dimensions and the geometry needed for a particular girder. The only adjustment to girder elevations and haunch dimensions when laying out the steel girder

bridge is that regarding cross slope. Figure 6.18 shows the haunch for a bridge deck on a steel plate girder. As flange thickness can vary along the length of the girder, the working point for geometric calculations is often at the top of the web.

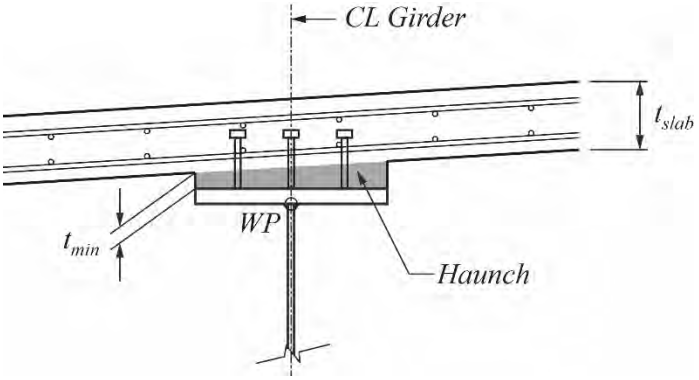

Source: PCI

Figure 6.18 Haunch for Steel Plate Girder

6.4.4 Haunch Thickness for Steel Trapezoidal Box Girders

For a detailed discussion of steel trapezoidal box girders, refer to Chapter 12.

As with steel plate girders, the fabricator can control the shape of the steel trapezoidal box girder to account for deflections resulting from girder self-weight and superimposed dead loads (noncomposite and composite). Similar to the precast concrete U-girder, the steel trapezoidal box girder is rotated to be aligned with the cross slope of the bridge. As such, the only adjustment to girder elevations and haunch dimensions that may be needed is to compensate for fabricated versus theoretical differences. **Figure 6.19** shows the haunches for a typical trapezoidal box girder.

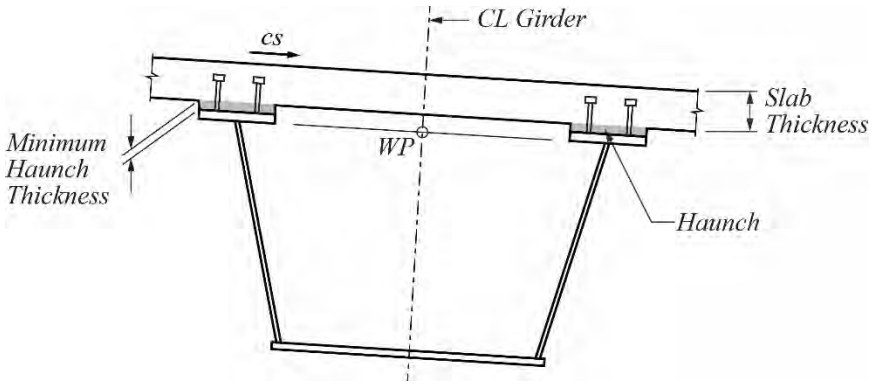

Source: PCI

Figure 6.19 Haunches for Steel Trapezoidal Box Girders

6.5 Bearing Seat Thickness and Pier Top Elevations

Accurate bearing seat elevations are needed to ensure that superstructure girders are erected in the correct position. Bearing seat elevations are computed using the following information:

- Top-of-deck elevations
- Haunch thicknesses at the pier
- Superstructure dimensions
- Dimensions and details of bearing components

Figure 6.20 shows a typical cross section of a concrete girder superstructure and a portion of the supporting substructure of bridge 1. The precast concrete girders are erected as simple spans, supported on the pier cap by a bearing assembly composed of a bearing plate, the bearing itself, and the bearing seat. The centerlines of the bearings are offset longitudinally from the centerline of pier to accommodate the width of the bearings and appropriate edge distances from the end of the girders and pier cap.

The stations of the centerlines of the bearings for a straight bridge are found by adding or subtracting the bearing offset (*s* in **Figure 6.20**) from the station of the centerline of the pier. Top-of-deck elevations Z_D and Z_U at the stations of the centerlines of bearings are found from the vertical profile. Working points are established at the center of the bearings at the bottom of the girders. The elevations of the working points are found by subtracting the depth of the superstructure from deck elevations Z_D and Z_U.

Note that **Figure 6.20** shows the condition with the end of the precast concrete girder cast so that the joint between girders is vertical. Many transportation agencies cast the beams square and allow the joint to be inclined perpendicular to the grade of the bridge.

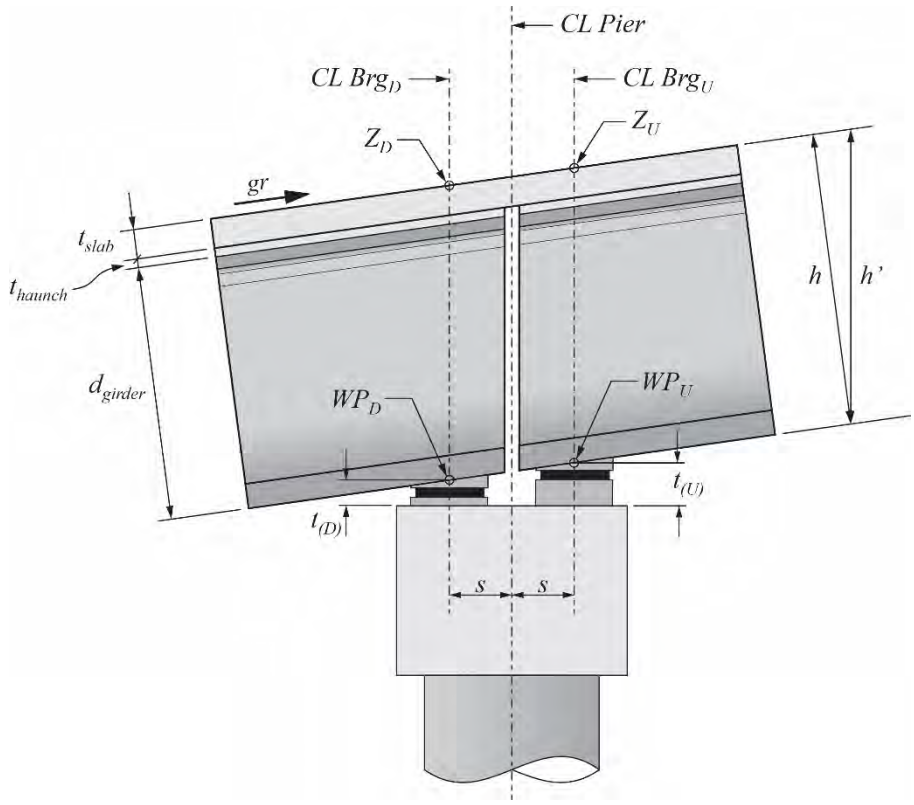

Source: PCI

Figure 6.20 Precast Concrete Girder Bridge Geometry at a Pier

The total bridge depth, *h* perpendicular to the roadway grade is found as the sum of the slab thickness, the haunch thickness at the end of the girder, and the depth of the precast concrete girder:

$$h = t_{slab} + t_{haunch} + d_{girder} \tag{6.41}$$

The vertical height of the bridge at the centerlines of bearing is found by making an adjustment for the grade of the vertical profile at the bearings.

$$h' = \frac{h}{\cos\left(\tan^{-1}\left(gr\right)\right)} \tag{6.42}$$

where

gr = Grade of the profile in decimal form

Though Eq. (6.42) is theoretically true, it is noted that there has to be substantial girder depth *h* or grade *gr* to produce a vertical height that is much different from the height perpendicular to the grade. For example, the combination of an 8 ft deep superstructure on a 6 percent grade increases the vertical depth by only ⅛ in. It is also noted that the grades of the girders on either side of the pier may be different from each other and from the local grades at the centerlines of the bearings. For most highway bridges, the changes in grade are small and a single value equal to that of the centerline of the pier may be used.

The elevations of the working points are found by

$$Z_{WPD} = Z_D - h' \tag{6.43}$$

$$Z_{WPU} = Z_U - h' \tag{6.44}$$

Continuing with the example bridge, bridge 1, consider pier 2 as it supports the end of girder 3 of span 1 and the beginning of girder 3 in span 2. Assuming a bearing spacing of 1 ft 0 in., the top-of-deck elevations at the centerline of bearing are

$$Z_D = 120.8575 \text{ ft} \tag{6.45}$$

$$Z_U = 120.8925 \text{ ft} \tag{6.46}$$

The grade of the vertical profile at the centerline of pier is 1.75 percent. The depth of the girder is 72 in., the thickness of the slab is 9 in., and the depth of the haunch at pier 2 (from the previous section) is 2.4 in. The total depth of the superstructure is then 83.4 in. or 6.95 ft. Correcting for grade according to Eq. (6.42), the vertical depth of the superstructure is

$$h' = \frac{6.95}{\cos\left(\tan^{-1}\left(0.0175\right)\right)} = 6.9511 \text{ ft} \tag{6.47}$$

The results of Eq. (6.47) show that the grade correction for the example bridge is negligible, considering tolerances that can be achieved in the field.

The elevations of the working points can now be found as

$$Z_{WPD} = 120.8575 - 6.9511 = 113.9064 \text{ ft} \tag{6.48}$$

$$Z_{WPU} = 120.8925 - 6.9511 = 113.9414 \text{ ft} \tag{6.49}$$

Figure 6.21 shows more detail of the bearings and the top of the pier cap. The top-of-pier elevation is found by subtracting the minimum thickness of the bearing plate, bearing, and bearing seat from the lowest working point elevation.

Bearing thicknesses are determined by the bridge designer. The bearing plate and bearing seat thickness are controlled by minimum dimensions, typically set by constructability considerations. Bearing plates are typically beveled steel plates. In cases of flat or small grades (as permitted by the owner agency) and flexible bearing such as elastomeric pads, sometimes flat plates, or no plate at all is

used. When used, a practical minimum thickness of plate is selected. The thickness of the bearing plate at the centerline of the bearing is then found as

$$t_{plate} = t_{plate}(\min) + \left(\frac{l_{plate}}{2} gr\right) \tag{6.50}$$

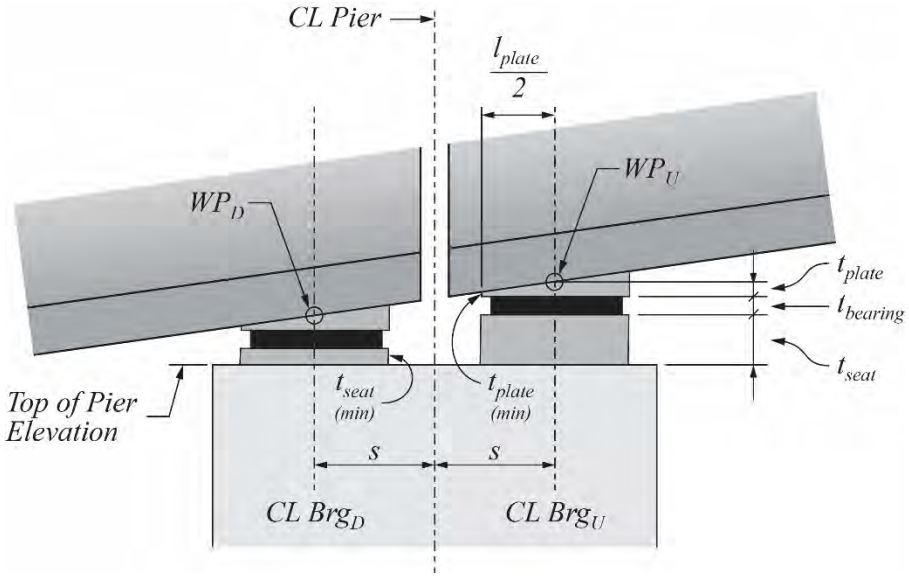

Source: PCI

Figure 6.21 Bearing Details and Geometry

Bearing seats are typically cast as a secondary placement on top of the pier to achieve better accuracy in top of seat elevation. Unreinforced bearing seats of thicknesses of 1 in. are not uncommon. If the bearing seats are reinforced a minimum dimension of 3 or 4 in. is typically used.

If the vertical profile at the pier has positive grade, as shown in **Figure 6.21**, the minimum height of the bearing "stack" (plate, bearing, and seat) is on the down-station side of the pier. A negative grade would have the minimum height of stack on the up-station side of the pier. The total thickness of the stack is

$$t_{stack}(\min) = t_{plate} + t_{bearing} + t_{seat}(\min) \tag{6.51}$$

The top-of-pier elevation for the layout shown in **Figure 6.21** is found by subtracting the bearing stack thickness from the working point elevations:

$$Z_{TOP} = Z_{WP(D)} - t_{stack}(\min) \tag{6.52}$$

If a flat pier top is used, then the bearing stack thickness on the up-grade side should be greater than on the down-grade side. The difference in height is typically made up in the height of the bearing seats. The thickness of this bearing seat is found by

$$t_{seat(U)} = Z_{WP(U)} - t_{plate} - t_{bearing} - Z_{top} \tag{6.53}$$

Continuing with the example of the bearings supporting girder 3 of span 1 and girder 3 of span 2 at pier 2 of bridge 1, and assuming a minimum thickness of bearing plate of ½ in. and a length of plate of 14 in., the thickness of the plate at the centerline of the bearing would be

$$t_{plate} = 0.5 \text{ in.} + \left(\frac{14 \text{ in.}}{2} (.0175) \right) = 0.6225 \text{ in.} \tag{6.54}$$

The bearing thickness for this example is 1½ in., and the minimum bearing seat elevations is 4 in. The total height of the bearing stack is then

$$t_{stack}(\min) = .6225 \text{ in.} + 1.5 \text{ in.} + 4 \text{ in.} = 6.1225 \text{ in.} \tag{6.55}$$

The top-of-pier elevation is

$$Z_{TOP} = 113.9064 \text{ ft} - \frac{6.1225 \text{ in.}}{12 \text{ in./ft}} = 113.3962 \text{ ft} \tag{6.56}$$

The thickness of the up-grade bearing seat is

$$t_{seat(U)} = 113.9414 \text{ ft} - 113.3962 \text{ ft} - \frac{0.6225 \text{ in.}}{12 \text{ in./ft}} - \frac{1.5 \text{ in.}}{12 \text{ in./ft}} = 0.3683 \text{ ft} = 4.4196 \text{ in.} \tag{6.57}$$

As with **Figure 6.20**, **Figure 6.21** shows the condition with the end of the precast concrete girder cast so that the joint between girders is vertical. Some transportation agencies cast the beams square and allow the joint to be inclined perpendicular to the grade of the bridge.

Chapter 7 – Geometry of Concrete Curved Bridges with Straight Precast Concrete Girders

7.1 Introduction

The previous chapter presented geometric calculations typical to bridges that lie on tangent horizontal alignments. This chapter presents additional geometric considerations for bridges following curved alignments with straight precast concrete girders.

The geometry of curved precast concrete segmental box girder bridges is presented separately in Chapter 8. Chapter 9 presents geometric considerations for curved precast concrete U-girders.

7.2 Curved Bridges with Straight Precast Girders

Curved bridge superstructures can be constructed using straight girders placed as chords between supports. **Figure 7.1** shows a typical curved bridge constructed with straight pretensioned concrete girders and cast-in-place deck slab. The chorded girder layout produces angle changes along the girder lines at the piers and variable deck slab overhangs.

Source: PCI

Figure 7.1 Curved Bridge with Chorded Girders

Figure 7.2 shows a framing plan view of a curved bridge consisting of prestressed concrete girders chorded between radially placed piers. The locations of the bearings on the piers lie along girder layout lines that are concentrically offset from the centerline of alignment. The deck slab overhangs increase on the outside of the curve from a minimum value at the piers to a maximum value at midspan. The opposite is true for the inside of the curve.

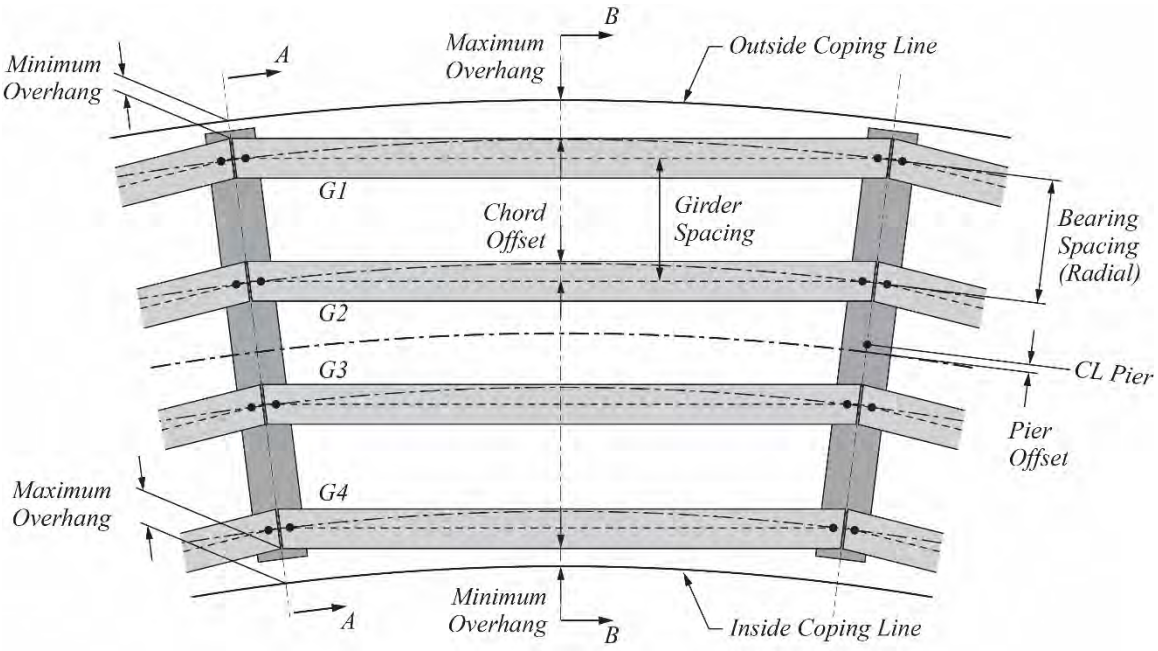

Source: PCI

Figure 7.2 Curved Bridge with Chorded Girders

Figure 7.2 also shows that the centerline of the pier is offset transversely from the centerline of alignment, shifting the girders transversely. This offset is provided so that the maximum overhang at the pier on the inside coping line is approximately equal to the maximum overhang at midspan along the outside coping line, while the minimum overhang at midspan along the inside coping line is approximately equal to the minimum overhang at the pier along the outside coping line. **Figure 7.3** and **Figure 7.4** show the resulting transverse cross sections at the centerline of the pier and at midspan of the structure shown in **Figure 7.2**. The pier offset to produce equal overhangs is shown in **Figure 7.3**.

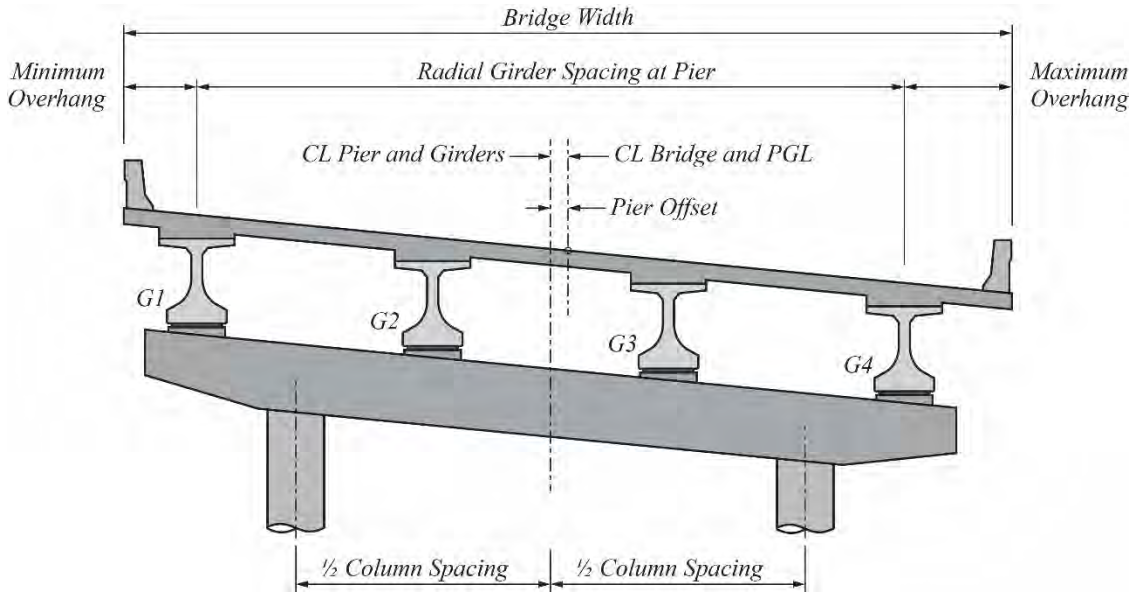

Source: PCI

Figure 7.3 Cross Section at Pier Placed Radial to Curved Alignment (Section A-A, Fig. 7.2

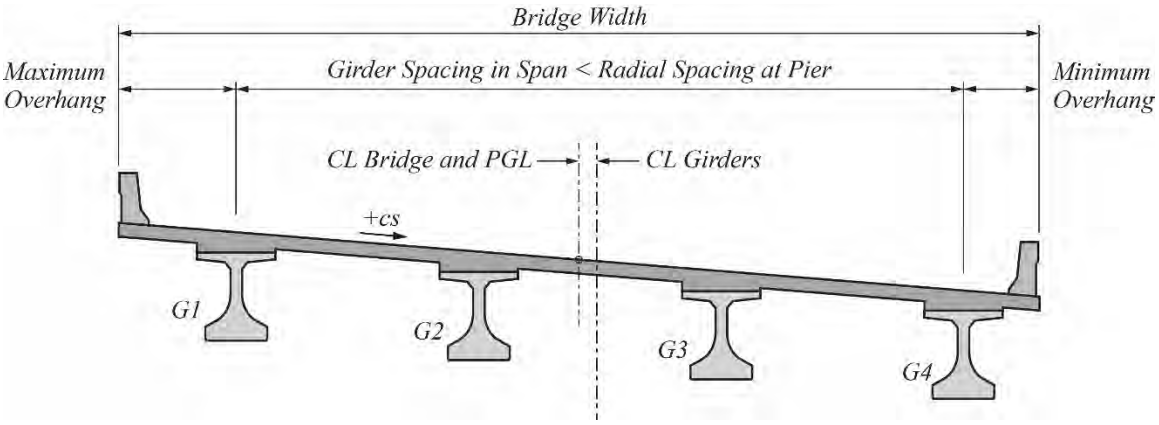

Source: PCI

Figure 7.4 Cross Section at Midspan (Section B-B, Fig. 7.2)

The offset of the centerlines of the chorded girders relative to the centerline of horizontal alignment varies along the span. The varying offsets need adjustments to the elevation of the girders so that minimum haunch dimensions can be respected along the length of the girders. **Figure 7.5** shows a closer look at cross sections of girder G1 at the pier and at midspan. These cross sections have been arranged so that they are aligned along the left coping line. Considering for the moment that this bridge has no vertical profile (lies along a zero grade and the girder has no camber), the elevation of the girder at the pier should be lower than that of the girder at midspan by an amount equal to the girder offset multiplied by the cross slope.

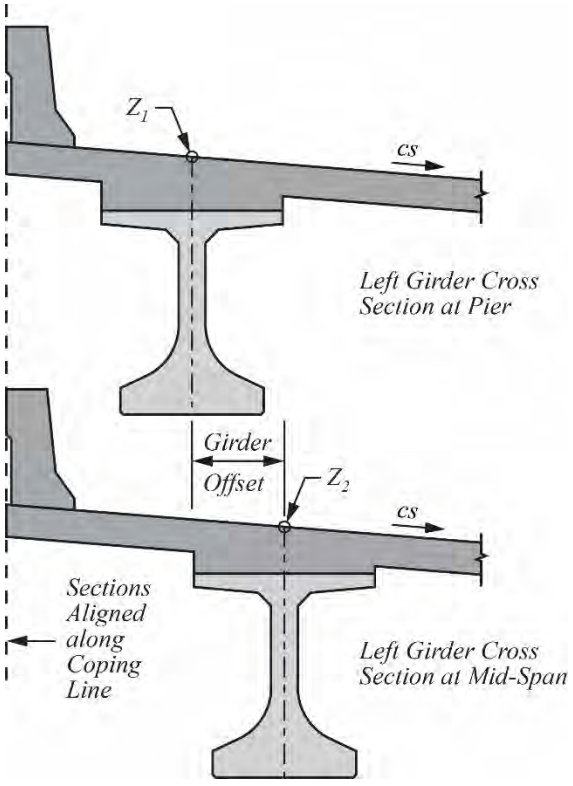

Source: PCI

Figure 7.5 Cross Sections through Left Girder at Midspan and at Pier Aligned along the Left Coping Line

Figure 7.6 shows the two cross sections of **Figure 7.5** superimposed on one another, aligned along the coping line. The girder moves toward the center of curvature of the horizontal alignment between its location at the piers and midspan. The downward cross slope makes it necessary to lower the entire girder to maintain the minimum haunch thickness at midspan, thus the haunch at the support becomes thicker.

This change can be expressed as an adjustment to the haunch thickness at the piers. This adjustment would be in addition to the other haunch adjustments presented in chapter 6 for straight alignments. Recalling Eq. (6.39), the total haunch thickness now becomes

$$t_{total} = t_{\min} + \Delta t_{cs} + \Delta t_{pr} + \Delta t_{nc} + \Delta t_{off} \tag{7.1}$$

where

t_{min} = Minimum haunch thickness

Δt_{cs} = Haunch adjustment for cross slope

Δt_{pr} = Haunch adjustment for profile

Δt_{nc} = Haunch adjustment for net camber

Δt_{off} = Haunch adjustment for girder offset in a curved bridge for chorded girders

The haunch thickness adjustment Δt_{off} is found by

$$\Delta t_{off} = Girder\ Offset \times Cross\ Slope \tag{7.2}$$

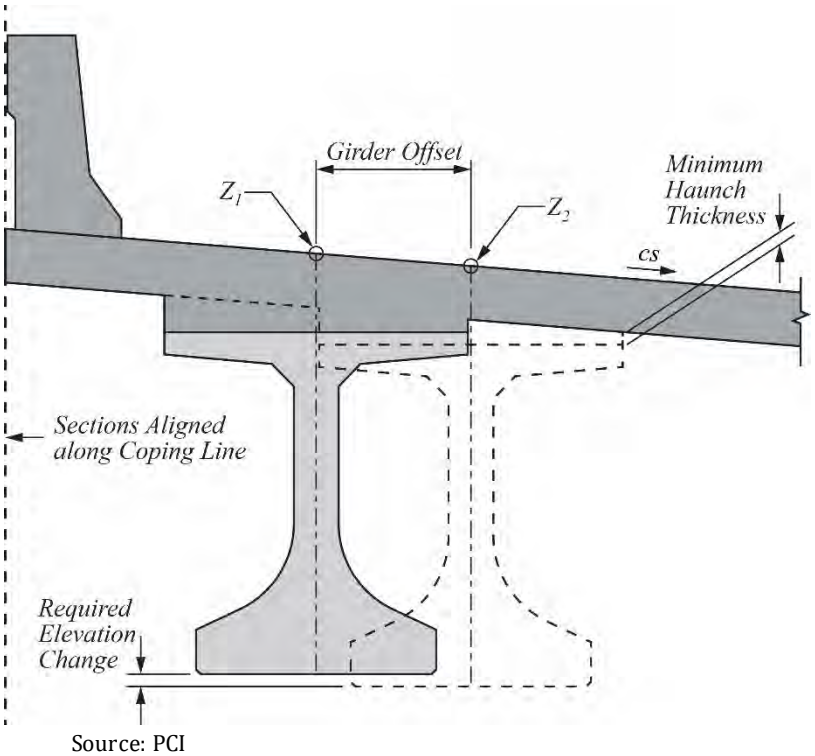

Source: PCI

Figure 7.6 Haunch Adjustment for Chorded Girders

The girder offset in Eq. (7.2) is the offset between the girder chord and a curve concentric to the horizontal alignment, both passing through the center of the bearings at the piers. This offset is shown

in the center of **Figure 7.2**. **Figure 7.7** shows the layout details at a pier used to determine the offset curved alignments and girder chords that are used to determine the girder offset of Eq. (7.2). The offset curved alignment can be created using the procedures shown in Section 5.10 of this manual. The offset used for each girder line is the radial offset from the horizontal alignment to the girder line, taking into account a pier offset used to balance inside and outside overhang lengths. The bearings are typically located on the pier caps using dimensions along the length of, and perpendicular to, the pier caps. The bearing offset from the centerline of pier (dimension *s*) is then measured perpendicularly to the pier to locate the center of the bearings. The theoretical location of the center of the bearings along the offset girder alignment is often approximately equal to the dimension*s*.

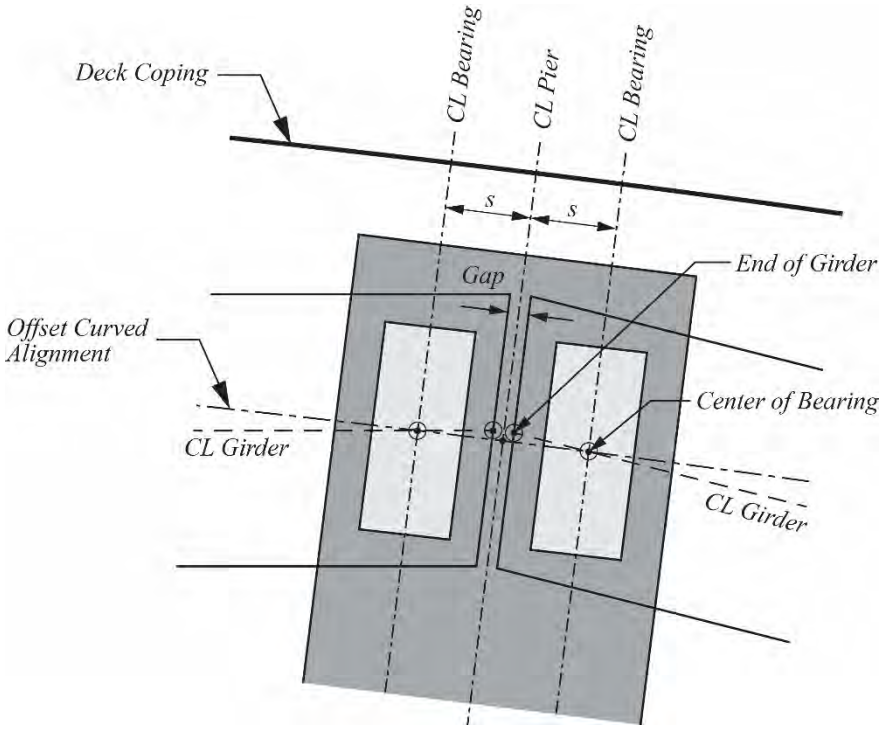

Source: PCI

Figure 7.7 Plan View of Girder Geometry at a Support

Figure 7.7 shows a particular arrangement of bearings aligned with the pier cap and girder ends angled to achieve a constant-width gap between the girder ends. Other configurations are possible. For example, the bearings may be place perpendicular to the centerlines of the girders and the girders cast square at their ends. The orientation of the bearing pad can affect stability at erection. This should be checked in the design phase.

7.3 Example Bridge

Example calculations for curved bridges built with straight girders in this chapter are based on a curved bridge that follows the horizontal alignment, vertical profile, and superelevation descriptions developed in previous chapters. **Figure 7.8** shows the location of example bridge 2, which lies within the second horizontal curve (radius = 1250 ft) of the example horizontal alignment. The bridge begins at station 167+00 and ends at station 172+15, resulting in a length along centerline of alignment of 515 ft.

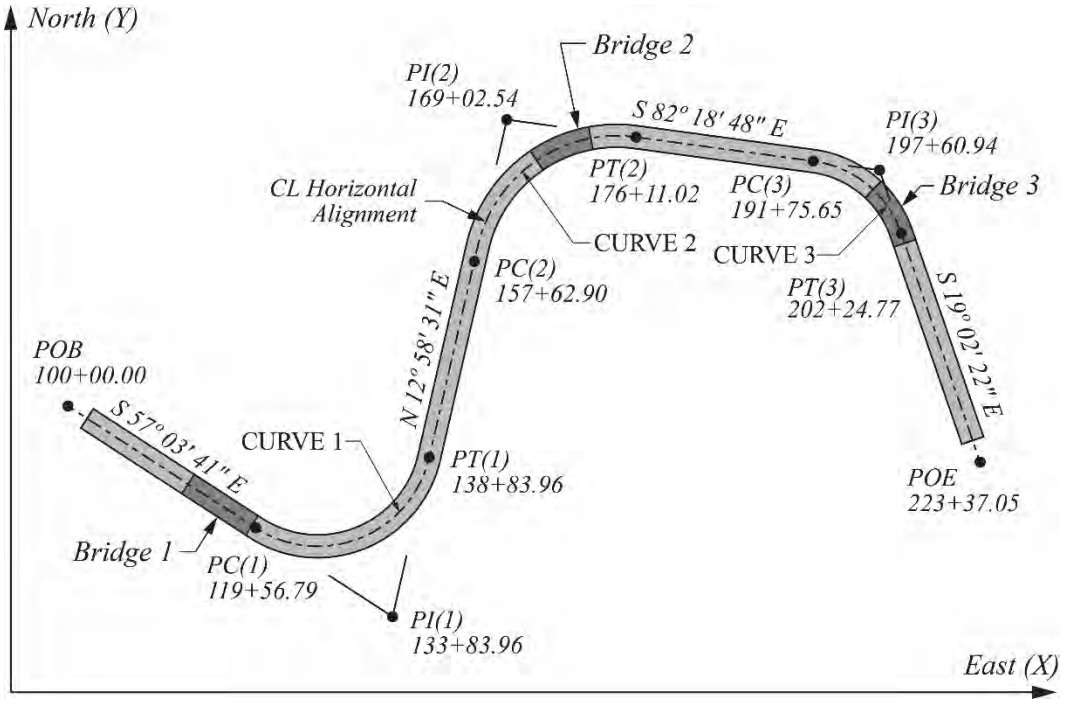

Source: PCI

Figure 7.8 Example Horizontal Alignment

Figure 7.9 shows the vertical profile for the examples of the manual. Example bridge 2 lies on the crest curve located at *VPI*(3). **Figure 7.10** shows a closer view of the vertical curve at *VPI*(3), also showing the location of the bridge.

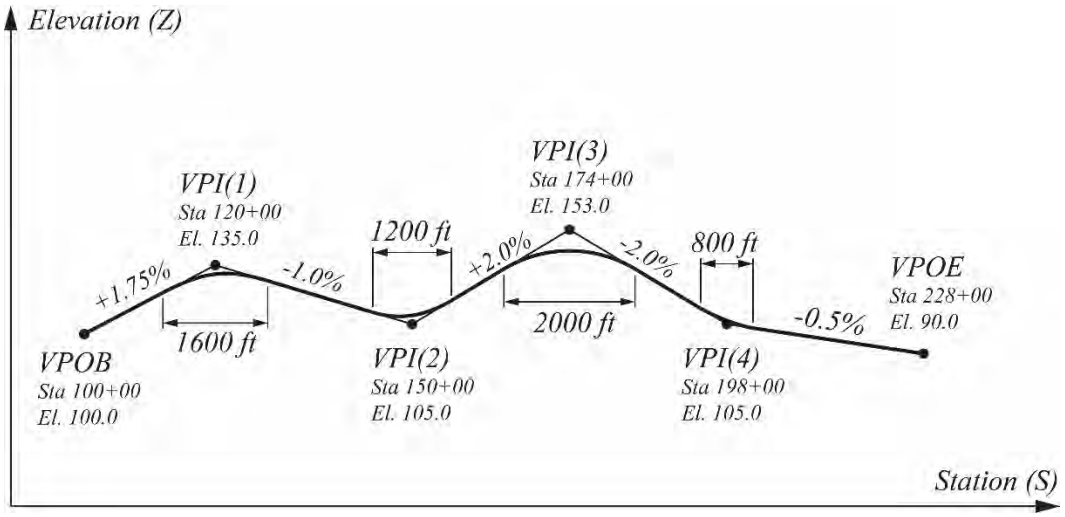

Source: PCI

Figure 7.9 Vertical Profile for the Example Alignment

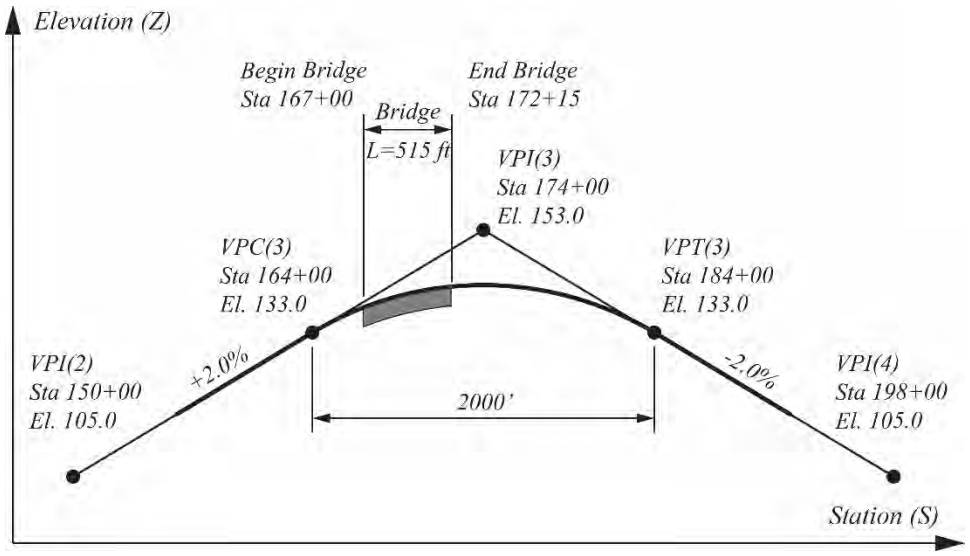

Source: PCI

Figure 7.10 Vertical Profile in the Vicinity of Example Bridge 2

A review of **Figure 4.16** from Chapter 4 shows that the example bridge is located completely within the constant superelevation portion of curve 2. The superelevation along the total length of the bridge is +5 percent.

Figure 7.11 shows a plan view of the span layout for bridge 2. The 515 ft long bridge is made up of five simple spans, each with a length of 103 ft, measured along the *PGL*. Stations of the piers are shown in **Table 7.1**. The spans of this bridge will be composed of straight precast concrete girders spanning as chords between radially located piers. The typical cross section of bridge 2 for this span option is shown in **Figure 7.12**.

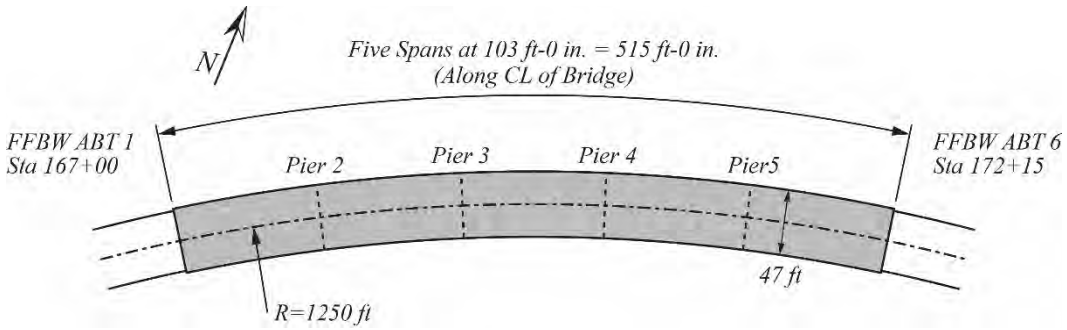

Source: PCI

Figure 7.11 Plan View of Example Bridge (Bridge 2) with Span Layout 1

Table 7.1 Location of Abutments and Piers for Span Layout 1 of Bridge 2

Pier	Station
Abutment 1	167+00.0
2	168+03.0
3	169+06.0
4	170+09.0
5	171+12.0
Abutment 6	172+15.0

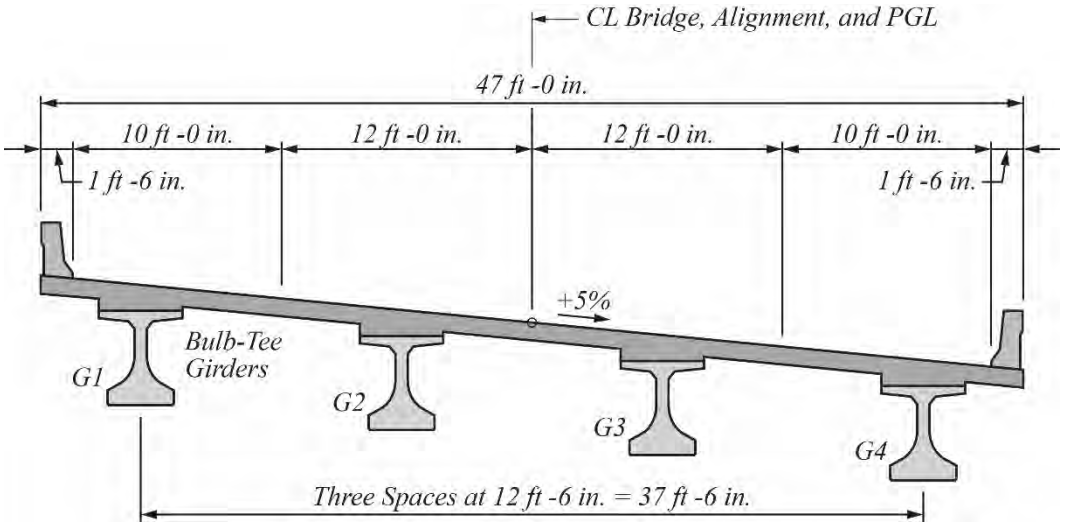

Source: PCI

Figure 7.12 Bridge 2 Cross Section, Span Layout 1

7.4 Example Geometry Calculations—Curved Bridge with Straight Precast Girders

The calculations in this section will consider girder G1 of span 3 in the example bridge. The calculations will compute the haunch thicknesses over the bearings and at the centerline of the span using the haunch thickness adjustments presented in Eq. (7.1). The thickness o will then be verified using general geometric calculations working from the bridge deck down to the top of the girder. Chapter 5 calculation methods are referenced in parentheses.

This example assumes:

- The offset of the girders and piers from the *PGL* to balance deck overhangs is 6 in.
- The distance from the centerline of pier to the centerline of the bearings is 1 ft 0 in. (dimension *s* in **Figure 7.7**).
- The minimum haunch thickness for this example is ½ in.
- The girder net camber is 1 in.

7.4.1 Establish Offset Alignment at Centerline of Girder G1

A horizontal alignment offset to the left of the *PGL* at the centerline of girder G1 is created (Section 5.10). The amount of the offset is 18.75 ft (1½ girder spacings) plus the 6 in. offset to balance deck overhangs. The total offset is 19.25 ft to the left. The resulting *PI* coordinates of this offset alignment are shown in **Table 7.2**. **Table 7.3** shows the curve data for the offset alignment.

Table 7.2 Coordinate Information for Alignment Offset 19.25 ft Left

Point	Number	*X*	*Y*
POB	1	510.4670	2516.1556
PI(1)	2	3327.4101	691.0939
PI(2)	3	4325.1821	5021.4245
PI(3)	4	7614.3280	4577.4907
POE	5	8498.1969	2016.2797

Table 7.3 Curve Data for Alignment Offset 19.25 ft Left

Curve	*R*	*L*	*T*
1	980.75	1882.2776	1399.7034
2	1269.25	1876.5768	1157.1860
3	1519.25	1677.7633	935.9986

7.4.2 Determine Centerline of Bearing Coordinates for Girder G1 in Span 3

Coordinates at the centerlines of pier 3 (169+06) and pier 4 (170+09) are found along the *PGL* (Section 5.7). Coordinates at the centerlines of pier 3 and pier 4 offset to the girder G1 alignment are then found by offsetting the *PGL* points 19.25 ft radially to the left (Section 5.8). Finally, the centerlines of the bearings for girder G1 in span 3 are found by locating a point 1 ft up-station of the pier 3 offset point, and a point 1 ft down-station from the pier 4 offset point, along the offset girder G1 alignment (Section 5.7). The coordinates of the six located points are shown in **Table 7.4.**

Table 7.4 Coordinate Information for Points at Pier 3 and Pier 4

Point	*X* (E)	*Y* (N)
Pier 3 – CL pier (on *PGL* at 169+06)	4781.2642	4745.0760
Pier 3 – CL G1 at pier (19.25 ft left of *PGL*)	4773.2418	4762.5747
Pier 3 – CL G1 brg (1 ft up-station)	4774.1510	4762.9911
Pier 4 – CL pier (on *PGL* at 170+09)	4876.5551	4784.0972
Pier 4 – CL G1 at pier (19.25 ft left of *PGL*)	4870.0001	4802.1968
Pier 4 – CL G1 brg (1 ft down-station)	4869.0601	4801.8559

7.4.3 Determine Elevations at Centerlines of Bearing and at Centerline of Span

The points at the centerline of the bearings along the offset alignment found in the previous section are projected back onto the *PGL* alignment (Section 5.9). The projected *PGL* stations, elevations on the *PGL*, and elevations on the deck over the offset alignment are shown in **Table 7.5**. The same information is shown for the centerline of the girder.

Table 7.5 Deck Elevations along Concentrically Offset Girder G1 Alignment

Location	Station	*PGL* elevation, ft	Offset, ft	*CS*	CL G1 elevation, ft
P3 CL brg	169+06.9848	140.5694	-19.25	0.05	141.5319
CL span	169+57.5000	141.0419	-19.25	0.05	142.0044
P4 CL brg	170+08.0152	141.4635	-19.25	0.05	142.4260

7.4.4 Determine Chord Length and Middle Ordinate of Girder G1

The span length along the *PGL* between centerlines of piers is 103 ft 0 in. The span length along the girder G1 alignment is

$$L_{G1} = 103.0\left(\frac{1269.25}{1250}\right) = 104.5862 \text{ ft} \tag{7.3}$$

Assume that the length along the girder G1 alignment between the centers of the bearings is approximately equal to the bearing spacing across the pier cap. In this case, the length along the girder G1 alignment between bearings is then

$$L_{G1} = 104.5862 - 2(1) = 102.5862 \text{ ft} \tag{7.4}$$

The deflection angle between the bearing centerlines is found by rearranging Eq. (2.34):

$$\alpha = \left(\frac{L}{R}\right) = \frac{102.5862}{1269.25} = 0.080824 \text{ rad} = 4.63089 \text{ degrees} \tag{7.5}$$

The long chord of girder 1 between centerlines of bearing is found using Eq. (2.36):

$$LC_{G1} = 2R\sin\left(\frac{\alpha}{2}\right) = 2(1269.25)\sin\left(\frac{4.63089}{2}\right) = 102.5583 \text{ ft} \tag{7.6}$$

The middle ordinate from this long chord is found using Eq. (2.39):

$$M_{G1} = R\left(1 - \cos\left(\frac{\alpha}{2}\right)\right) = 1269.25\left(1 - \cos\left(\frac{4.63089}{2}\right)\right) = 1.0363 \text{ ft} \tag{7.7}$$

7.4.5 Determine Haunch Thicknesses at Piers and Center of Girder

The haunch thickness will be the minimum ½ in. thickness chosen for this example with adjustments made as presented in this chapter and Chapter 6. The haunch adjustment for cross slope is found using Eq. (6.21):

$$\Delta t_{cs} = 0.05\left(\frac{48 \text{ in.}}{2}\right) = 1.20 \text{ in.} \tag{7.8}$$

The correction for profile is found from Eq. (6.24):

$$\Delta t_{pr} = 142.0044 - \left(141.5319 + \left(\frac{142.4260 - 141.5319}{102.5862}\right)51.2931\right) = 0.0255 \text{ ft} \tag{7.9}$$

or

$$\Delta t_{pr} = 0.31 \text{ in.} \tag{7.10}$$

The haunch adjustment for bridge curvature is found by using Eq. (7.2):

$$\Delta t_{off} = 1.0363(0.05) = 0.0518 \text{ ft} = 0.62 \text{ in.} \tag{7.11}$$

Total haunch thicknesses are found by using Eq. (7.1), using the terms applicable to the problem specifics. The haunch thickness at the centerline of the span is found by using the minimum thickness and adjustments for cross slope and bridge curvature:

$$t_{haunch} = 0.5 + 1.20 + 0.62 = 2.32 \text{ in.} \tag{7.12}$$

The haunch thickness at the centerline of the bearings is equal to the centerline haunch thickness plus the adjustments for camber and profile:

$$t_{haunch} = 0.5 + 1.20 + 0.62 + 1.00 + 0.3 = 3.62 \text{ in.} \tag{7.13}$$

7.4.6 Verify Haunch Thickness at Centerline of Girder

The haunch thickness at the centerline of the girder is verified by the following operations:

- Determine the top-of-girder elevations at the centerline of the bearings.
- Determine the top-of-girder elevation at midspan of the chorded girder using end-of-girder elevations plus the girder net camber.
- Determine the top of deck elevation over the midspan of the chorded girder.

- Subtract the top-of-chorded-girder elevation and deck thickness from the top-of-deck elevation.

Elevations at the top of the girders at the centerlines of bearings are found by subtracting deck elevations, slab thickness, and end haunch thickness from the deck elevations.

$$\text{Elevation of G1 at } CL\ P3\ Brg = 141.5319 - 0.6667 - \frac{3.62}{12} = 140.5636 \text{ ft} \tag{7.14}$$

$$\text{Elevation of G1 at } CL\ P4\ Brg = 142.4260 - 0.6667 - \frac{3.62}{12} = 141.4577 \text{ ft} \tag{7.15}$$

The elevation at the centerline of G1 is the average of these two elevations plus the net camber.

$$\text{Elevation of } G1 \text{ at Midspan} = \left(\frac{140.5636 + 141.4577}{2}\right) + \left(\frac{1}{12}\right) = 141.0940 \text{ ft} \tag{7.16}$$

The elevation of the top of the deck over the centerline of chorded girder G1 is found by taking the *PGL* elevation at the middle of span 3 and adjusting it for superelevation multiplied by the distance to the middle of the girder chord.

$$\text{Elevation of } CL\ G1 = 141.0419 = (19.25 - 1.0363) = 141.9526 \text{ ft} \tag{7.17}$$

The haunch thickness is determined by subtracting the slab thickness and top of girder elevation from the deck elevation.

$$t_{haunch} = 141.9526 - 0.6667 - 141.0940 = 0.192 \text{ ft} = 2.30 \text{ in.} \tag{7.18}$$

This result is approximately equal to the result shown for Eq. (7.12).

Chapter 8 – Geometry of Precast Concrete Segmental Bridges

8.1 Introduction

Precast concrete segmental bridge construction benefits long spans, increased speed of construction, and construction "from above" over environmentally sensitive landscapes or complex urban highway systems. Key to the design and construction of precast concrete segmental bridges are proper geometric design of the individual segments and the control of geometry during segment precasting. This chapter discusses both of these elements.

Segments of precast concrete segmental bridges can be cast to follow the most challenging of bridge geometrics. **Figure 8.1** shows the Foothills Parkway Bridge No. 2, located in Blount County, Tennessee, a precast concrete segmental box girder bridge constructed over challenging terrain. This 790 ft bridge consists of five spans with lengths of 125 ft, three of 180 ft, and 125 ft. The bridge follows an S-shaped alignment with curve radii of 262 and 650 ft. Superelevations vary from 7.8 percent (right) to 5.8 percent (left) over a 315 ft transition length. The vertical profile of the bridge begins at a +6.75 percent grade and transitions through a vertical curve to a +8.02 percent grade.

Source: PCI

Figure 8.1 Foothills Parkway Bridge No. 2

The segments for the Foothills Parkway Bridge No. 2 were cast 40 miles from the project site in a PCI-certified precasting plant. Ninety-two superstructure segments were each precast with their own unique chorded shapes so that, when assembled, they produced the desired bridge geometry.

Figure 8.2 shows a few of the precast concrete segments for this bridge. Typical segment lengths were 8 ft 8 in. and pier/abutment segment lengths were 5 ft 0 in. Each segment was 36 ft 10 in. wide and 9 ft 0 in. deep. Weights of the precast segments ranged from 40 to 45 tons.

Source: PCI

Figure 8.2 Precast Concrete Segments for the Foothills Parkway Bridge No. 2

8.1.1 Construction Methods

Most precast concrete segmental bridges are built by one of two erection methods: the balanced cantilever method or the span-by-span method. **Figure 8.3** shows two common erection schematics for balanced cantilever construction. The top schematic, which presupposes ground access to the site, shows precast concrete segment placement using a ground-based crane. Temporary towers are used to stabilize the superstructure during the placement of segments on either side of the cantilever. The bottom schematic shows segment erection using an overhead gantry. In this case, the precast concrete segments are delivered over the completed portion of bridge. **Figure 8.4** shows the ground-based balanced cantilever construction of a precast concrete segmental bridge in Jacksonville, Fla.

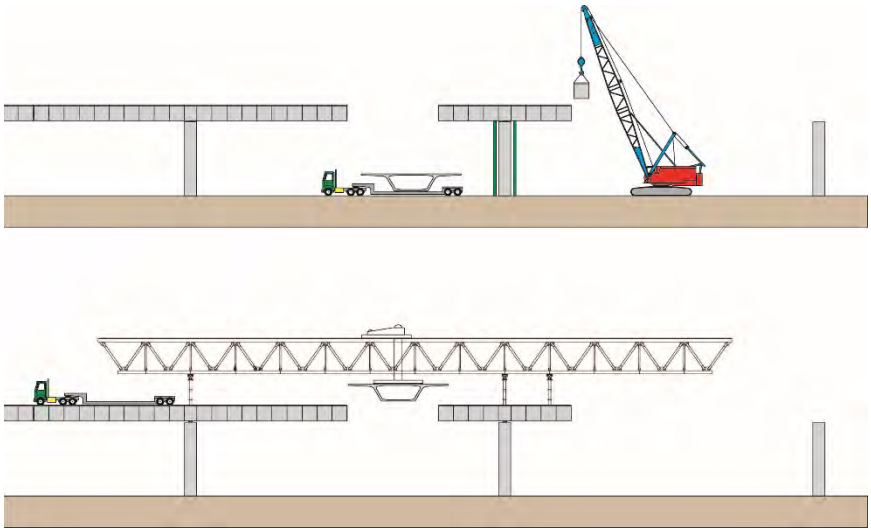

Source: PCI

Figure 8.3 Common Balanced Cantilever Erection Schematics

Source: PCI

Figure 8.4 I-95/I-295 Ramp Balanced Cantilever Construction, Jacksonville, Fla.

Figure 8.5 shows two common erection schematics for span-by-span segmental construction. The top schematic utilizes temporary erection trusses to support a full span of segments until post-tensioning tendons can be stressed, making the span complete. Ground access is shown in this top schematic, but segments can be delivered over the completed portion of bridge to a deck-mounted crane or segment placer for erection. The bottom schematic shows segment erection using an overhead gantry, with segments delivered over the completed portion of bridge. Overhead gantries with ground delivery of segments were used to erect five miles of segmental spans in Phase 1 of the Dulles Corridor Metrorail Project in Tysons Corner, Va. **Figure 8.6** shows a span just completed using an overhead gantry.

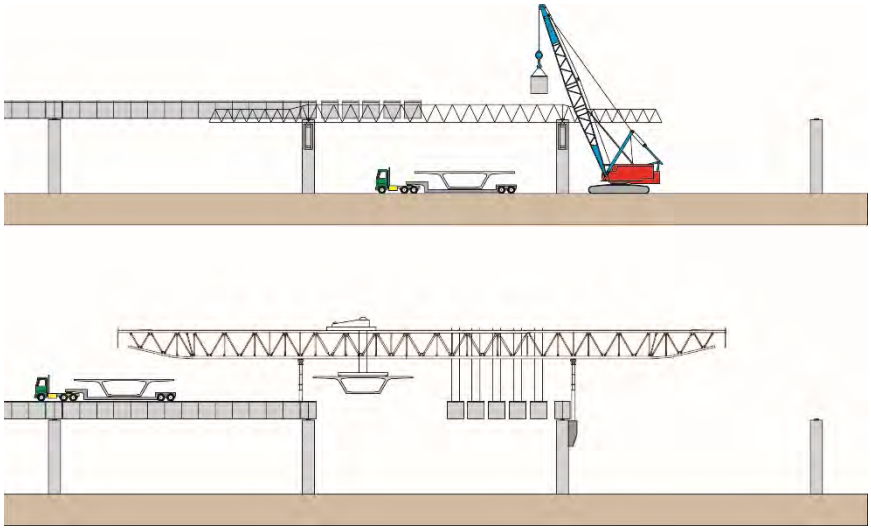

Source: PCI

Figure 8.5 Span-by-Span Erection Schematics

Source: PCI

Figure 8.6 Span-by-Span Construction with Overhead Gantry on the Phase 1 Dulles Corridor Metrorail Project

8.1.2 Match-Casting by the Short-Line Method

Segments of precast concrete segmental bridges are cast against one another to ensure a precise fit when they are erected. This process of casting against one another is called *match-casting*. The most common method of match-casting, called the *short-line method*, uses a casting machine to cast new segments between a fixed bulkhead and the previously cast segment. The basic components of a casting machine for short-line casting, as shown in **Figure 8.7,** are as follows:

- Permanent bulkhead: The bulkhead has the cross section of the precast concrete segments, shear and alignment keys, and holes for the support of ducts for the post-tensioning tendons. The bulkhead is rigidly supported so that it does not move throughout segment casting. The bulkhead location and the axis of the casting machine serve as the local coordinate system for segment casting.
- Bottom soffits: Two soffits are needed: one to support the segment being cast and one to support the previously cast segment. The soffits roll on rails and are outfitted with hydraulic jacks to move the soffit beds vertically and laterally to the desired segment geometry.
- Outside web and cantilever wing forms: These two forms, one for each side of the segment, are made snug against the permanent bulkhead and previously cast segment prior to casting the new segment. These forms should be stiff enough to maintain casting tolerances, yet sufficiently flexible to warp to the desired segment geometry.
- Core form: This form is collapsible and retractable so that it can be inserted through the bulkhead and expanded to the desired core dimensions.

Figure 8.8 shows a photograph of a typical casting machine used to cast segments at the I-4/Lee Roy Selmon Expressway Interchange in Tampa, Fla.

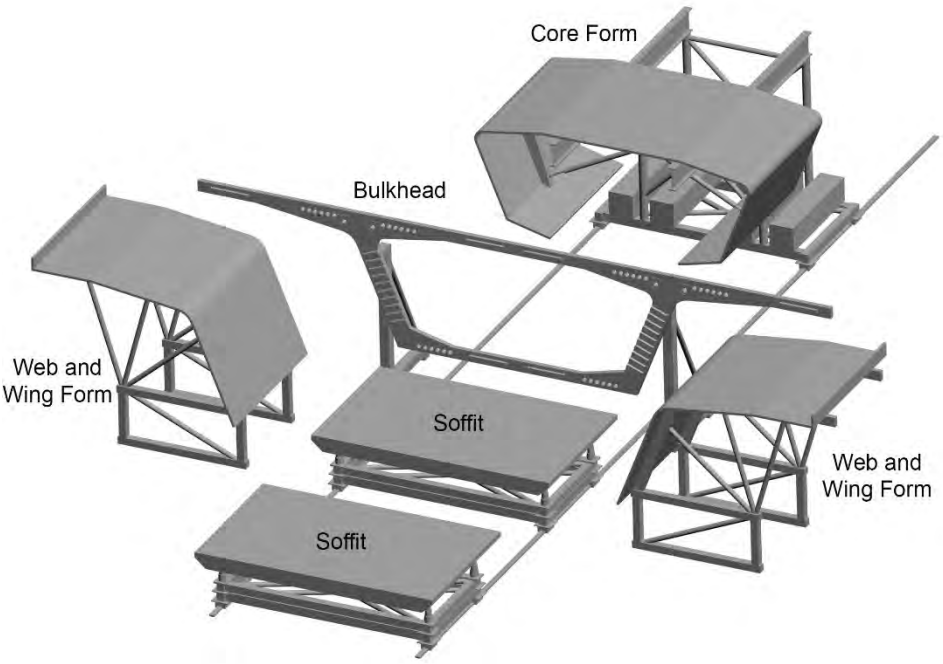

Source: PCI

Figure 8.7 Casting Machine for Short-Line Segment Casting

Source: PCI

Figure 8.8 Casting Machine for the I-4/Lee Roy Selmon Expressway Interchange

The casting machine is fabricated and delivered to the site, where it is assembled on a prepared foundation. The two soffits will support precast concrete segments in two positions: the match-cast position and the new-cast position. The match-cast segment was cast in a previous cycle. The new-cast segment is cast between the permanent bulkhead and the match-cast segment.

The typical sequence for casting a continuous run of segments, as shown in **Figure 8.9**, is:

1. A starter segment (first new-cast segment of the continuous run of segments) is cast between the permanent bulkhead and a temporary bulkhead. A segment from a previous run of segments that has the appropriate end cross section is typically used in lieu of a temporary bulkhead.
2. When the newly cast concrete reaches a strength sufficient for form stripping and segment moving, the starter segment moves from the new-cast to the match-cast position. The hydraulic jacks on the soffit are used to orient the match-cast segment to achieve the desired geometry of the next new-cast segment.
3. The next segment of the run of segments is cast in the new-cast position between the permanent bulkhead and the match-cast segment.
4. When the newly cast concrete reaches a strength sufficient for form stripping and segment moving, the match-cast segment is transported to storage, awaiting assembly in the bridge. The new-cast segment moves to the match-cast position. The soffit supporting the previous match-cast segment is leapfrogged over the new-cast segment to support the next segment to be cast.

Steps 3 and 4 are repeated until the continuous run of segments is complete.

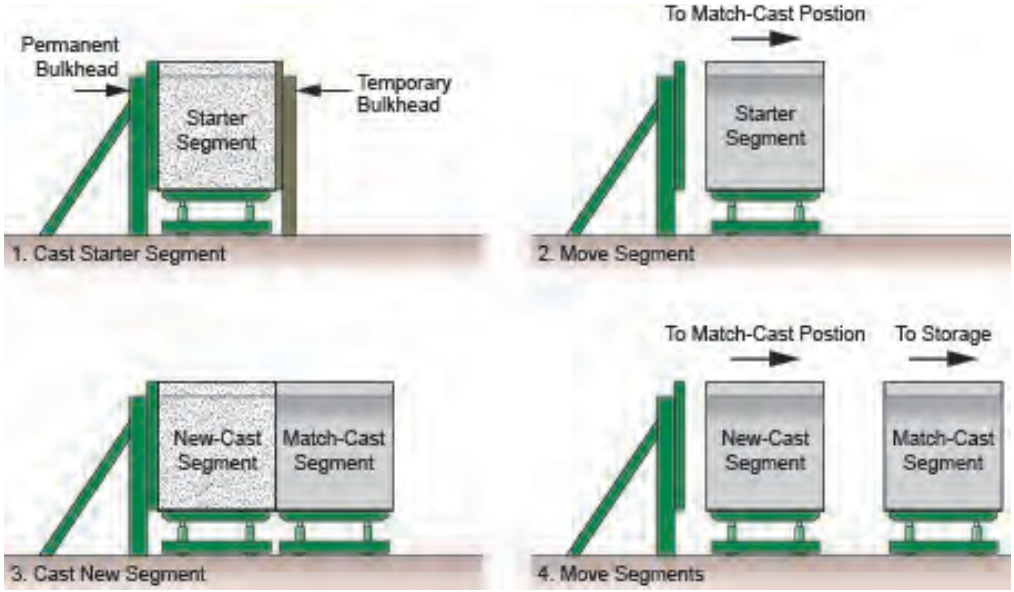

Source: PCI

Figure 8.9 Casting Machine Components

Figure 8.10 shows the short-line casting machine for the I-95/I-295 Ramp in Jacksonville, Fla. In this photograph, the match-cast segment is in position to achieve the desired segment geometry of the new-cast segment and the side wing forms have been made snug against the match-cast segment and the bulkhead.

Source: PCI

Figure 8.10 Casting Machine for the I-95/I-295 Ramp in Jacksonville, Fla.

Geometry of precast concrete segmental bridges is achieved by casting the new-cast segment between the fixed bulkhead and the previously cast segment (match-cast segment), which has been oriented in a manner that when the segments are erected they follow the desired bridge geometry. Taken together, the bulkhead, forms, and segments are typically called the casting cell. The orientation of the segments when they are cast is set within a local coordinate system referred to as the casting cell system. **Figure 8.11** shows the layout of the local casting cell coordinate system. The local y axis is oriented horizontally along the line of sight between a fixed instrument tower and target tower. The local x axis is oriented horizontally and perpendicular to the local y axis. The z axis is vertical and passes through the intersection of the local x axis and y axis. The bulkhead is in the local xz plane.

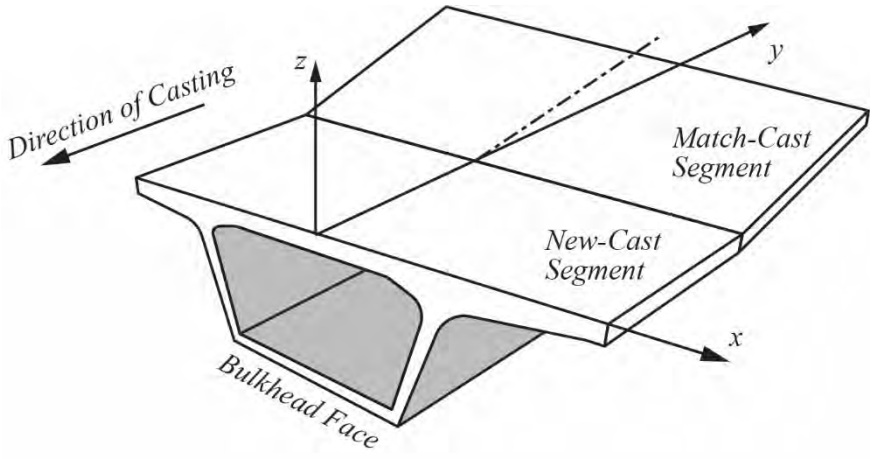

Source: PCI

Figure 8.11 Local Casting Cell Coordinate System

8.2 Establishing Precast Concrete Segment Geometry (Global Coordinates)

8.2.1 Centerline of Segment Beginning and Ending Points

8.2.1.1 Centerline of Segment Alignments

Locating precast concrete segments in the 3D global coordinate system begins with locating the beginning and ending segment centerline points. These beginning and ending points are located by reference to stations along a control horizontal alignment and the associated vertical profile and superelevation design.

Figure 8.12 shows an example portion of a precast concrete segmental bridge located in the global coordinate system (N, E, Elev.). The horizontal alignment controlling the project layout in this example is the profile grade line (*PGL*), along which the vertical profile and the superelevations are specified.

A horizontal alignment that defines the centerline of box girder is typically established to facilitate geometric computations. The centerline of box girder horizontal alignment for the example shown in **Figure 8.12** is defined by a constant offset distance between the *PGL* and the desired centerline of the precast concrete segments. The stationing of this new centerline alignment is arbitrary, as information about points along the new alignment is found by projecting the points onto the control horizontal alignment, in this case the PGL. For example, elevations of points along the centerline of the box girder are found as the sum of the elevation at the projected station on the profile grade line plus a differential elevation equal to superelevation (plus or minus) multiplied by the offset between the alignments.

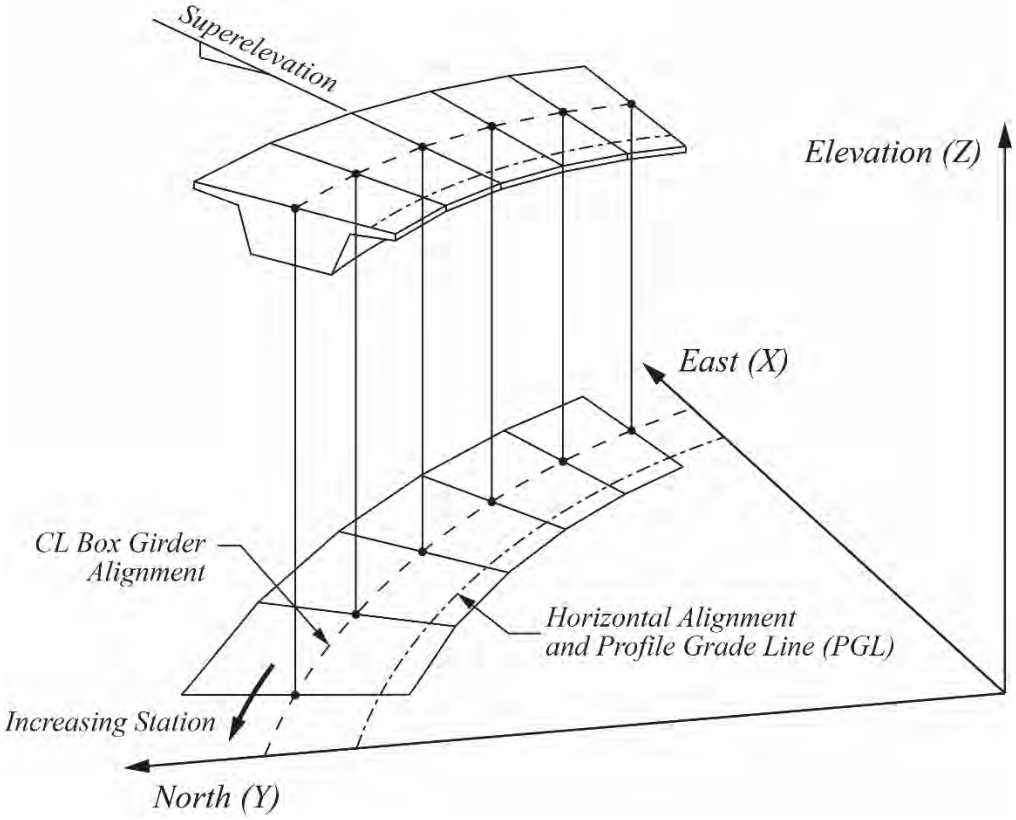

Source: PCI

Figure 8.12 Centerline Segment Points

It is important to note a few things regarding the interaction between the horizontal alignment of the centerline of the box girder and the controlling highway geometrics:

Roadway geometric definitions can vary significantly from highway agency to highway agency. In some cases, the controlling horizontal alignment follows a roadway centerline or lane line and is related to a *PGL* via a fixed offset. In other cases, superelevations may be applied about a point offset from a *PGL*, such as the edge of a travelway. In this instance, elevations at the centerline of the box girder may be controlled by a *PGL* that is offset from superelevation pivot point, whose elevations are related to the *PGL* via the normal crown.

A project may contain multiple box girders that need unique alignments to accommodate merging roadways and ramp structures. The control of the individual box girder alignments may be by a single control horizontal alignment, with associated vertical profile and superelevation design that is not concentric to the box girders.

Figure 8.13 shows a portion of a precast concrete segmental bridge similar to that shown in **Figure 8.12**. **Figure 8.13** is different in that the controlling horizontal alignment to which the vertical profile and superelevations are based on is the horizontal alignment of the centerline of the box girder. This common location of horizontal alignments will be used to facilitate the development of concepts in the remainder of this chapter.

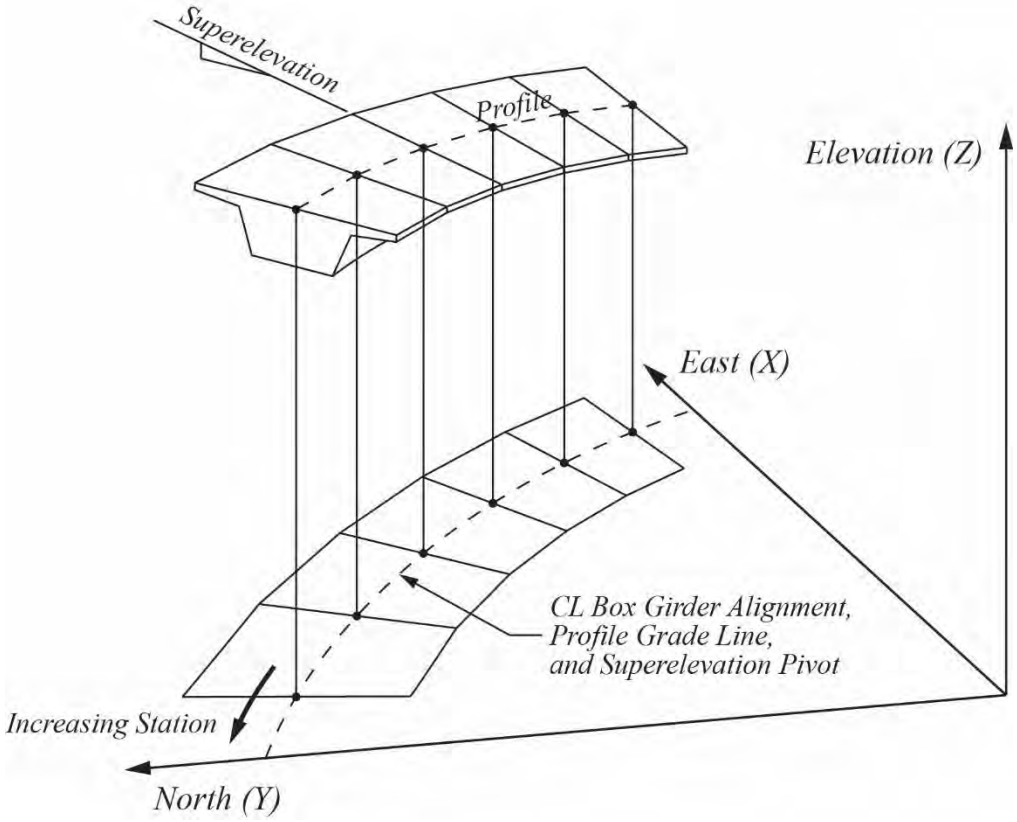

Source: PCI

Figure 8.13 Centerline Segment Points

8.2.1.2 Locating Pier Segments

The first points located on the centerline of the box girder superstructure are those of the pier segments. These segments, which rest on bearings at the piers, contain diaphragms to provide torsional

stiffness to the box girders and to transfer superstructure loads to the bearings. **Figure 8.14** shows a side view and vertical section through a box girder superstructure at the location of a pier.

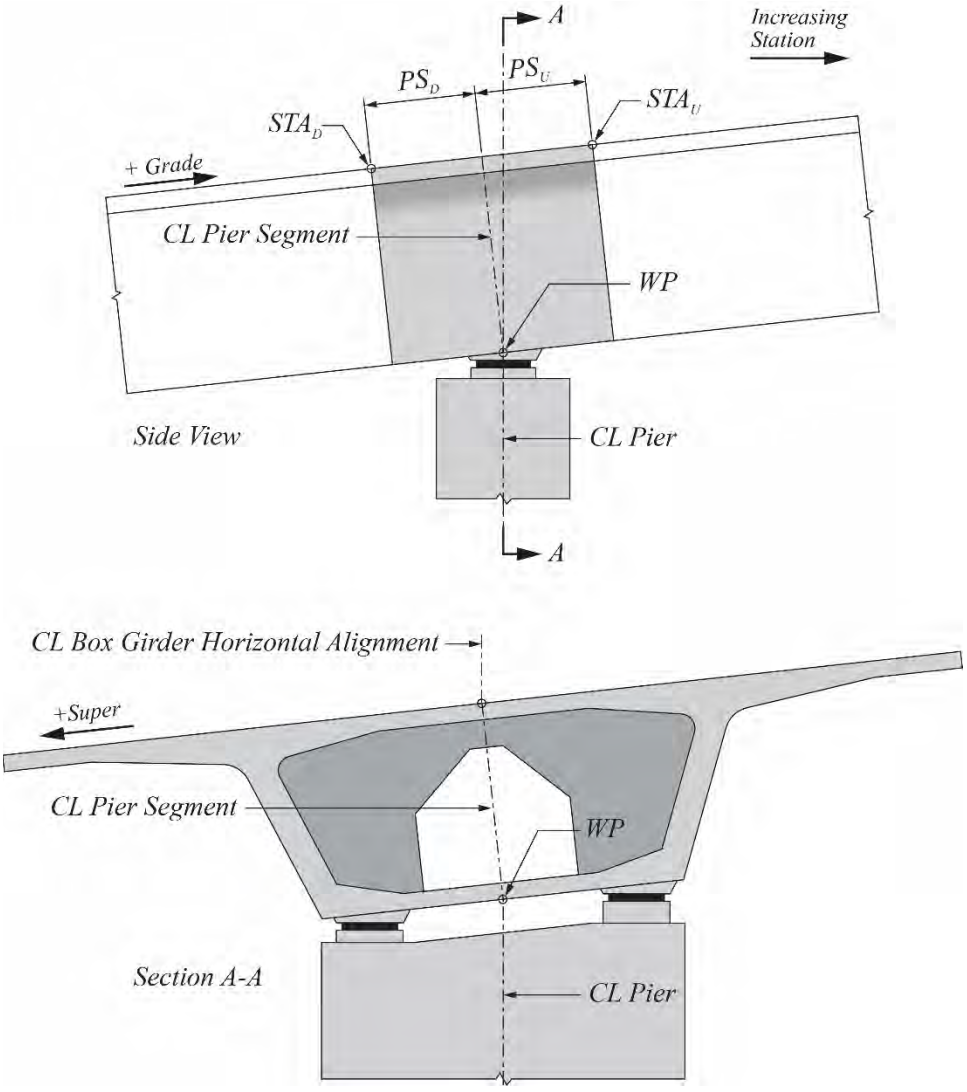

Source: PCI

Figure 8.14 Side View and Cross Section at a Pier

The chorded length of the pier segment between beginning and ending points in **Figure 8.14** is equal to the sum of two lengths measured from the pier segment centerline. PS_U is the portion of length of the pier segment from the centerline of the pier segment to the end of the segment in the up-station direction. PS_D is the portion of length of the pier segment in the down-station direction. In some instances, to reduce handling weights, two partial-length pier segments with lengths PS_U and PS_D are match-cast to form a complete pier segment.

The pier segment is located by finding the stations of the beginning point (STA_D) and ending point (STA_U) such that the following conditions are satisfied:

- The location of the supporting pier, defined by station along the control horizontal alignment, should remain in its project-defined location.

- The two points should lie on the 3D global geometry as defined by horizontal alignment, vertical profile, and superelevation.
- The chord length between the two points is equal to the sum of PS_D and PS_U.

The first of these three conditions suggests that the pier segment "rock" about its base to achieve desired grade and to keep the centerline of the pier at a specified location. This rocking takes place about a point at the bottom middle of the pier segment called the *working point (WP)*. As shown in **Figure 8.14**, positive grade (increasing elevation with stationing) requires that the pier segment rock in the down-station direction. An up-station rocking is needed for negative grades. Only at a zero grade would the centerline of the pier segment and centerline of the pier align in side view.

Figure 8.15 shows another side view of the pier segment rocked to accommodate the grade of the bridge. Also shown in **Figure 8.15** is the change in station Δ_{STA} of the center of the pier segment from the centerline of the pier. The dimension h is the depth of the box girder when observed in side view.

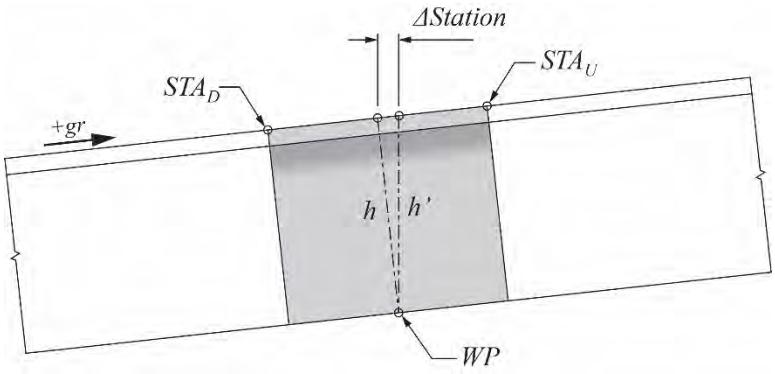

Source: PCI

Figure 8.15 Side View Pier

Knowing the station of the centerline of pier and the elevation, grade, and cross slope at that station can be computed. This information and the segment dimensions lead to the following equations for the beginning and ending points of the pier segment.

The grade expressed in degrees is

$$\theta_{gr} = \tan^{-1}(gr) \tag{8.1}$$

The change in station from the centerline of pier is

$$\Delta Station = h \sin(\theta_{gr}) \tag{8.2}$$

The stations of the beginning and ending points are

$$STA_D = STA_{CL} - \Delta Station - PS_D \cos(\theta_{gr}) \tag{8.3}$$

$$STA_U = STA_{CL} - \Delta Station + PS_U \cos(\theta_{gr}) \tag{8.4}$$

The elevations of the beginning and ending points are

$$Z_D = Z_{CL} - \left(\Delta_{STA} + PS_D \cos(\theta_{gr})\right) gr \tag{8.5}$$

$$Z_U = Z_{CL} - \left(\Delta_{STA} - PS_U \cos(\theta_{gr})\right) gr \tag{8.6}$$

The depth of the box girder projected onto the centerline of the pier is

$$h' = \frac{h}{\cos\left(\theta_{gr}\right)} \tag{8.7}$$

The working point is also used with respect to cross slope to satisfy the second condition for pier segment placement: maintaining the beginning and ending points of the pier segment on the 3D geometry. Section A-A in **Figure 8.14** shows that a transverse offset of the working point relative to the horizontal alignment of the centerline of box girder is needed to keep the centerline of the box girder in the correct position. This offset is specified on a project's foundation layout drawings.

Figure 8.16 shows another depiction of section A-A showing the transverse offset Δ_{TRVS}. Remembering that this cross section is taken vertically through a box girder with grade, the depth of the box girder in this vertical section is that found by Eq. (8.7). This depth is used to find the transverse offset and elevation of the working point.

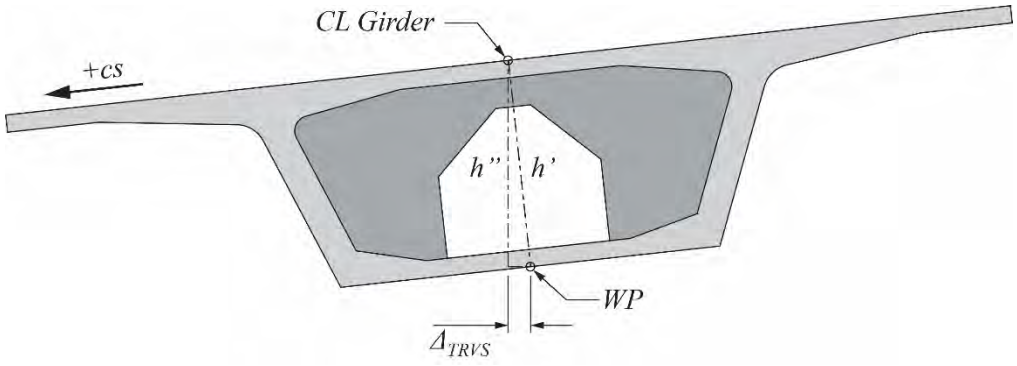

Source: PCI

Figure 8.16 Cross Section at a Pier

The cross slope expressed in angular form is

$$\theta_{CS} = \tan^{-1}\left(cs\right) \tag{8.8}$$

The transverse offset is then

$$\Delta_{TRVS} = h'\sin\left(\theta_{cs}\right) \tag{8.9}$$

Or when combined with Eq. (8.7):

$$\Delta_{TRVS} = \left(\frac{\sin\left(\theta_{cs}\right)}{\cos\left(\theta_{gr}\right)}\right)h \tag{8.10}$$

The vertical change in elevation from the profile grade line at the station of the centerline of the pier to the working point is

$$Z_{WP} = Z_{CL} - h" = Z_{CL} - h'\cos\left(\theta_{cs}\right) \tag{8.11}$$

Or when combined with Eq. (8.7):

$$Z_{WP} = Z_{CL} - \left(\frac{\cos\left(\theta_{cs}\right)}{\cos\left(\theta_{gr}\right)}\right)h \tag{8.12}$$

Eq. (8.1) through (8.12) are based on simplifying assumptions that, for most highway geometries, produced results of sufficient accuracy. These assumptions and their 3D realities are shown in **Table 8.1.**

Table 8.1 Simplified Pier Segment Placement Assumptions and 3-D Placement Realities

Simplified assumption	3-D reality
The vertical grade of the pier segment is equal to that of the instantaneous grade at the station of the centerline of the pier.	The grade of the chord of the centerline of the pier segment is slightly different than the instantaneous grade when the pier segment lies in a portion of a profile that contains vertical curves.
The length of the pier segment in plan view is equal to the station difference between the beginning and ending points.	The chord length is different from the station difference when the pier segment lies along a curving horizontal alignment.
The transverse offset of the working point is radial to the horizontal alignment at the station of the centerline of the pier.	The transverse offset is perpendicular to the chord of the pier segment, which is different from the radial bearing if the pier segment lies along a curving horizontal alignment.

A more exact solution for locating pier segments with an accuracy that may be needed for more severe combinations of highway geometrics is depicted in **Figure 8.17**. The procedure is based on an iterative process with the following steps:

1. Use Eq. (8.3) to approximate station of the beginning point of the pier segment (point P_1 in **Figure 8.17**).
2 Calculate data associated with point P_1 (X, Y, Z, gr, cs).
3. Approximate the station of the ending point of the pier segment using Eq. (8.4) (point P_2 in **Figure 8.17**).
4. Calculate data associated with point P_2 (X, Y, Z, gr, cs).
5. Compute the chord length between points P_1 and P_2 and compare the chord length with the length of the pier segment.
6. Iterate on the location of point P_2 until the chord length is sufficiently the same as the pier segment length.
7. Compute the data associated with point P_{CL} at the section of the pier segment containing the working point. Coordinate information is found along the chord between points P_1 and P_2, proportioned by relative dimensions of PS_D and PS_U. Pier segments are often cast square as starter segments (square and without superelevation variation). If this is the case, the cross slope for the segment cs_{CL} is proportioned between cs_1 and cs_2 by the relative dimensions of PS_D and PS_U. The grade of the pier segment is the elevation change between points P_1 and P_2 divided by the length of the plan projection of the pier segment chord. The bearing of the pier segment is the plan view bearing of the plan projection of the pier segment chord.
8. Find two vectors: Vector 1 is a unit vector from point P_{CL} in a direction perpendicular to the bearing of the pier segment chord. Vector 2 is a unit vector from point P_{CL} in the direction of point P_2.

9. Find the cross product of the two unit vectors of step 8 and scale it to a length equal to the depth of the box girder superstructure (h).
10. Locate the working point by adding the vector found in step 9 to point P_{CL}. The results will be coordinate information X, Y, and Z.
11. Project the X and Y coordinates of the working point onto the horizontal alignment of the centerline of box girder.
12 If the station found by projecting the working point equals the centerline of pier station, then determine the pier and footing offset Δ_{TRVS}. The bearing of the footing is the bearing of the pier segment. If the station found does not equal the centerline of pier station, adjust initial assumption for the station of point P_1 and repeat steps 2 through 11 until the stations reasonably converge.

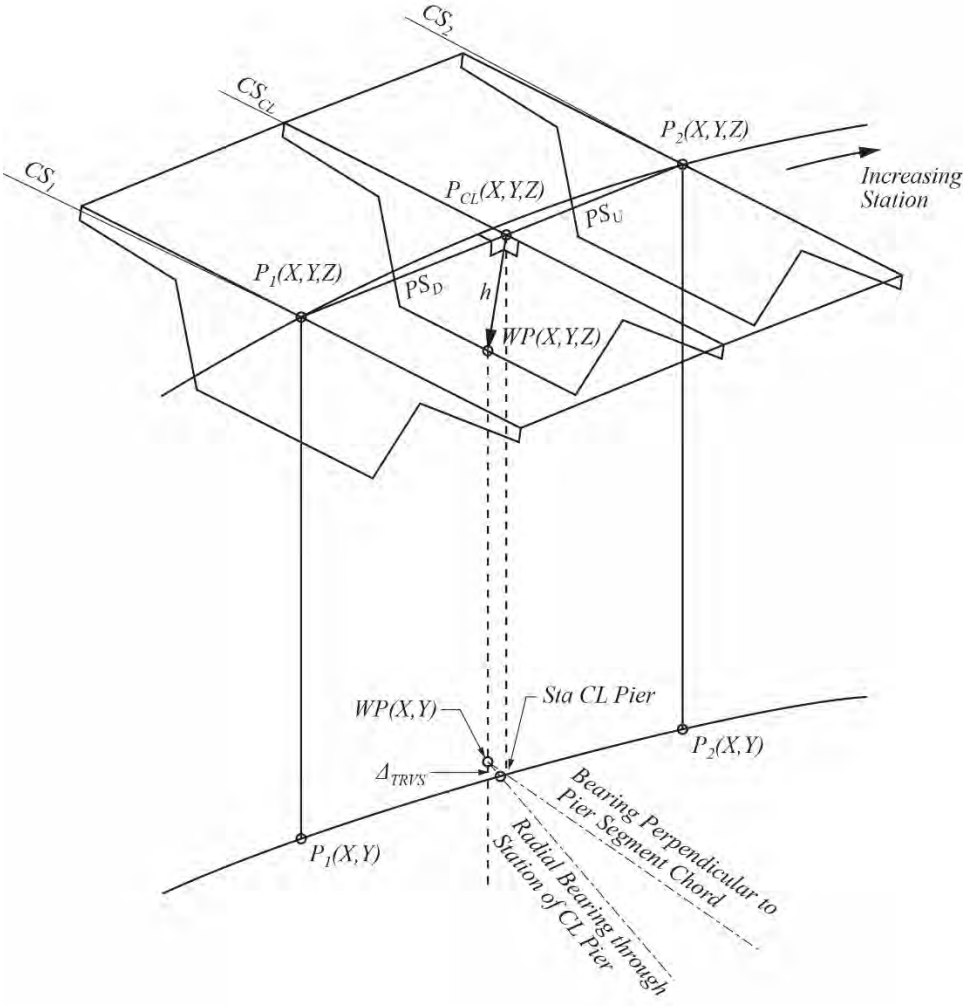

Source: PCI

Figure 8.17 3D Iterative Approach to Locating Pier Segments

8.2.1.3 Typical Segment Centerline Points

Typical segments within a bridge are cast straight as chords between their beginning and ending points. The lengths of these chords are the desired segment lengths. Once the global coordinates of the points at the beginning of a continuous run of segments are located, the global coordinates of other points along the continuous run can be found by a series of iterations. An iteration is complete when

the 3D chord length along the centerline of the box girder is equal to the desired segment length. A flow chart for this procedure for the segment layout and highway geometry shown in **Figure 8.12** is shown in **Figure 8.18**.

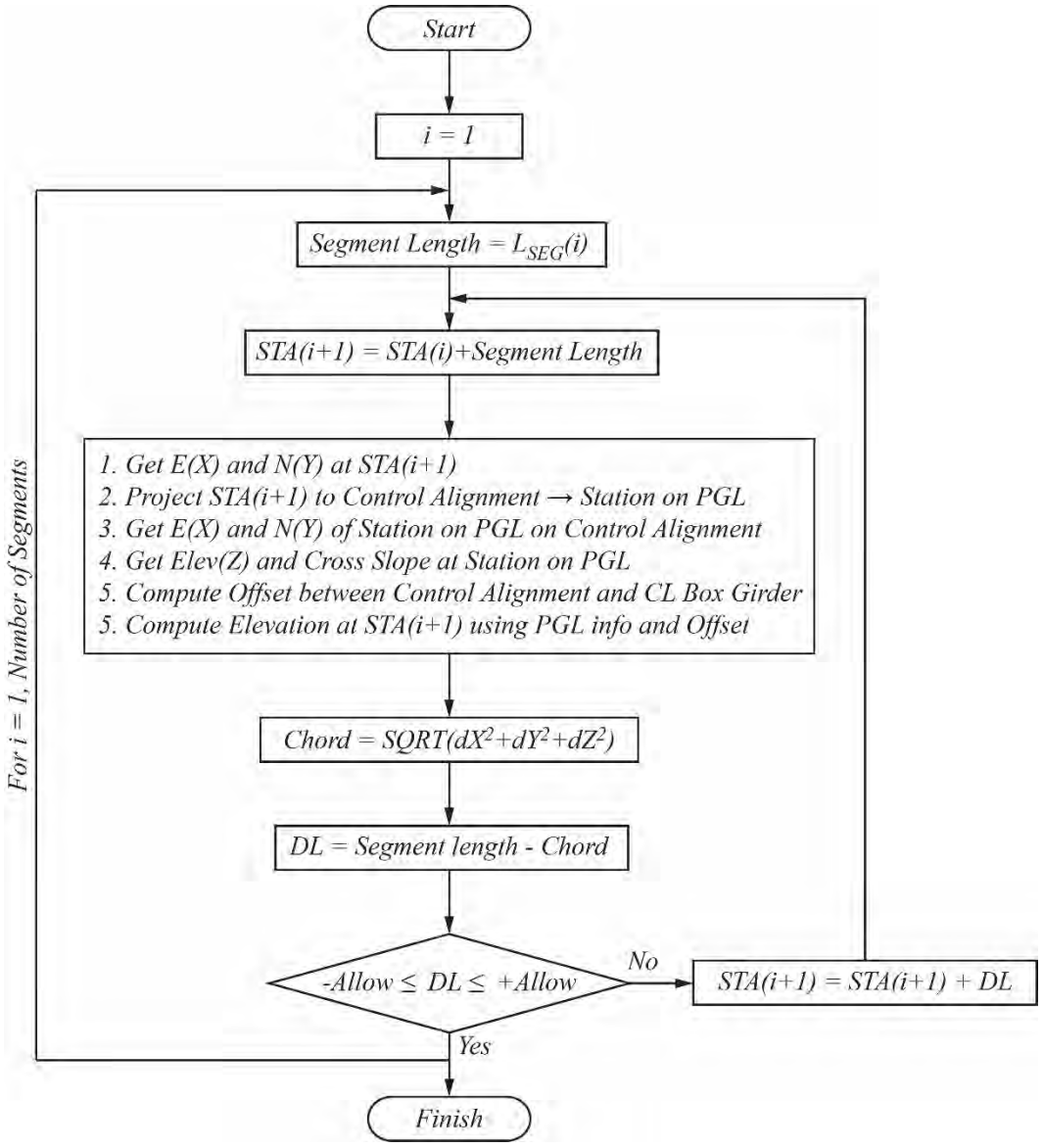

Source: PCI

Figure 8.18 Flow Chart for Iterative Approach to Centerline Points

The terms used in **Figure 8.18** are

L_{SEG} = lengths of the segments in a continuous run of segments

Chord = computed chord length for the current iteration

DL = difference between computed chord length and the segment length

Allow = acceptable accuracy of *DL*

8.2.1.4 Centerline of Girder Points Based on Construction Method

The approach to establishing centerline of segment points differs depending on the method of segment erection. **Figure 8.19** shows the centerline of segment points for two adjacent cantilevers in a bridge built in balanced cantilever. In **Figure 8.19**, the pier segments of the two balanced cantilevers have been located as discussed in Section 8.2.1.2. The centerline of segment points for typical segments are then found by applying the iterative approach of Section 8.2.1.3 in both the up-station and down-station directions beginning at the pier segments. Within a span, the distance between the ends of the cantilevers determines the length of the cast-in-place closure joint making the span continuous.

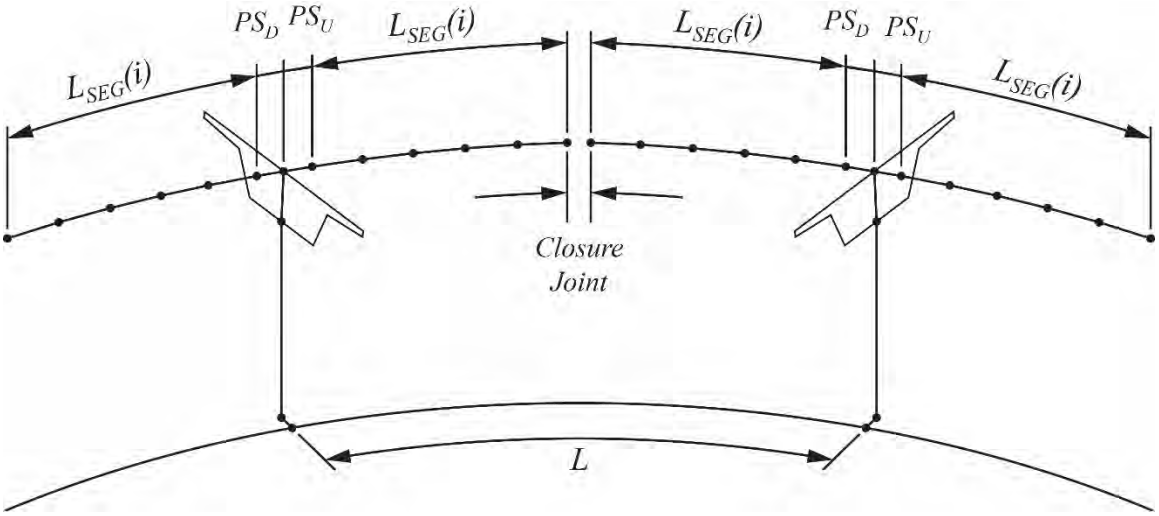

Source: PCI

Figure 8.19 Centerline of Segment Points for a Balanced Cantilever Bridge

Figure 8.20 shows centerline of segment points for a bridge built using the span-by-span method of construction. Closure joints are shown at either end of the span between the pier segments and first and last typical segments. These closure joints allow for the pier segments to be precast in their own forms off the critical path of typical segment casting. The pier segments located at either end of the span are located as discussed in Section 8.2.1.2. The typical segments are located as a continuous run of segments, the first of which is cast as a starter segment. The centerline of segment points for the typical segments is found using the approach of Section 8.2.1.3, but with one additional computation: an iterative adjustment of the beginning of the first segment of the span until the closure joints at either end of the span are equal in length.

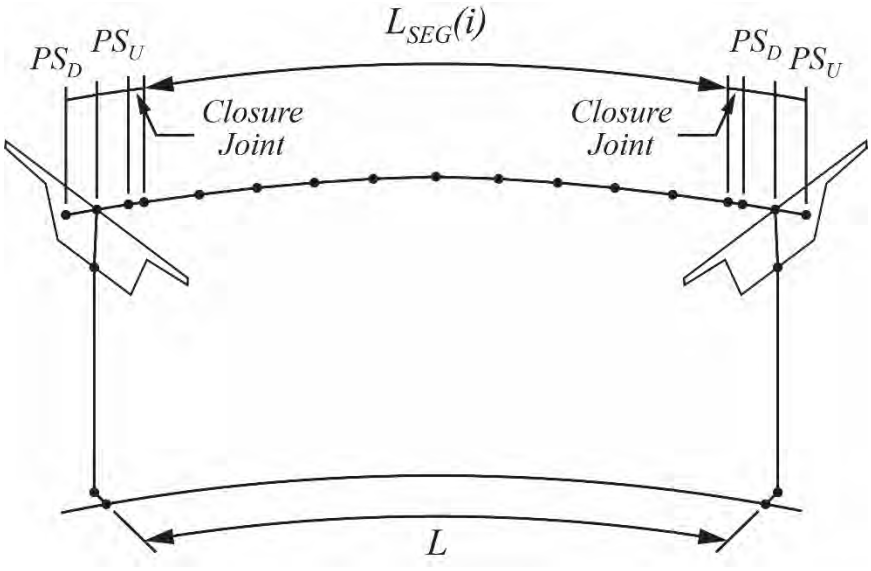

Source: PCI

Figure 8.20 Centerline of Segment Points for a Span-by-Span Bridge

There are several variations available for establishing the centerline of segment points for span-by-span bridges. Transit bridges, for example, are often constructed of simple spans with no closure joints within the span. In this case, typical segment lengths are adjusted to fit between pier segments located at either end of the span.

8.2.2 Segment Wingtip and Geometry Control Coordinates

The previous section provided an approach for locating points along the centerline of a box girder once the beginning station of a continuous run of segments is known. Other points located along the joints between segments are needed to establish the shapes of the precast concrete segments. Four points are typically needed along each bulkhead. Two points are located at the ends of the cantilever wingtips. For symmetrical bridge segments, the offset along the bulkhead for these points is equal to half of the width of the segment. Two other points are located to serve as geometry control points for the surveying of the segments as they are cast. These points are located symmetrically off the line of sight, along the bulkhead. They are located over a portion of the box girder cross section top slab that is not subject to local deflection. These points are typically located over the webs of the box girder.

Figure 8.21 shows a pair of segments taken from the layout of segments in **Figure 8.21**. Global coordinates for the points along the centerline of the segment have been located as discussed in the previous section. Inset at the bottom left of **Figure 8.21** is the pair of segments oriented in the casting yard coordinate system. Points have been located along the bulkhead at the wingtips and at survey locations. The coordinates of these points, known in the casting cell, are translated so that the origin of the casting cell (middle of the new-cast segment) is located at the beginning of the new-cast segment in the global coordinate system. The relocated points are then transformed so that the casting cell y axis is oriented along the chord of the segment (producing the y' axis) and the casting cell x axis is oriented to produce the cross slope at the station of the beginning of the segment (producing the x' axis). The cross product of the x' axis and y' axis produces the orientation of the z' axis. This transformation yields the global coordinates of the bulkhead points in the global coordinate system.

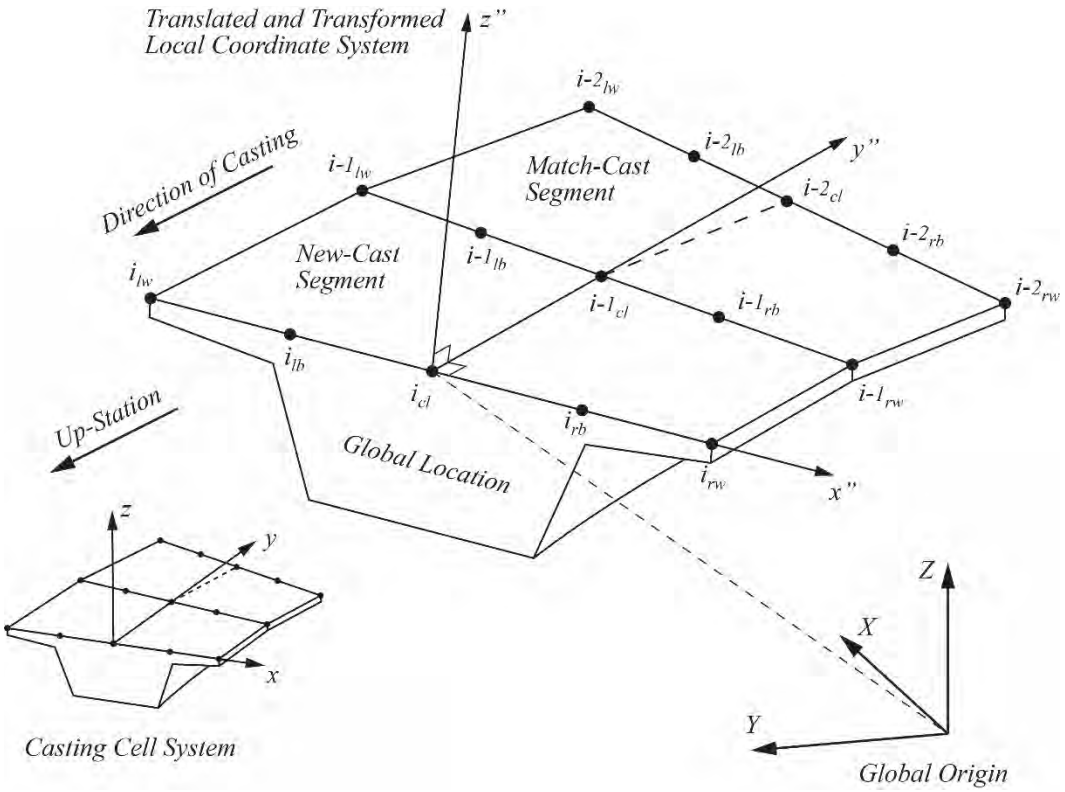

Source: PCI

Figure 8.21 Finding Bulkhead Coordinates in the Global Coordinate System

Figure 8.21 shows the translated and transformed axes of the local casting yard coordinate system to its desired global location and orientation. Also shown in **Figure 8.21** is the direction of casting consistent in the up-station direction with the properly oriented x', y', and z' axes. This coordinate system always looks back toward previously cast segments. This is important to recognize when a continuous run of segments begins with a middle starter segment, with casting proceeding from that starter segment in both up-station and down-station directions, as is the case for balanced cantilever construction.

Figure 8.22 shows a portion of bridge that is to be built using the balanced cantilever method of construction. The starter segment for the casting of the cantilevered segments is the pier segment shown located at the supporting pier. Casting in the up-station direction proceeds with the x', y', and z' axes looking down-station. The down-station segments are with the x', y', and z' axes oriented to be looking up-station. It is important to track "left" and "right" bulkhead points correctly when transforming them from the casting yard coordinate systems to the global system.

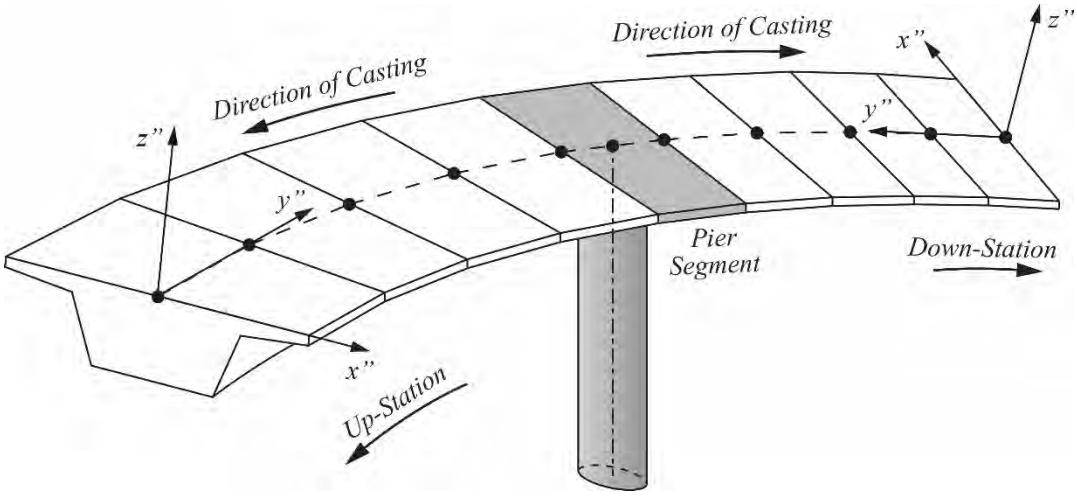

Source: PCI

Figure 8.22 Coordinate System Orientation as a Function of Direction of Casting

8.3 Geometry Control

8.3.1 General

Individual segment shapes can be established by the 3D global coordinates found using procedures described in the previous section. Achieving segment shapes involves a method of geometric control that is performed during segment casting. The short-line method of casting is based on making very fine adjustments to each match-cast segment by activating hydraulic jacks in the casting machine soffits. These fine adjustments are found by transforming the global coordinates of successive pairs of segments (match-cast and new-cast) to the casting cell. The relative position of a pair of segments is set and verified using conventional surveying equipment and targets with refined gradations to achieve desired accuracy.

Figure 8.23 shows the casting cell and features of the geometry control surveying needs. The local y axis of the casting cell is established along the line of sight from an instrument tower to a target tower. These towers are firmly founded so that they do not move during the casting of all segments. The towers are located between a set of benchmarks, one behind the instrument tower and one beyond the target tower. The benchmarks allow for daily verification of the line of sight. During assembly of the forms, the bulkhead is surveyed into place such that the x axis is horizontal, the z axis is vertical, and the xz plane is perpendicular to the line of sight (y axis).

Three different adjustments to the orientation of the match-cast segments are used to achieve the appropriate dimensions of the new-cast segment. Horizontal curvature is established by a lateral offset of the match-cast segment relative to the line of sight as shown in **Figure 8.24**. The y axis is aligned along the chord of the new-cast segment and the bulkhead is perpendicular to the segment chord. **Figure 8.25** shows another approach to achieving horizontal geometry, where the beginnings of both the match-cast and new-cast are offset from the line of sight. The y axis in this case is located tangentially to the horizontal alignment at the bulkhead, which is located radially to the horizontal alignment. Chorded joint layouts are more commonly used than radial joints and are used in this manual.

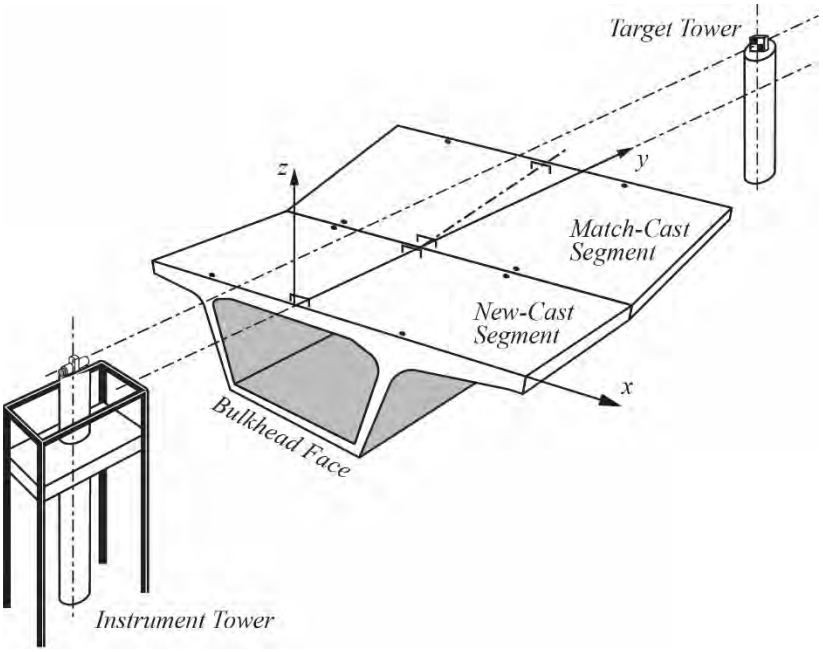

Source: PCI

Figure 8.23 Surveying Set-Up in the Casting Cell

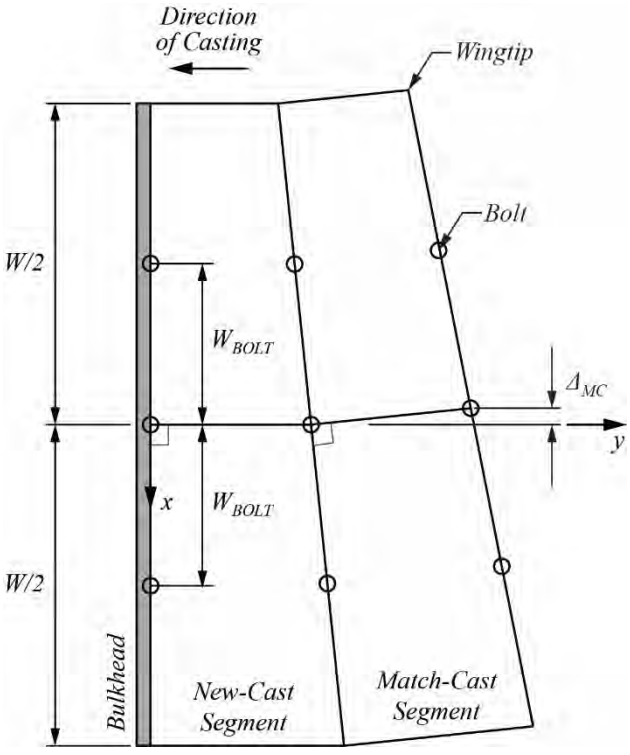

Source: PCI

Figure 8.24 Casting Cell Horizontal Alignment—Chorded Joints

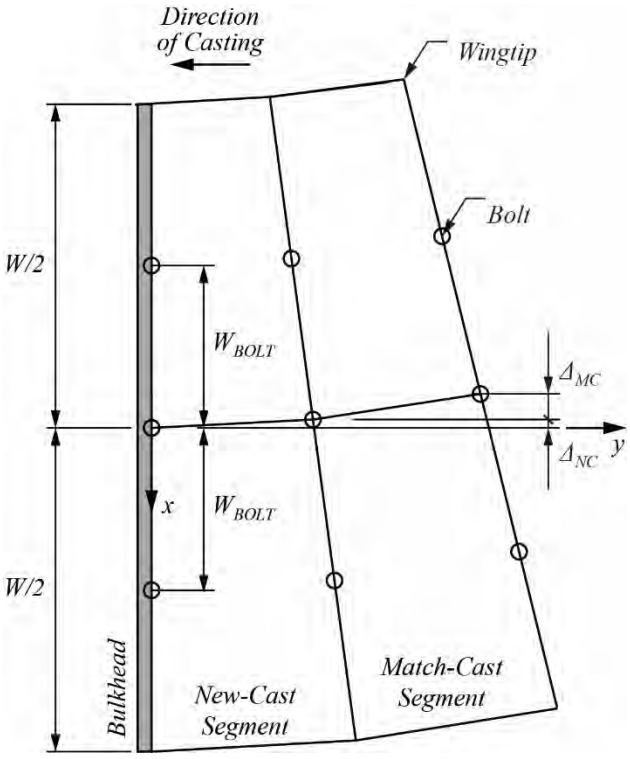

Source: PCI

Figure 8.25 Casting Cell Horizontal Alignment—Radial Joints

Vertical profile is achieved in the casting yard by elevating the beginning of the match-cast segment relative to the top of the bulkhead as shown in **Figure 8.26**. Superelevation variation is cast into the segments by rotating the soffit of the match-cast segment as shown in **Figure 8.27**.

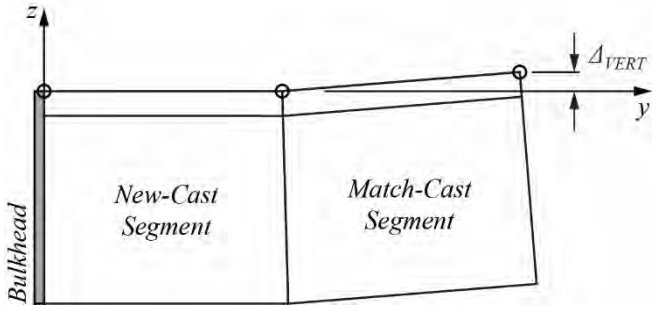

Source: PCI

Figure 8.26 Casting Cell Vertical Profile

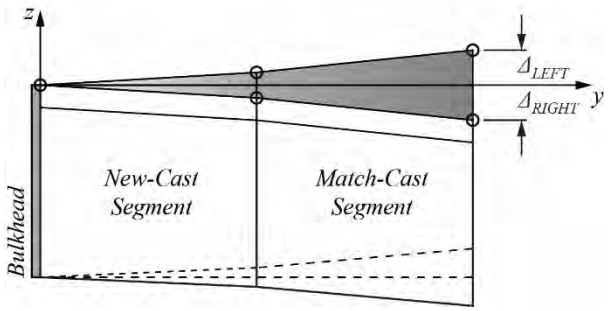

Source: PCI

Figure 8.27 Casting Cell Superelevation

8.3.2 Geometry Control Embedded Hardware

Marking survey locations directly on top of the precast concrete segments is not a reliable practice for surveying small changes in segment geometry. This is overcome by embedding hardware into the segments, as shown in **Figure 8.28**, on which geometric measurements are made. Galvanized steel bolts are embedded in the top slab of the segments at fixed offsets along the bulkhead. The bolt locations coincide with segment geometry points previously computed. The bolts serve as the fixed locations on which elevation measurements are taken. As they cannot be located directly at the segment joint, the bolts are located slightly off the bulkhead at a constant dimension. Galvanized steel hairpins are embedded in the top slabs of the segments to establish lateral segment location in the casting cell. When the concrete has hardened, a punch mark is made on the hairpins in line with the casting cell y axis.

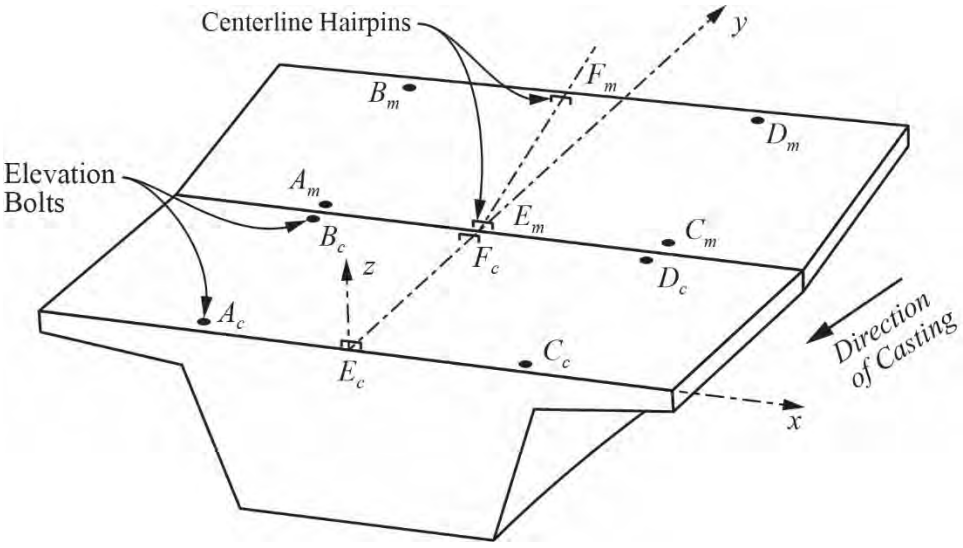

Source: PCI

Figure 8.28 Geometry Control Embedded Hardware

8.3.3 Measuring Tools and Read Accuracy

Special tools are needed to measure elevations and offsets accurately:

- Elevation readings on the bolts can be made with a precision level placed on top of the bolt (**Figure 8.29**). The leveling rod should be fitted with a scale divided down to at least 0.005 ft. A side-mounted spirit bubble level aids in keeping the rod vertical. The leveling rod should be fitted with a center point that sets into a punch mark on the top of the bolt.

- Centerline offsets can be measured from the casting cell centerline using a metal scale fitted with a center point that sits in a punch mark on the hairpins (**Figure 8.30**). The scale should be divided down to at least 0.005 ft. A spirit level should be attached to this scale so that it can be held in a horizontal position. The scale should be held so that is at right angles to the casting cell line of sight (y axis).
- A steel tape can be used for length measurements between the bolts and hairpins. The scale of the tape should be such that readings can be made with an accuracy of 0.002 ft.

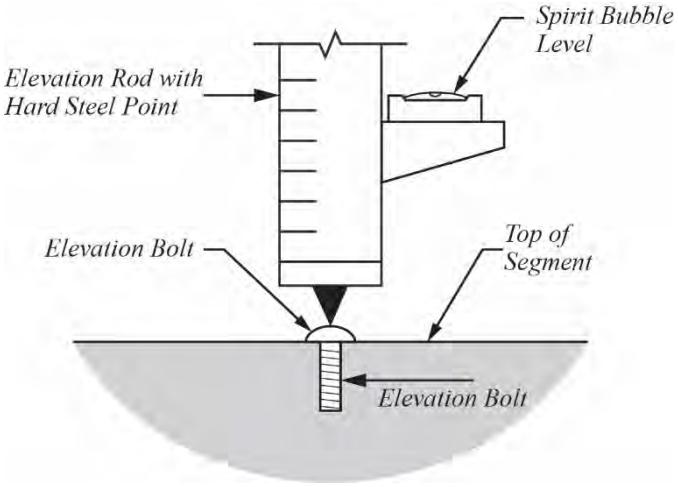

Source: PCI

Figure 8.29 Level Rod for Elevation Measurements

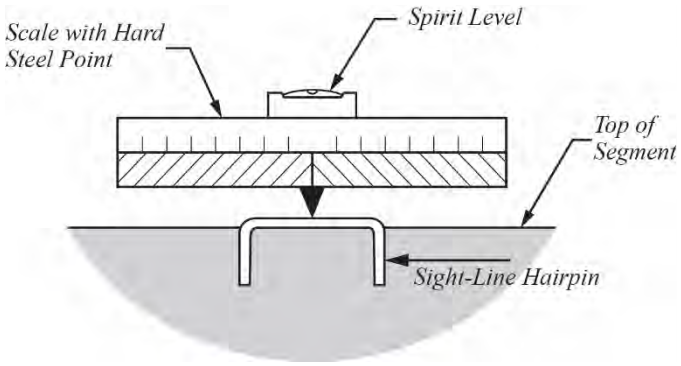

Source: PCI

Figure 8.30 Horizontal Level for Offset Measurements

8.3.4 Geometry Control Procedures

Geometry control of the precast concrete segments involves establishing, monitoring, and adjusting the relationship between new-cast and match-cast segments in the casting cell. 3D transformations from global location to the casting cell, within the casting cell, and back from the casting cell to global locations are performed for each casting cycle. The data transformed in this process are the coordinates determined in the casting cell based on elevation and offset readings. This 3D process of successive transformations to track as-cast positions to produce casting setups for the next segments was first developed for the Linn Cove Viaduct on the Blue Ridge Parkway in North Carolina in 1979.

Figure 8.31 shows the geometric transformations sequence. The rotation aspects of the transformations are made using direction cosines as described in appendix A.

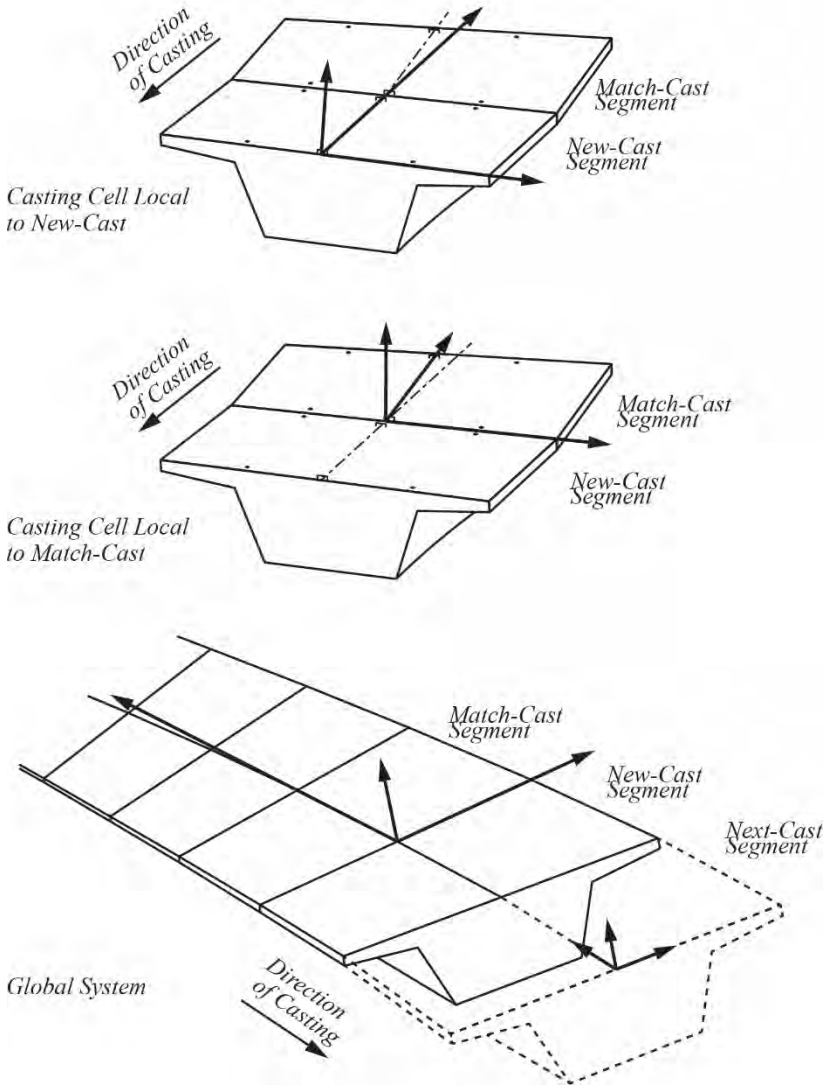

Source: PCI

Figure 8.31 Geometry Control Transformations

Following is a typical sequence of events for geometric control of precast concrete segmental bridges:

Starter segment (typically a pier segment in balanced cantilever construction)

- Global coordinates of the starter segment are transformed to the casting cell bulkhead.
- The temporary bulkhead is surveyed into position relative to the permanent bulkhead.
- The reinforcing cage is installed, forms are secured, and concrete is placed into the forms.
- Four elevation bolts (A_c, B_c, C_c, and D_c shown in **Figure 8.28**) and centerline hairpins E_c and F_c are installed after the top slab has been finished.
- When the concrete has sufficiently hardened, the elevations of the tops of the bolts are recorded and the centerline scribed onto the centerline markers.
- When the concrete reaches sufficient strength, the forms are released, and the starter segment is rolled into the match-cast position.

- The as-cast coordinates of the bolts and centerlines are established from the elevation and offset readings.
- The as-cast coordinates are transformed from the casting cell to their global position using the transpose of the transformation matrix of the starter segment.

Typical segment

- The global coordinates of the new-cast segment to be cast and the as-cast points of the match-cast segment are transformed from the global system to the casting cell using the transformation matrix of the new-cast segment.
- The match-cast segment is adjusted so that the bolts and punched centerlines are aligned to the transformed starter segment coordinates.
- The bolts are now in the A_m, B_m, C_m, and D_m position and the punch marks are in the E_m and F_m position (**Figure 8.28**).
- The reinforcing cage for the new-cast segment is installed, forms are secured, and concrete is placed into the forms.
- The new-cast segment is cast and new bolts A_c, B_c, C_c, and D_c and hairpins E_c and F_c are placed after the top slab is finished.
- When the concrete has sufficiently hardened, the elevations of all bolts are measured, hairpins in the new-cast segment are punched, and offsets in the match-cast segment are measured.
- Elevation and offset readings are used to establish coordinates of the geometry control points in the casting cell.
- A twist check is performed to determine whether the match-cast segment has twisted under the weight of the as-cast segment wet concrete. A twisted match-cast segment will untwist when separated from the new-cast segment. When realigned during erection, the relative angular changes between the segments will be incorrect. As a result, the next new-cast segment is adjusted to compensate for the measured twist.
- A transformation matrix located at the beginning of the match-cast segment is created and the as-built coordinates are transformed from the casting cell bulkhead to the match-cast joint location.
- The coordinates are then transformed from the match-cast joint in the casting cell to the global system, establishing the location of the new-cast segment.

Chapter 9 – Geometry of Curved Precast Concrete U-Girder Bridges

9.1 Introduction

Use of precast concrete U-girder segments may benefit many curved bridge projects. Geometrically, these bridges can support a wide range of highway horizontal curvatures with any combination of vertical profile and roadway superelevation. Structurally, the torsional stiffness of the U-girders, formed into a box by the top slab, enables moderate span lengths to be reached with radii as small as 500 ft. Span lengths approaching 300 ft can be achieved with variable depth girders when curvature is small. Aesthetically, the bridge type offers fewer girder lines, smooth webs, and a gracefully curving superstructure. Economically, this bridge type is typically cost-effective compared with curved steel bridges. Precast concrete U-girder bridge construction is typically cost-effective compared with precast concrete segmental bridges when the project size does not warrant the development of a project-specific segmental casting yard.

Figure 9.1 shows a typical curved bridge constructed using curved U-girder segments. The bridge shown is the Ramp Y Bridge at the I-270/I-76 Interchange in Denver, Colo. The Colorado Department of Transportation played a leading role in the development of this bridge type.

Source: PCI

Figure 9.1 Curved U-Girder Bridge in Colorado

Curved U-girder segments are fabricated in casting yards using forms that themselves are curved to achieve the desired girder radius. A variety of forming systems have been used, including full-length forms with sufficient lateral flexibility to be bent into shape, and modular systems composed of multiple, short sections of rigid forms that are individually arranged to the girder radius. **Figure 9.2** shows four aspects of the modular forming system. At the upper left of the figure is a rendering of the two pieces that make up a unit of the modular forming system, the outer and inner forms. The upper right picture shows an assembly of outer forms positioned to follow the radius to be cast. The reinforcing cage and post-tensioning tendons have been positioned in the outer forms in the bottom left

photograph, and inner form placement has begun. The bottom right photograph shows a completed curved U-girder segment being transported from the casting bed to storage.

Source: PCI

Figure 9.2 Curved U-Girder Fabrication

The construction sequences of curved U-girder bridges vary from project to project, but typically include the following phases:

- Falsework towers that will temporarily support the U-girder segments are erected at the girder longitudinal splice locations.
- The precast concrete curved U-girder segments are shipped from the casting yard to the bridge site. Sufficient longitudinal post-tensioning tendons are stressed in the casting yard to limit tensile stresses during handling, shipping, and placement on the temporary towers.
- Precast concrete curved U-girders are erected on the temporary towers. Temporary lateral bracing between the top flanges may be needed. The erected U-girders are stabilized against overturning at the temporary supports.
- Post-tensioning tendon ducts are spliced at the closure joints, closure joint reinforcing is tied, and the closure joint concrete is placed.
- When the closure concrete has reached sufficient strength, some of the remaining longitudinal tendons are stressed, making the girder segments continuous between expansion joints.
- A lid slab between the top flanges of the U-girders is formed and cast to provide a torsionally stiff closed box cross section. Additional post-tensioning tendons are stressed when the lid slab concrete has reached sufficient strength.

- The remainder of the deck and haunch buildups are formed, reinforced, and cast.

Figure 9.3 shows four views during the construction of two curved spliced U-girder bridges at the SR417/Boggy Creek Road Interchange. These bridges, located just south of Orlando International Airport, were the first curved spliced U-girder bridges built in Florida. The upper left photograph shows several U-girder segments that have been erected on temporary towers. The upper right photograph shows the placement of a U-girder segment. Two cranes were used for placing these girder segments because of the weight of the pick and to adjust the inclination of the girder segment for grade. The rigging of the cranes was such that girder segments were lifted with their final superelevation. The bottom left photograph shows a girder segment erected on temporary bearings. Surveying operations are taking place to ensure the position of the girder segment. The turnbuckles in the lifting rigging shown in this photograph set the cross slope of the girder segment as it is lifted. Splicing of the longitudinal post-tensioning tendon ducts at the cast-in-place closure joints is shown in the bottom right photograph. In regions of variable superelevation, the cross slopes of adjacent girder segments may need to be adjusted to minimize angular deviations in the tendons at these closure joints (see Section 9.2.3).

Source: PCI

Figure 9.3 Curved U-Girder Field Assembly

9.2 Geometric Considerations for Girder Precasting and Erection

Curved U-girder segments are precast with horizontal curvature but are cast flat and without superelevation variations along their length. Final bridge geometry is achieved by locating the girder segment correctly in 3D space and then casting the bridge deck to the needed appropriate roadway geometry. In addition to girder segment setting elevations, the geometric calculations are performed to

predict haunch thicknesses needed between the precast concrete girder segments and cast-in-place deck.

This mixture of precast and cast-in-place concrete needs a combination of geometric principles for precast segmental box girders (Chapter 8) and curved steel girders (Chapter 10). Like segmental bridges, the geometry of the curved U-girder is set locally in a casting bed so that it transforms to its correct global location in the bridge. Like curved steel bridges, haunch thicknesses over the webs of the U-girders are computed as the difference between the globally located U-girder and the deck slab cast to the roadway geometry.

9.2.1 Horizontal Layout

Curved U-girder horizontal layout is typically established by setting a control horizontal alignment for the working point of the U-girder cross section. The working point of the cross section is located along the girder centerline at the level of the top of top flanges. **Figure 9.4** shows a typical U-girder cross section and the working point. Also shown in the figure is a *nominal setting dimension*, which is the vertical dimension from roadway surface to the working point of the girder segment. This dimension allows for a range of haunch thickness along the girder segments and is refined as necessary as the haunch thicknesses are verified.

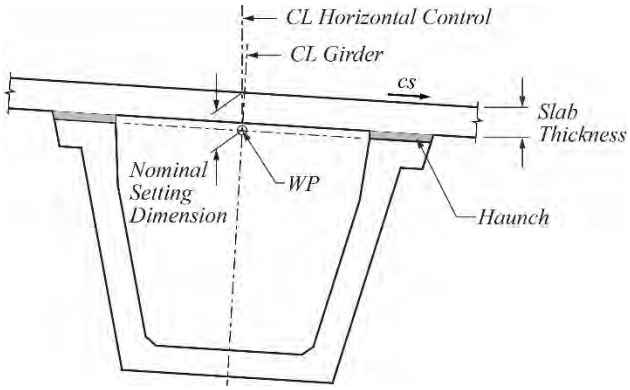

Source: PCI

Figure 9.4 Typical U-Girder Cross Section Showing Horizontal Control and Working Point

Figure 9.5 shows the plan layout of U-girders for a bridge consisting of two girder lines similar to the bridge shown in **Figure 9.1**. The girders are divided into segments with lengths chosen by shipping limitations, which take maximum width (with offset middle ordinate), and maximum weights into account. The girder segments are separated by longitudinal gaps typically 2 ft 0 in. in length. These gaps are the locations for cast-in-place closure joints, called splices, cast on-site when the girders are made continuous. The bridge horizontal geometry in **Figure 9.5**, defined along the centerline of the bridge, has a constant radius R. Offset horizontal alignments are defined to establish the locations of the working points at the ends of the girder segments. In this case, the offsets to these alignments are equal to half of the girder spacing, $S/2$. The resulting radii of the two offset alignments are $R+S/2$ and $R–S/2$.

Figure 9.5 also shows points along the centerline of the horizontal alignment with the labels *Begin station* and *End station*. These stations are projected onto the offset horizontal alignments to identify the location of the beginnings and endings of the girder segments. This results in splices with annular segment shapes. The splices have slightly different lengths along the left and right girder offset alignments. The differences in length are small relative to the 2 ft 0 in. centerline length (plus or minus ⅜ in. for a bridge with a 750 ft radius and girder spacing of 22 ft 6 in.). If preferred, the length of the

girder segments can be chosen such that the splice lengths are equal to 2 ft 0 in. along each offset control alignment.

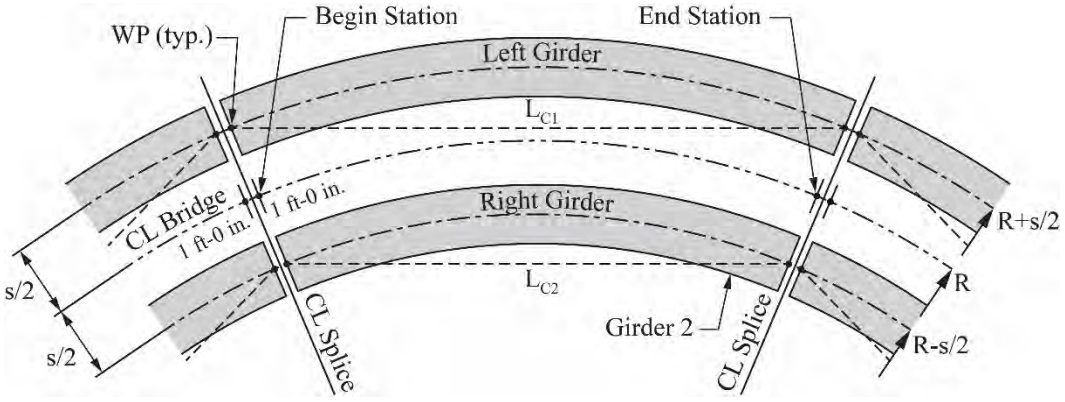

Source: PCI

Figure 9.5 Plan View Layout of a Two-Girder Bridge with Individual Girder Radii

Each of the girders shown in **Figure 9.5** follows its offset control alignment. This can be accomplished by casting the girders with slightly different radii. The small changes in radii necessitate resetting of the forms between the inner and outer girders, which negatively affects casting and construction schedules and increases costs. **Figure 9.6** shows the preferred approach, where both girder segments are cast with radii equal to that of the centerline of bridge. The offset of the girder segment from the control alignment is seen in the differences between the external dimensions ΔE_1 and ΔE_2. There is also an angle change in the girder geometry at the splices ($\Delta\alpha$). For a centerline of alignment radius of 750 ft, girder spacing of 22 ft 6 in., and a length of girder segment of 90 ft, the difference in external distance is equal to approximately ¼ in. The corresponding angle change at the splices is 0.1 degree. These small values indicate that girders cast with constant radii are appropriate for curved U-girder bridges.

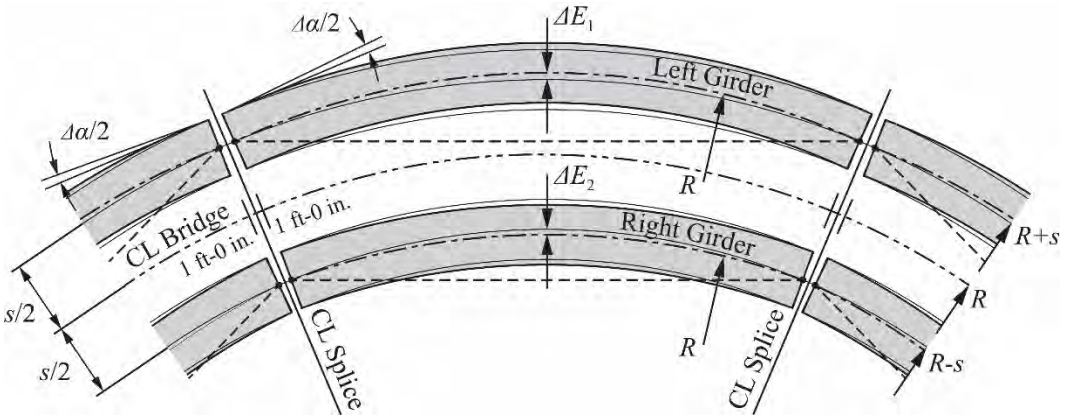

Source: PCI

Figure 9.6 Plan View Layout of a Two-Girder Bridge with Equal Girder Radii

9.2.2 Girder Segment Length

Chord lengths of the U-girder segments in plan view are adjusted for bridge grade to determine the length to be cast. **Figure 9.7** shows a 3D view of a U-girder segment following a constant radius curve in plan view. The begin and end stations of the girder segment are located along the centerline bridge alignment. Working points WP_1 and WP_2 for a girder segment of the right girder are found in the xy plane by projecting these points onto the control horizontal alignment. The elevations at points on the

bridge deck over the working points are found from the elevations at the begin station and end station plus or minus the superelevation multiplied by the offset to the control horizontal alignment. The elevations of the working points are found as the deck elevations above them minus the nominal setting dimension shown in **Figure 9.4**. The chord length for the girder segment is then found as the distance between the two working points including their elevations.

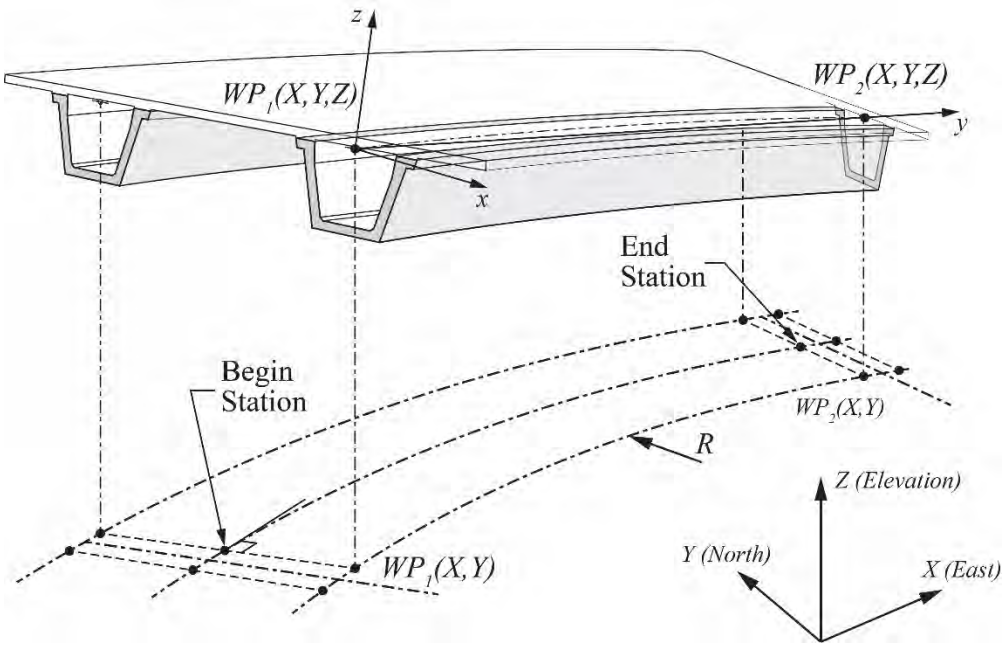

Source: PCI

Figure 9.7 Determining the Girder Segment Chord Length

9.2.3 Girder Segment Superelevation

U-girder segments are cast flat and have sufficient torsional stiffness to retain their cast shape during shipping and lifting. Crane rigging used to erect the girder segments is setup to lift the girder segments at a single superelevation. In regions of constant roadway superelevation, the superelevation of the lifted girder segment is the same as that of the roadway geometry. As superelevation is applied about the chord of the torsionally stiff curved U-girder, only the cross section at the midpoint of the girder will be aligned with the superelevation of the bridge deck. The superelevation of the girder from the midpoint to the ends will vary slightly from radial roadway superelevations.

In regions of superelevation transition, adjacent girder segments may need to be superelevated by different amounts. The change in superelevation at the girder splices will cause misalignment of the longitudinal post-tensioning tendons. **Figure 9.8** shows a cross section taken at a splice where the superelevations of the girder segments are different. The two girders are located at their working points with their individually preferred superelevations. Also shown in the figure are typical tendon locations at splices in positive and negative moment regions. Depending on the distance of a duct from the working point, the misalignment can be significant. The post-tensioning ducts are coupled across cast-in-place closure joints between the ends of the girders. Cases of expected significant misalignments can be treated by increasing the length of the closure joint. Horizontal reinforcing ties confining the change in direction of the post-tensioning force may be needed.

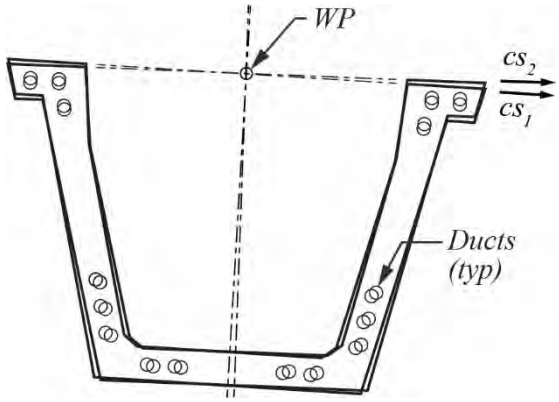

Source: PCI

Figure 9.8 Misalignment of Girder Segment Ends in Regions of Superelevation Transition

Two methods of improving tendon alignment are shown in **Figure 9.9**. Correction is made in the cross section at the left by applying corrective rotations (plus or minus *Δcs*) to the two girder segments and then aligning the working points on the offset control alignment. The cross section on the right makes correction by placing one of the girder segments on a control alignment offset slightly different from the other. Cross slopes of the girder segments are not changed using this method of correction. The direction of the offset is selected based on the locations of the post-tensioning tendons. For the example shown in the right sketch, an offset to the outside of the curve was made to better align the tendons in the positive moment region.

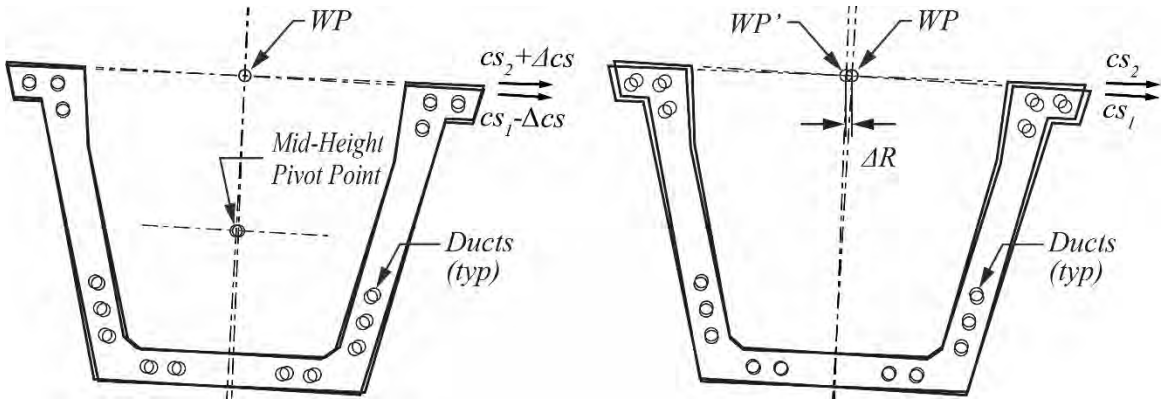

Source: PCI

Figure 9.9 Adjustments to Improve Duct Alignment: Rotate Each Segment about a Mid-Height Pivot Point (left) and Offset Working Points (right)

9.2.4 Deck Slab Varying Dimensions

Figure 9.10 shows a typical cross section of a bridge with two curved U-girders. The transverse deck slab dimensions are shown as variable in this figure. These variations come from a combination of things:

- Changes in superelevation while maintaining constant horizontal control alignments
- Using the same radius to cast both the left and right girders
- 3D transformation of a horizontal curvature from the casting bed to the permanent location in the bridge

The resulting variations in deck slab dimensions are small and can be easily accommodated within the flexibility of the forming details.

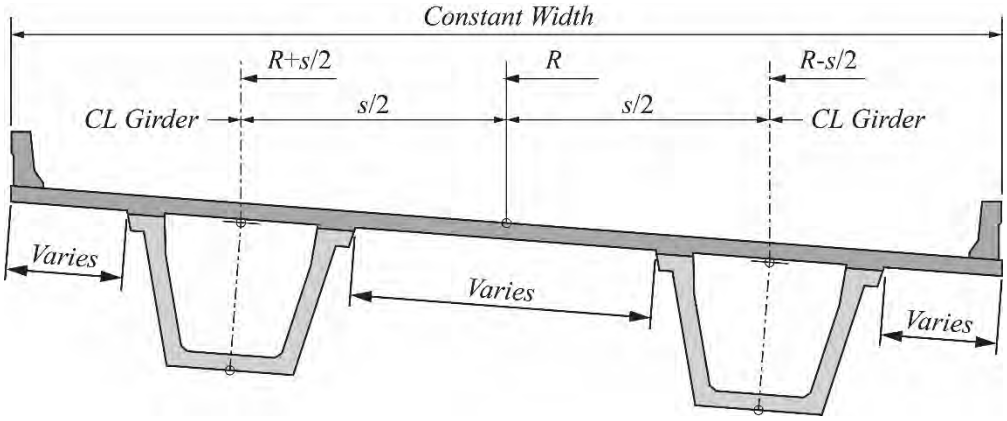

Source: PCI

Figure 9.10 Bridge Cross Section Showing Variable Deck Dimensions

9.3 Transformation from the Casting Bed to Location in the Bridge

Locating a curved precast concrete U-girder in its position within a bridge involves transforming the girder from a local casting bed coordinate system to the global coordinate system. A curved U-girder segment in the local coordinate system of the casting bed is shown in **Figure 9.11**. The coordinate system is shown with the local y axis oriented horizontally and along the chord of the girder segment defined by the working points. The local x axis is also horizontal and is oriented perpendicular to the local y axis. The local z axis is vertical and passes through the intersection of local x axis and y axis. The beginning and ending bulkheads will be skewed to the xz plane.

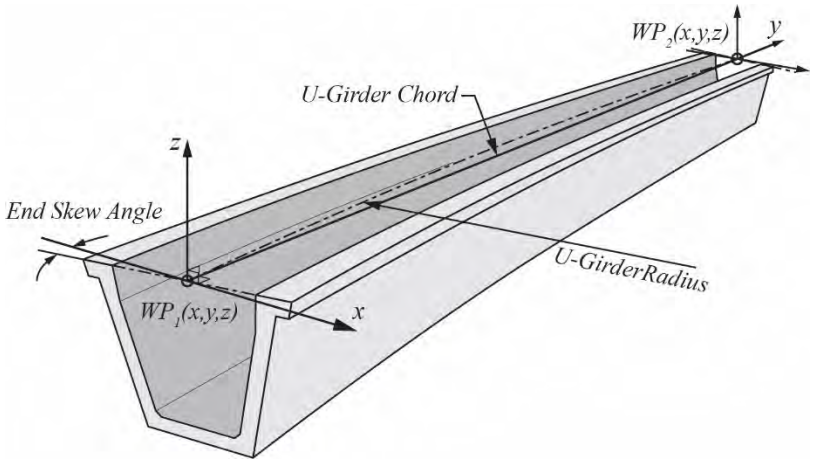

Source: PCI

Figure 9.11 Casting Bed Local Coordinate System

Figure 9.12 shows the U-girder segment in its final location within a bridge. The location in the global system of coordinates is found by performing three rotational transformations (angles λ, β, and γ) and one translation from the origin of the local system ($\Delta X, \Delta Y, \Delta Z$) to the beginning working point (WP_1).

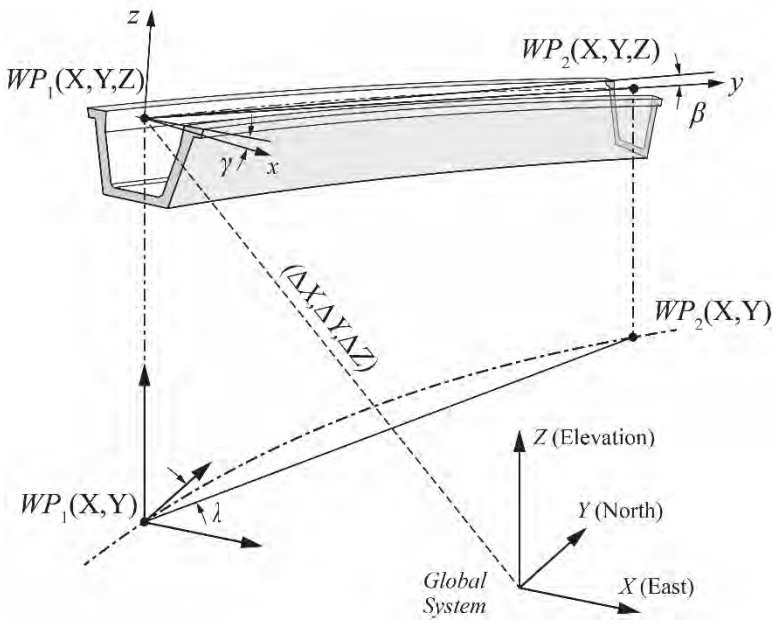

Source: PCI

Figure 9.12 3D Location of Curved Girder Segment

The steps of the three transformations and one translation is as follows:

- Transform about the y axis by the angle γ, which is equal to the inverse tangent of the girder segment superelevation.
- Transform about the x axis by the angle β, which represents the grade of the girder segment. The angle is the inverse tangent of the elevation difference between the two working points divided by the plan view chord between the two working points.
- Transform about the z axis by the angle λ, which is the angle between the chord of the casting bed (local y axis) and the global y axis.
- Translate the resulting coordinate system by adding the coordinates of WP1 to the origin of the resulting local coordinate system.

This process can be expressed in equation form as

$$[P]_{global} = [T]_{\lambda}^{T}[T]_{\beta}^{T}[T]_{\gamma}^{T}[P]_{casting\ bed} + [P]_{begin} \tag{9.1}$$

The points [*P*] are 3×1 matrices containing the x, y, and z coordinates of points. The transformation matrices $[T]^T$ are shown in Section A.5.2 of appendix A. Points in the local system of the casting bed, such as tenth points on the top flanges or the locations of temporary bearings, can be determined in the global system using Eq. (9.1).

9.4 Example Bridge

Example calculations in this chapter are based on a curved bridge that follows the horizontal alignment, vertical profile, and superelevation descriptions in previous chapters. **Figure 9.13** shows the location of bridge 3, which lies within the third horizontal curve (radius = 950 ft) of the example horizontal alignment. The bridge begins at station 197+65 and ends at station 203+15, resulting in a length along centerline of alignment of 550 ft.

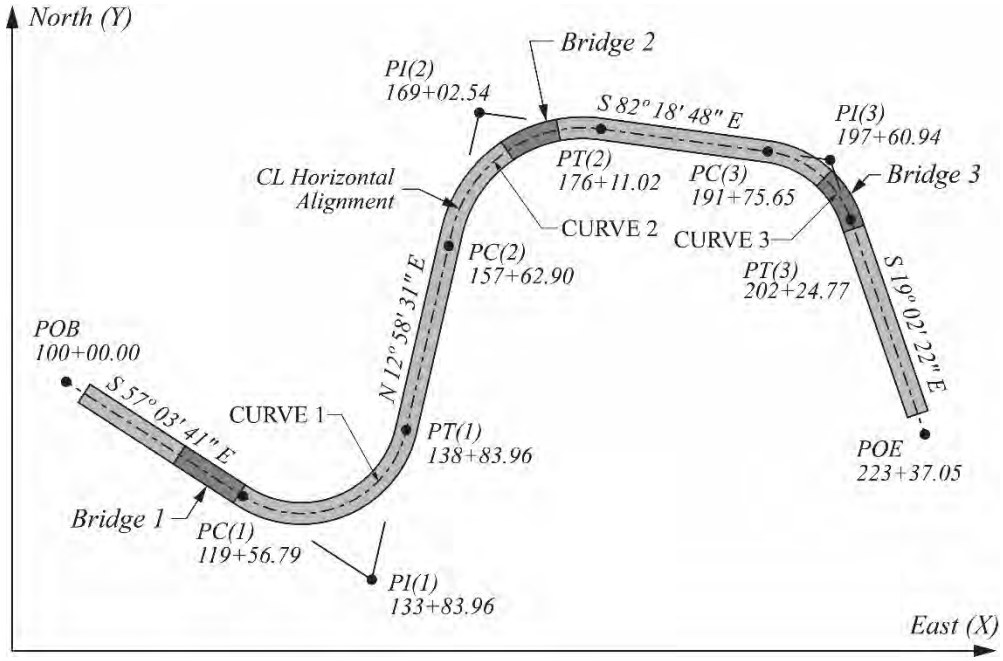

Source: PCI

Figure 9.13 Example Horizontal Alignment

Bridge 3 lies mostly on the sag curve located at *VPI*(4) of the profile previously developed in this manual. **Figure 9.14** shows the vertical curve at *VPI*(4) and the location of the bridge.

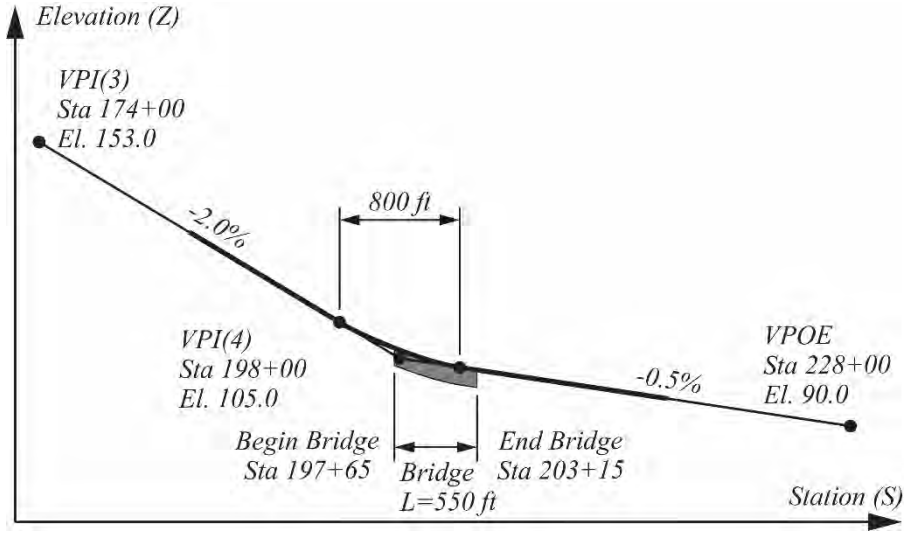

Source: PCI

Figure 9.14 Vertical Profile in the Vicinity of Bridge 3

Figure 9.15 shows a portion of the superelevation diagram at the location of the example bridge. Most of the curve lies in constant curvature with a superelevation of 7.5 percent. The end of the bridge undergoes superelevation transition, as a portion of the last span lies beyond the *PT* of the horizontal curve.

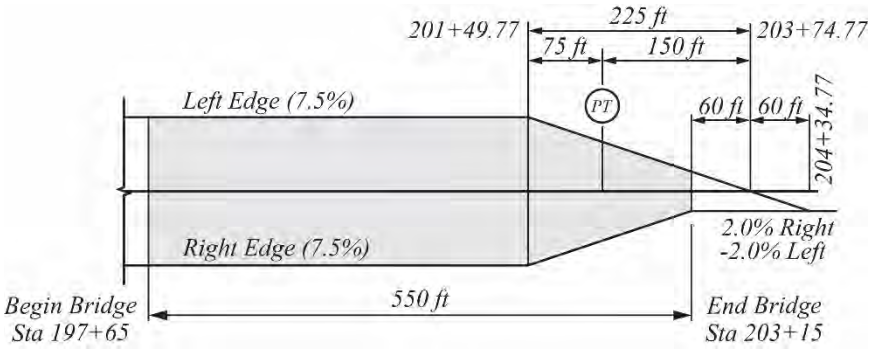

Source: PCI

Figure 9.15 Superelevation Diagram at Bridge 3

Figure 9.16 shows an elevation view layout of bridge 3. **Figure 9.17** shows the bridge in plan view. The spans of this bridge utilize curved precast concrete U-girders divided into six 90 ft girder segments. The cross section of the bridge is shown in **Figure 9.18**.

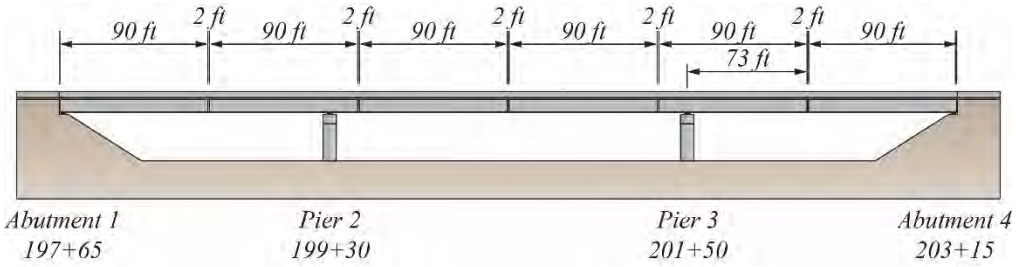

Source: PCI

Figure 9.16 Elevation View of Bridge 3

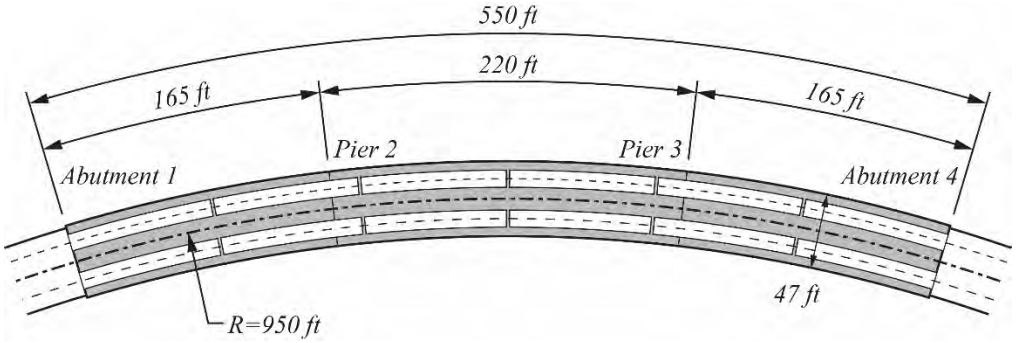

Source: PCI

Figure 9.17 Plan View of Bridge 3

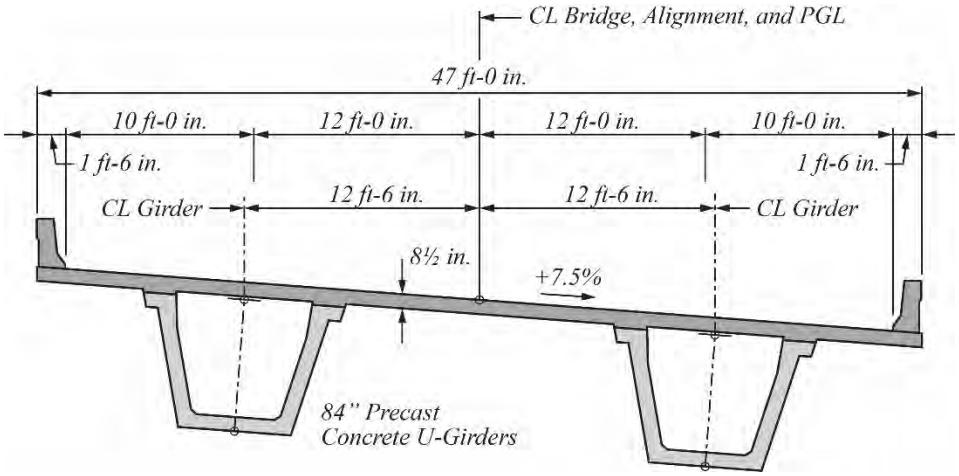

Source: PCI

Figure 9.18 Bridge 3 Cross Section in Full Superelevation

9.5 Example Calculations

Example calculations in this section are made for the second girder segment of the right girder (G2R) of bridge 3. The calculations include

- Locating the working points of the of the girder segment
- Determining the girder segment length
- Transforming girder segment control points from the casting bed coordinate system to the global system of coordinates (tenth points)
- Determining the elevations of the of the bridge deck over the global locations of the control points and evaluating the available haunch thickness

For this example, it is assumed that all girder segments will be cast with a radius equal to the radius of the bridge horizontal alignment.

9.5.1 Locating Working Points

The beginning and ending stations along the bridge horizontal alignment are found from the dimensions shown in the elevation and plan views shown in **Figure 9.16** and **Figure 9.17**. These stations are

$$Begin\ Segment = 198 + 57 \qquad End\ Segment = 199 + 47 \tag{9.2}$$

The working points are located radially offset to these points at a distance of 12.5 ft to the right (one-half of the girder spacing as shown in **Figure 9.18**). The procedures previously developed in this manual are used to determine the X and Y coordinates of the working points. The vertical profile and superelevation diagrams are used to establish the elevations of the working points at deck level. The resulting coordinates of the working points are

$$[P]_{WP1} = \begin{bmatrix} 7598.0645 \\ 4314.6033 \\ 104.8805 \end{bmatrix} \qquad [P]_{WP2} = \begin{bmatrix} 7653.3415 \\ 4245.1281 \\ 103.9276 \end{bmatrix} \tag{9.3}$$

9.5.2 Determining Girder Segment Length

The 3D chord length of the girder segment is the distance between the two working points:

$$L_{C2} = \sqrt{(\Delta X)^2 + (\Delta Y)^2 + (\Delta Z)^2} = 88.7877 \text{ ft} \tag{9.4}$$

The length of the girder segment along its curve with a 950 ft radius is found by solving for the deflection angle using the chord length and then multiplying it (in radians) by the radius. Recalling that

$$L_{C2} = 2R\sin\left(\frac{\alpha}{2}\right) \tag{9.5}$$

then

$$\alpha = 2\sin^{-1}\left(\frac{88.7877}{2(950)}\right) = 5.35686^\circ = 0.0934948 \text{ rad} \tag{9.6}$$

and

$$L_G = R\alpha = 950(0.0934948) = 88.8200 \text{ ft} \tag{9.7}$$

9.5.3 Transforming Tenth Points from Local to Global System

Tenth points are located along the center and on the outer edge of the top flanges of girder segment G2R in the casting cell coordinate system. These points are then located in the global location of the girder segment using the three rotational transformations and one translation presented in Section 9.3.

Figure 9.19 shows the layout of points to be located in the global system. **Table 9.1** presents the coordinates of these points in the local system of the casting bed.

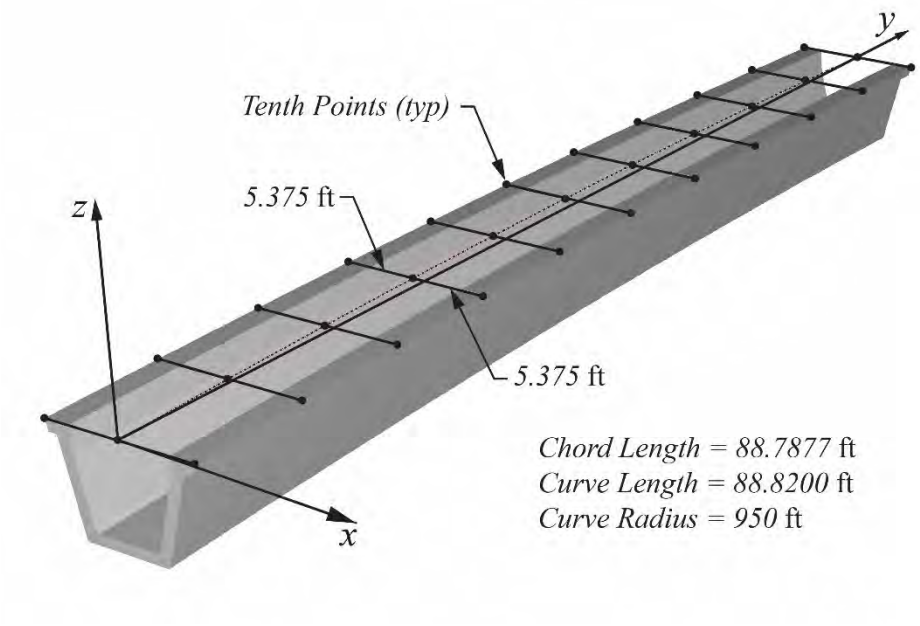

Source: PCI

Figure 9.19 Tenth Points in Girder Segment G2R in Casting Bed

Table 9.1 Tenth-Point Coordinates in Casting Bed Local System

Node	X, ft	Y, ft	Z, ft
1(CL)	0.0000	0.0000	0.0000
2(CL)	-0.3736	8.8741	0.0000
3(CL)	-0.6642	17.7513	0.0000
4(CL)	-0.8718	26.6309	0.0000
5(CL)	-0.9963	35.5120	0.0000
6(CL)	-1.0378	44.3938	0.0000
7(CL)	-0.9963	53.2757	0.0000
8(CL)	-0.8718	62.1568	0.0000
9(CL)	-0.6642	71.0364	0.0000
10 (CL)	-0.3736	79.9136	0.0000
11(CL)	0.0000	88.7877	0.0000
1(L)	-5.3691	-0.2512	0.0000
2(L)	-5.7448	8.6731	0.0000
3(L)	-6.0371	17.6006	0.0000
4(L)	-6.2458	26.5304	0.0000
5(L)	-6.3711	35.4617	0.0000
6(L)	-6.4128	44.3938	0.0000
7(L)	-6.3711	53.3260	0.0000
8(L)	-6.2458	62.2573	0.0000
9(L)	-6.0371	71.1871	0.0000
10(L)	-5.7448	80.1145	0.0000
11(L)	-5.3691	89.0389	0.0000
1(R)	5.3691	0.2512	0.0000
2(R)	4.9977	9.0751	0.0000
3(R)	4.7087	17.9021	0.0000
4(R)	4.5023	26.7314	0.0000
5(R)	4.3784	35.5622	0.0000
6 (R)	4.3372	44.3938	0.0000
7(R)	4.3784	53.2255	0.0000
8(R)	4.5023	62.0563	0.0000
9(R)	4.7087	70.8856	0.0000
10 (R)	4.9977	79.7126	0.0000
11(R)	5.3691	88.5365	0.0000

The three angles to be used in the transformations to the global system are found next. The rotation in plan view established by angle λ is found from the plan coordinates of the working points of the girder segment, expressed relative to an assumed orientation of the casting bed y axis. For this example, it is assumed that the casting bed y axis is aligned with the global y axis. The angle from the coordinates of the working points is

$$\lambda' = \tan^{-1}\left(\frac{Y_{WP2} - Y_{WP1}}{X_{WP2} - X_{WP1}}\right) = \tan^{-1}\left(\frac{-69.4752}{55.2770}\right) = -51.49296^\circ \tag{9.8}$$

This represents an angle from the local system to the plan view global location of

$$\lambda = 270^\circ + \lambda' = 270 + \left(-51.49296^\circ\right) = 218.50706^\circ \tag{9.9}$$

The angle β, used to transform the girder segment to grade, is the inverse tangent of the elevation difference between the two working points divided by the plan view chord between the points.

$$\text{Chord length in planview} = L_{C2P} = \sqrt{(\Delta X)^2 + (\Delta Y)^2} = 88.7826 \text{ ft} \tag{9.10}$$

$$\beta = \tan^{-1}\left(\frac{Z_{WP2} - Z_{WP1}}{L(plan\ chord)_{G2R}}\right) = \tan^{-1}\left(\frac{-0.9529}{88.7826}\right) = -0.6149^\circ \tag{9.11}$$

Girder segment G2R is in a region of constant superelevation equal to 7.5 percent. The adjacent girder segments, G1R and G3R, are also in a region of constant superelevation of 7.5 percent. As a result, the girder segment G2R will be transformed for cross slope using the angle γ:

$$\gamma = \tan^{-1}(0.075) = 4.2892^\circ \tag{9.12}$$

The three transforms of the transformation matrices are assembled:

$$[T]_\alpha^T = \begin{bmatrix} \cos\alpha & -\sin\alpha & 0 \\ \sin\alpha & \cos\alpha & 0 \\ 0 & 0 & 1 \end{bmatrix} = \begin{bmatrix} -0.7825 & 0.6226 & 0.0000 \\ -0.6226 & -0.7825 & 0.0000 \\ 0.0000 & 0.0000 & 1.0000 \end{bmatrix} \tag{9.13}$$

$$[T]_\beta^T = \begin{bmatrix} 1 & 0 & 0 \\ 0 & \cos\beta & -\sin\beta \\ 0 & \sin\beta & \cos\beta \end{bmatrix} = \begin{bmatrix} 1.0000 & 0.0000 & 0.0000 \\ 0.0000 & 0.9999 & 0.0107 \\ 0.0000 & -0.0107 & 0.9999 \end{bmatrix} \tag{9.14}$$

$$[T]_\gamma^T = \begin{bmatrix} \cos\gamma & 0 & \sin\gamma \\ 0 & 1 & 0 \\ -\sin\gamma & 0 & \cos\gamma \end{bmatrix} = \begin{bmatrix} 0.9972 & 0.0000 & 0.0748 \\ 0.0000 & 1.0000 & 0.0000 \\ -0.0748 & 0.0000 & 0.9972 \end{bmatrix} \tag{9.15}$$

The coordinate information in **Table 9.1** is premultiplied by the transpose of the transformation matrices in accordance with Eq. (9.1). To these results are added the coordinates of WP_1 shown in Eq. (9.3). The last adjustment to locate the girder is to drop the girder vertically by the nominal setting dimension. The value of this parameter for this example is 1 ft 0 in. The tenth points transformed and translated to the global system are shown in **Table 9.2**.

Table 9.2 Tenth-Point Coordinates in the Global Coordinate System

Node	X, ft	Y, ft	Z, ft
1(CL)	7598.0645	4314.6033	103.8805
2(CL)	7603.8810	4307.8911	103.8132
3(CL)	7609.6347	4301.1251	103.7396
4(CL)	7615.3249	4294.3057	103.6598
5(CL)	7620.9514	4287.4336	103.5739
6(CL)	7626.5134	4280.5094	103.4816
7(CL)	7632.0106	4273.5337	103.3832
8(CL)	7637.4425	4266.5071	103.2786
9(CL)	7642.8086	4259.4302	103.1678
10(CL)	7648.1084	4252.3037	103.0508
11(CL)	7653.3415	4245.1281	102.9276
1(L)	7602.1006	4318.1300	104.2847
2(L)	7607.9500	4311.3798	104.2170
3(L)	7613.7362	4304.5755	104.1431
4(L)	7619.4587	4297.7175	104.0628
5(L)	7625.1169	4290.8066	103.9763
6(L)	7630.7104	4283.8432	103.8836
7(L)	7636.2387	4276.8280	103.7846
8(L)	7641.7014	4269.7617	103.6794
9(L)	7647.0978	4262.6448	103.5680
10(L)	7652.4276	4255.4779	103.4503
11(L)	7657.6903	4248.2617	103.3264
1(R)	7594.0285	4311.0766	103.4762
2(R)	7599.8121	4304.4024	103.4093
3(R)	7605.5332	4297.6746	103.3362
4(R)	7611.1912	4290.8938	103.2569
5(R)	7616.7858	4284.0606	103.1714
6(R)	7622.3164	4277.1756	103.0797
7(R)	7627.7825	4270.2394	102.9818
8(R)	7633.1837	4263.2525	102.8778
9(R)	7638.5194	4256.2157	102.7676
10(R)	7643.7892	4249.1295	102.6512
11(R)	7648.9927	4241.9945	102.5287

9.5.4 Deck Elevations and Available Haunch Thickness over Tenth Points

The global X and Y coordinates are projected onto the centerline of bridge alignment, which is the *PGL* for this example. The results of these projections are offsets from the *PGL*, which are used with superelevation information to determine the deck elevations over the tenth points. **Table 9.3** lists the results of the stations to which the tenth points project, offsets from the *PGL*, and deck elevations over the tenth points.

Table 9.3 also presents the available haunch thickness. This thickness is the available distance from the bottom of the deck slab to the top of the uncambered girder. The slab thickness for this example is 8.5 in. The designer should evaluate the available haunch thicknesses considering the anticipated cambers and adjust the elevation of the globally located working points (one or both points). These adjustments added or subtracted from the nominal setting dimension establish the final girder setting dimensions.

Table 9.3 Deck Elevations and Available Haunch Thickness at Tenth Points

Node	CL station	Offset, ft	Deck	Haunch
1(CL)	19857.0000	12.5000	104.8805	0.2917
2(CL)	19866.0002	12.5060	104.7779	0.2564
3(CL)	19875.0004	12.5107	104.6769	0.2290
4(CL)	19884.0006	12.5140	104.5776	0.2094
5(CL)	19893.0007	12.5160	104.4799	0.1977
6(CL)	19902.0008	12.5166	104.3838	0.1938
7(CL)	19911.0009	12.5160	104.2893	0.1978
8(CL)	19920.0008	12.5140	104.1964	0.2095
9(CL)	19929.0007	12.5106	104.1052	0.2291
10(CL)	19938.0004	12.5060	104.0156	0.2565
11(CL)	19947.0000	12.5000	103.9276	0.2917
1(L)	19857.0070	7.1402	105.2824	0.2893
2(L)	19866.0067	7.1462	105.1798	0.2545
3(L)	19875.0063	7.1508	105.0789	0.2275
4(L)	19884.0060	7.1541	104.9795	0.2084
5(L)	19893.0056	7.1561	104.8818	0.1971
6(L)	19902.0052	7.1567	104.7857	0.1938
7(L)	19911.0047	7.1560	104.6913	0.1983
8(L)	19920.0041	7.1539	104.5984	0.2107
9(L)	19929.0034	7.1506	104.5072	0.2309
10(L)	19938.0026	7.1458	104.4176	0.2589
11(L)	19947.0017	7.1398	104.3296	0.2948
1(R)	19856.9929	17.8598	104.4786	0.2940
2(R)	19865.9937	17.8658	104.3760	0.2583
3(R)	19874.9944	17.8705	104.2750	0.2305
4(R)	19883.9951	17.8739	104.1757	0.2105
5(R)	19892.9958	17.8759	104.0779	0.1982
6(R)	19901.9965	17.8766	103.9818	0.1938
7(R)	19910.9970	17.8760	103.8873	0.1972
8(R)	19919.9975	17.8740	103.7945	0.2084
9(R)	19928.9979	17.8707	103.7032	0.2273
10(R)	19937.9982	17.8661	103.6136	0.2540
11(R)	19946.9983	17.8602	103.5256	0.2885

PART 3 – STEEL TOPICS

Chapter 10 – Geometry of Steel I-Girder Bridges

10.1 Introduction

This chapter presents geometric considerations and topics specific to bridges supported by steel superstructure members and will expand on discussions, examples, and calculations as presented in earlier chapters. The representative steel superstructure types include the following:

- I-Girders (Straight and Curved Girders)
- Girder-Substringer Systems
- Trusses
- Arches
- Trapezoidal Box Girders

Although tangent bridges with straight steel girders are relatively basic to design and construct, the designer should still consider the implications of geometric layout during design. For example, as the skew angle of the substructure units increases, the level of analysis for the superstructure design also increases. In this regard, straight steel girder bridges with skews less than or equal to 20 degrees are typically designed using a line girder method of analysis, while more severely skewed bridges may need a 2D Grid Analysis or ultimately a 3D Finite Element Analysis. As will be shown in this section, a similar logic follows for the severity of curvature for curved girders.

10.2 Vertical Camber

Steel girders are fabricated based on predetermined camber (See 6.4.3) calculated based on girder weight, superimposed dead loads, and the bridge geometry to minimize variations in girder elevations and haunch along the structure. A constant haunch depth along the length of the steel girder is the typical industry convention. (However, designers should refer to project specific design criteria or owner preference when deciding whether to design for a constant or variable depth haunch.) Steel girder haunch is measured from top-of-web to bottom-of-deck slab. The haunch thickness is measured from top-of-web rather than top-of-flange because the flange thickness typically changes along the length of the girder. The top-of-web provides a constant point of reference relative to the top-of-deck slab. If haunch were measured from top-of-flange, the value would change every time the flange thickness changed.

The constant haunch depth approach to steel girders contrasts with that of precast concrete beams. Precast concrete beams use a varying haunch to account for the difference between cambered shape and bridge deck profile (see 6.4.1.). The reason for the difference is a steel girder can be fabricated to match an irregular vertical profile while the cambered shape of a precast concrete beam is inherently parabolic.

Camber values typically are computed at quarter or tenth points along the length of the span. The number of points along the girder may vary depending on the bridge owner. Some owners will specify specific increments of length not to be exceeded; however, if no owner-specific guidance is available, fabricators often work with the tenth points in practice. Regardless, at each point, the change in the vertical profile is added to the composite and non-composite deflection to produce a total anticipated camber deflection. The girder is then fabricated with a camber equal to the inverse shape of the total

anticipated camber deflection. As a result, after placement of the full dead load, the top of the web will settle to a deflected shape that parallels the bridge deck profile.

10.2.1 Camber for Self-Weight Deflection

Common practice in calculating the vertical camber of a steel girder is to start by evaluating the deflection along the girder due to its self-weight and the tributary weight of miscellaneous steel. Miscellaneous steel can include, but is not limited to, cross frames, diaphragms, shear connectors, and connection hardware. The self-weight deflection values are typically extracted from the girder analysis. Computerized design software simplifies calculating deflections, especially for continuous steel girders and where section properties vary along the length of the girder.

10.2.2 Camber for Non-Composite Dead Load Deflection

The deflection due to non-composite dead loads is determined next. Non-composite dead loads, or loads applied to the non-composite girder section, generally include the weight of the concrete deck, concrete haunch, and stay-in-place forms, as applicable. Again, these values are typically obtained from the girder analysis results. It should be noted that each program is different, and as such, the deflections reported may combine multiple non-composite loads. However, designers should be aware and understand what is and is not included in the deflection report. The common practice is to separate various dead load deflection results to allow the user greater flexibility.

10.2.3 Camber for Composite Dead Load Deflection

The dead load deflection due to composite loads, often referred to as superimposed loads, include those applied to the composite deck/girder section. This can include the deflections due to the weight of bridge barriers, sidewalks, curbs, fences, lighting, signs, or other permanent appurtenances. The designer should consult the bridge owner's policy and project-specific design criteria to determine the extent to which these values are included in the camber calculations. Similarly, the weight of wearing surfaces may or may not be included in this group of deflection values. In instances where a *permanent* wearing surface is applied to the deck and composite section as part of initial construction, this can be included in the superimposed dead load deflections; however, if the project criteria stipulates the design accommodate a *future* wearing surface, this is traditionally not included in the deflections for camber, as these loads may never be applied.

10.2.4 Camber for Vertical Profile

The last component of the camber calculation is the adjustment used to compensate for vertical curvature of the bridge deck profile. As mentioned previously, steel girders and beams can be fabricated to closely follow the vertical profile of the bridge, whether the bridge is on a constant grade or is situated partially or fully within a vertical curve. When located within a vertical curve, the calculation to account for the profile is typically based on: (1) theoretical haunch is constant along the length of the girder; (2) no deflection occurs at the supports. A similar procedure for adjusting for the profile is presented in Section 6.4.1.3, but whereas that section uses it as a modification for haunch, here the same geometrical constraints are used to adjust the final girder camber values. The point of reference for this calculation is a chord drawn from the top of the web at the near support to the top of the web at the far support. From this the designer can measure the offset to the top of the web along the length of the girder.

As shown in **Figure 10.1**, for a span completely within a constant grade, the reference line and the top of web are coincident and therefore no adjustment for vertical curvature is needed. **Figure 10.2** and **Figure 10.3** illustrate the adjustment for a crest and sag vertical curve, respectively. Some bridge owners prefer to avoid locating a bridge within a sag vertical curve, the primary reason being

aesthetics. For example, passersby may be alarmed by the appearance of a bridge designed with sag curves, even though the bridge is structurally sound. Moreover, any geometric sag configuration, be it directly resulting from a sag curve or indirectly via the combination of cross-slope transition and vertical alignment can lead to ponding on the bridge. That is, potentially poor drainage can be a significant safety concern.

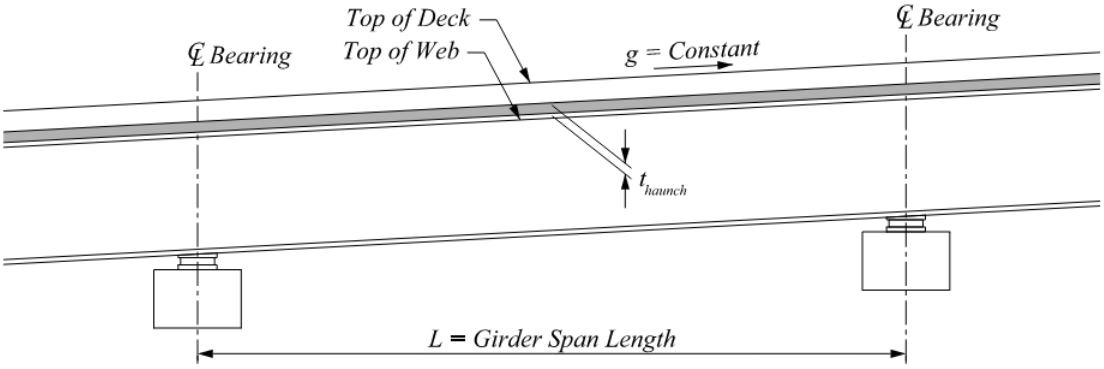

Source: FHWA

Figure 10.1 Steel Girder Span on Constant Grade

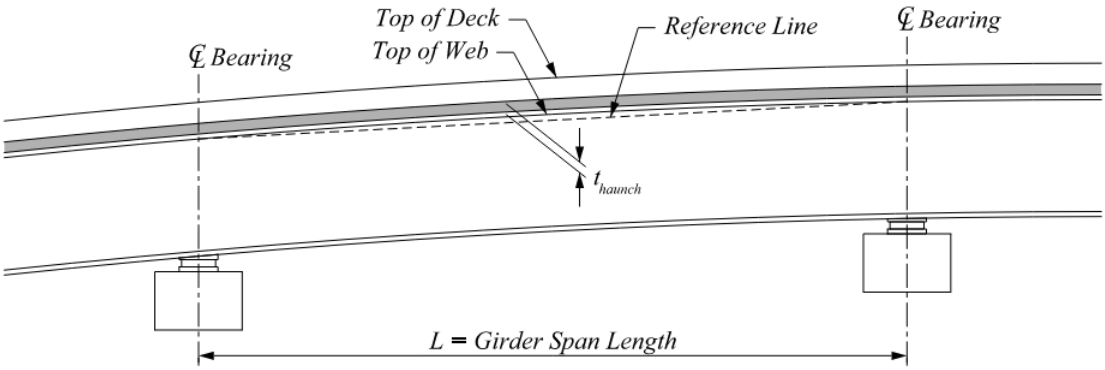

Source: FHWA

Figure 10.2 Steel Girder Span Profile Grade Adjustment for Crest Curves

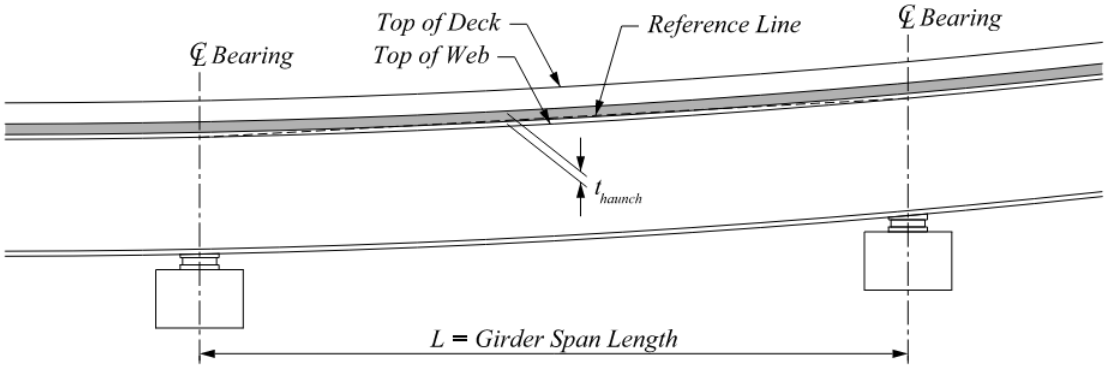

Source: FHWA

Figure 10.3 Steel Girder Span Profile Grade Adjustment for Sag Curves

Expressed in equation form, the adjustment due to vertical curvature is an adaption of Eqn. 6.24:

$$\Delta_{vc} = Z(x) - \left(Z_1 + \left(\frac{Z_2 - Z_1}{L}\right)x\right) \qquad \text{(Eqn. 10.1)}$$

Where: Δ_{vc} = adjustment for vertical curvature
$Z(x)$ = centerline of girder top of web elevation at "x" along the span
Z_1 = centerline of girder top of web elevation at beginning of the span
Z_2 = centerline of girder top of web elevation at end of the span
L = span length

Consider the Bridge 1 example used in Chapter 6, adapted here for steel I-girders and shown in **Figure 10.4** and **Figure 10.5**. The adjustment due to vertical curvature will be calculated for Girders 2 and 3 in Span 3. Additionally, both Girders 2 and 3 are presented to show the effect of the skew at Pier 4.

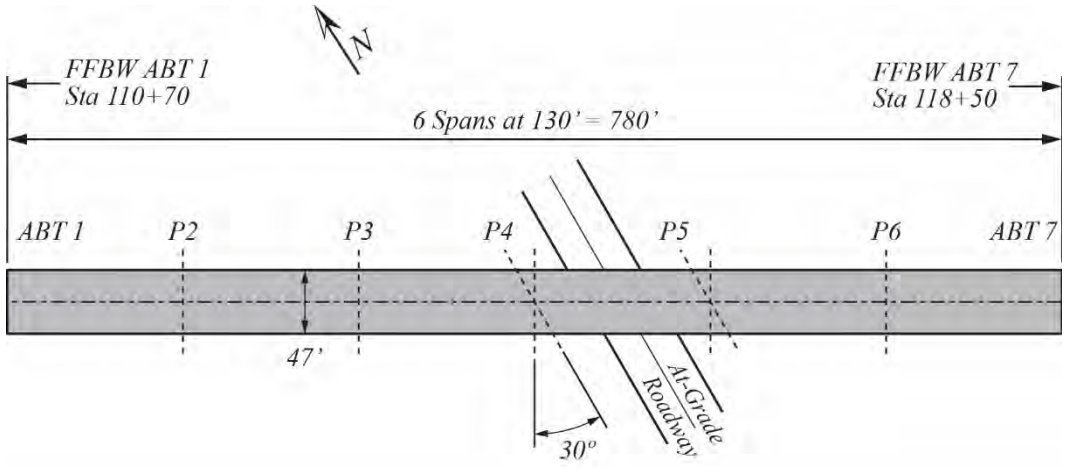

Source: FHWA

Figure 10.4 Plan View of Example Bridge (Bridge 1)

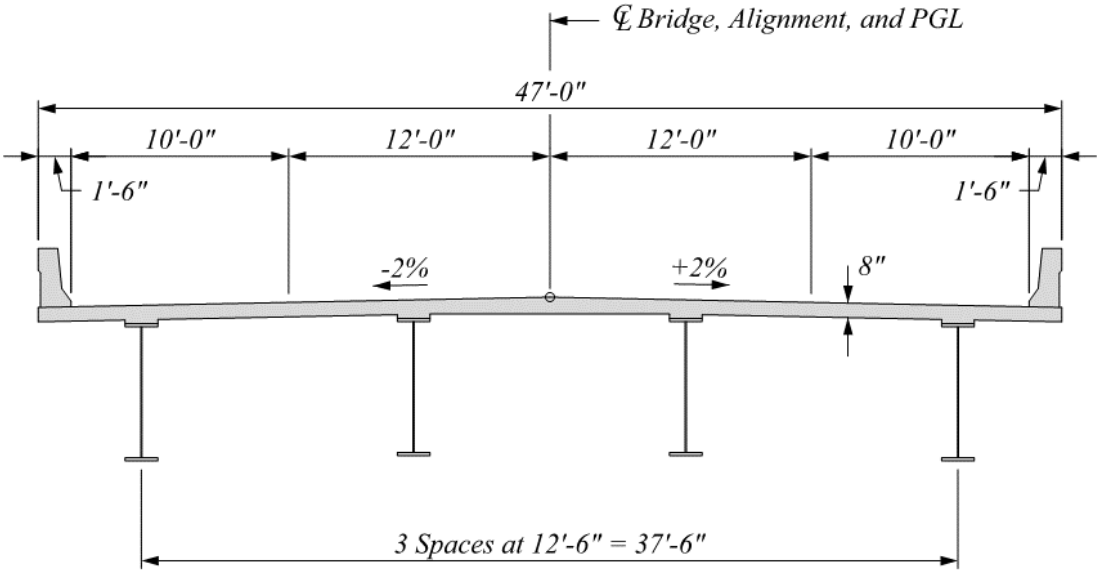

Source: FHWA

Figure 10.5 Bridge 1 Cross Section

Before looking at the calculated vertical curvature adjustment values, several other geometry items that differ from the example presented in Chapter 6 are calculated. The haunch thickness at the centerline of the girder will be based on the widest top flange and a minimum haunch thickness of two inches at the edge of the flange. For this example, the maximum top flange dimensions are 18 in. wide by 1.75 in. thick.

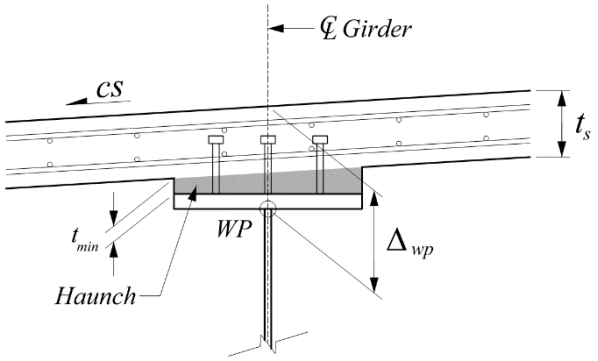

Source: FHWA

Figure 10.6 Typical Haunch for Steel Girder Bridges

The depth to the working point, or top of web, can be calculated as:

$$\Delta_{wp} = t_{tf} + t_{min} + |cs|\frac{b_t}{2} + t_s$$

(Eqn. 10.2)

Where: Δ_{wp} = depth from top of deck to working point, or top of web
t_{tf} = thickness of the top flange of the girder
$t_{\min}$ = minimum haunch thickness
$|cs|$ = absolute value of the cross slope at the cross section under consideration

b_t = width of the top flange of the girder
t_s = thickness of the deck slab

For Span 3, the depth to the working point is:

$$\Delta_{wp} = 1.75" + 2" + |0.02|\frac{18"}{2} + 8" = 11.93"$$

Next, Equation 10.1 is calculated at the tenth points, as shown in **Table 10.1** and **Table 10.2** for Girder 2 and Girder 3, respectively. In both Tables, Column 4 is the top of web elevations, which are obtained by subtracting the depth to the working point, Δwp (calculated above), from the top of deck elevations (Column 3). Column 6 is the adjustment for vertical curvature, Δvc, equal to the difference between the top of web (Column 4) and reference line elevations (Column 5).

Table 10.1 Bridge 1, Girder 2 Adjustments for Vertical Curvature in Span 3 (all elevations/dimensions in feet)

Location (1/10 Points) (Column 1)	Station (Column 2)	Top of Deck Elevations at CL Girder (Column 3)	Top of Web Elevations at CL Girder (Column 4)	Elevations Along Reference Line (Column 5)	Δ_{vc} (Column 6)
CL Pier 3	112+00.00	120.8750	119.8808	119.8808	0
0.10	112+12.64	121.1010	120.1006	120.0883	0.0124
0.20	112+25.28	121.3242	120.3177	120.2957	0.0220
0.30	112+37.92	121.5444	120.5320	120.5032	0.0288
0.40	112+50.56	121.7618	120.7436	120.7107	0.0329
0.50	112+63.20	121.9762	120.9524	120.9181	0.0343
0.60	112+75.83	122.1877	121.1585	121.1256	0.0329
0.70	112+88.47	122.3963	121.3619	121.3330	0.0288
0.80	113+01.11	122.6021	121.5625	121.5405	0.0220
0.90	113+13.75	122.8049	121.7603	121.7479	0.0124
CL Pier 4	113+26.39	123.0048	121.9554	121.9554	0

Table 10.2 Bridge 1, Girder 3 Adjustments for Vertical Curvature in Span 3 (all elevations/dimensions in feet)

Location (1/10 Points) (Column 1)	Station (Column 2)	Top of Deck Elevations At CL Girder (Column 3)	Top of Web Elevations At CL Girder (Column 4)	Elevations Along Reference Line (Column 5)	Δ_{vc} (Column 6)
CL Pier 3	112+00.00	120.8750	119.8808	119.8808	0
0.10	112+13.36	121.1073	120.1131	120.0993	0.0138
0.20	112+26.72	121.3365	120.3423	120.3178	0.0245
0.30	112+40.08	121.5626	120.5685	120.5363	0.0322
0.40	112+53.44	121.7857	120.7915	120.7547	0.0368
0.50	112+66.80	122.0057	121.0116	120.9732	0.0384
0.60	112+80.17	122.2227	121.2285	121.1917	0.0368
0.70	112+93.53	122.4365	121.4424	121.4102	0.0322
0.80	113+06.89	122.6473	121.6532	121.6286	0.0245
0.90	113+20.25	122.8551	121.8609	121.8471	0.0138
CL Pier 4	113+33.61	123.0597	122.0656	122.0656	0

10.2.4.1 Finalize the Vertical Camber Calculations

Once the dead load deflections and profile adjustment (if any) have been completed, the Required Shop Camber, RSC_i, is calculated for inclusion on the design plans, per bridge owner policy. When reporting final camber values, proper sign convention is critical. Downward deflection (negative) is reported as upward camber (positive), such that the girder settles into the correct position after anticipated loads are applied. Note that camber could be negative to counteract upward deflection caused by span arrangement of adjacent spans.

Two typical camber diagrams are shown in **Figure 10.7** and **Figure 10.8.** The reference chords used to calculate the vertical curvature adjustments are also shown in the figures; the first figure shows a constant chord between abutments (without blocking), and the second figure shows a chord with elevation changes from one support to another (with blocking). The sign of the adjustment due to vertical curvature is used as-calculated rather than applying the opposite sign convention because it is not a deflection but a distance relative to the reference line. The RSC_i reported at intervals along the girder length are determined as:

$$RSC_i = -(\Delta_{stl} + \Delta_{ADL} + \Delta_{BDL}) + \Delta_{vc} \qquad \text{(Eqn. 10.3)}$$

Where: RSC_i = Required Shop Camber (as may be established by a bridge owner)
Δ_{stl} = deflection due to girder self-weight
Δ_{ADL} = deflection due to other non-composite dead loads
Δ_{BDL} = deflection due to composite dead loads
Δ_{vc} = adjustment due to vertical curvature

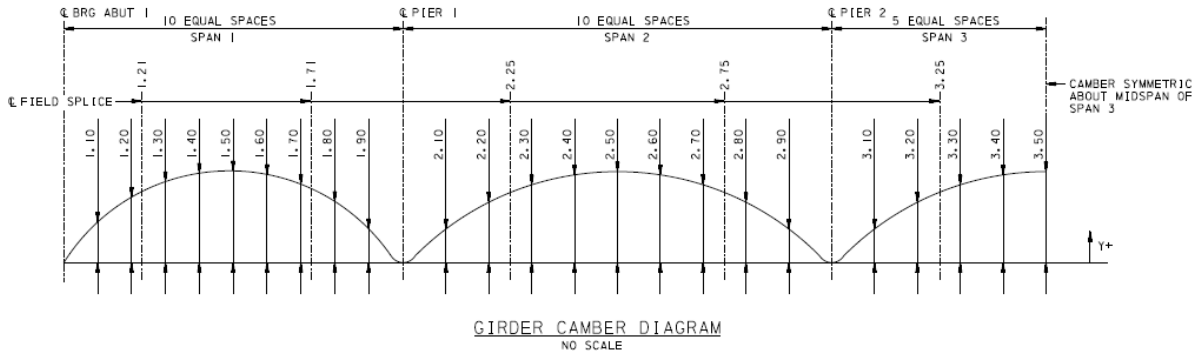

Source: FHWA

Figure 10.7 Typical Camber Diagram for a Steel Girder without Blocking

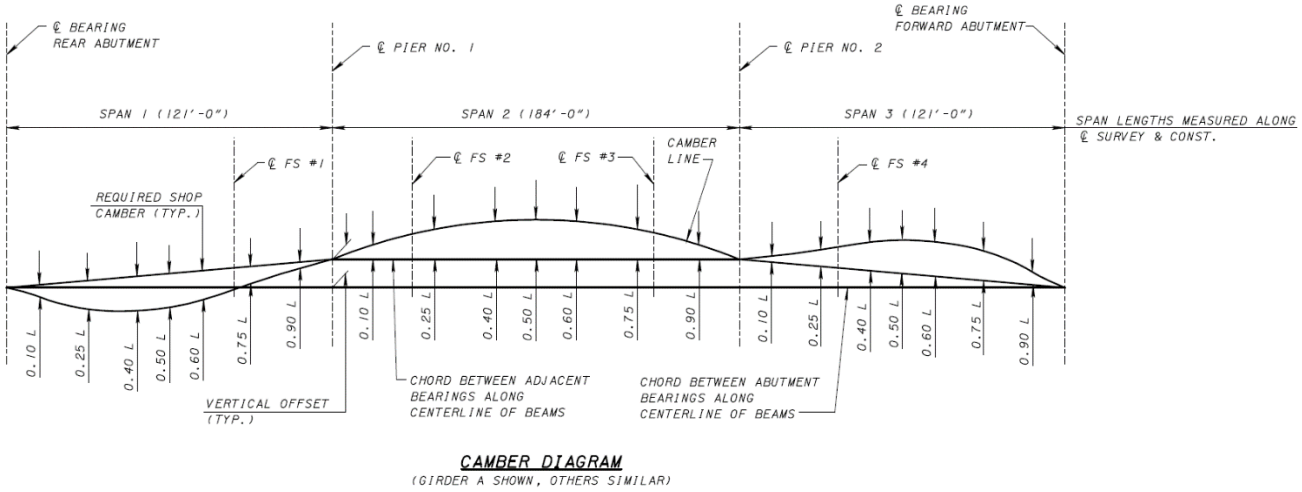

Source: FHWA

Figure 10.8 Typical Camber Diagram for a Steel Girder with Blocking

10.3 Additional Vertical Displacement Considerations

Other conditions may influence how vertical camber is calculated. These include, but are not limited to, deck pouring sequences for longer bridges, staged construction, and curved bridges. They are discussed in the following sections.

10.3.1 Deck Placement Effects

Up to this point, discussions regarding steel girder camber did not address the effect of deck placement. As deck concrete is placed sequentially and left to cure, the deck and girder section progressively transition from a non-composite to a composite section. The deflection calculation is no longer a simple investigation of load and response of a single section, but a complex combination of composite and non-composite responses working in concert that change with every new pour in the sequence. For this reason, when modeling a continuous bridge, the effects of the sequential engagement of composite action (i.e., deck pour sequence) should be considered in the analysis and design calculations.

The deck pour sequence is typically included in design plans. The deck pour sequence communicates to the contractor the order in which the deck placement was analyzed during design. The reported calculated deflections are intrinsically tied to the sequence, and if the contractor chooses another plan,

unpredictable deflections and fit-up complications may result. This can occur with both straight and curved girder bridges. The deck pour sequence typically starts with the positive moment regions between points of dead load contraflexure. After curing time, concrete is then placed in the negative moment regions. This sequence is intended to reduce potential cracking in the negative moment regions and limit the amount of concrete the contractor needs to place in a single day.

The first analysis uses the non-composite, steel-only section along with the weight of the wet concrete to be placed during Pour #1. In the second analysis, the model includes the loading used in the previous analysis, plus the weight of the wet concrete to be placed during Pour #2; however, the girder properties within Pour #1 regions are modified to now reflect composite section properties. In these analyses, the modulus of elasticity of concrete will reflect the curing time of the previously placed concrete. This process progresses until the deck pour sequence is complete. The results of each analysis iteration are then summed to arrive at a net final moment, shear, and deflection. While it is possible for an intermediate effect to control the girder design, camber calculations rely upon the net final effect. In some instances, the pour sequence effect may even be small enough to be neglected but should be evaluated on a project by project basis.

On short multi-span bridges, it is possible to pour the entire deck before the wet concrete cures. Modifications to the concrete mix, including the use of admixtures may be needed to slow the curing rate. The benefits of placing the deck in a single pour include reducing the cracking potential in the negative moment region and simplifying the placement process. In addition, there is no need for a deck pour sequence or analysis, as deflections can be calculated by placing the entire wet concrete dead load on the non-composite girder section.

10.3.2 Staged Construction Effects

Project constraints often prevent the full width construction of a bridge during one stage (or "phase"). Projects that include densely populated or urban areas, high volume roadways, and bridge replacements on existing alignments typically maintain partial use of the bridge during construction. Likewise, rehabilitation projects where a viable traffic detour is not feasible typically use staged construction to facilitate bridge widening, deck slab replacement, or superstructure modifications.

To the extent that it is possible without knowing a contractor's plan, it is important to take the staged construction sequencing into consideration when performing the girder design and analysis. Specifically, the designer should plan for a feasible staged construction and evaluate the dead load deflections that occur at each stage of construction to fully understand and account for "locked-in" effects of the staged construction. The locked-in effect of permanent dead load deflections has the potential to impact the camber calculations/diagram, the cross frame/diaphragm details, the haunch detail, and the girder design. Consider the following example. **Figure 10.9** through **Figure 10.11** depict a common straight girder scenario. In **Figure 10.9**, Stage 1 has been constructed and most of the permanent dead load deflections have already occurred, where the Stage 2 portion is subject to only steel dead load deflection. As shown by the reference line in the figures, the structural members are at different stages of vertical alignment due to the difference in applied dead loads to the respective members. This condition is exaggerated with horizontally curved girders, which may twist in addition to deflecting vertically (see Section 10.5.3).

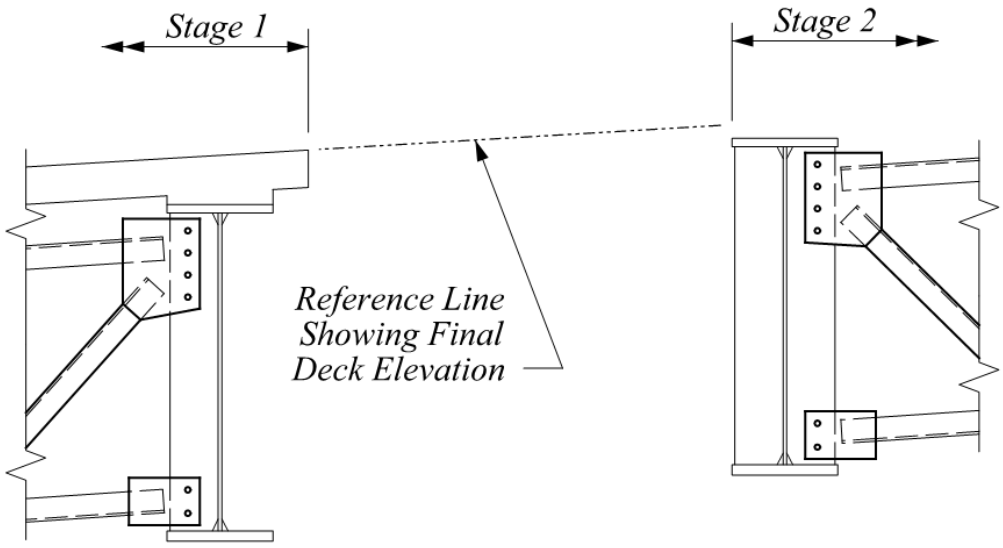

Source: FHWA

Figure 10.9 Detail of Stage 1 Construction Complete and Stage 2 before Deck Pour

The designer should evaluate whether to erect the cross frames between the two stages before or after pouring the Stage 2 deck slab. If the Stage 2 deflection (Δ_{DL} as shown in **Figure 10.10**) at the cross frame locations due to the wet concrete is small, e.g., below S/100 (where S is the girder spacing in inches), the cross frame can likely be erected between stages prior to the Stage 2 deck pour with limited adverse effect. The cited limit of S/100, which is used by the Ohio Department of Transportation, typically results in inconsequential locked-in stresses in the girders and cross frames after the deck is placed. If Stage 2 deflection is greater than S/100, connecting the cross frames between stages prior to the Stage 2 deck pour will more likely lead to significant locked-in stresses. (Note that this is also a consideration for actual fit-up of the cross frame, and that the connection may not properly align if there is excessive differential girder deflection.)

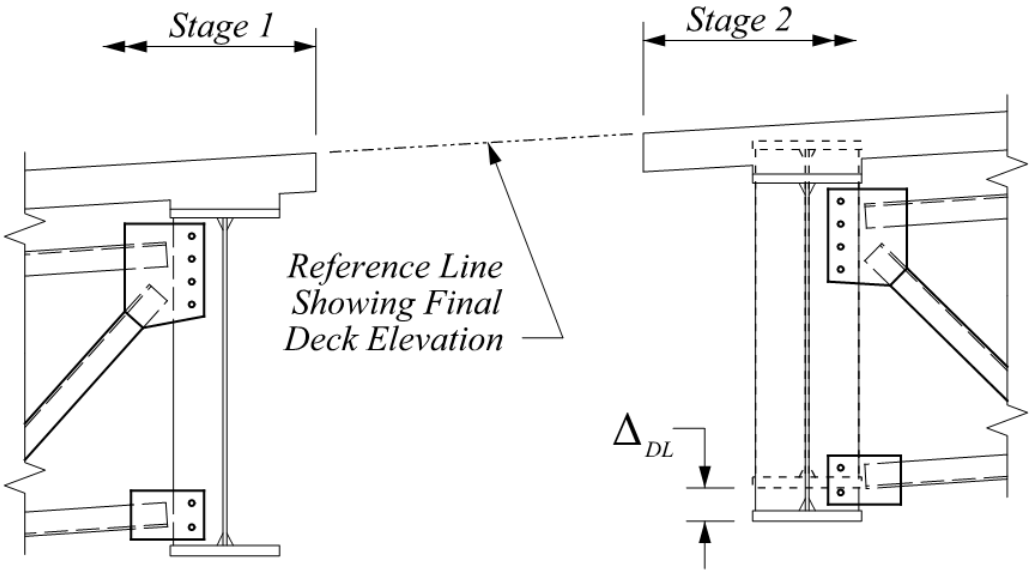

Δ_{DL} = Deflection due to deck slab dead load in Stage 2

Source: FHWA

Figure 10.10 Detail of Stage 2 Deflected Position

When greater than S/100, the designer should consider delaying connection of the cross frame until after the deck slab is poured for Stage 2, thereby reducing fit-up issues and locked-in stresses. The cross frame can be connected with t field drilled bolt holes at one girder, or by field welding the cross-frame gusset plate to the stiffener. To complete the deck slab, a closure pour (Stage 3) is performed after the cross frames are securely fastened, as shown in **Figure 10.11.**

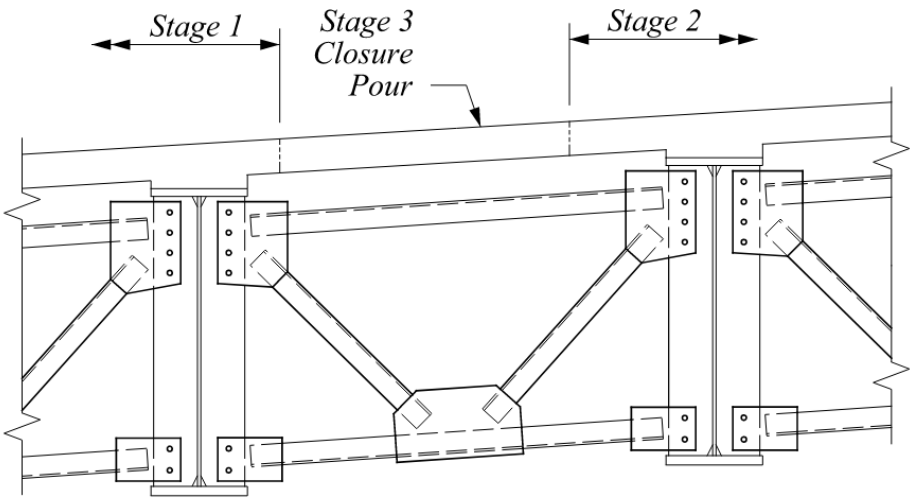

Source: FHWA

Figure 10.11 Detail of Completed Construction with Stage 3 Closure

This example is intended to serve as a simplified demonstration of the importance of staged construction considerations during design. The analysis of existing versus proposed deflections for

bridge widening can be thought of in a similar fashion. For example, bridge widening projects typically include removal of portions of the existing deck slab, concrete barriers, and miscellaneous appurtenances connected to the bridge overhang (e.g., utilities, lighting, etc.). This may cause some rebounding of the existing girder deflection following the partial demolition, and the designer should coordinate those rebound deflections with the anticipated deflections of the bridge's new portions. As presented in the prior example, the old construction to remain can be thought of Stage 1 and the new construction as Stage 2. Additionally, the timing of cross frame installation will be critical, and it may be necessary to remove and re-install existing cross frames to limit locked-in stresses or allow the necessary freedom of movement.

Discussions regarding the design of bridges using staged construction, specific to steel girder design, can be found in the AASHTO/National Steel Bridge Alliance (NSBA) Collaboration *G13.1 Guidelines for Steel Girder Bridge Analysis* (AASHTO/NSBA, 2019). This non-Federal guideline provides additional information specific to cross frame attachment methods, as well as consideration of live load deflections during construction.

10.3.3 Vertical Camber for Curved Steel I-Girders

Curving I-girders introduces a complex 3D aspect to cambering. It is important to understand the way in which a curved girder deflects under load, and how it differs from that of a straight girder. The AASHTO/NSBA Collaboration *G13.1 Guidelines for Steel Girder Bridge Analysis* (AASHTO/NSBA, 2019) and the NSBA document *Skewed and Curved I-Girder Bridge Fit* (Chavel et al., 2016) are non-Federal guidelines that present descriptions. The key consideration for curved girders is recognizing that they experience torsional deformations as a result of the eccentricity of vertical loads relative to the horizontal chord between centerline of supports. As such, curved girders will tend to not only deflect vertically but twist laterally in response to loading. A 3D model can capture the vertical component of out-of-place deformation directly, while a 2D model generally does not include a vertical component associated with girder twist deformations (although some programs will provide approximations). The accuracy of the modeling relies on the designer fully incorporating the anticipated sequential loading, both longitudinally as a result of an incremental deck pour sequence, and transversely due to staged construction. For more detailed discussion related to this topic, refer to the AASHTO/NSBA document mentioned above and the non-Federal guidelines of NCHRP 20-07/Task 355 *Guidelines for Reliable Fit-Up of Steel I-Girder Bridges* (White et al., 2015).

Basic considerations for vertical geometry are presented in the Example Bridge in the following section.

10.3.4 Considerations on Two AASHTO Optional Criteria

Live load deflections are addressed separately by the AASHTO BDS, which is incorporated by reference at 23 CFR 625.4(d) as a required design standard for projects on the National Highway System (23 CFR 625.3). Section 2.5.2.6 of the AASHTO BDS (AASHTO, 2017a) (23 CFR 625.4(d)(1)(v)) lists live load deflection criteria but refers to it as "optional." Some owners maintain deflection criteria requirements that differ from the AASHTO BDS. These criteria were originally intended to ensure some minimum measure of stiffness and help avoid potential dynamic vibration problems. Designers may still find limiting live load deflection following Section AASHTO BDS 2.5.2.6 (AASHTO, 2017a) (23 CFR 625.4(d)(1)(v)) to be a simple but practical means of ensuring enough structural stiffness to render a dynamic analysis unnecessary in some cases.

Similarly, AASHTO BDS Section 2.5.2.6.3 (AASHTO, 2017a) (23 CFR 625.4(d)(1)(v)) presents span-to-depth limits but calls them "optional" as well. Many structures have been successfully designed and built with higher span/depth ratios (i.e., shallower superstructures) than suggested by these limits. But

the AASHTO BDS (AASHTO, 2017a) (23 CFR 625.4(d)(1)(v)) includes these limits in its publication because they represent a good starting point for proportioning a design. For some structure types, these limits might be near the low end of the economical design spectrum. Some steel girder bridges with depths deeper than these suggested limits could be more economical, if proven by a case-by-case evaluation.

10.4 Example Bridge

This section presents additional geometric considerations for curved bridges with curved steel plate girders. Unlike curved bridges with straight beams, the use of curved beams or girders reduces some complexity involved in calculating the bridge framing geometry and can be beneficial in situations where straight beams might be problematic, such as bridges with tight radii. Curving the girders to follow the horizontal roadway alignment allows for constant overhangs at the exterior girders instead of shifting chorded beams to optimize overhangs. Similar to straight beams laid parallel to a tangent roadway alignment, curved girders mimic the roadway horizontal alignment with concentric offsets to each beam line. While the girder lengths will vary from one to the next, this is often easier to work with in design than the varying overhang of chorded beams.

The bridge example used in Chapter 7 will be revisited. The number of spans and the span lengths, however, will be modified to better represent a typical steel girder bridge arrangement. The horizontal alignment, vertical profile, and superelevation for the Bridge 2 location (**Figure 10.12**) remain as developed in earlier chapters. The bridge lies within the second horizontal curve (radius = 1250') of the example alignment, beginning at station 167+00 and ending at station 172+15. The total bridge length is 515' along the centerline of alignment.

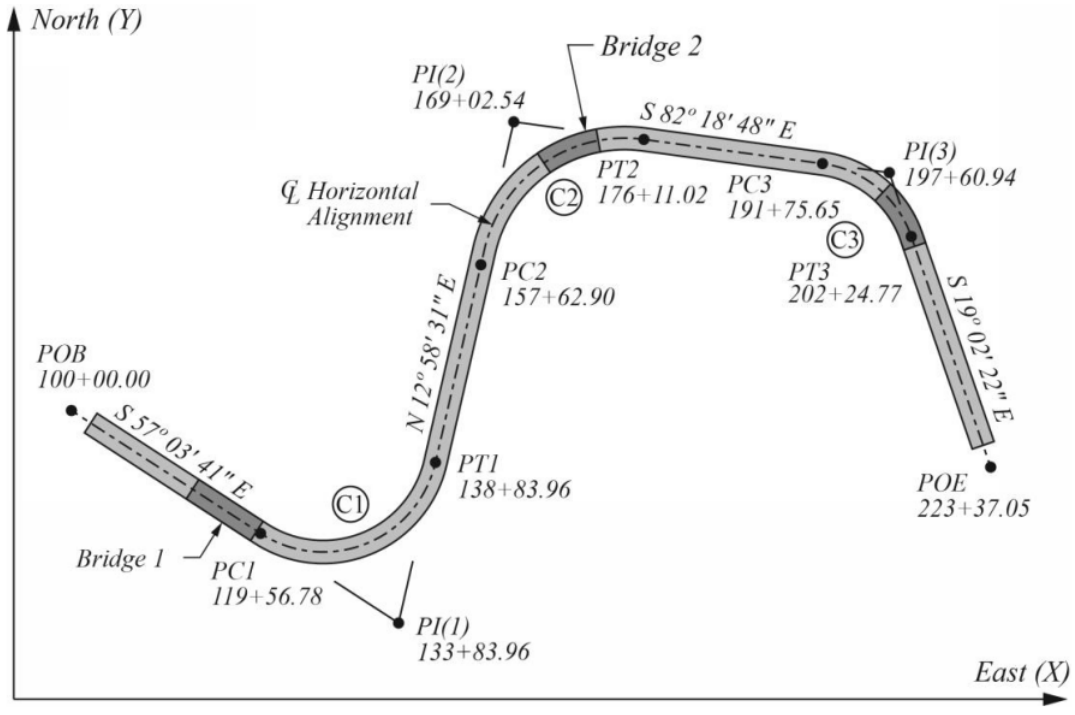

Source: PCI

Figure 10.12 Example Horizontal Alignment

Bridge 2 exists entirely within the crest vertical curve VPI(3), shown in **Figure 10.13** and **Figure 10.14.**

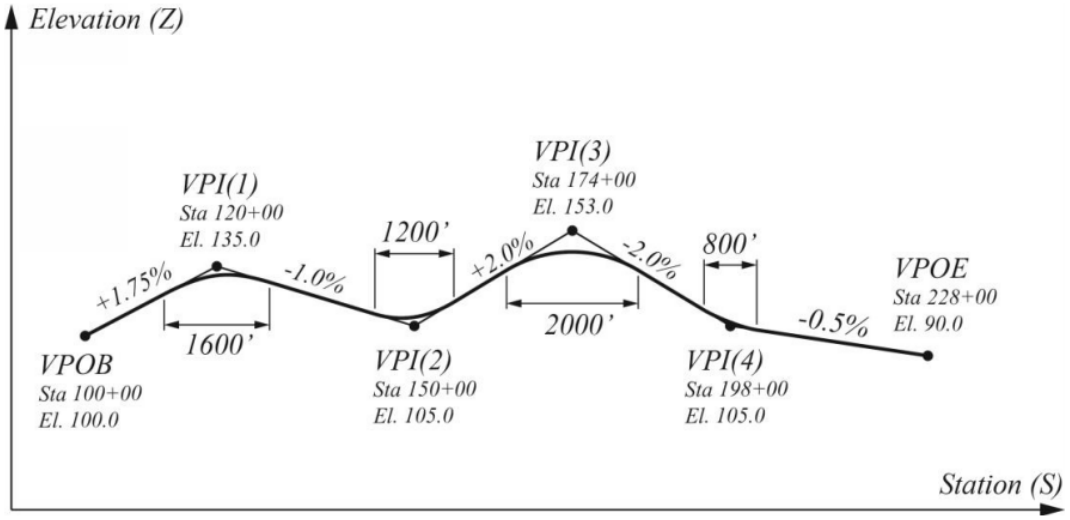

Source: PCI

Figure 10.13 Vertical Profile for the Example Alignment

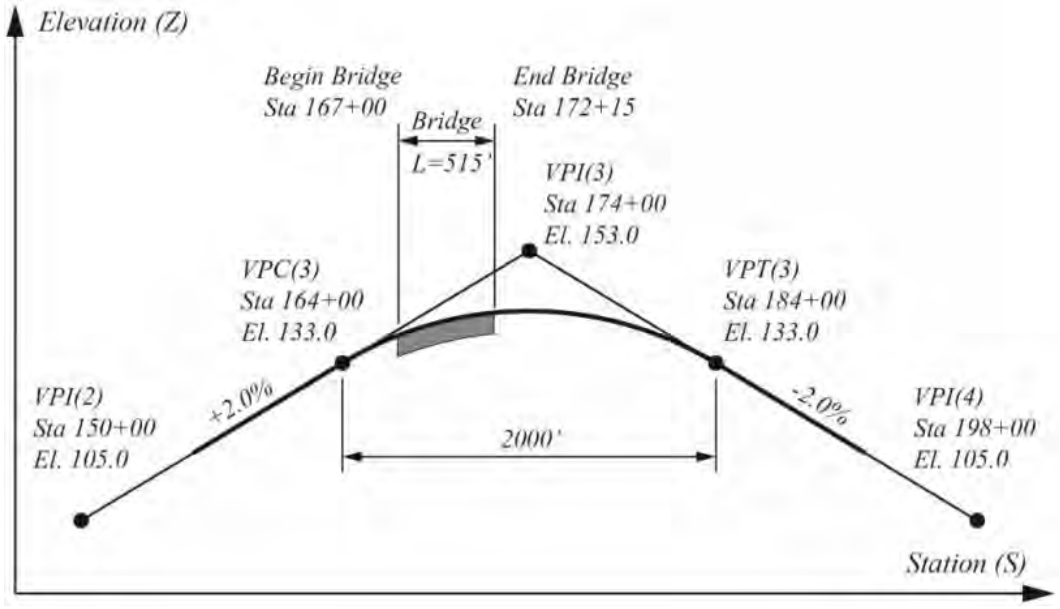

Source: PCI

Figure 10.14 Vertical Profile in the Vicinity of Example Bridge 2

Bridge 2 is also located completely within the constant superelevation portion of horizontal Curve 2. The superelevated cross-slope is +5 percent (refer to Section 4.1 for cross slope sign convention).

The modified span arrangement for the curved steel girder version of Bridge 2 is shown in **Figure 10.15** and consists of three spans (157 ft 6 in., 200 ft, 157 ft 6 in.). Total bridge length is 515 ft. The five equal span arrangement used in Chapter 7 is commonly employed for prestressed concrete beams, but the optimal span arrangement for continuous steel girders seeks to balance positive and negative moments by limiting the end spans to approximately 80 percent of the center span(s). The orientation of the piers is radial to the curved roadway alignment. The pier stations are provided in

Table 10.3. Where the beams in the previous example were straight, chorded beams, this example will develop the geometry for curved girders following concentric offsets from the roadway alignment. The typical cross section for this adaptation of Bridge 2 is provided in **Figure 10.16**.

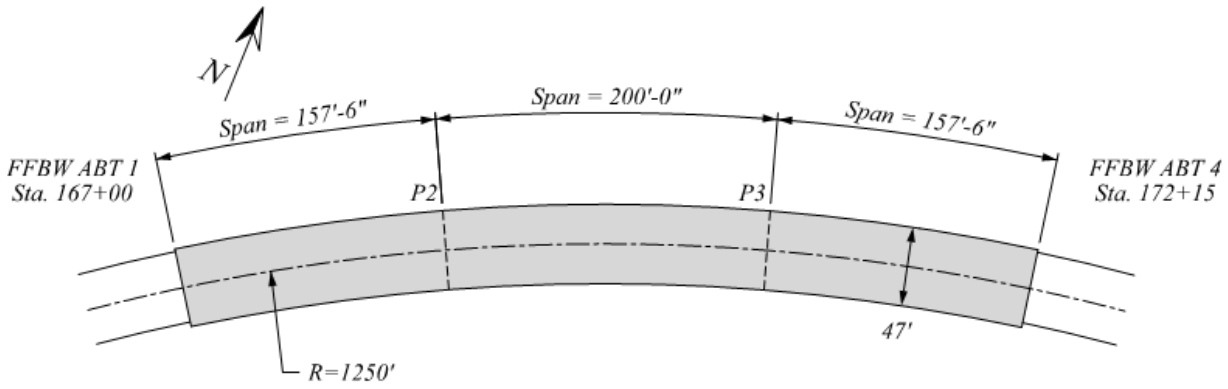

Source: FHWA

Figure 10.15 Plan View of Bridge 2 with a Three-Span Layout

Table 10.3 Location of Abutments and Piers for Bridge 2 with a Three-Span Layout

Pier	Station
Abt. 1	167+00.0
2	168+57.5
3	170+57.5
Abt. 4	172+15.0

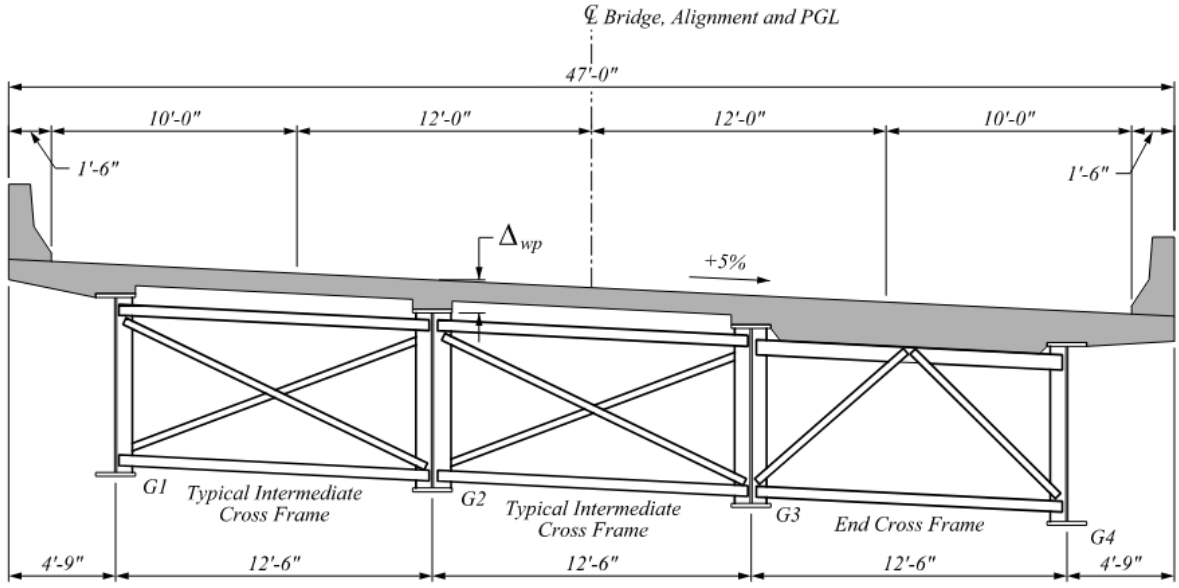

Source: FHWA

Figure 10.16 Bridge 2 Cross Section for Curved Steel Plate Girder Example

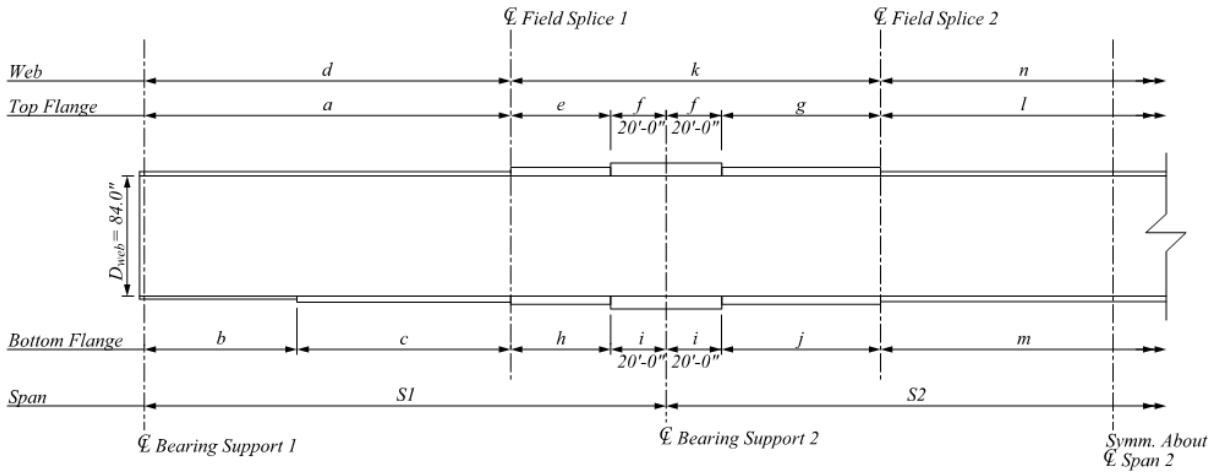

Source: FHWA

Figure 10.17 Elevation View of Bridge 2 Curved Steel Girder

The calculations presented in this section are based on Girder 4, Span 2. The calculations show how to compute the total haunch thickness along the length of the girder using the haunch thickness formula presented in Equation 8.2. The total haunch is then used to calculate the adjustment for vertical curvature for the girder. Although not shown in this example (the procedure is detailed in Chapter 6 and Chapter 7), the adjustment for vertical curvature is used to calculate the total shop camber for the girder.

For this example:

- The deck overhangs are a constant 4.75 ft. at each fascia girder. This is different from the example in Chapter 7, where the overhangs varied because straight beams were used to support a curved deck.
- The centerline of bearing and the centerline of piers are the same because the girders are continuous over the piers.
- The minimum concrete thickness between bottom of deck and top of top flange (haunch) for this example is 2 in., measured at the edge of top flange.
- The top flange is 28 in. x 2.5 in. and 17 in. x 1 in. at the centerline of Pier and midspan of Span 2, respectively.
- The deck thickness is 9.5 in.

10.4.1 Establish Offset Alignment at Centerline of Girder G4

A girder G4 horizontal alignment offset of 18.75 ft to the right of the PGL is created following the procedure outlined in Section 5.10. The resulting PI coordinates are shown in **Table 10.4**. **Table 10.5** shows the curve data for the offset alignment.

Table 10.4 Coordinate Information for Alignment Offset 18.75 ft Right

Point	Number	East (X)	North (Y)
POB	1	489.8049	2484.2640
PI(1)	2	3352.2629	629.7137
PI(2)	3	4354.4330	4979.1320
PI(3)	4	7586.0441	4542.9636
POE	5	8462.2757	2003.8834

Table 10.5 Curve Data for Alignment Offset 18.75 ft Right

Curve	R (ft)	L (ft)	T (ft)
1	1018.75	1955.2081	1453.9361
2	1231.25	1820.3941	1122.5410
3	931.25	1028.4134	573.7362

10.4.2 Determine Centerline of Bearing Coordinates for Girder G4 in Span 2

Coordinates at the centerlines of Pier 2 (168+57.50) and Pier 3 (170+57.50) are found along the PGL (Section 5.7). Coordinates at the centerlines of Pier 2 and Pier 3 offset to the centerline of girder G4 alignment are then found by offsetting the PGL points 18.75 ft radially to the right (Section 5.8). The coordinates of the four located points are shown in **Table 10.6.**

Table 10.6 Coordinate Information for Point at Pier 2 and Pier 3

Pier	Point	East (X)	North (Y)
Pier 2	CL Pier (PGL Sta. 168+57.50, offset 0.00)	4737.5798	4724.0136
	CL G4 at Pier (PGL Sta. 168+57.50, offset 18.75 ft Right)	4746.0491	4707.2854
Pier 3	CL Pier (PGL Sta. 170+57.50, offset 0.00)	4922.4656	4799.7235
	CL G4 at Pier (PGL Sta. 170+57.50, offset 18.75 ft Right)	4928.1616	4781.8596

10.4.3 Determine Deck Elevations at Centerline of Bearing and Tenth Points of Span 2

The top of deck elevations along both the PGL and the centerline of girder G4 are calculated next. The elevations along the PGL are determined from the vertical curve information provided in **Figure 10.14**. Using the elevations on the PGL and the known cross slope of the deck, the top of deck elevations along girder G4 can be found. The calculated elevations are provided in **Table 10.7**.

Table 10.7 Deck Elevations along Girder G4 Alignment (all elevations/dimensions in feet)

Location (1/10 Points) (Column 1)	PGL Station (Column 2)	PGL Elevation (Column 3)	Offset (Column 4)	CS (Column 5)	CL G4 Elevation (Column 6)
CL Pier 2	168+57.50	140.0569	18.75	0.05	139.1194
0.10	168+77.50	140.2699	18.75	0.05	139.3324
0.20	168+97.50	140.4749	18.75	0.05	139.5374
0.30	169+17.50	140.6719	18.75	0.05	139.7344
0.40	169+37.50	140.8609	18.75	0.05	139.9234
0.50	169+57.50	141.0419	18.75	0.05	140.1044
0.60	169+77.50	141.2149	18.75	0.05	140.2774
0.70	169+97.50	141.3799	18.75	0.05	140.4424
0.80	170+17.50	141.5369	18.75	0.05	140.5994
0.90	170+37.50	141.6859	18.75	0.05	140.7484
CL Pier 3	170+57.50	141.8269	18.75	0.05	140.8894

10.4.4 Determine Haunch Thickness and Depth to Working Point

Recalling the discussion in Section 8.2.1, the theoretical haunch for steel girder superstructures is generally set at a constant depth along the length of the entire bridge or superstructure unit. The theoretical haunch for this example will be based on the largest top flange plate (28 in. wide x 2.5 in. thick) located over the piers. Using **Figure 10.6** for reference and the assumption above, the total haunch thickness and depth to the working point can be calculated as:

$$\Delta_{wp} = 2.5" + 2" + |0.05|\frac{28"}{2} + 9.5" = 14.70"$$

The girder flanges vary in height and width along their length as illustrated in the partial girder elevation, **Figure 10.17**. Holding a constant distance from top of deck to working point along the length of the girder simplifies construction, forming the concrete deck, and the geometry presented in the construction plans. Additional concrete haunch is used to compensate for any differences in flange thickness.

10.4.5 Determine Girder Length along Girder G4

The length along girder G4 will now be calculated to use in determining the adjustment for vertical curvature as part of the girder camber calculations. The span length along the PGL between the bearings at Pier 2 and Pier 3 is 200 ft. The span length measured along the centerline of girder G4 (located 18.75 ft radially to the inside of the curve) is:

$$L_{G4} = 200'\left(\frac{1231.25'}{1250'}\right) = 197'$$

10.4.6 Determine the Vertical Curve Adjustment for Camber

The vertical curve adjustment can now be calculated for the horizontally curved girders. In this example the substructure units have been set radial to the roadway alignment. The radial geometry, along with the constant girder offset from the PGL, simplifies the calculation of the shop camber. The segmented tenth point distances (or any other owner-preferred increment) along the PGL are radially offset to the tenth points of the girder whether to a larger or smaller radius curve. If the piers were not radial, the direct correlation of segmented lengths along the PGL would not match those of the girders, making the calculation of deck elevations more complicated and involving additional points of interest along the bridge length. For example, the midpoint of the span at the girder would not line up radially with the midpoint of the span at the PGL; therefore, a new point along the PGL should be calculated that corresponds to the radial location of the midspan point along the girder being investigated.

Similar to the calculation in Section 8.2.1.4, **Table 10.8** provides the individual components needed to calculate the Adjustment for Vertical Curvature. The top of deck elevations (Column 3) are taken from **Table 10.7**. The depth to the working point is then subtracted from the top of deck elevations to determine the top of web elevations (Column 4). Next, using the G4 span length, the elevations along the reference line (**Figure 10.2**) are calculated (Column 5). The difference between the top of web elevation and reference line elevation is the Adjustment for Vertical Curvature, Δ_{vc}.

Table 10.8 Girder G4 Adjustment for Vertical Curvature in Span 2 (all elevations/dimensions in feet)

Location (1/10 Points) (Column 1)	Station (Column 2)	Top of Deck Elevation at CL G4 (Column 3)	Top of Web Elevation at CL G4 (Column 4)	Reference Line Elevation (Column 5)	Δ_{vc} (Column 6)
CL Pier 2	168+57.50	139.1194	137.8944	137.8944	0
0.10	168+77.50	139.3324	138.1074	138.0714	0.0360
0.20	168+97.50	139.5374	138.3124	138.2484	0.0640
0.30	169+17.50	139.7344	138.5094	138.4254	0.0840
0.40	169+37.50	139.9234	138.6984	138.6024	0.0960
0.50	169+57.50	140.1044	138.8794	138.7794	0.1000
0.60	169+77.50	140.2774	139.0524	138.9564	0.0960
0.70	169+97.50	140.4424	139.2174	139.1334	0.0840
0.80	170+17.50	140.5994	139.3744	139.3104	0.0640
0.90	170+37.50	140.7484	139.5234	139.4874	0.0360
CL Pier 3	170+57.50	140.8894	139.6644	139.6644	0

As shown in previous sections, this vertical curve information can now be incorporated into the camber calculations.

10.5 Structure Behavior and Geometry Change under Load

10.5.1 Straight Skewed I-Girder Bridges

In straight skewed I-girder bridges prior to cross frame connection, the girders deflect only vertically under their self-weight. Once the cross frames are connected to the girders and are engaged in transfer of internal shear and moment, the interconnected girders deflect as a 3D system under subsequent loading. The primary function of cross frames in straight skewed bridges is to brace the girders, but they also serve as an additional transverse load path in the system. As a result, the girders deflect vertically and simultaneously twist under dead loads. When cross frames are perpendicular to the girders, twisting of the cross section occurs primarily because of the differential vertical deflections at intermediate cross frames. This behavior is illustrated in **Figure 10.18.**

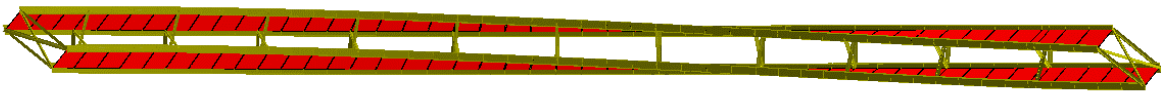

Source: FHWA

Figure 10.18 3D Top View of Magnified Girder Deflection and Twist for Two Simple Span I-Girders Connected with Perpendicular Cross Frames, with Skewed Supports and Subjected to Vertical Loading After the Cross Frames Have Been Installed

In a straight skewed bridge, the total internal torsion tends to be relatively small and the girder torques are induced predominantly by the compatibility of deformations between the girders and the cross frames. In a straight skewed bridge, if the girders are not interconnected by the cross frames, there is no tendency for them to twist under the primary vertical loads.

10.5.2 Girder Layover Considerations for Skewed Bridges

The girder layover at the bearings of severely skewed bridges can have an impact on both design and construction. First, the layover causes out of plane rotation at the skewed bearing lines. It is possible for this induced rotation to exceed the tolerance of the bearing and if not accounted for in the bearing design, bearing failure may occur during construction or in the future. The layover of the girders at the skewed bearing lines can also be problematic when installing the expansion joints. If layover is not given proper consideration during design, construction, or both, the girder top flanges can shift, making the joint difficult to install properly. This can also lead to unintended racking during its service life.

10.5.3 Horizontally Curved I-Girder Bridges

Horizontally curved I-girder bridges are subjected to significant internal torsional moments because the resultant of the bridge vertical loads within each span has an eccentricity relative to a straight chord drawn between the supports. Contrasting to the discussion on torsion in skewed bridges the internal torsion in curved bridges exists regardless of the interconnection of the girders and cross frames. If the curved I-girders are not connected to the bridge structural system by the cross frames, the girders alone can exhibit large torsional deflections and could potentially become unstable.

Horizontally curved I-girders generally exhibit significant coupling between major-axis bending and torsional rotations. Major-axis bending of curved girders cannot occur without also inducing twisting of the girders and twisting of curved girders cannot occur without inducing major-axis bending. This behavior, if not accounted for, can exacerbate fit-up problems in curved girder bridges since it is difficult to adjust the twist of the girders while attempting to connect the cross frames.

10.6 Geometric Considerations for Bridge Modeling

The geometric configuration, or framing plan, of a bridge can dictate the level of modeling complexity needed to accurately predict loading and behavioral response in steel girders and cross frames. In most cases, the best approach to developing a framing plan is the simplest approach. A clean and simple framing plan will lead to a bridge that is easy to design, fabricate, and construct, while the converse is equally true. The designer is referred to the compendium of AASHTO/NSBA Steel Bridge Collaboration documents and the FHWA's *Steel Bridge Design Handbook*. In addition, NCHRP Report 725 provides information for analysis methods and construction engineering of curved and skewed steel bridges. Note that these AASHTO, NSBA and NCHRP documents are non-Federal guidelines. The research

compared 1D (line girder analysis) and 2D (grid analysis) methods to 3D (finite element analysis) models as the geometry of the subject bridges became increasingly more complex.

This section will provide discussion related to choosing an appropriate level of analysis based on the severity of the bridge geometry.

10.6.1 Skew Index

NCHRP Report 725 provides the concept of the Skew Index, I_s:

$$I_s = \frac{w_g \tan\theta}{L_s} \qquad \text{(Eqn. 10.4)}$$

Where: I_s = bridge skew index
w_g = maximum width between exterior girders of the bridge cross-section in feet
L_s = span length in feet at the centerline of the bridge cross-section
θ = maximum skew angle of the bearing lines in degrees measured from a line taken perpendicular to the span centerline

Steel girder bridges with little to no skew may be considered among the least complex to analyze and model, as the behavior of this bridge type experiences only vertical deflections and negligible torsional bending. Cross frames connect adjacent girders at nearly the same location along the length of both girders. It follows that adjacent girders demonstrate very little, if any, differential deflection.

The research results from the nonbinding NCHRP 725 (White et al., 2012) found that if a bridge has a skew index less than 0.3, 1D line girder analysis will yield the accuracy needed for major-axis bending stresses and vertical displacements when compared to a 3D finite element model. Line girder analysis does not produce results for forces in cross frames. This is adequate for design purposes since cross frames are considered secondary members for straight steel bridges, and generally only serve as stability bracing during construction and to brace the bottom flange (in the completed structure) against lateral forces passing from superstructure to substructure.

As skew increases, perpendicular cross frames (as shown in **Figure 10.19**) connect increasingly disparate points along the length of adjacent girders. The result is a different vertical displacement at one end of the cross frame versus the other (i.e., Point A versus Point B), known as differential deflection. It induces a twisting effect in the girders and can lead to flange lateral bending, girder layover at the bearings, and significant loading in the cross frames. This behavior is not captured in a 1D line girder analysis. As the cross frames are engaged to distribute girder reactions, shears, and moments, the designer should consider 2D and 3D analysis methods to capture the cross-frame forces appropriately. Refer to NCHRP 725 (White et al., 2012) (not in Federal regulation) for a more developed discussion of the analysis and approach to estimating cross frame forces.

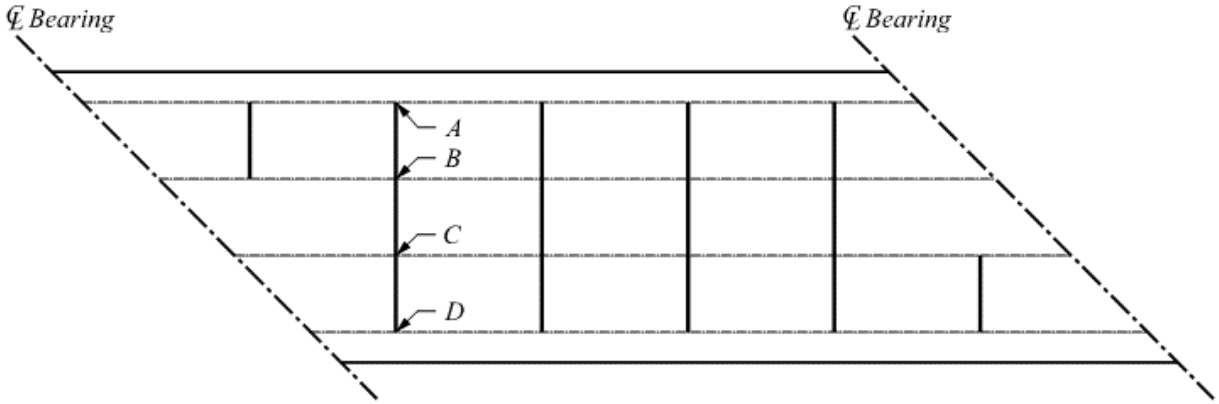

Source: FHWA

Figure 10.19 Framing Plan Showing Differential Deflections Due to Skew

Table 10.9 Vertical Displacements at Points A, B, C, and D as Indicated in Figure 10.19

Point	A	Differential (A-B)	B	Differential (B-C)	C	Differential (C-D)	D
Deflection (in.)	6.12	-0.78	5.34	-2.05	3.29	-2.44	0.85

10.6.2 Connectivity Index

Appendix B of the nonbinding AASHTO/NSBA *G13.1 Guidelines for Steel Girder Bridge Analysis* (AASHTO/NSBA, 2019) provides information about the selection of analysis methods and construction engineering of curved and skewed steel bridges. The information is based on research that compared the accuracy of 1D and 2D methods versus 3D models as the geometry of the bridges became more complex. This section will discuss the effects curvature has on the bridge framing and the appropriate level of modeling and analysis needed to account for the additional loads not present in a straight bridge.

AASHTO/NSBA G13.1 *Guidelines for Steel Girder Bridge Analysis* Table B.2-1 (AASHTO/NSBA, 2019) (not in Federal regulation) provides a matrix of non-composite dead load analysis of I-girder bridges and assigns a letter grade for different load responses based on a variety of geometric variables. The letter grades, designated A through F, indicate the varying levels of normalized mean error a designer can expect relative to the 3D FEA benchmark models. Curved bridges with no skew are further subdivided by their connectivity index, I_C (Equation 10.5). The connectivity index provides an indication of the potential loss of accuracy in capturing the I-girder torsion effects, which can result from poor modeling of a curved bridge.

$$I_C = \frac{15000}{R(n_{cf}+1)m} \qquad \text{(Eqn. 10.5)}$$

Where: R = the minimum radius of curvature at the centerline of the bridge cross-section in feet throughout the length of the bridge
n_{cf} = the number of cross frames in the span
m = a constant taken equal to 1 for simple-span bridges and 2 for continuous-span bridges

Bridges with a connectivity index greater than 1.0 would be appropriate to model with a full 3D analysis.

To demonstrate the connectivity index, recall the example in Section 10.4. The bridge is made up of three spans measuring 157 ft 6 in., 200 ft, and 157 ft 6 in. on a curved alignment with a radius of 1250 ft, measured at the centerline of the bridge. It is considered to have "regular" geometry, since the supports are radial and the girder spacing and deck width are constant. The end spans have six intermediate cross frames spaced at 22.5 ft along the alignment, and the center span has nine intermediate cross frames spaced at 20.0 ft along the alignment.

For Span 1 and Span 3:

$$I_C = \frac{15000}{1250(6+1)2} = 0.86$$

And for Span 2:

$$I_C = \frac{15000}{1250(9+1)2} = 0.60$$

For multiple span bridges, the connectivity index for the overall bridge is the greatest value of any of the individual spans; therefore, for the example bridge, $I_C = 0.86$.

For illustration purposes, were the same bridge designed with a tighter radius, say 970 ft, the connectivity index would be:

$$I_C = \frac{15000}{970(6+1)2} = 1.10$$

Once the connectivity index value has been calculated, the designer can use the matrix provided in AASHTO/NSBA *G13.1 Guidelines for Steel Girder Bridge Analysis* Table B.2-1 (AASHTO/NSBA, 2019) (not in Federal regulation) to help determine an appropriate level of analysis for the girders. The example bridge with the alignment radius of 970 ft has a connectivity index value of greater than 1.0, and the designer wants to determine major axis bending forces, as well as vertical displacements of the girders during erection and prior to placement of the concrete deck. This designer's first choice is to perform a traditional 2D-grid model for the bridge. Table B.2-1 shows the worst-case major axis bending score for the 2D-grid model, with an $I_C > 1.0$, is a "D," while the mode score is a "B." The worst-case grade indicates a normalized mean error between 21 percent and 30 percent, which may suggest a bridge with some extreme geometry. As this bridge is considered "regular," the designer can evaluate whether the bridge in question would fall within the mode grade of "B," which would indicate a normalized mean error of 7 to 12 percent. On the other hand, a 1D-line girder analysis would yield a grade of "C" for both the worst-case and mode scores, with a 13 to 20 percent normalized mean error. The designer should determine if the difference in the level of effort to produce a more complicated model outweighs the amount of inaccuracy expected. Some inaccuracy in a model can be overcome by conservatively designing the members, such as reducing the target performance ratio by the normalized mean error of the model type selected.

In general, a 1D-line girder analysis can be used when designing straight, non-skewed bridges, if the presence of lateral loading effects are minimal. The simple 2D grid analysis method can be used for member design but is not accurate when looking at deflections during intermediate construction stages and when the geometry imposes lateral load effects to the girders. The use of an improved 2D grid analysis, such as a plate with eccentric beam (PEB) model, can eliminate a number of the inaccuracies

of the simple 2D grid, but may not provide accurate results when significant second-order effects are present. A 3D model may provide the most representative theoretical behavior of the bridge and the most accurate results, especially with significant second-order and lateral effects on the girder system.

Each of the different bridge modeling methods, going from 1D to 3D, has increased complexity, which in turn equates to an increased amount of time to produce the models. Increased accuracy of a 3D model may be achieved by inputting both the correct bridge geometry and member stiffness but should not go beyond the need of engineering application. There is a diminishing return to the added complexity of a 3D model. Some adjustments can be made to minimize modeling time and still achieve acceptable results.

One practical approach is to connect cross frame member elements directly to girder flange nodes. This eliminates modeling connection plates and adding individual cross frame member nodes. While this approach typically yields more accurate results than an improved 2D analysis, it reduces the production effort of a 3D model. It is the responsibility of the designer to determine the appropriate method of analysis based on the desired level of precision.

10.7 Geometric Considerations for Thermal Movement

The thermal movement is very different for a tangent, non-skewed bridge compared to that of a skewed or curved girder bridge. The following sections will describe the expected response from each bridge configuration and the effects for consideration in design.

10.7.1 Non-Skewed Bridges

In a non-skewed bridge, expansion flows perpendicularly from the fixed line of bearings (single span) or point of fixity (multi-span). Standard use of expansion bearings aligned in the longitudinal direction of the bridge allow the bridge to expand without resistance. Thermal load transfer from superstructure to substructure in this scenario is effectively negated.

10.7.2 Skewed Bridges

The thermal movement in skewed bridges is typically asymmetrical following an imaginary diagonal axis connecting acute corner-to-acute corner, as shown in **Figure 10.20**. The thermal movement along the diagonal axis can cause racking (shearing) along the bearing lines. When racking occurs, resistance to the free movement of thermal expansion builds in the bearings. The designer should account for these forces not only in the superstructure design, but likewise in the load transfer to the substructure units.

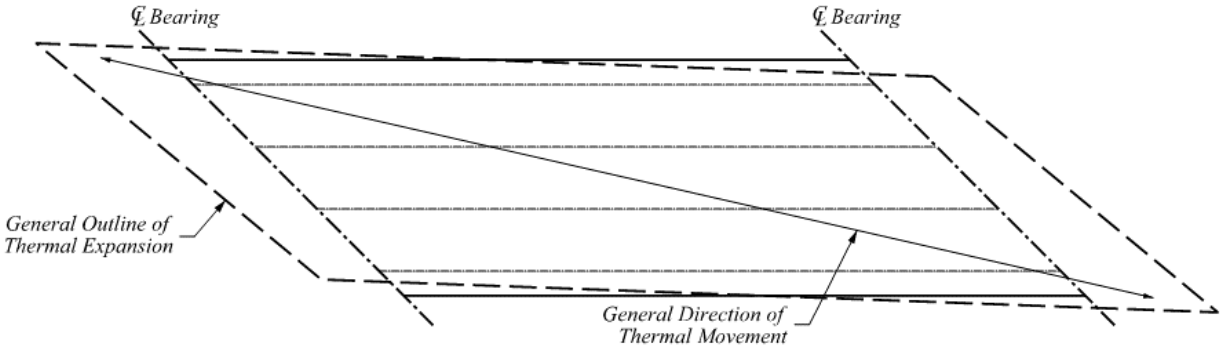

Source: FHWA

Figure 10.20 Plan View Showing Typical Thermal Movement on a Single Span Steel Girder Bridge with Parallel Skewed Supports

The designer has several options to limit the amount of unintended thermal loading in the superstructure and substructure. Designing and detailing the bearings to limit the amount of force resulting from racking and binding of the bearings is one option. This is accomplished by orienting the bearings relative to the direction of racking. In doing so, the designer can limit the amount of racking and the bearing's binding resistance to thermal movement. Similarly, the use of free moving bearings in locations experiencing the most severe racking can prove advantageous. Many bearing products on the market include variations that accommodate free movement. The designer should evaluate the placement of the different bearing styles (i.e., fixed, unilateral movement, free movement) to maintain overall stability of the bridge. Bridges consisting of multiple spans with severe skew can benefit from fixing one or more of the intermediate piers. The axis of thermal movement will generally follow the same diagonal path; however, the magnitude of movement and racking at the abutments will be reduced.

Additionally, there are considerations for semi-integral and integral bearing types since the skew and resulting thermal movement place asymmetrical forces upon the integral substructure. Not considering this phenomenon has led to unintended displacement of the superstructure relative to the foundations over time.

10.7.3 Curved Bridges

For a curved I-girder bridge, the directionality of thermal expansion and contraction is expected to follow a chord connecting the expansion support to the thermal point of fixity. The first step in determining the geometric response to the bridge thermal movements is to determine where the thermal point of fixity is located. This exercise will vary from bridge to bridge and is dependent on the number of spans, radius of curvature, the width of the superstructure, and support fixity. Where a bridge only has a single fixed support along its length, that support can be assumed to be the point of fixity. For longer structures with multiple and sometimes consecutively fixed supports, additional analysis should be used to locate the point of fixity. An overall refined stiffness analysis of the entire bridge, including the piers, abutments, and bearings, should be performed to locate the point of fixity.

The selection of the fixed support or supports for a curved steel girder bridge is at the discretion of the designer but should include consideration of the overall movement of the superstructure. In **Figure 10.21**, a two-span curved girder bridge is shown where the first support is fixed. The thermal

movement at the expansion supports will follow chorded lines connecting them back to the first support. The image is exaggerated but shows that the translation of the bridge will compound at each subsequent expansion support leading to misalignment of the roadway at the far support.

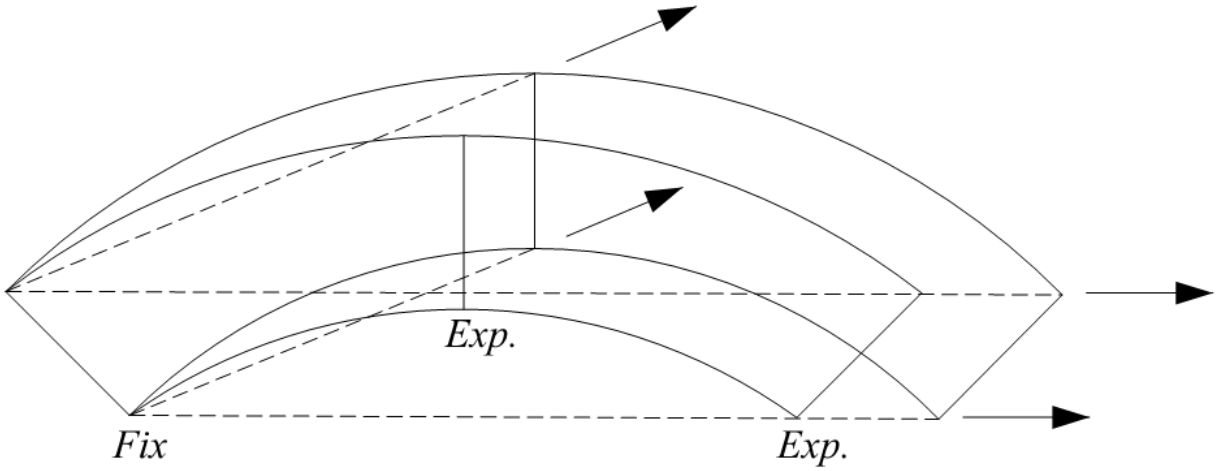

Source: FHWA

Figure 10.21 Thermal Movement with Rear Support Fixed

If the fixed support location is changed to a centrally located pier (**Figure 10.22**), the misalignment witnessed in **Figure 10.21** is equally distributed between the end supports. The structure will translate in the direction of each end's respective chord, but the magnitude and directional severity of the movement is more easily managed by distributing to each end. Only after considering how the bridge will behave can the designer effectively select the type and size of expansion joint needed.

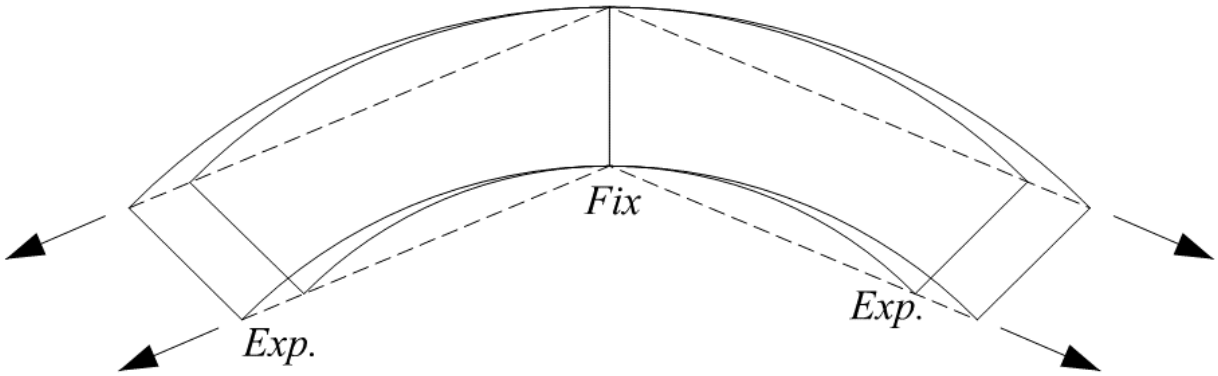

Source: FHWA

Figure 10.22 Thermal Movement with Center Support Fixed

On multi-fixed support bridges, once the thermal point of fixity is located, the designer can establish directionality of the theoretical thermal movement at each of the substructure supports, and can begin to evaluate bearing styles (i.e., fixed, unilateral movement, and free movement) to minimize locked-in forces along the length of the steel girders. Bearings that allow unilateral movement, also called guided bearings, will be oriented to allow movement along the established chords at expansion supports, while

still providing lateral restraint. In some cases, it might be advantageous to provide a combination of guided bearings and free moving bearings at the same substructure support. The guided bearings can share the total lateral restraint at that support, while the free bearings can be released of any restraint and reduce the potential for locked-in forces. This is often the case for shorter, curved girder bridges with a small radius.

10.8 Bridge Fit Condition Considerations

To help inform and standardize the steel bridge design and construction industry, an ad-hoc task group affiliated with the National Steel Bridge Alliance (NSBA) published information featuring fit-up considerations and design, detailing, and erection specifications in *Skewed and Curved Steel I-Girder Bridge Fit* (Chavel et al., 2016). The information is largely based on research conducted as part of NCHRP Project 20-07 Task 355, *Guidelines for Reliable Fit-Up of Steel I-Girder Bridges* (White, 2015) and anecdotal experience of the authors, fabricators, and erectors. These documents are voluntary, nonbinding information, and are not Federal requirements.

The "fit" or "fit condition" is the provision in design/fabrication/erection to achieve the target geometry under a specified dead load condition. A typical target geometry is to make I-girder webs reasonably plumb. It is achieved by compensating in design for the tendency of the I-girders to twist due to differential deflections (skewed bridges) or internal torsional moment (curved girder bridges). The fit condition selected is intended to facilitate the structure "fit-up."

Fit-up refers to the assembly of the structural steel during the bridge erection. It is desirable that the fit-up be manageable without the need for excessive jacking or pulling forces from the erector. The fit-up of the structural steel and fit condition are interrelated, but distinct attributes of the bridge construction process. Consideration of fit condition during design is important because it affects the magnitude of the locked-in force effects in the cross frames and the girders, and consequently the forces in-play during fit-up and erection.

10.8.1 Common Fit Conditions

The three most common fit conditions considered in skewed or curved I-girder bridges are:

- No-Load Fit (NLF) - The cross frames are detailed to fit to the girders plumb in the fabricated, fully-cambered and plumb position of the girders under zero load. NLF is also sometimes referred to as Fully-Cambered Fit.
- Steel Dead Load Fit (SDLF) - The cross frames are detailed to fit to the girders in an ideal plumb position where the girders are assumed deflected vertically under the self-weight of the structural steel at the completion of the steel erection. SDLF is also sometimes referred to as Erected Fit.
- Total Dead Load Fit (TDLF) - The cross frames are detailed to fit to the girders in an ideal plumb position where the girders are assumed deflected vertically under the total as-constructed dead loads. TDLF is also sometimes referred to as Final Fit.

The term "Total Dead Load" typically is assumed to include either all dead loads that are present when the bridge is opened to traffic, or the as-constructed dead loads, taken as the weight of the structural steel plus the weight of the concrete deck, but not including the weight of barrier rails, sidewalks, etc.

Although the use of refined analysis methods is not necessary for all skewed I-girder bridges, these methods, when utilized, do allow for direct consideration of cross frame forces and girder flange lateral bending stresses. However, it is important to recognize that the dead load force effects, when determined from a refined analysis model, typically do not include the locked-in force effects from

SDLF or TDLF detailing of the cross frames. That is, the analysis model corresponds to the assumption of NLF. This is a simplifying assumption that does not account for the influence of the actual fit condition on the bridge response. However, the choice of fit condition directly influences the cross frame fabricated geometry, as well as the bridge constructability and subsequent internal forces. Therefore, the fit condition is selected and clearly specified by the design engineer, often in consultation with a fabricator or steel erector.

A fit decision is made so that the fabricator/detailer can complete the shop drawings and fabricate the bridge components in a way that allows the steel erector to assemble the steel and achieve the desired geometry in the field. The fit decision also affects design decisions regarding the rotation demands on the bearings as well as the internal forces for which the cross frames and girders should be designed. The fit condition should generally be selected to accomplish the following objectives, in order of priority as suggested in the nonbinding *Skewed and Curved Steel I-Girder Bridge Fit* (Chavel et al., 2016):

1. facilitate the construction of the bridge;
2. offset large girder dead load twist rotations and corresponding lateral movements at the deck joints and barrier rails, which occur predominantly at sharply skewed abutment lines;
3. in straight skewed bridges, reduce the dead load forces in the cross frames or diaphragms and the flange lateral bending stresses in the girders; and
4. in horizontally curved bridges, limit the magnitude of additive locked-in dead load force effects.

According to Article 6.7.2 of the AASHTO BDS (AASHTO, 2017a) (23 CFR 625.4(d)(1)(v)), the cross frame or diaphragm fit condition should be specified, one per structure, for the following I-girder bridges:

- straight bridges where one or more support lines are skewed more than 20 degrees from normal;
- horizontally curved bridges where one or more support lines are skewed more than 20 degrees from normal and with an L/R in all spans less than or equal to 0.03; and
- horizontally curved bridges with or without skewed supports and with a maximum L/R greater than 0.03,
  where:
  L = the span length, bearing to bearing along the centerline of the bridge (ft)
  R = the radius of the centerline of the bridge cross-section (ft)

10.8.2 Detailing of Cross Frames

Based on the findings presented in the nonbinding *Skewed and Curved Steel I-Girder Bridge Fit* (Chavel et al., 2016), NLF presents a concern for straight skewed bridges because it can lead to lateral girder rotation by the support bearings that could otherwise be avoided under SDLF or TDLF. It should be noted that when there is no skew (or curvature) and the bridge is "square," the fit-up effects are inconsequential and result in the same detailing procedure regardless of fit condition.

The remainder of this section will focus on SDLF and TDLF for straight bridges with skewed supports and for curved I-girder bridges. Typically, to accomplish SDLF or TDLF at intermediate cross frames connected normal to the girders, the detailer determines the girder geometry in the targeted fit condition by subtracting the steel dead load or total dead load deflection from the girder plumb, fully-cambered no-load geometry. The fully-cambered, no-load girder profile is based on the roadway profile plus the total vertical camber. The girders are assumed to be vertically plumb in their initial fully-

cambered, no-load geometry as well as in their targeted steel dead load or total dead load positions. In other words, only the girder vertical deflections are considered, and any twisting of the cross section due to dead load is disregarded. The fabricated SDLF or TDLF cross frame geometry is then calculated such that the cross-frame fits to the work points at the girder connection plates.

A common term used by detailers and fabricators when referencing cross frames is "drops." Drops are the resulting difference in elevations between two ends of a cross frame with the girders in their targeted steel dead load or total dead load positions, as illustrated in **Figure 10.23**. The drops generally will be different at each cross frame. Furthermore, drops for individual cross frames typically differ between the SDLF and TDLF positions.

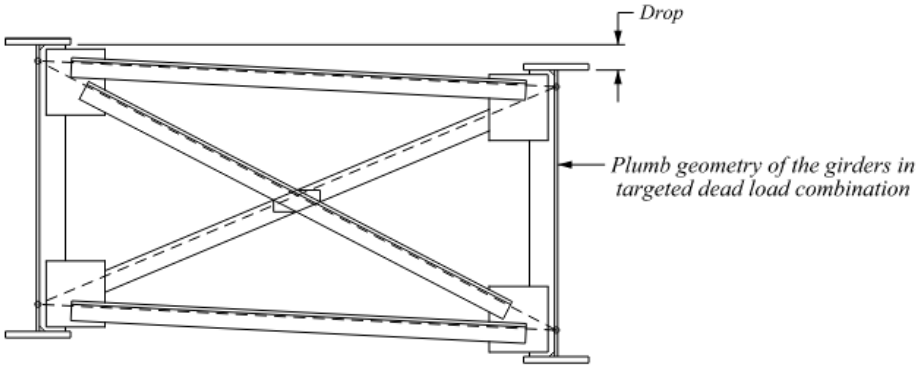

Source: NSBA (reprinted with permission)

Figure 10.23 Drop of an Intermediate Cross Frame Between Two Adjacent Girders

For cross frames oriented parallel to the support skew, the rotated positions of the girder connection plates should also be considered by the detailer when determining the cross-frame geometry. Due to major axis dead load bending and rotation of the girders, the connection plates move longitudinally as the girders deflect vertically. In addition, the cross frames rotate about their own axes. As a result, the corners of skewed cross frames move both longitudinally and transversely when the girders deflect vertically, as illustrated in **Figure 10.24** (AASHTO/NSBA, 2020).

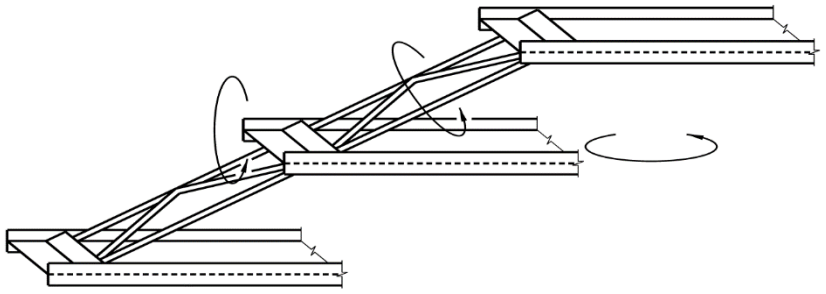

Source: NSBA (reprinted with permission)

Figure 10.24 End Cross Frame Showing Three Rotations That Should be Considered by the Detailer: Major Axis Bending Rotation of the Girder, Twist Rotation of the Girder, and Rotation About the Cross Frame Axis (AASHTO/NSBA, 2020)

10.8.3 Effect of Fit Condition on Cross Frame Forces

For skewed I-girder bridges, SDLF or TDLF detailing "pre-twists" the girders in the direction opposite of the expected dead load roll. In doing so, the final dead load force effect in the cross frame is cancelled out. As a result, it is conservative to neglect the SDLF or TDLF effect and design the cross frames using the results from an accurate 2D grid or 3D FEA model. This is common practice when the engineer chooses to utilize more than a line girder analysis for design. In certain I-girder bridges (those with severe skew and large width/span ratios) the cross-frame forces determined in this manner can be very conservative. This can lead to excessively large cross frames. In lieu of adding SDLF or TDLF effects to the refined analysis, the nonbinding NCHRP 20-07 Task 355 Report (White et al., 2015) suggests a range of reduction factors that can be applied to cross frame forces and flange lateral bending stresses. The designer should determine their applicability based on specific owner/agency policy. The use of these factors is not a Federal requirement.

Alternatively, for skewed I-girder bridges detailed for TDLF, the total dead load cross frame forces and flange lateral bending stresses can be reduced to account for locked-in force effects following AASHTO BDS Commentary Article C6.7.2-1 (AASHTO, 2017a) (23 CFR 625.4(d)(1)(v)). This allows for the application of a net reduced load factor $(\gamma_p)_{red}$ to the dead load cross frame forces and flange lateral bending stresses. The result is a lower-bound estimate of the corresponding beneficial locked-in force effects from TDLF detailing (White et al., 2015) (not in Federal regulation). The use of the net reduced load factor $(\gamma_p)_{red}$ is not used in combination with the reduction factors in the NCHRP 20-07 Task 355 Report .

For curved I-girder bridges, the use of SDLF and NLF are most common. Practice has demonstrated that the use of TDLF on curved bridges can potentially render the bridge unconstructible. This is because curved girders cannot be twisted as readily as straight girders to facilitate erection. Therefore, AASHTO BDS Section 6.7.2 (AASHTO, 2017a) (23 CFR 625.4(d)(1)(v)) indicates that the use of TDLF detailing should not be specified for horizontally curved bridges with an L/R greater than 0.03. Note, even though AASHTO BDS allows for TDLF under specific stipulations, the nonbinding *Skewed and Curved Steel I-Girder Bridge Fit* (Chavel et al., 2016) suggests that Total Dead Load Fit (TDLF) be avoided for horizontally curved steel I-girder bridges.

10.9 Variable Depth Girders

Variable depth girders, also called haunched girders, are designed and detailed with deeper web depths over interior supports than at mid-span. The use of variable depth girders can be advantageous when designing continuous long-span bridges, when designing bridges with short end spans compared to the center span(s), and when vertical clearance below the bridge is limited. The variation in depth can be either linear or parabolic, and generally terminates near a field splice for ease of fabrication.

The use of variable depth rather than constant depth sections affords designers greater flexibility in distributing girder weight efficiently along the span. Web depth typically transitions from deepest at supports (areas of high shear force) to shallowest at midspan (relatively low shear force). In addition, due to the increased stiffness of the deeper girder section at the supports, moment naturally shifts toward the supports, which further facilitates the use of a shallower midspan web depth. Long span bridges (those with a maximum span exceeding 500 ft) are particularly economical at leveraging the benefits of variable depth optimization.

As noted, the variation in web depth can be linear or parabolic. A parabolic taper is generally considered more aesthetically pleasing; however, aesthetics notwithstanding, the straight taper reduces the geometric complexity of modeling and detailing. In the past it was also more economical

from a fabrication standpoint to detail the web with a straight taper. Today, fabricators' use of modern Computer Numerical Control (CNC) equipment has eliminated much of the premium cost associated with fabricating complex geometric shapes.

Source: FHWA

Figure 10.25 Application of Parabolic Variable Depth Girders

It is important to consider several detailing limits when establishing the geometry of the variable depth section, as follows:

- AASHTO *LRFD Bridge Construction Specifications* Section 11.4.3.3 (AASHTO, 2017b) (23 CFR 625.4(d)(1)(iv)) limits the flange cold bend radius to *5.0t*, where "*t*" is the thickness of the flange. This is typically applicable at the beginning and end of the haunched section. The minimum radius is measured at the concave face of the flange.
- For most cases, flange plate bend lines will be oriented perpendicular to the direction of final rolling; however, where the bend line is parallel to the final direction of rolling, the minimum bend radius should be *7.5t*.
- When modeling and detailing the tapered web, as the taper approaches the pier, the bottom flange should return to parallel with the top flange. This parallel section at the support should be long enough to accommodate the sole plate, bearing stiffeners, and jacking stiffeners, as needed.

Source: FHWA

Figure 10.26 Application of Straight Taper Variable Depth Girders

Field splices have the potential to impact the shipping and erection cost of variable depth steel plate girders. Designers should evaluate the cost/benefit of confining the variable depth portions to a single field section via field splices versus minimizing field splices and combining constant and variable depth sections. The former may ease shipping the girders to the field because the variable depth sections are generally shorter in length, but designers should exercise caution not to unjustifiably add field splices to the detriment of increased handling and erection costs. Including an optional field splice at both ends of variable depth field sections should be considered to improve shipping and erection flexibility.

Chapter 11 – Geometry of Girder-Substringer Systems

11.1 Introduction

Prior to the 1970s, it was common to design steel bridges with only two girders in the cross section and make use of transverse floorbeams at regular intervals. Longitudinal stringers were also employed, either continuous over the floorbeams or framed into the floorbeam web. Deck girders and through girders were common configurations of the two-girder system. Today, the two-girder system is generally considered fracture critical. AASHTO BDS (AASHTO, 2017a) (23 CFR 625.4(d)(1)(v)) defines a fracture critical member as a "component in tension whose failure is expected to result in the collapse of the bridge or the inability of the bridge to perform its function." Subsequently, the multi-girder system gained popularity as the fabrication of welded plate girders became more economical and redundancy concerns surrounding two-girder systems sparked awareness among state agencies and industry officials.

A variation of the multi-girder system is the girder substringer system. This system typically becomes economical for long span bridges (greater than 275 ft) that have a wide cross section. A girder substringer bridge utilizes a minimal number of heavy girders combined with a relatively large girder spacing. For example, the West Virginia Department of Highways suggests a girder spacing of 20 to 22 feet for a girder-substringer system. To complement the wide spacing, inverted K-type cross frames are used to support the deck between girders. The cross frame system is comprised of a rolled beam placed midway between the girders, atop the cross frames, as shown in **Figure 11.1** and **Figure 11.2**. Refer to the controlling agency/owner's specifications for specific girder-substringer system criteria.

Source: FHWA

Figure 11.1 Girder-Substringer System

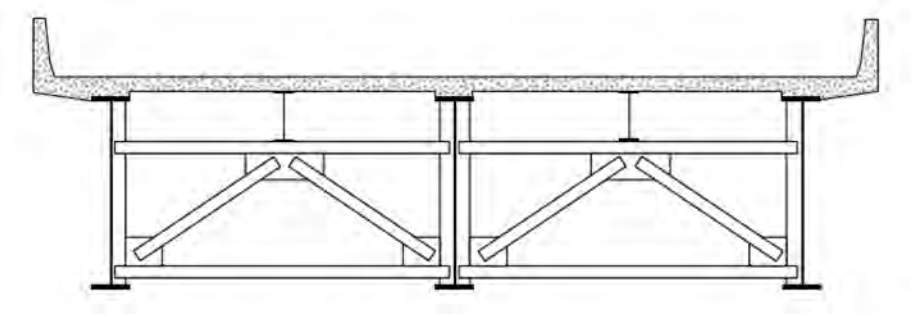

Source: FHWA

Figure 11.2 Cross-Section of a Girder-Substringer System

11.2 Live Load Distribution Factors

For conventional multi-girder bridges, AASHTO BDS (AASHTO, 2017a) (23 CFR 625.4(d)(1)(v)) assumes the live load distribution between girders is transferred by way of deck stiffness as opposed to the frame action of cross frames. For multi-girder substringer systems, however, AASHTO live load distribution factors are not applicable due to the large differences in the longitudinal stiffness of the members. A more rigorous analysis technique such as a 2D grid or 3D model should be employed to determine the live load distribution.

11.3 Geometric Considerations

With advancements in software, curved and highly skewed multi-girder bridges are becoming more prevalent. Introducing either curvature or skew can lead to differential deflections between the girders resulting in challenging issues when erecting the cross frame and substringer systems. Designers may modify approach span alignment or abutment arrangements to avoid introducing curvature or skew into a substringer bridge.

As with conventional long span bridges, multiple spans may be needed. Girder-Substringer Systems can be used for single span arrangements or made continuous over conventional piers or delta piers as used on the Shenandoah River Bridge in West Virginia (**Figure 11.3**).

Source: HDR

Figure 11.3 Shenandoah River Bridge in West Virginia

Since the use of substringer bridges is often only considered for long spans, thermal expansion and contraction is an inherent factor in design. As with most long span bridges, significant longitudinal

movement calls for proper expansion joints to avoid issues with bearings and the substructure. Compatibility of thermal effects between the girders and substringers should be considered if fixity or connections of the substringers to the floorbeams prevents equal thermal movements between the members. Localized differences in movement may create unanticipated loads. Refer to the previous discussion in Section 10.7.

The cross frames in substringer bridges provide support for the rolled beams as well as laterally bracing the girders against lateral torsional buckling. Cross frames should be as deep as possible. Deep cross frames are efficient because the diagonals of the cross frame are at a large enough angle to prevent the gusset plates from becoming too large. Helwig suggested that the minimum cross frame depth be at least ¾ of the girder depth (Helwig 2015).

Skew should be avoided in substringer bridges, so that the cross frames and connection plates are normal to the girders, as in the simple case of conventional plate girder bridges. Transverse stiffeners provide shear resistance and web stability for the girders and are typically not welded to the tension flange of the girder. Connection plates allow for the attachment of cross frames using either bolts or welds. Connection plates should run the entire depth of the girder and are typically welded to both girder flanges and the web. To account for the plate girder web-to-flange fillet weld, the stiffener or connection plate is clipped. Typically, a clip of one to two inches is used at both top and bottom corners of the stiffener or connection plate.

The designer can select how the cross frames are oriented with respect to the deck surface. The cross frames are erected either truly vertical (plumb) or normal to the deck surface. If the true vertical configuration is chosen, beveled fill plates are used to compensate for the divergence from the deck surface normal direction.

Work points for cross frames are typically located at the intersection of the centroids of the individual members. As with conventional steel girder bridges, it is preferable to have cross frames delivered to the construction site as one unit. The benefit is twofold. It assists the erector with girder alignment and reduces the number of individual pieces to handle.

11.4 Camber Considerations

Consistent with Section 8.2.1, the designer should consider dead load camber for substringer bridges. AASHTO BDS Section 6.7.2 (AASHTO, 2017a) (23 CFR 625.4(d)(1)(v)) requires the designer report deflection separately for the self-weight, concrete deck including stay-in-place formwork, and any anticipated future wearing surface. The camber of the girders should be accounted for in the cross frames and rolled beams because the camber will affect the cross frame fit up. In addition to camber, differential deflection resulting from both staged construction and the erection sequence should be accounted for in cross frame fit up. Where permitted, a common approach to ensure cross frame fit up in staged construction is to use vertically slotted holes, field drilled holes, or field welded connections to provide flexibility in mating components. Finally, the connection between the substringer and cross frames should account for differential dead load deflection of the girders. Longitudinal slotted holes in the stringer to floorbeam flange connection may be beneficial to compensate for differential dead load deflection as well as fabrication and erection tolerance.

Chapter 12 – Geometry of Steel Trapezoidal Box Girder Bridges

12.1 General Considerations

Steel trapezoidal box girders are comprised of several distinct components. This section will discuss the design decisions and layout considerations that influence the geometry of each.

A trapezoidal box girder is a three-sided steel section consisting of a wide bottom flange connecting two inclined webs. A composite concrete deck slab forms the top surface, making the tub a closed section. The inherent advantage of a trapezoidal box is derived from its geometric shape. It has an extremely high degree of torsional stiffness, making it ideal for curved girder applications. While curved structures take full advantage of the trapezoidal box's torsional stiffness, straight sections can also be desirable despite their premium cost due to the structure's simple aesthetics and clean lines.

Source: HDR

Figure 12.1 Dual Steel Trapezoidal Box Girders

Aside from the girder itself, a trapezoidal box girder system also includes a bracing system. The primary purpose of the bracing system is to provide stability to the individual girder as well as the girder system prior to and during the deck pouring sequence. While the bracing system in some instances may no longer be needed after the deck has hardened, it is commonly left in place to accommodate future deck slab replacement. The bracing system is generally comprised of internal and external cross frames as well as a lattice structure of top flange lateral bracing within each girder. Internal and external cross frames are typically K-frames (within the span) or solid plate diaphragms (at supports). Geometric considerations for cross frames and top flange lateral bracing are discussed in Sections 8.6.3 and 8.6.4, respectively.

12.2 Superstructure Fabrication

Historically, steel trapezoidal boxes have generally been more costly to fabricate than other steel superstructure types. This is due in large part to their complex geometry, which leads to difficulty in

fabricating and assembling the various components. In addition, highly skilled and specialized labor is typically necessary for both fabrication and erection. While material costs may be competitive with similarly sized plate girders, labor cost is a significant contributor to the overall cost. However, given careful consideration during design, trapezoidal box girders can be detailed and fabricated to their full economic potential. Indirect savings in the form of reduced erection costs, resulting from fewer diaphragms to connect and fewer girder lines to set, may partially offset premium fabrication costs (Coletti et al., 2005).

Several steel detailing guides offer suggestions for economic box girder design, such as the Texas Department of Transportation (TxDOT) *Preferred Practices for Steel Bridge Design, Fabrication, and Erection* (TxDOT, 2006) (not in Federal regulation) and Section 6.11.2 of the AASHTO BDS (AASHTO, 2017a) (23 CFR 625.4(d)(1)(v)). Designers may refer to these guidelines when developing steel trapezoidal box designs as well as discuss detailing decisions regarding plate proportioning versus the cost of stiffeners with local steel bridge fabricators.

Fabrication costs are also influenced by structure geometry. Where at all possible, designers should avoid skewed supports, or at minimum, skewed ends. Skewed end diaphragms may be more expensive and complicated to detail, fabricate, and erect. Diaphragms at skewed piers, however, can be detailed using parallel connections as a workaround to the complexity of skewed details (Coletti et al., 2005) (not in Federal regulation).

Working with local steel bridge fabricators can also provide insight regarding the placement of field splices. Field splice placement will influence shipping length (many States limit shipping lengths to approximately 120 feet) and erection weight. Box girders are generally heavier than plate girders, leading to excessive equipment and labor costs for shipping and erection. Appendix B of the NSBA document *Practical Steel Tub Girder Design* (Coletti et al., 2005) (not in Federal regulation) includes suggested details for the economic development and layout of trapezoidal box girders. In addition, designers can refer to the nonbinding guidelines within FHWA's *Steel Bridge Design Handbook* (FHWA, 2015) and the AASHTO/NSBA Steel Bridge Collaboration's *G12.1-2020 Guidelines to Design for Constructability* (AASHTO/NSBA, 2020) and *G1.4-2006 Guidelines for Design Details* (AASHTO/NSBA, 2006).

12.3 Internal and External Diaphragms

Numerous resources suggest steps and design considerations to take into account when developing an efficient framing plan, spacing diaphragms and lateral support, and proportioning member sizes. This section discusses the influence of the bridge geometry on internal and external cross frames.

Internal intermediate diaphragms are provided to control cross sectional distortion of the box girder. They are typically composed of K-frame cross frames to allow easy access for inspectors. Locating intermediate diaphragms at every other panel point of the top flange lateral bracing has been demonstrated by Li to produce better performance than pairing an intermediate diaphragm with every panel point (Li, 2004, Helwig et al., 2004) (not in Federal regulation).

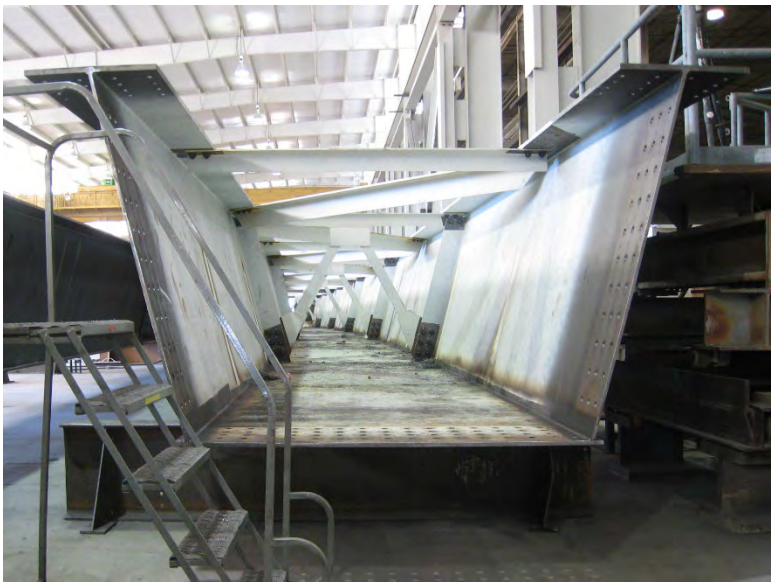

Source: HDR

Figure 12.2 Internal Intermediate Cross Frames and Top Flange Lateral Bracing

Exterior intermediate diaphragms are provided to control differential displacement and rotation of individual box girders during slab placement. The presence of exterior intermediate diaphragms helps to ensure a more uniform deck slab thickness is achieved across the width of the bridge. Li further showed that sufficient control of deck slab thickness can be achieved with only a few intermediate braces between supports (Li, 2004, Helwig et al., 2004) (not in Federal regulation). Bracing at the midspan was also shown to be more sensitive to rotational influences, so an uneven distribution of intermediate braces concentrated toward the midspan is a more efficient layout than evenly spaced braces throughout. For information in determining the number and spacing of exterior, as well as interior, intermediate diaphragms, the reader is directed to Section 5 of the nonbinding NSBA document *Practical Steel Tub Girder Design* (Coletti et al., 2005).

Interior and exterior support diaphragms are typically steel plate elements. The only notable geometric consideration in detailing of these diaphragms is the need for a properly braced access hole (**Figure 12.3**).

Source: HDR

Figure 12.3 Solid Plate Interior Support Diaphragm with Access Hole

12.4 Top Flange Lateral Bracing

Trapezoidal box girders in their finished, closed-section condition (including a cured, composite deck slab) are torsionally much stiffer than comparably sized plate girders. This makes the trapezoidal box an ideal candidate for curved structure applications. The problem, however, is the trapezoidal box, is not a closed, torsionally stiff section during transport or erection. Only after the concrete deck slab has cured, and formed a composite top to the section, does the member realize its torsional rigidity. Therefore, to stabilize the box girder prior to the finished deck condition, lateral bracing should be considered to stabilize the otherwise independent top flanges. The top flange lateral bracing is formed in either a Warren or Pratt truss configuration. For further information, the benefits of one versus the other is discussed in detail in the AASHTO BDS (AASHTO, 2017a) (23 CFR 625.4(d)(1)(v)) with additional nonbinding information available in *Design Guidelines for Steel Trapezoidal Box Girder Systems* (Helwig et al., 2007). Regardless of the truss type, the angle formed by the truss diagonal and top flange is very important for the geometric layout. Some research (Helwig et al., 2007) showed that an angle beyond 35 and 50 degree could result in an inefficient use of bracing material and fabrication labor.

A secondary consideration in the layout of the top flange lateral bracing truss is the relationship of the patterns between adjacent boxes. The truss patterns are said to be "parallel" when both girders use the same diagonal orientation. The truss patterns are "mirrored" when the diagonal orientation of one girder is mirrored about the centerline between the adjacent girders. The advantage of the mirrored pattern is the diagonals of both girders coincide with the external K-frame connection. This provides for a better distribution of forces into the top flange, relieving the top strut of the truss/internal diaphragm of the full load transfer burden. Helwig suggests this is a particularly beneficial approach for structures with support skews exceeding 20 degrees (Helwig et al., 2007).

Chapter 13 – Geometry of Truss Bridges

13.1 Introduction

Trusses have been in use for bridge construction since at least the 1840s and were developed to provide longer spans than could be achieved by arches or other common structure types of the day. Early truss construction used wood and progressed to iron and finally steel by the late 19th century. While this structure type has been largely supplanted by higher strength materials and other construction techniques, they still offer an aesthetically pleasing and efficient structural system.

Modern trusses continue to have applications for roadway, rail, pedestrian, and temporary bridges. Various manufacturers provide pre-engineered truss structures for use on low volume roads, private developments, and projects such as bike and walking trails.

Trusses can be categorized into three broad types: deck trusses, through trusses and pony trusses. Deck trusses have the roadway surface placed on top of the truss; through trusses have the deck surface at the bottom of the truss with a fully braced system above the deck surface, as shown in **Figure 13.1**; and, a pony truss is a modification of a through truss where there is no bracing between top chords of the truss. The section discusses geometric considerations that are broadly applicable across the spectrum of truss structures.

Source: HDR

Figure 13.1 Through Truss Bridge, Point Marion Bridge, State Route 88 over the Monongahela River in Fayette and Green Counties, Pennsylvania

13.2 General Geometric Considerations

Truss design is addressed in the AASHTO BDS (AASHTO, 2017a) (23 CFR 625.4(d)(1)(v)) in several locations. AASHTO BDS Table 2.5.2.6.3-1 (AASHTO, 2017a) (23 CFR 625.4(d)(1)(v)) provides minimum depths for superstructures of various materials and notes a minimum depth of 0.1L, where L is the span length in feet, for a truss. For example, a 250 ft span truss would result in a total depth of at least 25 ft.

The 0.1L minimum depth is only valid if the bridge owner chooses to invoke the criteria. AASHTO BDS Section 2.3.3.2 (AASHTO, 2017a) (23 CFR 625.4(d)(1)(v)) further specifies the minimum vertical clearance from the roadway carried to any overhead bracing members in a through truss configuration is 17.5 ft.

Trusses are typically designed to function with discrete members acting in a series of triangles to form the structural system. The truss members are typically designed as axially loaded members with little or no flexural load. The member joints are idealized pin connections often referred to as panel points. Older trusses used pins at the joints, but modern trusses typically use gusset plates or fully welded connections to join the members. Depending on the truss configuration, individual members may carry only tension or compression, or may be subject to stress reversal.

Floor systems are made up of transverse floor beams and in some cases, stringers that are perpendicular to the floor beams. The floor beams connect the joints of the parallel trusses. This system will support the deck. Additional bracing may also be present for either a deck truss or a through truss to provide lateral stability, transverse load resistance, and bracing against buckling. This bracing may exist in the plane of the truss chords as well as vertically between the trusses. The latter, known as sway bracing, minimizes differential deflections between the trusses similar to cross bracing in a steel girder system. The major components of a through truss system are shown in **Figure 13.2**.

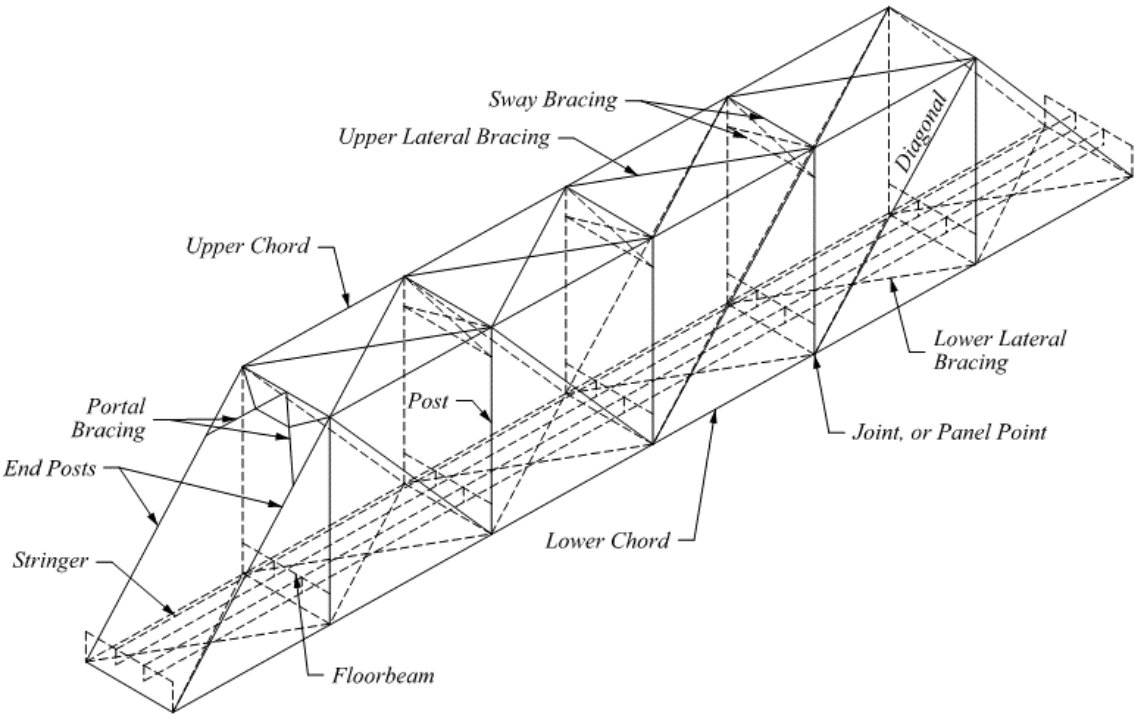

Source: FHWA

Figure 13.2 Components of a Typical Through Truss (deck not shown)

In general, based on the basic geometric shape, truss configurations with a parabolic shape to the non-roadway supporting chord (the bottom chord of a deck truss or the top chord of a through or pony truss) may provide better structural performance than one with a straight chord. In this regard, a Parker truss configuration for the through truss is more efficient than a Pratt truss configuration due to the shape of the top chord (see **Figure 13.3**).

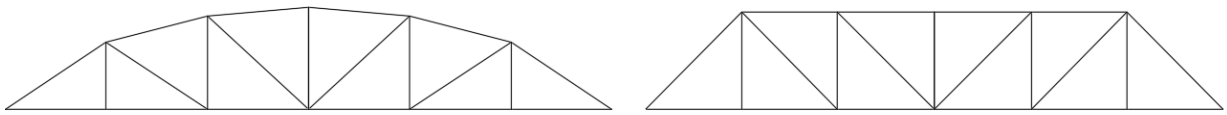

Source: FHWA

Figure 13.3 Parker Truss (left) vs Pratt Truss (right)

In developing the layout and geometry of a truss structure, a number of factors should be considered early in project development. Through or pony trusses are often used in applications where vertical clearance below the bridge is critical either due to the bridge crossing another roadway or similar feature, or due to the hydraulic opening. The profile of the roadway should be developed considering the depth of the truss below the roadway surface. This may be controlled by either the depth of the bottom chord or the depth of the floorbeam.

Other factors can influence configuration of trusses, such as:

- Aesthetics;
- Fabrication, delivery and erection limitations that exist on a project site;
- The ability to prefabricate z assemble portions of the bridge off site;
- Member types, whether they are rolled steel sections, fabricated beam sections, box sections, or some combination of individual members; and
- Future maintenance and inspectability.

The configuration of the floor system should likewise be considered. Floor systems with stringers and floorbeams can be either stacked systems where the stringer sits on top of the floorbeam, or framed systems where the stringers frame into the webs of the floorbeams. Stacked systems offer several advantages over framed systems. These include the ability to make the stringers continuous over several floorbeams allowing for more efficient designs and a reduction in the number of field pieces; and, a reduction in the number and complexity of the connections to the floorbeams. The disadvantages of the stacked system are they generally result in a deeper floor system, and the stacked system will typically prevent the floorbeams from being made composite to the deck resulting in a larger steel section.

Skewing truss structures should be avoided. Introducing skew into a truss can lead to problems with differential deflections inducing bending or additional forces into bracing members, and ultimately longer and heavier floorbeams, and complicating connections between floorbeams and truss joints. Whenever possible, skews should be addressed in approach spans or by modifying the orientation of abutments on single span structures.

Steel fabrication and detailing practices can accommodate reasonable vertical curves in trusses, especially in custom built longer span structures. Prefabricated truss structures for pedestrian use or smaller projects may be difficult to procure with vertical curvature. Significant changes in cross slopes that cannot be accommodated with variations in stringer haunch depth should be avoided. Deck trusses have been constructed with ramp tie-ins for acceleration and deceleration lanes. This can be accomplished using sloped secondary trusses or cantilever brackets.

For the layout of the truss system, it is a typical practice to develop an arrangement that keeps the truss diagonal angles at a relatively steep slope between 45 and 60 degrees. This arrangement will generally

reduce the size of the diagonal members and help to control the size of the stringers by reducing their span length. This also helps to minimize the size of the gusset plates at the truss joints. Bottom chord members are to be fabricated straight in each panel.

Other considerations for truss geometry are similar to any other type of bridge. Fixity and continuity of the spans as well as thermal expansion and contraction is important for serviceability and design of both the superstructure and the substructure. Often, through truss structures are arranged with a single truss span and conventional approach spans. Deck trusses, on the other hand, are frequently made continuous, often with three or more spans (see **Figure 13.4**). Continuous deck trusses are typically arranged with a variable depth truss with the bottom chord following a parabolic shape. Multiple span truss structures can result in very large longitudinal movements, and consideration of expansion joint types will be important.

Source: HDR

Figure 13.4 Deck Truss Bridge, Liberty Bridge over the Monongahela River in Pittsburgh, Pennsylvania

13.3 Camber and Constructability Considerations

Designers should understand and account for various constructability, fabrication, and erection considerations for trusses from the earliest stages of design development. How the bridge is to be built can directly affect much of the decision-making process in how a project comes together. Contract plans should specify whether the truss has been designed for cambered lengths and cambered angles, or for camber lengths and geometric angles. This section will examine a number of these factors.

Any steel bridge, regardless of whether it is designed for a vertical curve, will be constructed with camber to account for dead load deflection. This camber should be accounted for in the truss as well as the floor system. How and when the dead load is applied to the bridge is important, as the application of load due to erection can introduce locked-in stresses in members that a standard analysis may not take into account. As an example, if a model of a complete, in-place truss structure is developed and the self-weight and imposed dead loads from the deck or other components are instantaneously "turned on" in the analysis, the analysis would not account for progressive loading of members during erection. This condition would assume that the structure is always fully shored against gravity during erection, which is highly unlikely. **Figure 13.5** shows the expected dead load deflections of a truss from its cambered position to its final loaded position.

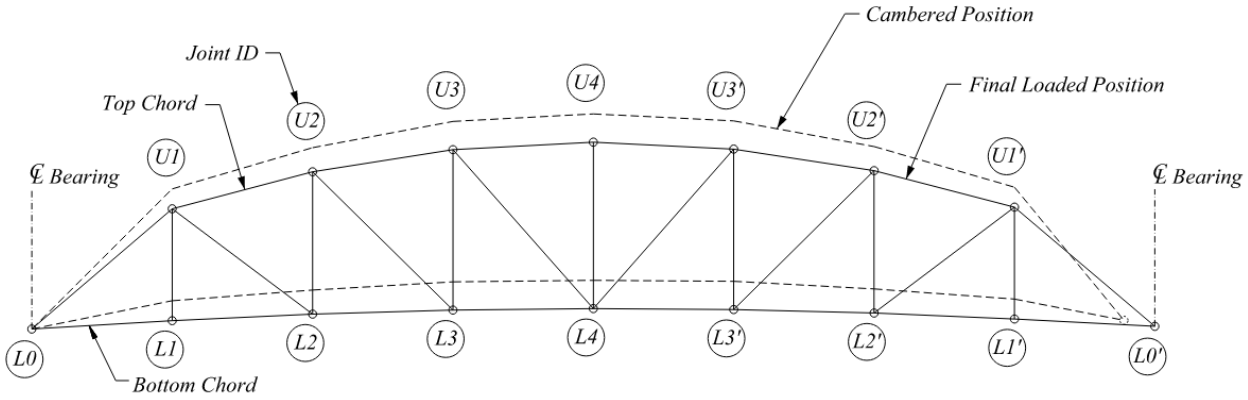

Source: FHWA

Figure 13.5 Truss Deflections from Cambered Position to Final Position

In addition to the camber considerations of the trusses, the designer should select how the floorbeams are oriented with respect to the deck surface and if the floorbeams and stringers are assumed to be detailed in a cambered or final position. The floorbeams can be erected either in a truly vertical (plumb) position or normal to the deck surface. The orientation of the floorbeam should match the orientation of the truss vertical assuming the truss configuration includes vertical floorbeam. However, if the bridge is oriented on a vertical curve or a grade, the connections between the floorbeams and stringers should account for the grade as the flanges of the stringer would not necessarily be in the same plane as the flanges of the floorbeam. On stacked systems, this will lead to beveled fill plates between the bottom of the stringer and the top of the floorbeam. Setting the floorbeam normal to the road surface would bring these planes closer to agreement but could introduce out of plane bending as well as detailing issues at the connection to the truss joints.

Camber in the stringers may be a combination of dead load camber to address deflections and geometric camber to address vertical curves. Detailing of the connection for cambered position would have the member fabricated in either a no load or self-weight only loaded position prior to the deck being placed. The deflection from the deck placement would introduce forces into the "locked in" connection since it may not rotate as a pinned connection. Detailing for a final position would assume that the stringer end is permitted to rotate in response to dead load deflection before being fully assembled. This can be accomplished with slotted holes or with the installation of only a portion of the bolts prior to the deck placement.

Camber in the floorbeams can be addressed by detailing the member for its cambered profile. Floorbeams are frequently detailed with both web and flange connections to the truss, so proper detailing of the flange connections will be beneficial to allow the floorbeam to "fall" into its final position. The end rotation of the floorbeams in the fully cambered position should be accommodated in the field during erection. This can be achieved by leaning out the trusses (slightly twisting the chords and vertical members) to match the end rotation of the floorbeams. This will allow the truss bottom chord to rotate into position as dead load is applied. Another important consideration is any impact that rotation or introduction of locked-in forces has in applying forces into the truss joint and truss system laterally. If significant forces or displacements are anticipated, consideration in design and detailing of sway and lateral bracing may be warranted. Finally, differential movement of the truss and the stringers should also be considered.

Accommodating cross slope is another important factor in floorbeam detailing. For stacked systems, cross slope is typically addressed with fill plates or bearing support assemblies of various height. For framed systems, the height of the top of the stringer can be varied as shown in **Figure 13.6** to create the cross slope while minimizing haunch depth for the stringers. Several factors should be accounted for if this method is used. Adequate connection depth of the stringer to the floorbeam needs to be provided. For constructability, connection holes in the floorbeam should be detailed at the same relative elevation to the deck cross slope across the width of the floorbeam leaving the clip angles between stringers and floorbeams at different elevations. The depth of the haunch over the floorbeam should also be considered if the floorbeam is composite with the deck. Reinforcement of the haunch may be needed if the depth is excessive.

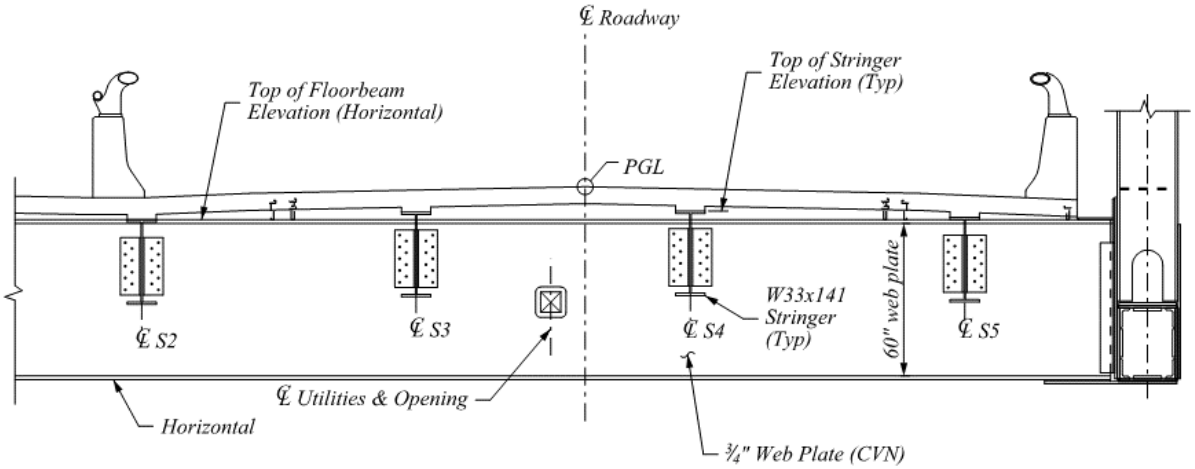

Source: FHWA

Figure 13.6 Partial Cross Section of Floorbeam and Stringers in a Through-Truss Bridge

Similar to conventional girder type structures, floor system camber is generally provided in a tabular format that breaks down the camber by steel self-weight, non-composite deck load, and composite deck load. Geometric camber, if present, can also be tabulated. Floorbeam camber is typically provided at all stringer locations at a minimum. Stringer camber may be provided at quarter points or at additional points at the judgment of the designer based on the length of the stringers.

Detailing of the truss geometry begins with the development of the truss elevation including elevations at each panel point along the top and bottom chords. The designer should indicate whether the panel point elevations are provided under consideration of full dead load application. The profile grade and vertical curve, if present, also need to be accounted for in these elevations. It is also customary to provide member lengths from center-to-center of the panel points. Where chords are continuous over two or more panel points, chords can either be kinked or straight-lined from end-to-end, if the offset is negligible. Again, most importantly, the designer should indicate the assumptions used in developing the lengths and elevations presented on the plans.

Each joint of the truss should be fully detailed on the design plans including an elevation and appropriate views and sections to clearly indicate the member sizes, hole patterns, edge distances and other details. Locations of manholes or handholes as well as cover plates should also be detailed. As previously discussed with the floorbeams, the need for tie and seat plates and web connections should be evaluated for constructability purposes. These features may only be an adjunct to erection of the structure and may not provide adequate rigidity to fix the end of the floorbeam for the purposes of

structural analysis. Any desire to assume fixity in the connection should also be weighed against any influence end moments would have on the design of the remainder of the joint. It is typical practice to design the floorbeam support as a pinned connection.

For joints located at bearings, designs should have bearing stiffeners as well as stiffeners between the gusset plates to provide adequate rigidity and buckling resistance since the members will not run "through" the connection. Stiffeners may be welded plates, bolted angles, or a combination of the two. Levelling and bearing plates may also be needed. Appropriate clearances for weld access and bolt clearances should be considered for these details.

While final detailing of gusset and connection plates is left to the fabricator, bridge owners typically rely on designers to develop details and bolt patterns that are constructible and economical. Consideration of the field assembly and erection conditions is very important. Trusses can be assembled and erected using several methods depending on project circumstances and conditions. Trusses can be erected in pieces using falsework towers that are moved and reset as assembly progresses. One or more truss panels would cantilever over the falsework while other components are attached. If this method is used, some owners may find it desirable to detail the truss members and connections for cambered lengths and cambered angles that would allow the components to fit together in a no-load condition. This fit up method could introduce some permanent distortion into the members once the falsework is removed. Any locked in stresses from this method should be considered in the design of the members and the connections.

Trusses can also be partially or fully assembled in a no-load condition and launched into place. While the geometric considerations for this method may be similar to the cambered length and cambered angle condition, additional consideration should be given to the launching method used and how the truss is supported and braced in temporary conditions. Moreover, owners are becoming more accepting of virtual assembly with advances in state-of-the-art computer programs that can also be linked directly to CNC fabrication. Experience has shown this can effectively eliminate the practice of full or partial shop fit up. Similarly, trusses can also be erected using a drop in method with one or more cranes after being assembled in a no-load condition.

The other general method of truss assembly and erection which can influence connection geometry is known colloquially as "Chicago Style" assembly, which uses cambered member lengths but geometric final angles. This method is similar to the floorbeam erection method where the beam is allowed to "fall" into position with end rotation being permitted. If this method is employed, the truss members are either permitted to fall into position or are forced into position. Proper detailing of the connections including staged installation of bolts should be investigated if this method is used. A drawback of the "Chicago Style" assembly is that the truss cannot be fully shop assembled.

Chapter 14 – Geometry of Steel Arch Bridges

14.1 Introduction

Steel arch structures are an effective long span option where pier placement is not possible: the roadway is over a feature that is in a deep cut or ravine; favorable geological conditions exist; structure aesthetics are critical; or some combination of these factors are present. Steel arch structures are a logical outgrowth of stone or other types of arch structures that represent some of the earliest forms of bridges. They incorporate many of the same concepts of taking advantage of the strength of the arch shape to span the crossing including strength and rigidity of the arch to resist compression.

Steel arch bridges can be of several general types. Deck arch structures incorporate the arch to support a more conventional superstructure, typically a floorbeam-stringer configuration. Deck arch structures frequently use spandrel columns to support the floorbeams in a manner similar to a steel truss. This arrangement minimizes superstructure depth and dead loads. An example of this type of structure is the Greenfield Bridge in the City of Pittsburgh (**Figure 14.1**).

Source: HDR

Figure 14.1 Greenfield Bridge in the City of Pittsburgh, an Open-Spandrel Deck Arch Structure Completed in 2017

Through arch and tied-arch type bridges represent the other major types of steel arch structures. While similar in configuration with the deck passing through the arch, the major difference between these types of structures is how horizontal loads are resisted. A traditional through arch structure transmits the horizontal thrust of the arch action into the foundation. This calls for a robust foundation or pier capable of resisting the large lateral forces. This is often accomplished with the use of a substantial anchorage similar to a suspension bridge on each end. Examples include the Hell Gate Bridge, a railroad

bridge in New York City; the Sydney Harbor Bridge; and the Bayonne Bridge between Staten Island and New Jersey.

Tied-arch bridges use a deck system that is designed to not only support superstructure and vehicle loads but to resist the longitudinal forces created by the arch. The lateral forces induce large tension forces in the superstructure system and act structurally similar to the lower chord of a through truss. This can reduce or eliminate the thrust loads acting on the substructure allowing for a corresponding reduction in foundation and pier size. Tied arch structures introduce fracture critical considerations into the design of the superstructure, however, and costs of the increased demands on the superstructure, including long term maintenance and inspection, should be weighed against the costs of the larger foundation system. An example of a tied arch structure is the Fort Duquesne Bridge in the City of Pittsburgh (see **Figure 14.2**).

Source: HDR

Figure 14.2 Fort Duquesne Bridge in the City of Pittsburgh, a tied arch structure

14.2 Arch Configuration Layout

Arches for highway bridges generally use a parabolic curve. The geometry can be developed using classical mathematic equations to find the length of the curve and points along the curve. A parabolic curve and a catenary are not the same. A catenary, which is the shape a weighted chain or rope would assume when supported from the ends, is the shape suspension bridge cables typically follow. The mathematical derivation of a catenary is different from that of a parabola. Inverted parabolic curves, such as the ones used in arch bridges, tend to be more efficient in transmitting forces through the arch when loads are applied. They do, however, generate higher thrust loads at the supports.

Several considerations contribute to the selected configuration of the structure. Common steel arch rib configurations consist of built-up box members or I-shapes. Longer span arch structures often have arch ribs that consist of trussed members. Many of the same concerns and techniques used for trusses can be applied to trussed arch ribs. As arch structures are frequently used over waterways, navigational clearances are an important issue. For through arch structures, vertical clearances to portal frames and bracing, similar to a through truss, should be considered. Structures in a ravine type

setting will often have their configuration dictated by geotechnical conditions as placement of anchorages are dependent on sufficient geotechnical resistance.

Other general considerations were suggested by Nettleton in *Arch Bridges* (Nettleton and Torkelson, 1977) (not in Federal regulation). It was reported that, existing steel arch structures have a typical rise-to-span ratio of between 0.16 to 0.20 with a minimum of 0.12 and a maximum of 0.30. Nettleton then discusses rib depth as a function of span and distinguishes between non-tied and tied arches. For non-tied arches, Nettleton suggests limiting live load deflection of an arch to $L / 1200$ where L = the span length in feet, and plotted values of L / d with d being the depth of the rib in feet to derive an equation of $L / d = 44 + 0.6 \sqrt{L}$ to approximate the depth of the rib. Consideration should also be given to the type of arch being used as trussed arches typically have less live load deflection, therefore a "flatter" arch may be acceptable. Nettleton also notes that fixed arches can have ratios of about 0.8 times the calculated value since they tend to have smaller live load deflections.

For rib depth on tied arch structures, the distribution of live load between the tie and the rib is a consideration. If the tie is assumed to carry much of the live load in flexure, the rib would primarily only resist the thrust in the arch. This could reduce the demand on the rib; however, it could yield a more robust tie structure.

Source: HDR

Figure 14.3 West End Bridge in the City of Pittsburgh

Considerations for an arch floor system are very similar to those for a truss. Both stacked and framed systems of floorbeams and stringers can be used. Connectivity of the floorbeams to a tied arch system consisting of girders or a truss structure in a manner similar to a truss. In the case of a deck arch structure with spandrel columns, the connection of the floor system to the columns can occur in several ways. Depending on thermal expansion or other movement, the deck system can be supported on conventional bearings on top of the columns. This system permits expansion and contraction of the superstructure while reducing or eliminating longitudinal loads acting on the columns. It can also release the connection between the column and superstructure which influences load development due to global deflection of the arch. This effect should be considered in the analysis of the structure.

Spandrel column height in deck arches is directly related to the layout of the rib geometry. Taller columns may necessitate additional bracing or more robust members to meet buckling requirements of the owner. End connectivity between the column and the rib, or between the column and the floorbeam will influence the selection of k value and the unbraced length of the column as well as the overall

performance of the structure. The rigidity of the connection will directly relate to the moment transmitted into the columns due to overall displacement of the rib.

14.3 Camber and Constructability Considerations

As with trusses, a variety of constructability, fabrication, and erection considerations should be considered throughout the development of the project s. The erection method to be used will directly influence geometry considerations as well as design loads. Site specific conditions will often dictate what methods can be used to erect the structure.

Smaller arch structures with relatively light ribs can sometimes be erected as complete units. The rib would be assembled on site in a no-load condition and then set with cranes. The assumed locations of the pick points for the erection will figure into detailing of the members. If an arch rib is picked at its center, the outstanding legs would tend to deflect inward. This deflection is counter to the normal deflection the structure would see in service. This could be addressed by detailing the rib for the assumed amount of deflection so that when it is lifted, the legs "fall" into their final position. The arch could also be detailed for its final, in-place position and have the legs jacked into position on the bearings during erection. A final option may be to use a temporary strut to brace the legs and remove the strut once the arch has been erected. In any case, proper detailing of connections, including accounting for displacements and stresses during erection should be carried out.

Tied arch structures can also be prefabricated and erected in a unit. In the nonbinding *Arch Structures* (Nettleton and Torkelson, 1977), the author discusses a procedure used for the Fremont Bridge in Portland, Oregon where the center span, which acts as a tied arch, was jacked into place after being prefabricated off site. The rib and tie sections are forced into a cambered position introducing stresses that are equal and opposite to the final dead load stresses. Once they are erected and the temporary struts are removed, the structure deflects into final position resulting in little to no net dead load stress.

Larger and longer span structures are typically erected using temporary shoring towers or tie back structures. An example of the construction of an arch using these methods is shown in **Figure 14.4**. This method is similar to truss erection and presents many of the same design and construction challenges. The structure should be designed for temporary loading conditions, including accounting for temporary bearing locations and often incomplete or different bracing systems and locations in the temporary condition.

Source: HDR

Figure 14.4 Erection of the Arch Rib of the Greenfield Bridge in the City of Pittsburgh Using Temporary Supports

Phasing of the erection should be considered if temporary supports are used. If members are permitted to cantilever beyond the temporary support, the designer should consider if the member should be detailed using the cambered length – cambered angle method previously discussed for truss erection or other methods. Consideration of the chosen method may influence the design of gusset plates or other connections. Detailing of the key or final segment to be erected should also be considered if phased erection is used. Field drilling of connection holes or other methods to account for discrepancies during erection should be expected to ensure proper fit.

Design for camber and deflection should also consider erection of the remainder of the structure and placement of the deck as these loads can impart greater stresses and displacements on the ribs than its self-weight. The development of hinge points as the bridge is constructed should also be considered since hinge locations may move as load is added. For tied arch structures, if the connections in the rib are detailed for the overall camber of the structure under full dead load, the action of the tie, or the location and amount of forces present in the tie, could vary greatly during various stages of construction. Loads in the tie may also vary during the construction of the bridge.

For non-tied arches, movement at the bearings as load is added is a consideration. As dead load is added, the arch will deflect, adding translation to the expansion bearing. This translation can either be relieved by resetting the bearings once dead load is applied or detailing the bearings to account for this longitudinal translation. Footing forces can also vary during staged construction, and evaluation of the footing including bearing resistance checks or checks for deep foundation forces and uplift conditions may be warranted. This condition may also be a factor in future redecking operations on the bridge. The designer may wish to address the future redecking in the plans. It is also prudent to consider this on any rehabilitation of existing tied arch structures.

As with trusses, some amount of geometric camber can be accounted for in an arch structure. Most changes in deck geometry, including cross slopes or vertical curve, can be addressed in the floor system. Significant variations in the cross slope or grade should be avoided wherever possible to simplify detailing and fabrication. Similar to trusses, camber in the floor system can be tabulated in the design plans to distinguish between dead load cambers at various stages and geometric camber.

APPENDICES

Appendix A – Vector Geometry

A.1 Introduction

The geometry of complex bridge types, such as curved steel and concrete girder bridges and precast concrete segmental box girder bridges, often involves the use of vector geometry. This appendix presents aspects of vector geometry important to these bridge types. Basic characteristics of vectors are introduced in two dimensions and then expanded to 3D vectors. Unless indicated by citation to Federal law or regulations, the definitions, notations, and equations that follow are provided to assist in using this manual and their use is not required.

A.2 2D Vectors

A.2.1 Definitions and Notations

A geometric vector is a linear object that has both magnitude and direction. **Figure A.1** shows a 2D vector *U* lying in the X-Y plane beginning at point *A*(*x*,*y*) and extending to point *B*(*x*, *y*).

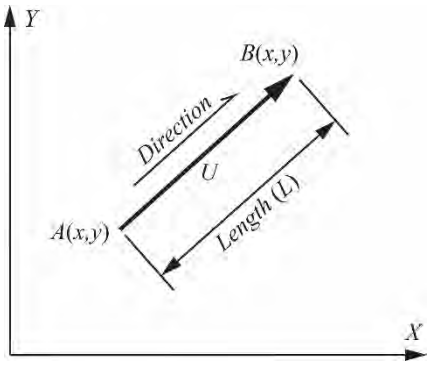

Source: PCI

Figure A.1 2D Vector from A to B

Figure A.2 shows parameters used to further define the 2D vector *U*.

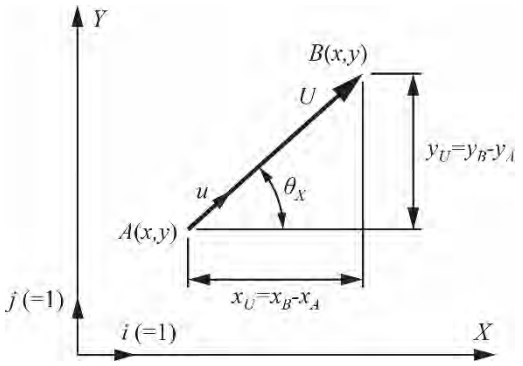

Source: PCI

Figure A.2 Additional Features of a 2D Vector

Set within the orthogonal coordinate system in the X-Y plane, the length of a 2D vector can be expressed by the projected lengths of the vector along the two axes. The length of vector *U* projected onto the X axis is

$$x_U = x_B - x_A \tag{A.1}$$

The length of vector *U* projected onto the Y axis is

$$y_U = y_B - y_A \tag{A.2}$$

The length of vector *U* is found by the Pythagorean theorem:

$$|U| = \sqrt{x_U^2 + y_U^2} \tag{A.3}$$

The direction of the 2D vector can be expressed by the angle from the X axis to the vector. The convention adopted for this manual is that vector directions are given by direction cosines within the coordinate system. Remembering from trigonometry that the cosine of an angle is equal to the length of the adjacent leg of a right triangle divided by the length of the hypotenuse, the direction cosine of vector *U* with regard to the X axis is

$$\cos\theta_{UX} = \left(\frac{x_U}{|U|}\right) \tag{A.4}$$

Vector *U* can be expressed in equation form by the components of the vector parallel with the axes of the coordinate system multiplied by unit vectors along each axis.

$$U = x_U i + y_U j \tag{A.5}$$

The integers *i* and *j*, shown in **Figure A.2**, are unit vectors along the X and Y axes, respectively.

Example 1: Given the 2D vectors *U* and *V* in the figure below, compute their lengths and direction cosines. Also, express the vectors in equation form.

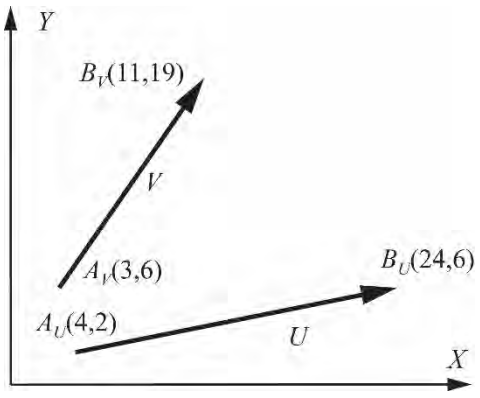

Source: PCI

Figure A.3 Example 2D Vectors

For vector *U*:

$$x_U = 24 - 4 = 20 \tag{A.6}$$

$$y_U = 6 - 2 = 4 \tag{A.7}$$

$$|U| = \sqrt{20^2 + 4^2} = 20.3961 \tag{A.8}$$

$$\cos\theta_{UX} = \left(\frac{20}{20.3961}\right) = 0.9806 \tag{A.9}$$

$$U = 20i + 4j \tag{A.10}$$

For vector *V*:

$$x_V = 11 - 3 = 8 \tag{A.11}$$

$$y_V = 19 - 6 = 13 \tag{A.12}$$

$$|V| = \sqrt{8^2 + 13^2} = 15.2643 \tag{A.13}$$

$$\cos\theta_{VX} = \left(\frac{8}{15.2643}\right) = 0.5241 \tag{A.14}$$

$$V = 8i + 13j \tag{A.15}$$

It should be noted that the equations for vector direction cosine and resulting direction angles are quadrant dependent. Vector components' signs should be assigned using a convention similar to that presented in section 2.3, Eq. (2.8)–(2.15).

A.2.2 Vector Addition and Subtraction

Vectors are added by summing values associated with common unit vectors. The two vectors *U* and *V* of Example 1 can be added together to form a third vector *W* by

$$W = U + V = (x_U - x_V)i + (y_U - y_V)j \tag{A.16}$$

The addition of vectors *U* and *V* is shown graphically in **Figure A.4**. Vector *V* is placed at the end of vector *U*. The vector connecting the beginning of vector *U* to the end of vector *V* is the summation vector *W*. As addition is a commutative property, note that

$$W = U + V = V + U \tag{A.17}$$

The commutative property of vector addition is shown in **Figure A.4** by the dashed vectors.

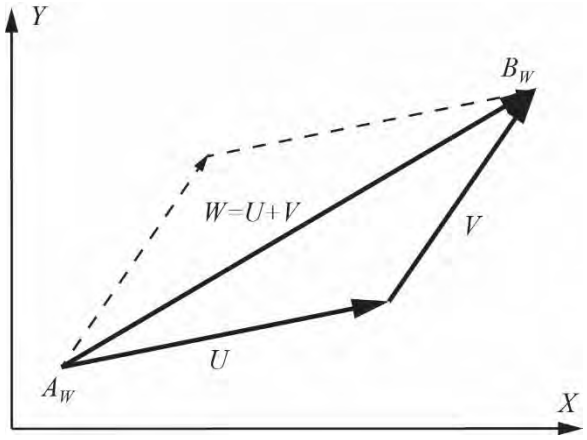

Source: PCI

Figure A.4 Vector Addition

Vector subtraction is

$$W = U - V = (x_U - x_V)i + (y_U - y_V)j \tag{A.18}$$

Figure A.5 shows the graphical representation of the subtraction of the two vectors of Example 1, vectors *U* and *V*. The beginnings of the two vectors are first collocated. Vector *W* is then drawn from the end of the vector being subtracted (vector *V* in this case) to the end of the vector being subtracted from (vector *U*).

Note that subtraction is not a commutative property in that subtracting vector *U* from vector *V* would result in a vector of appropriate length, but of wrong direction. Also note that the same subtracted result can be achieved by adding the negative of the vector to be subtracted (see **Figure A.6**).

$$W = U - V = U + (-V) \tag{A.19}$$

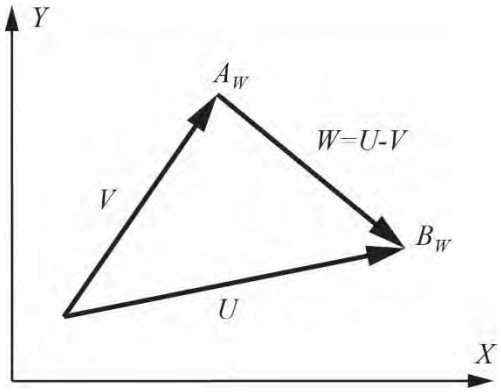

Source: PCI

Figure A.5 Vector Subtraction

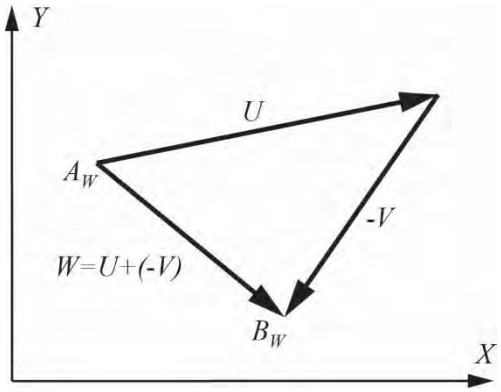

Source: PCI

Figure A.6 Vector Addition by Adding a Negative Vector

Example 2: Add and subtract vectors *U* and *V* from Example 1.

$$U = 20i + 4j \tag{A.20}$$

$$V = 8i + 13j \tag{A.21}$$

$$W = U + V = (20 + 8)i + (4 + 13)j = 28i + 17j \tag{A.22}$$

$$W = U - V = (20 - 8)i + (4 - 13)j = 12i - 9j \tag{A.23}$$

A.2.3 Vector Multiplication—Scalar (Dot) Product

This form of vector multiplication, for vectors containing the same number of terms, returns a single scalar product. Algebraically, the scalar product is

$$U \cdot V = (x_u x_v) + (y_u y_v) \tag{A.24}$$

The scalar product can also be expressed geometrically:

$$U \cdot V = |U||V|\cos\theta \tag{A.25}$$

Figure A.7 depicts the graphical expression of the scalar product.

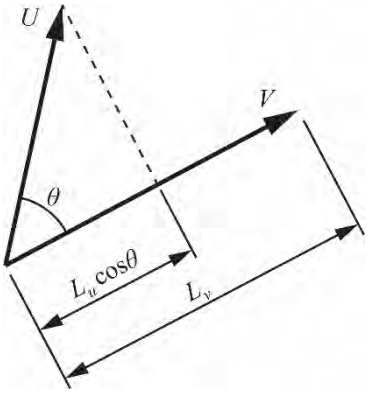

Source: PCI

Figure A.7 Example 3D Vector

Rearranging Eq. (A.25) by the commutative rule produces

$$U \cdot V = |U|\cos\theta|V| \tag{A.26}$$

This shows that the scalar product is equal to the length of the projection of vector *U* onto vector *V* multiplied by the length of vector *V*. This could alternatively be restated as the scalar product is equal to the length of the projection of vector *V* onto vector *U* multiplied by the length of vector *U*.

Eq. (A.24) and (A.25) can be combined to find the angle between the two vectors:

$$\theta = \cos^{-1}\frac{(x_U x_V) + (y_U y_V)}{|U||V|} \tag{A.27}$$

Note that the scalar product of nonzero vectors will be equal to zero when the angle between the two vectors equals 90 degrees. That is, two lines are perpendicular (geometrically orthogonal) if the scalar product of the vectors is equal to zero.

It should again be noted that the equations for vector direction cosine and resulting direction angles are quadrant dependent. Vector components' signs should be assigned using a convention similar to that presented in section 2.3, Eq. (2.8)—(2.15).

Example 3: Find the scalar product of vectors *U* and *V* in Example 1 using both the algebraic definition and the angle between the two vectors.

$$U = 20i + 4j \tag{A.28}$$

$$V = 8i + 13j \tag{A.29}$$

$$|U| = 20.3961 \tag{A.30}$$

$$|V| = 15.2643 \tag{A.31}$$

$$U \cdot V = (20 \times 8) + (4 \times 13) = 212 \tag{A.32}$$

$$\theta = \cos^{-1}\left(\frac{212}{(20.3961)(15.2643)}\right) = 47.0825^{\circ} \tag{A.33}$$

A.3 3D Vectors

A 3D vector is one in which the beginning and ending points are shown in 3D space. **Figure A.8** shows a coordinate system defined by three orthogonal axes, X, Y, and Z. Vector *U* in **Figure A.8** begins with point A(*x*, *y*, *z*) and ends with point B(*x*, *y*, *z*).

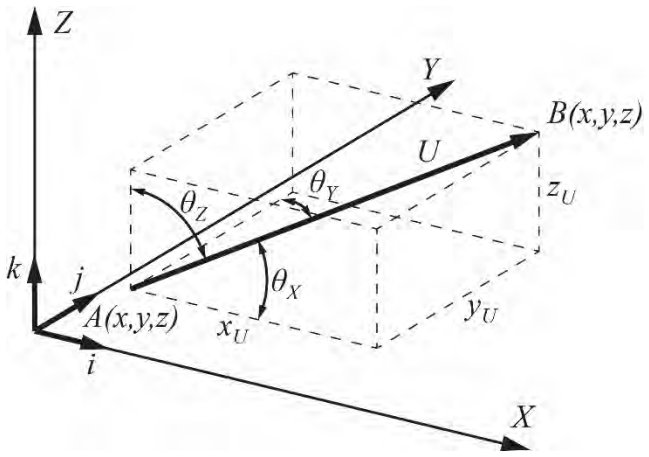

Source: PCI

Figure A.8 3D Vector

As with 2D vectors, 3D vectors can be shown by projected lengths along the three coordinate system axes. The projected lengths of vector *U* shown in **Figure A.8** onto the X, Y and Z axes are

$$x_U = x_B - x_A \tag{A.34}$$

$$y_U = y_B - y_A \tag{A.35}$$

$$z_U = z_B - z_A \tag{A.36}$$

The length of vector *U* is then

$$l_U = \sqrt{x_U^2 + y_U^2 + z_U^2} \tag{A.37}$$

Vector *U* can be expressed in equation form as

$$U = x_U i + y_U j + z_U k \tag{A.38}$$

The integers *i*, *j*, and *k*, shown in **Figure A.8**, are unit vectors coincident with the X, Y and Z axes, respectively.

The direction cosines of the vector relative to all three axes are used to establish the orientation of the vector. Equation A.44, which defines the angle between two vectors in two dimensions, can be expanded to three dimensions and written as

$$\cos\theta_{UV} = \left(\frac{x_U x_V + y_U y_V + z_U z_V}{|U||V|}\right) \tag{A.39}$$

The three direction cosines are found with respect to the unit vectors of the coordinate system:

$$X = 1i + 0j + 0k \tag{A.40}$$

$$Y = 0i + 1j + 0k \tag{A.41}$$

$$Z = 0i + 0j + 1k \tag{A.42}$$

The direction cosines of vector *U* are then

$$\cos\theta_{UX} = \left(\frac{x_U(1) + y_U(0) + z_U(0)}{|U|(1)}\right) = \frac{x_U}{|U|} \tag{A.43}$$

$$\cos\theta_{UY} = \left(\frac{x_U(0) + y_U(1) + z_U(0)}{|U|(1)}\right) = \frac{y_U}{|U|} \tag{A.44}$$

$$\cos\theta_{UZ} = \left(\frac{x_U(0) + y_U(0) + z_U(1)}{|U|(1)}\right) = \frac{y_Z}{|U|} \tag{A.45}$$

Note that Eq. (A.42) produces the same result as Eq. (A.4).

Example 4: Given the 3D vector *U* in **Figure A.9**, compute the direction cosines of the vector relative to the coordinate system.

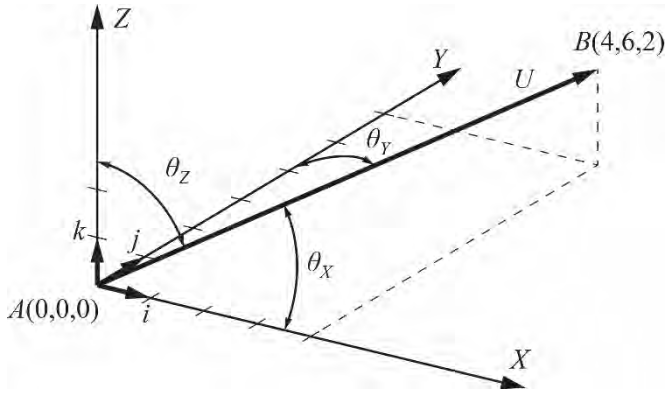

Source: PCI

Figure A.9 Example 3D Vector

The length of vector *U* is

$$|U| = \sqrt{4^2 + 6^2 + 2^2} = 2\sqrt{14} \tag{A.46}$$

The direction cosines are found using Eq. (A.42)–(A.44), and using the unit vectors *i*, *j*, and *k*.

$$\cos\theta_{UX} = \left(\frac{4(1) + 6(0) + 2(0)}{2\sqrt{14}(1)}\right) = \frac{4}{2\sqrt{14}} = \frac{2}{\sqrt{14}} \tag{A.47}$$

$$\cos\theta_{UY} = \left(\frac{4(0) + 6(1) + 2(0)}{2\sqrt{14}(1)}\right) = \frac{6}{2\sqrt{14}} = \frac{3}{\sqrt{14}} \tag{A.48}$$

$$\cos\theta_{UZ} = \left(\frac{4(0) + 6(0) + 2(1)}{2\sqrt{14}(1)}\right) = \frac{2}{2\sqrt{14}} = \frac{1}{\sqrt{14}} \tag{A.49}$$

A.4 Vector Multiplication—Vector (Cross) Product

The second method of vector multiplication, the vector or cross product, differs from the scalar product in that the result is a vector (scalar magnitude and direction). The resulting vector is perpendicular to the two vectors being multiplied, and its orientation is defined by the right-hand rule. The vector product is defined as

$$U \times V = |U||V|(\sin\theta)N \tag{A.50}$$

where

U = First vector being multiplied
V = Second vector being multiplied
θ = Angle between vectors U and V in the plane in which they lie
N = Unit vector perpendicular to the plane that contains U and V

Consider two 3D vectors U and V:

$$U = x_u i + y_u j + z_u k \tag{A.51}$$

$$V = x_v i + y_v j + z_v k \tag{A.52}$$

The vector product of U and V is found by multiplying the coefficients in like directions:

$$\begin{aligned} U \times V = {} & x_u x_v (i \times i) + x_u y_v (i \times j) + x_u z_v (i \times k) + \\ & y_u x_v (j \times i) + y_u y_v (j \times j) + y_u z_v (j \times k) + \\ & z_u x_v (k \times i) + z_u y_v (k \times j) + z_u z_v (k \times k) \end{aligned} \tag{A.53}$$

The cross products of the unit vectors are

$$i \times j = k \tag{A.54}$$

$$j \times k = i \tag{A.55}$$

$$k \times i = j \tag{A.56}$$

$$j \times i = -k \tag{A.57}$$

$$k \times j = -i \tag{A.58}$$

$$i \times k = -j \tag{A.59}$$

$$i \times i = j \times j = k \times k = 0 \tag{A.60}$$

Substituting Eq. (A.53)–(A.59) into Eq. (A.52) results in

$$\begin{aligned} U \times V = {} & x_u x_v (0) + x_u y_v (k) + x_u z_v (-j) + \\ & y_u x_v (-k) + y_u y_v (0) + y_u z_v (i) + \\ & z_u x_v (j) + z_u y_v (-i) + z_u z_v (0) \end{aligned} \tag{A.61}$$

or

$$U \times V = (y_u z_v - y_v z_u) i + (z_u x_v - z_v x_u) j + (x_u y_v - x_v y_u) k \tag{A.62}$$

The vector product can also be expressed in the form of a determinant:

$$U \times V = \begin{vmatrix} i & j & k \\ x_u & y_u & z_u \\ x_v & y_v & z_v \end{vmatrix} = \begin{vmatrix} y_u & z_u \\ y_v & z_v \end{vmatrix} i - \begin{vmatrix} x_u & z_u \\ x_v & z_v \end{vmatrix} j + \begin{vmatrix} x_u & y_u \\ x_v & y_v \end{vmatrix} k \tag{A.63}$$

When the two-by-two determinants are solved, it produces Eq. (A.61).

Example 5: Find the vector product of the two vectors below using Eq. (A.61). Verify the length of the perpendicular vector using Eq. (A.49).

$$U = 4i + 6j + 2k \tag{A.64}$$

$$V = -2i + 4j + 1k \tag{A.65}$$

$$U \times V = \left(6(1) - 4(2)\right)i + \left(2(-2) - 1(4)\right)j + \left(4(4) - (-2)(6)\right)k \tag{A.66}$$

$$U \times V = -2i + 4j + 1k \tag{A.67}$$

$$|U \times V| = \sqrt{-2^2 + -8^2 + 28^2} = 29.1890 \tag{A.68}$$

$$|U| = \sqrt{4^2 + 6^2 + 2^2} = 7.4833 \tag{A.69}$$

$$|V| = \sqrt{-2^2 + 4^2 + 1^2} = 4.5826 \tag{A.70}$$

$$\cos\theta_{UV} = \left(\frac{4(-2) + 6(4) + 2(1)}{7.4833(4.5826)}\right) \tag{A.71}$$

$$|U \times V| = 7.4833(4.5826)\sin\left(\cos^{-1}(0.52489)\right) = 29.1890 \tag{A.72}$$

Figure A.10 shows vectors *U* and *V* and the vector product $U \cdot V$. Note that the length of the vector product is equal to the area of the parallelogram created by vectors *U* and *V* and the included angle θ.

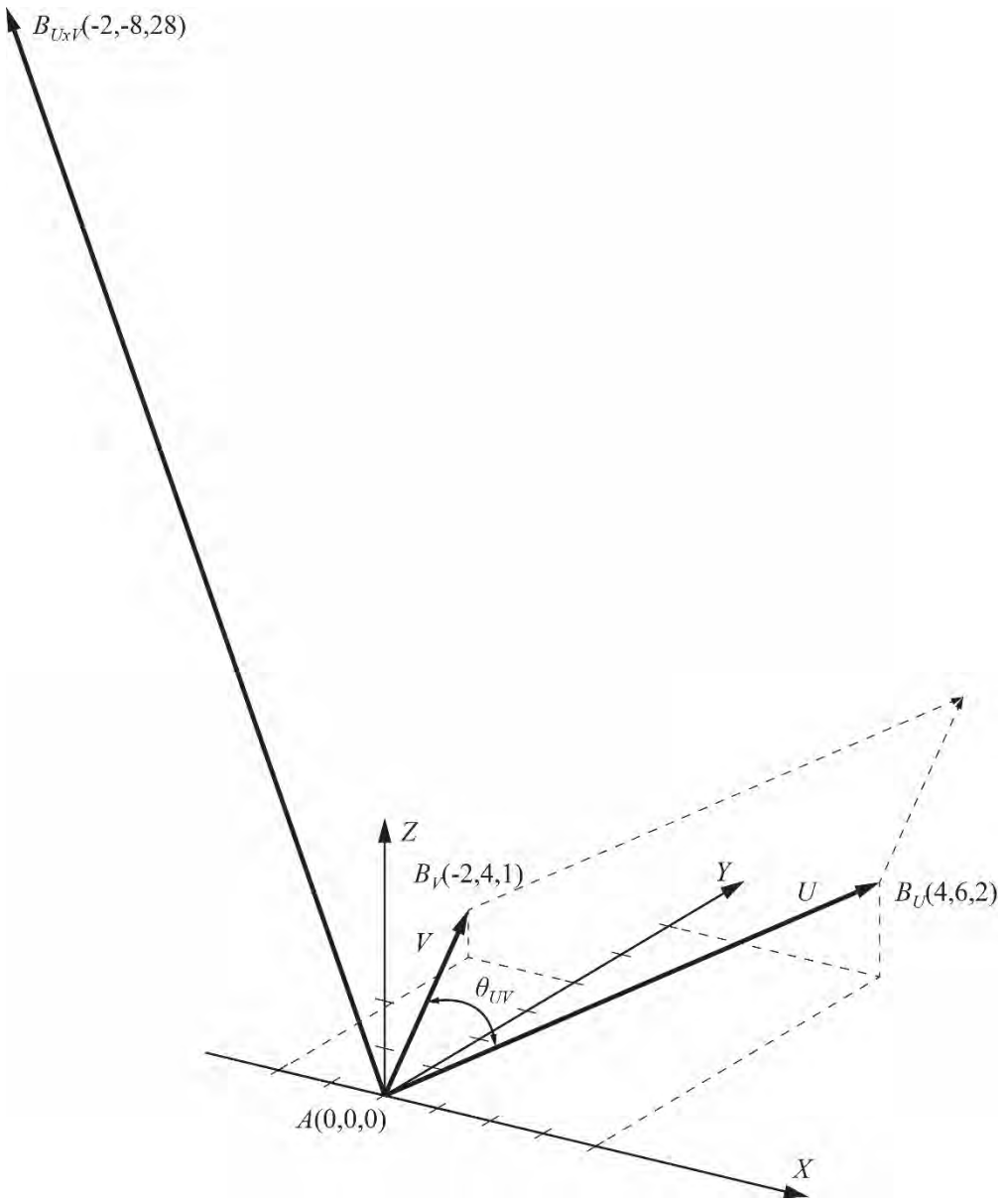

Source: PCI

Figure A.10 Vectors of Example 5

A.5 Coordinate Transformations

Development of a bridge's geometry often involves the expression of geometric information in alternative coordinate systems. This section begins with simple expressions of coordinate system translation and rotation in two dimensions. 3D rotational coordinate system transformations are then expressed using features of vector geometry presented in previous sections.

A.5.1 Coordinate System Translations

Consider the horizontal alignment used in Chapter 2 of this manual. **Figure A.11** shows the horizontal alignment in the global north (Y) and east (X) coordinate system. Also shown is a second coordinate system whose origin is located away from the origin of the global coordinate system.

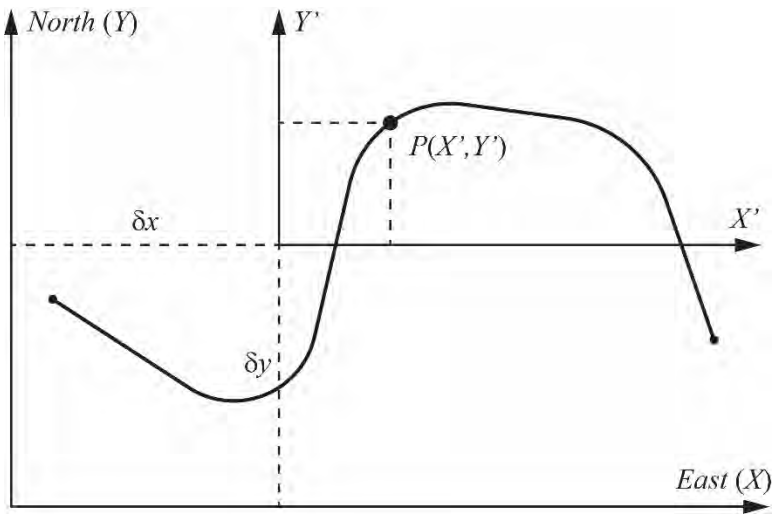

Source: PCI

Figure A.11 Translation of Coordinate System

The translation of the coordinate system from the global to the local system is achieved by subtracting the differential x and y dimensions δx and δy. In equation form, the x and y coordinates in the local coordinate system are

$$x' = x - \delta x \quad \text{(A.73)}$$

$$y' = y - \delta y \quad \text{(A.74)}$$

Coordinate system translations for 3D coordinate systems are achieved by adding an equation for translation relative to the Z axis:

$$z' = z - \delta z \quad \text{(A.75)}$$

A.5.2 2D Rotational Coordinate Transformations

Figure A.12 shows a closer view of **Figure A.11**, at the origin of the translated coordinate system X'Y'. **Figure A.12** also shows a coordinate system X''Y'', which is rotated by the angle θ in the counterclockwise direction.

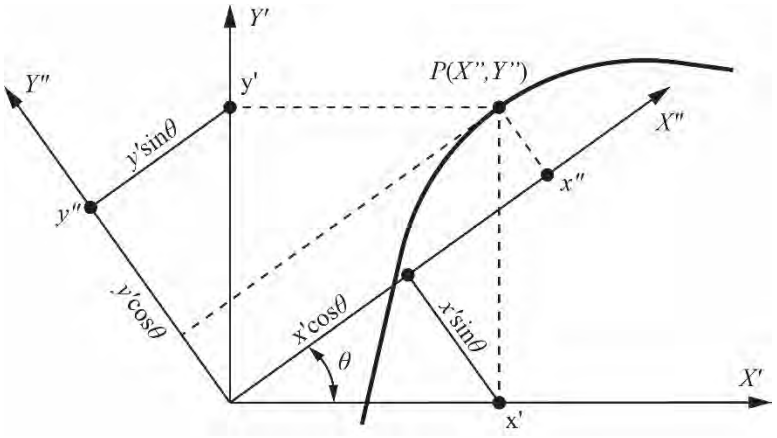

Source: PCI

Figure A.12 2D Coordinate System Rotation

The coordinates of point *P* in the rotated coordinate system are found by the following transformation equations for 2D systems:

$$x'' = x'\cos\theta + y'\sin\theta \tag{A.76}$$

$$y'' = -x'\sin\theta + y'\cos\theta \tag{A.77}$$

The transformation of the coordinates can be expressed as

$$\begin{bmatrix} x'' \\ y'' \end{bmatrix} = \begin{bmatrix} x'\cos\theta & y'\sin\theta \\ -x'\sin\theta & y'\cos\theta \end{bmatrix} \begin{bmatrix} x' \\ y' \end{bmatrix} \tag{A.78}$$

or, in terms of the point *P*,

$$[P''] = [T][P'] \tag{A.79}$$

The matrix [*T*] in Eq. (A.78) is the transformation matrix:

$$[T] = \begin{bmatrix} \cos\theta & \sin\theta \\ -\sin\theta & \cos\theta \end{bmatrix} \tag{A.80}$$

Transformations from the rotated system back to the system aligned with the global axes are made by premultiplying the rotated point coordinates by the transpose of the transformation matrix.

$$[T]^T [P'] = [T]^T [T][P] = [P] \tag{A.81}$$

The transpose of the transformation matrix is

$$[T]^T = \begin{bmatrix} \cos\theta & -\sin\theta \\ \sin\theta & \cos\theta \end{bmatrix} \tag{A.82}$$

It is often convenient to develop 2D transformations in a 3D system, where rotations are made about each of the 3D axes in sequence. **Figure A.13** shows a 3D coordinate system and three 2D views in the XY, YZ, and ZX planes. The rotation angles for the three systems are α, β, and γ, respectively. The transformation matrices and transforms of these matrices are given in Eq. (A.81)–(A.86).

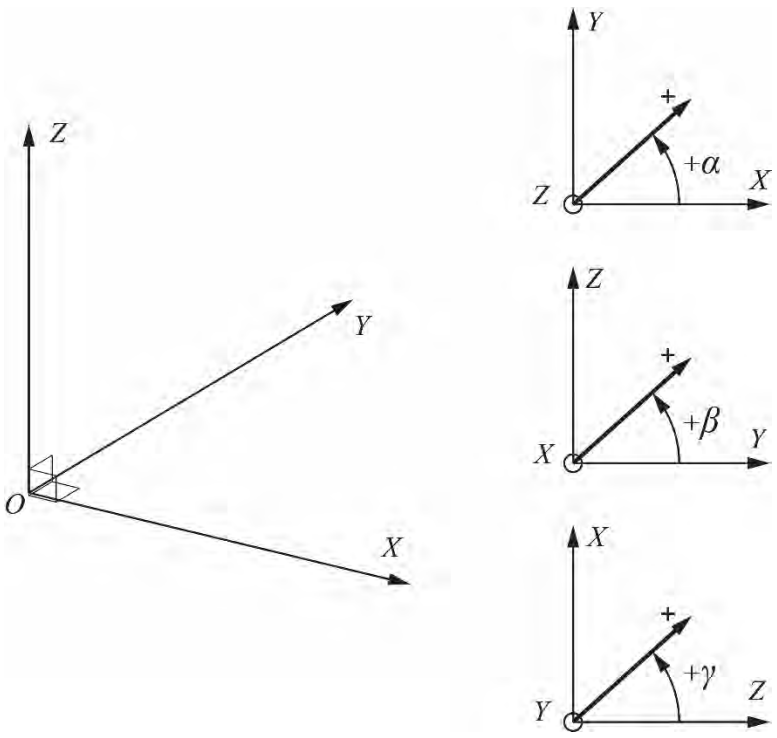

Source: PCI

Figure A.13 3D Coordinate System Rotation

$$[T]_Z = \begin{bmatrix} \cos\alpha & \sin\alpha & 0 \\ -\sin\alpha & \cos\alpha & 0 \\ 0 & 0 & 1 \end{bmatrix} \qquad [T]_Z^T = \begin{bmatrix} \cos\alpha & -\sin\alpha & 0 \\ \sin\alpha & \cos\alpha & 0 \\ 0 & 0 & 1 \end{bmatrix} \tag{A.83, A.84}$$

$$[T]_X = \begin{bmatrix} 1 & 0 & 0 \\ 0 & \cos\beta & \sin\beta \\ 0 & -\sin\beta & \cos\beta \end{bmatrix} \qquad [T]_X^T = \begin{bmatrix} 1 & 0 & 0 \\ 0 & \cos\beta & -\sin\beta \\ 0 & \sin\beta & \cos\beta \end{bmatrix} \tag{A.85, A.86}$$

$$[T]_Y = \begin{bmatrix} \cos\gamma & 0 & -\sin\gamma \\ 0 & 1 & 0 \\ \sin\gamma & 0 & \cos\gamma \end{bmatrix} \qquad [T]_Y^T = \begin{bmatrix} \cos\gamma & 0 & \sin\gamma \\ 0 & 1 & 0 \\ -\sin\gamma & 0 & \cos\gamma \end{bmatrix} \tag{A.87, A.88}$$

A.5.3 3D Rotational Coordinate Transformations using Direction Cosines

Figure A.13 shows two orthogonal coordinate systems with a common origin. The second coordinate system X'Y'Z' is arbitrarily rotated away from the original coordinate system XYZ. The orientation of each of the axes of the new coordinate system can be described by three direction cosines relative to the original coordinate system. **Figure A.14** shows the three angles of the X' axis to the original coordinate system axes.

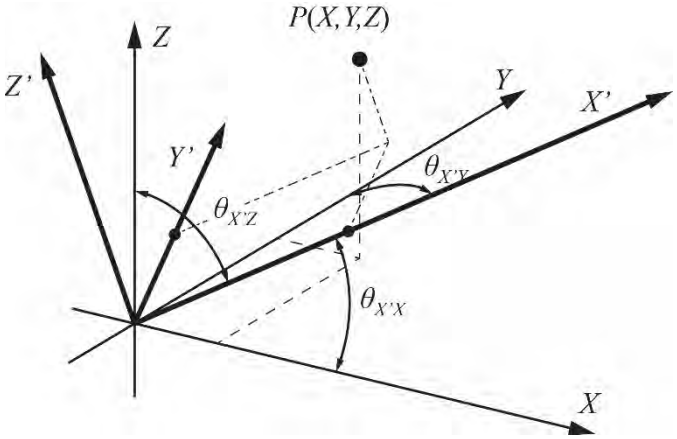

Source: PCI

Figure A.14 3D Coordinate System Rotation

The coordinates of point *P* in the X'Y'Z' system can be found by the matrix multiplication of the coordinates of point *P* in the XYZ system by a transformation matrix composed of the nine direction cosines.

$$[T] = \begin{bmatrix} \cos\theta_{X'X} & \cos\theta_{X'Y} & \cos\theta_{X'Z} \\ \cos\theta_{Y'X} & \cos\theta_{Y'Y} & \cos\theta_{Y'Z} \\ \cos\theta_{Z'X} & \cos\theta_{Z'Y} & \cos\theta_{Z'Z} \end{bmatrix} \tag{A.89}$$

The first row of the transformation matrix contains the direction cosines of the X' axis relative to the X (column 1), Y (column 2), and Z (column 3) axes. The second row contains the direction cosines for the Y' axis, and the third row contains the direction cosines for the Z' axis.

Transforming coordinates back to the original system is found by premultiplying the transformed results by the transpose of the transformation matrix. The transpose of the transformation matrix is

$$[T]^T = \begin{bmatrix} \cos\theta_{X'X} & \cos\theta_{Y'X} & \cos\theta_{Z'X} \\ \cos\theta_{X'Y} & \cos\theta_{Y'Y} & \cos\theta_{Z'Y} \\ \cos\theta_{X'Z} & \cos\theta_{Y'Z} & \cos\theta_{Z'Z} \end{bmatrix} \tag{A.90}$$

Appendix B – Example Alignment Geometry

B.1 Horizontal Alignment

The example horizontal alignment used in this manual was developed in Chapter 2. The alignment, which follows the centerline of the roadway, is shown in **Figure B.1**. Data of the example horizontal alignment are provided in this section.

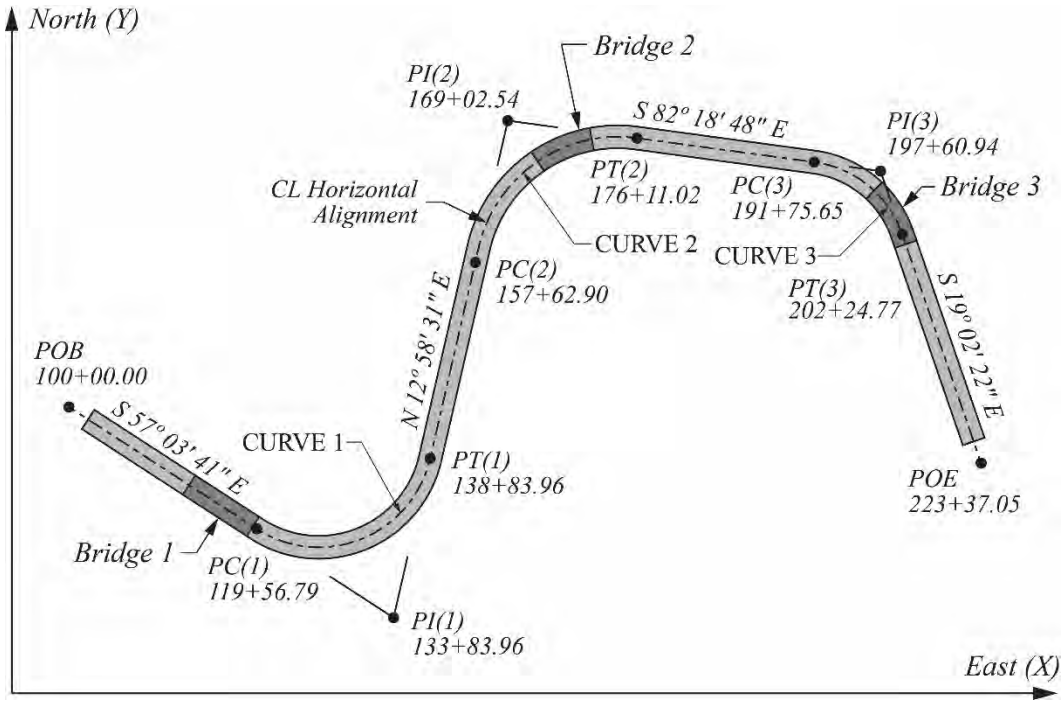

Source: PCI

Figure B.1 Example Horizontal Alignment

B.1.1 PI Data

PI	E(X)	N(Y)	STATION
POB	500.000000	2500.000000	100+00.000000
1	3340.000000	660.000000	133+83.962175
2	4340.000000	5000.000000	169+02.549349
3	7600.000000	4560.000000	197+60.953271
POE	8480.000000	2010.000000	223+37.070194

B.1.2 Baseline Data

BL	BEARING	LENGTH
1	S 57 03 40.7140 E	3383.962175
2	N 12 58 31.1944 E	4453.717548
3	S 82 18 47.8019 E	3289.559241
4	S 19 02 22.0343 E	2697.572983

B.1.3 Curve Data

CURVE 1		
TYPE = CIRCLE	LENGTH = 1919.222667	DELTA = 109 57 48.0916
RAD IN = 1000.000000	TAN IN = 1427.176521	DEG IN = 5 43 46.4806
RAD OUT = 1000.000000	TAN OUT = 1427.176521	DEG OUT = 5 43 46.4806
CURVE 2		
TYPE = CIRCLE	LENGTH = 1848.115835	DELTA = -84 42 41.0037
RAD IN = 1250.000000	TAN IN = 1139.635577	DEG IN = 4 35 01.1845
RAD OUT = 1250.000000	TAN OUT = 1139.635577	DEG OUT = 4 35 01.1845
CURVE 3		
TYPE = CIRCLE	LENGTH = 1049.119737	DELTA = -63 16 25.7677
RAD IN = 950.000000	TAN IN = 585.287899	DEG IN = 6 1 52.0849
RAD OUT = 950.000000	TAN OUT = 585.287899	DEG OUT = 6 1 52.0849

B.1.4 Alignment Data

POINT	STA	E(X)	N(Y)
POB	100+ 0.000000	500.000000	2500.000000

RUN = 1956.785654

CURVE	POINT	STA	E(X)	N(Y)	
1	PC	119+56.785654	2142.237995	1436.014820	LENGTH = 1919.222667
	PI(1)	133+83.962175	3340.000000	660.000000	TAN IN = 1427.176521
	PT	138+76.008321	3660.446123	2050.736173	TAN OUT = 1427.176521

RUN = 1886.905451

CURVE	POINT	STA	E(X)	N(Y)	
2	PC	157+62.913772	4084.115884	3889.462938	LENGTH 1848.115835
	PI(2)	169+ 2.549349	4340.000000	5000.000000	TAN IN 1139.635577
	PT	176+11.029607	5469.395067	4847.566310	TAN OUT 1139.635577

RUN = 1564.635765

CURVE	POINT	STA	E(X)	N(Y)	
3	PC	191+75.665372	7019.971367	4638.286073	LENGTH 1049.119737
	PI(3)	197+60.953271	7600.000000	4560.000000	TAN IN 585.287899
	PT	202+24.785109	7790.932128	4006.730765	TAN OUT 585.287899

RUN = 2112.285084

POINT	STA	E(X)	N(Y)
POE	223+37.070194	8480.000000	2010.000000

B.1.5 Curve Center Data

CURVE	CC E(X)	CC N(Y)
1	2685.979298	2275.267700
2	5302.199416	3608.798529
3	6892.902672	3696.822560

B.2 Vertical Profile Data

The vertical profile for the example horizontal alignment was developed in Chapter 3. The vertical profile, shown in **Figure B.2**, lies along the example horizontal alignment, which follows the centerline of the roadway. Data of the vertical profile are provided in this section.

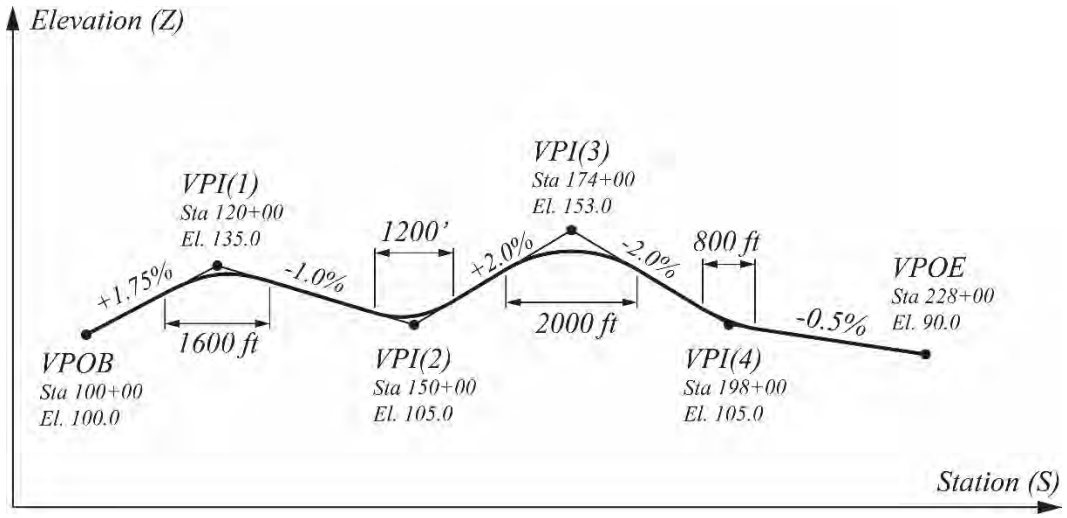

Source: PCI

Figure B.2 Example Vertical Profile

POINT	STATION	ELEVATION
VPOB	100+ 0.00000	100.00000

RUN = 1200.00000

CURVE	POINT	STATION	ELEVATION	
1	VPC	112+ 0.00000	121.00000	GRADE IN = 0.01750000
	VPI(1)	120+ 0.00000	135.00000	LENGTH = 1600.000000
	VPT	128+ 0.00000	127.00000	GRADE OUT = 0.01000000

RUN = 1600.00000

CURVE	POINT	STATION	ELEVATION	
2	VPC	144+ 0.00000	111.00000	GRADE IN = -0.01000000
	VPI(2)	150+ 0.00000	105.00000	LENGTH = 1200.000000
	VPT	156+ 0.00000	117.00000	GRADE OUT = 0.02000000

RUN = 800.00000

CURVE	POINT	STATION	ELEVATION	
3	VPC	164+ 0.00000	133.00000	GRADE IN = 0.02000000
	VPI(3)	174+ 0.00000	153.00000	LENGTH = 2000.000000
	VPT	184+ 0.00000	133.00000	GRADE OUT = -0.02000000

RUN = 1000.00000

CURVE	POINT	STATION	ELEVATION	
4	VPC	194+ 0.00000	113.00000	GRADE IN = -0.02000000
	VPI(4)	198+ 0.00000	105.00000	LENGTH = 800.000000
	VPT	202+ 0.00000	103.00000	GRADE OUT -0.00500000

RUN = 2600.00000

POINT	STATION	ELEVATION
VPOE	228+ 0.00000	90.00000

B.3 Superelevation Data

Superelevation diagrams for the three horizontal curves were developed in Chapter 4 of this manual. **Figure B.3** shows the three superelevation diagrams. Data of the superelevations are provided in this section.

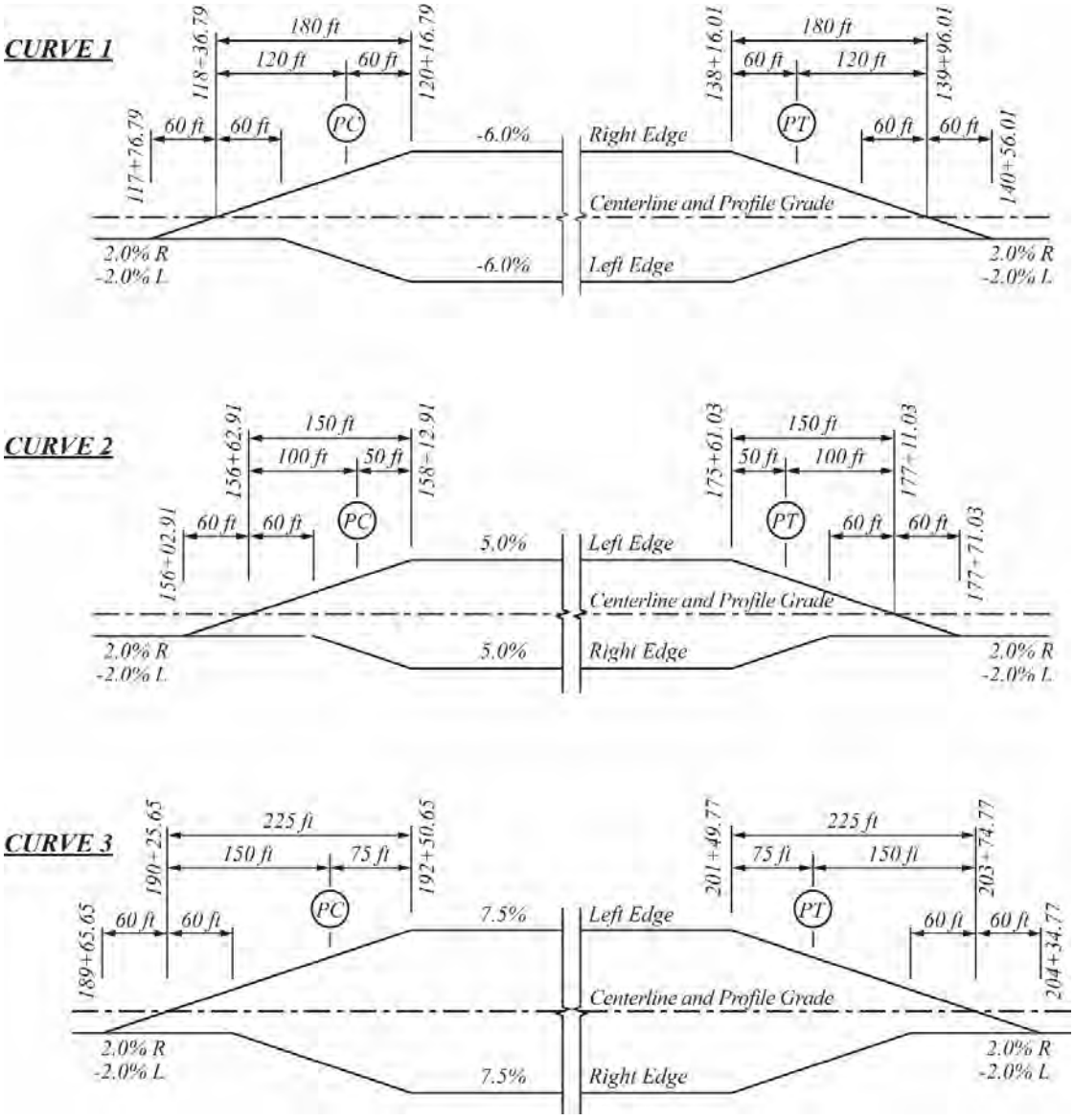

Source: PCI

Figure B.3 Superelevation Data for the Example Alignment

B.3.1 Right Superelevations

POINT	STATION	ELEVATION
SPOB	100+ 0.00000	-0.02000

RUN = 1776.78565

CURVE	POINT	STATION	ELEVATION	
1	SPC	117+76.78565	0.02000	RATE IN = 0.00000000
	SPI(1)	117+76.78565	0.02000	LENGTH = 0.000000
	SPT	117+76.78565	0.02000	RATE OUT = -0.00033333

RUN = 240.00000

CURVE	POINT	STATION	E ELEVATION	
2	SPC	120+16.78565	-0.06000	RATE IN = -0.00033333
	SPI(2)	120+16.78565	-0.06000	LENGTH = 0.000000
	SPT	120+16.78565	-0.06000	RATE OUT = 0.00000000

RUN = 799.22267

CURVE	POINT	STATION	ELEVATION	
3	SPC	138+16.00832	-0.06000	RATE IN = 0.00000000
	SPI(3)	138+16.00832	-0.06000	LENGTH = 0.000000
	SPT	138+16.00832	-0.06000	RATE OUT = 0.00033333

RUN = 240.00000

CURVE	POINT	STATION	ELEVATION	
4	SPC	140+56.00832	0.02000	RATE IN = 0.00033333
	SPI(4)	140+56.00832	0.02000	LENGTH = 0.000000
	SPT	140+56.00832	0.02000	RATE OUT = 0.00000000

RUN = 666.90545

CURVE	POINT	STATION	ELEVATION	
5	SPC	157+22.91377	0.02000	RATE IN = 0.00000000
	SPI(5)	157+22.91377	0.02000	LENGTH = 0.000000
	SPT	157+22.91377	0.02000	RATE OUT = 0.00033333

RUN = 90.00000

CURVE	POINT	STATION	ELEVATION	
6	SPC	158+12.91377	0.05000	RATE IN = 0.00033333
	SPI(6)	158+12.91377	0.05000	LENGTH = 0.000000
	SPT	158+12.91377	0.05000	RATE OUT 0.00000000

RUN = 1748.11584

CURVE	POINT	STATION	ELEVATION	
7	SPC	175+61.02961	0.05000	RATE IN = 0.00000000
	SPI(7)	175+61.02961	0.05000	LENGTH = 0.000000
	SPT	175+61.02961	0.05000	RATE OUT = -0.00033333

RUN = 90.00000

CURVE	POINT	STATION	ELEVATION	
8	SPC	176+51.02961	0.02000	RATE IN = -0.00033333
	SPI(8)	176+51.02961	0.02000	LENGTH = 0.000000
	SPT	176+51.02961	0.02000	RATE OUT = 0.00000000

RUN = 1434.63576

CURVE	POINT	STATION	ELEVATION	
9	SPC	190+85.66537	0.02000	RATE IN = 0.00000000
	SPI(10)	190+85.66537	0.02000	LENGTH = 0.000000
	SPT	190+85.66537	0.02000	RATE OUT = 0.00033333

RUN = 165.00000

CURVE	POINT	STATION	ELEVATION	
10	SPC	192+50.66537	0.07500	RATE IN = 0.00033333
	SPI(11)	192+50.66537	0.07500	LENGTH = 0.000000
	SPT	192+50.66537	0.07500	RATE OUT = 0.00000000

RUN = 899.11974

CURVE	POINT	STATION	ELEVATION	
11	SPC	201+49.78511	0.07500	RATE IN 0.00000000
	SPI(12)	201+49.78511	0.07500	LENGTH 0.000000
	SPT	201+49.78511	0.07500	RATE OUT -0.00033333

RUN = 165.00000

CURVE	POINT	STATION	ELEVATION	
12	SPC	203+14.78511	0.02000	RATE IN -0.00033333
	SPI(13)	203+14.78511	0.02000	LENGTH 0.000000
	SPT	203+14.78511	0.02000	RATE OUT 0.00000000

RUN = 2285.21489

B.3.2 Left Superelevations

POINT	STATION	ELEVATION
SPOB	100+ 0.00000	-0.02000

RUN = 1896.78565

CURVE	POINT	STATION	ELEVATION	
1	SPC	118+96.78565	-0.02000	RATE IN 0.00000000
	SPI(1)	118+96.78565	-0.02000	LENGTH 0.000000
	SPT	118+96.78565	-0.02000	RATE OUT -0.00033333

RUN = 120.00000

CURVE	POINT	STATION	ELEVATION	
2	SPC	120+16.78565	-0.06000	RATE IN -0.00033333
	SPI(2)	120+16.78565	-0.06000	LENGTH 0.000000
	SPT	120+16.78565	-0.06000	RATE OUT 0.00000000

RUN = 1799.22267

CURVE	POINT	STATION	ELEVATION	
3	SPC	38+16.00832	-0.06000	RATE IN 0.00000000
	SPI(3)	138+16.00832	-0.06000	LENGTH 0.000000
	SPT	138+16.00832	-0.06000	RATE OUT 0.00033333

RUN = 120.00000

CURVE	POINT	STATION	ELEVATION	
4	SPC	139+36.00832	-0.02000	RATE IN 0.00033333
	SPI(4)	139+36.00832	-0.02000	LENGTH 0.000000
	SPT	139+36.00832	-0.02000	RATE OUT 0.00000000

RUN = 1666.90545

CURVE	POINT	STATION	ELEVATION	
5	SPC	156+ 2.91377	-0.02000	RATE IN 0.00000000
	SPI(5)	156+ 2.91377	-0.02000	LENGTH 0.000000
	SPT	156+ 2.91377	-0.02000	RATE OUT 0.00033333

RUN = 210.00000

CURVE	POINT	STATION	ELEVATION	
6	SPC	158+12.91377	0.05000	RATE IN 0.00033333
	SPI(6)	158+12.91377	0.05000	LENGTH 0.000000
	SPT	158+12.91377	0.05000	RATE OUT 0.00000000

RUN = 1748.11584

CURVE	POINT	STATION	ELEVATION	
7	SPC	175+61.02961	0.05000	RATE IN 0.00000000
	SPI(7)	175+61.02961	0.05000	LENGTH 0.000000
	SPT	175+61.02961	0.05000	RATE OUT -0.00033333

RUN = 210.00000

CURVE	POINT	STATION	ELEVATION	
8	SPC	177+71.02961	-0.02000	RATE IN -0.00033333
	SPI(8)	177+71.02961	-0.02000	LENGTH 0.000000
	SPT	177+71.02961	-0.02000	RATE OUT 0.00000000

RUN = 1194.63576

CURVE	POINT	STATION	ELEVATION	
9	SPC	189+65.66537	-0.02000	RATE IN 0.00000000
	SPI(10)	189+65.66537	-0.02000	LENGTH 0.000000
	SPT	189+65.66537	-0.02000	RATE OUT 0.00033333

RUN = 285.00000

CURVE	POINT	STATION	ELEVATION	
10	SPC	192+50.66537	0.07500	RATE IN 0.00033333
	SPI(11)	192+50.66537	0.07500	LENGTH 0.000000
	SPT	192+50.66537	0.07500	RATE OUT 0.00000000

RUN = 899.11974

CURVE	POINT	STATION	ELEVATION	
11	SPC	201+49.78511	0.07500	RATE IN 0.00000000
	SPI(12)	201+49.78511	0.07500	LENGTH 0.000000
	SPT	201+49.78511	0.07500	RATE OUT -0.00033333

RUN = 285.00000

CURVE	POINT	STATION	ELEVATION	
12	SPC	204+34.78511	-0.02000	RATE IN -0.00033333
	SPI(13)	204+34.78511	-0.02000	LENGTH 0.000000
	SPT	204+34.78511	-0.02000	RATE OUT 0.00000000

RUN = 2165.21489

POINT	STATION	ELEVATION
SPI(14)	226+ 0.00000	-0.02000

ACKNOWLEDGMENTS

This report initially was envisioned as two documents addressing steel structures and concrete structures separately, and much work had been completed before the decision to combine them into one resource.

The primary authors of Part 1 (General), Part 2 (Concrete), and Appendices were John Corven, P.E. (Corven Engineering, a Hardesty Hanover Company) and William Nickas, P.E. (PCI). Many others engaged in discussions and reviewed drafts. Parts 1, Part 2, and the Appendices were developed with the 40 plus active Voting Members of the PCI Committee on Concrete Bridges. The outline and each draft were reviewed by the PCI Committee on Bridges and the AASHTO Committee on Bridges, Technical Subcommittee on Concrete (T-10).

For assistance in Part 3 (Steel) reviews, acknowledgments go to: Thomas Macioce, P.E. (PennDOT), Alex Lim, P.E (Caltrans), and Greg Turco, P.E. (TxDOT). Thanks are also due to committee members of AASHTO/NSBA Steel Bridge Collaboration, Task Group 1 on Detailing: Brad Dillman, P.E., Walter Gatti, P.E., Bill Lally, P.E., George Gorrill, P.E., Matthew Hellenthal, P.E., and Francesco Russo, PhD., P.E.

REFERENCES

1. AASHTO. 2017a. *LRFD Bridge Design Specifications*, Eighth Edition, LRFD-8. American Association of State Highway Transportation Officials, Washington, DC (23 CFR 625.4(d)(1)(v) (2022)).
2. AASHTO. 2017b. *LRFD Bridge Construction Specifications*, Fourth Edition, LRFDCONS-4. American Association of State Highway Transportation Officials, Washington, DC (23 CFR 625.4(d)(1)(iv) (2022)).
3. AASHTO/NSBA Steel Bridge Collaboration. 2006. *G1.4 Guidelines for Design Details,* 1st Edition. American Association of State Highway Transportation Officials, Washington, DC.
4. AASHTO/NSBA Steel Bridge Collaboration. 2019. *G13.1 Guidelines for Steel Girder Bridge Analysis,* 3rd Edition. American Association of State Highway Transportation Officials, Washington, DC.
5. AASHTO/NSBA Steel Bridge Collaboration. 2020. *G12.1 Guidelines to Design for Constructability and Fabrication,* 3rd Edition. American Association of State Highway Transportation Officials, Washington, DC.
6. Chavel, B.W., Coletti, D.A., Frank, K.H., Grubb, M.A., McEleney, W., Medlock, R.D., White, D.W. 2016. *Skewed and Curved Steel I-Girder Bridge Fit.* National Steel Bridge Alliance, August, Chicago, IL.
7. Coletti, D.A., Fan, Z. F., Gatti, W., and Vogel, J. 2005. *Practical Steel Tub Girder Design.* National Steel Bridge Alliance, April, Chicago, IL.
8. FHWA. 2015. Steel Bridge Design Handbook, FHWA Report No. HIF-16-002, Washington, DC.
9. Helwig, T. A., Herman, R. H., and Li, Dawei. 2004. *Behavior of Trapezoidal Box Girders with Skewed Supports*, TxDOT Research Report 0-4148-1, The University of Houston, May, Houston, TX.
10. Helwig, T. A., Yura, J. A., Herman, R. H., Williamson, E. B., and Li, Dawei. 2007. *Design Guidelines for Steel Trapezoidal Box Girder Systems*, TxDOT Research Report 0-4307-1, Center for Transportation Research, The University of Texas at Austin, April, Austin, TX.
11. Li, Dawei. 2004. *Behavior of Trapezoidal Box Girders with Skewed Supports*, Ph.D. Dissertation, Civil and Environmental Engineering Department, University of Houston, August, Houston, TX.
12. Nettleton, D.A., Torkelson, J.S. 1977. *Arch Structures*, Prepared for Bridge Division, Office of Engineering, Federal Highway Administration.
13. PCI. 2011. *PCI Bridge Design Manual, 3rd ed.,* MNL-133, Precast/Prestressed Concrete Institute, Chicago, IL.
14. Texas Department of Transportation. 2006. *Preferred Practices for Steel Bridge Design, Fabrication, and Erection*, January.
15. White, D. W., D. A. Coletti, B. W. Chavel, T. A. Sanchez, C. Ozgur, J. M. M. Chong, R. T. Leon, R. D. Medlock, R. A. Cisneros, T. V. Galambos, J. M. Yadlosky, W. J. Gatti, G. T. Kowatch. 2012. *Guidelines for Analytical Methods and Construction Engineering of Curved and Skewed Steel Girder Bridges*, NCHRP Report 725. Prepared for the Transportation Research Board of the National Academies under the auspices of the National Cooperative Highway Research Program, Washington, DC.
16. White, D.W., Nguyen, T.V., Coletti, D.A., Chavel, B.W., Grubb, M.A., Boring, C.G. 2015. *Guidelines for Reliable Fit-Up of Steel I-Girder Bridges*, NCHRP Report 20-07, Task 355, Prepared for the

Transportation Research Board of the National Academies under the auspices of the National Cooperative Highway Research Program, Washington, DC.